



**Optimisation des conditions réactionnelles et création
de nouveaux mutants à grande performance du
cytochrome p450 BM3 CYP102A1 utilisant les
cofacteurs alternatifs NADH et N-benzyl-1,4-
dihydronicotinamide**

Thèse

Thierry Vincent

Doctorat en génie chimique

Philosophiæ doctor (Ph. D.)

Québec, Canada

© Thierry Vincent, 2020

Résumé

Le cytochrome p450 CYP102A1, mieux connu sous le nom de BM3, provient de la bactérie *Bacillus megaterium*. Cette enzyme possède un groupement prosthétique hémique lui permettant de catalyser l'insertion d'oxygène dans un lien carbone-hydrogène menant généralement à une hydroxylation du substrat, ce qui en fait une monooxygénase. Ce genre de réaction demeure jusqu'à aujourd'hui difficile à effectuer par chimie traditionnelle ce qui confère un intérêt particulier à cette enzyme. Au contraire des autres cytochromes p450, BM3 est soluble (et non membranaire) et est naturellement fusionnée à son partenaire réductase formant ainsi une seule chaîne polypeptidique. Ainsi, au cours des dernières années, BM3 a attiré beaucoup d'attention de la part de l'industrie de la chimie fine et pharmaceutique due à son potentiel biocatalytique important. Cependant, son usage en industrie est restreint par son instabilité ainsi que par le coût prohibitif du cofacteur qui lui est nécessaire pour catalyser ses réactions, le NADPH. Cette thèse décrit le développement de différentes stratégies visant à libérer les réactions effectuées avec BM3 de leur dépendance au NADPH, tout en maximisant le rendement spécifique de la monooxygénase. En place du NADPH, deux autres cofacteurs de moindre coût furent utilisés comme alternative, soit le NADH et le N-benzyle-1,4-dihydronicotinamide (NBAH) en utilisant le mutant R966D/W1046S de BM3. Afin de maximiser le rendement spécifique de BM3, l'une des stratégies de cette thèse, l'optimisation du milieu réactionnel, repose sur deux éléments clés, soit favoriser la stabilité du cofacteur, car celui-ci est plus instable que l'enzyme elle-même, ainsi que d'abaisser au minimum la température de la réaction, car nous avons constaté que ceci avait pour effet d'augmenter le couplage entre les réactions réductase et monooxygénase et donc la stabilité de l'enzyme. L'effet net de la réaction ainsi optimisée fut d'augmenter le rendement spécifique du mutant R966D/W1046S par un facteur situé entre 2 et 2.6 en fonction du cofacteur utilisé. D'autre part, deux stratégies d'ingénierie enzymatique furent explorées afin de générer des mutations pouvant augmenter la performance de BM3. L'une d'entre elles, la mutagenèse par consensus guidé, généra une librairie de mutants de laquelle les mutants NTD5 et NTD6 furent identifiés, augmentant le rendement spécifique de l'enzyme comparativement à leur parent, R966D/W1046S, par un facteur de 5.2 et 2.3 pour le NBAH et le NADH, respectivement. L'autre stratégie explorée fut d'appliquer une pression sélective sur la bactérie *Bacillus megaterium* pour forcer, par évolution expérimentale, la performance de l'enzyme. De cette stratégie, un nouveau mutant de BM3 nommé DE, possédant 34 acides aminés substitués sur sa séquence, fut généré. Ce dernier a démontré une plus forte résistance aux solvants organiques ainsi qu'une augmentation de son rendement spécifique vis-à-vis le NADPH et le NADH d'un facteur de 1.23 et 1.76, comparativement à BM3 sauvage, respectivement. Les stratégies décrites dans cette thèse présentent une amélioration significative du rendement spécifique de BM3 ainsi que deux

nouvelles méthodologies avec lesquelles une enzyme peut être optimisée et de nouvelles mutations bénéfiques identifiées.

Abstract

The p450 cytochrome CYP102A1, better known as BM3, comes from the bacteria *Bacillus megaterium*. This enzyme possesses a prosthetic heme group enabling it to catalyze the insertion of oxygen into a carbon-hydrogen bond generally resulting in the hydroxylation of the substrate, the enzyme is therefore a monooxygenase. This type of reaction remains difficult to achieve by traditional chemistry. Unlike other p450 cytochromes, BM3 is soluble (is not membrane bound) and is naturally fused to its reductase partner forming a single polypeptide chain. As such, in recent years, BM3 has garnered much attention from the pharmaceutical and fine chemical industries, due to its high biocatalytic potential. However, its use in industry remains constrained by its instability as well as by the prohibitive cost of its cofactor, NADPH. This thesis describes the development of different strategies aiming at liberating reactions driven with BM3 from their dependence to NADPH whilst maximizing the specific yield of the monooxygenase. Instead of NADPH, two other inexpensive cofactors were used, namely NADH and N-benzyl-1,4-dihydronicotinamide (NBAH) by using the BM3 mutant R966D/W1046S. To maximize BM3 specific yield, one of the strategies used in this thesis work, the optimization of the reaction medium, rested on two key elements. Firstly, favouring the stabilization of the cofactor, as it was found to be more unstable than the enzyme itself and secondly lowering the reaction temperature as this effectively augmented oxidase/reductase reactions coupling and as such the stability of the enzyme. The net effect of the optimized reaction was to enhance the specific yield of the BM3 mutant R966D/W1046S by a factor of 2 and 2,6 depending on which cofactor was used. Two other enzymatic engineering strategies were explored to generate mutations which could enhance the performance of BM3. One of these, consensus guided mutagenesis, generated a library of mutants from which mutants NTD5 and NTD6 were identified enhancing the specific yield of the enzyme comparatively to their parent, R966D/W1046S, by a factor of 5,24 and 2,3 for NBAH and NADH respectively. The other strategy explored was to apply a selective pressure on *Bacillus megaterium* to force, by experimental evolution, the performance of the enzyme. From this strategy, a new mutant of BM3 called DE, possessing 34 new amino acid substitutions, was generated. This new mutant displayed a greater resistance to organic solvents as well as an augmentation of specific yields when used alongside NADPH and NADH comparatively to wild type BM3 by a factor of 1,23 and 1,76 respectively. The strategies described in this thesis allowed a significative enhancement of BM3 specific yield as well as represent two new methodologies by which new beneficial mutations can be identified.

Table of Contents

Résumé.....	ii
Abstract	iv
Table of Contents	v
List of tables.....	vii
List of figures	viii
Abbreviations	ix
Avant-Propos.....	xi
Introduction	1
Discovery	1
Cytochrome p450 functions	3
Cytochrome p450 BM3 oxidation.....	5
Catalytic cycle.....	5
Uncoupling.....	8
Kinetics of p450 BM3 oxidation.....	9
CYP based assays.....	10
Functional groups added by oxidation	13
Industrial and commercial interest in p450 cytochromes.....	15
Medical.....	15
Agriculture	16
Fragrance.....	17
Industry	17
1 Literature review - Cytochrome p450 BM3 biotechnology	20
1.1 Enzymatic process - Stability.....	20
1.1.1 Point mutations.....	23
1.1.2 Decoy molecules	27
1.1.3 Shuffle & fusion chimeras.....	29
1.1.4 Immobilisation	34
1.2 Enzymatic process - Electron source.....	41
1.2.1 Nicotinamide reduction and recycling	41
1.2.2 Electrode driven reduction	43
1.2.3 Light driven reduction.....	45
1.2.4 Peroxide driven reduction	47
1.2.5 Zinc/cobalt (III) sepulchrate (Zn/CoIIIsep) reduction.....	48
1.2.6 Enzymatic process - Biphasic systems	49
1.3 Whole-cell process	52
1.3.1 Permeability	54

1.3.2 Cell surface display	57
1.3.3 Cofactor regeneration.....	58
1.3.4 Cascade reactions	62
1.3.5 Biphasic systems	62
1.3.6 Alternative microorganisms	65
1.4 Objectives.....	76
2 Buffer formulation optimization for improved BM3 enzymatic reaction yield.	78
2.1 Introduction.....	81
2.2 Material and Methods.....	83
2.3 Results	87
2.4 Discussion	95
2.5 Conclusion.....	100
3 Optimisation of the p450BM3 cytochrome assisted by consensus-guided evolution	101
3.1 Introduction.....	104
3.2 Methods.....	108
3.3 Results	113
3.4 Discussion	119
3.5 Conclusion.....	124
4 Oleic acid based experimental evolution of Bacillus megaterium yielding an enhanced BM3 variant	125
4.1 Introduction.....	128
4.2 Materials & Methods.....	130
4.3 Results	137
4.4 Discussion	142
4.5 Conclusion.....	145
General conclusion.....	146
References	150

List of tables

Table 1 Commercially relevant biosynthesis products derived from various CYPs	166
Table 2 Whole cell and free enzyme process factors to consider for each chemical production strategy.....	211
Table 3 TON data for various free enzyme strategies discussed in sections 1.5.1, 1.5.2 & 1.5.3 ..	222
Table 4 Product outputs for various whole cell strategies discussed in chapter 1.5.4.....	74
Table 5 Effect of common buffers at increasing concentrations on the denaturation temperature of BM3 N-D, ranked in decreasing order of T _m . Conditions: 750 nM enzymes, 2X SYPRO orange, pH 7.....	88
Table 6 Tolerance of the N-D mutant towards organic cosolvents at increasing concentrations in regards to melting temperature with the ideal buffer at the top and the worst at the bottom of the table. Conditions: 750nM enzymes & 2X SYPRO orange.....	88
Table 7 Exploration of optimal cosolvent/buffer combination in regards to melting temperature. Conditions: 750nM enzymes & 2X SYPRO orange.....	89
Table 8 Kinetics of BM3 mutant R966D/W1046S in dual buffer 10 mM PBS/100 mM BTP pH 8 at both 4 and 25 °C	93
Table 9 Nucleotide sequence of each primer used in this work	113
Table 10 Mutations carried by every BM3 mutant in this work and primer used in their creation.	109
Table 11 Kinetics of promising BM3 mutants in dual buffer 10 mM PBS/100 mM BTP pH 8 at 25 °C	118
Table 12 Kinetics of promising BM3 mutants in 100 mM Tris pH 8 at 25 °C	118
Table 13 Amino acid substitutions accumulated by p450 BM3 DE compared to its parent sequence p450 BM3	138
Table 14 Sequence alignment of new evolved DE mutant compared to members of the CYP102 family	139
Table 15 Kinetic data for pNP production using NADPH as a cofactor for both wild type BM3 and the DE mutant	140

List of figures

Figure 1 The 10 classes of CYPs labelled by their respective domain architecture, cellular localization and their respective redox partners.....	3
Figure 2 Key natural reactions of CYPs which highlight their function in nature. A Hormone metabolism in humans. B Xenobiotic compound breakdown in humans. C Insect repellent in plants. D Microbial defense in bacteria	4
Figure 3 Illustrations of the heme prosthetic group.....	6
Figure 4 BM3 catalytic cycle	7
Figure 5 Examples with human CYP3A4 of the characteristic spectral alterations in the UV-visible spectrum seen in CYP's in the presence of a compound to the heme domain's active site11	
Figure 6 pNCA assay mechanism and difference in the absorption spectra once pNP release	122
Figure 7 NADH absorption spectra.....	133
Figure 8 Possible chemical modification outcomes resulting from the activity of CYPs	144
Figure 9 Example of the generation of valuable precursor chemicals by BM3 through the conversion of 6-iodotetralone	188
Figure 10 Example of the generation of valuable precursor chemicals by BM3 through the conversion of undecanoic acid to 9-hydroxy-10-undecanoic	19
Figure 11 Examples of shuffled chimeras & fusion chimeras	30
Figure 12 Assembly the PCNA fusion constructs.....	36
Figure 13 N-benzyl-1,4-dihydronicotinamide structure.....	37
Figure 14 Zinc dust (Zn)/Cobalt sepulchrate (Co (II/III)Sep) electrons transfer scheme	38
Figure 15 BM3m2 (Y51F/F87A) fused to phasin P and immobilised unto poly P3HB	40
Figure 16 Light driven reduction generic outline.....	45
Figure 17 Cholesterol cleavage by CYP11A1 yielding pregnenolone and 4-methylpentanal	68
Figure 18 Melting temperature of BM3 N-D mutant for different pH.....	87
Figure 19 Cofactor degradation rates at 25° C in buffers at both 1M and 0.1M concentrations.....	91
Figure 20 Turnover numbers of 10-pNCA conversion to <i>p</i> -nitrophenolate by wild type BM3 using as a cofactor either NADPH or NADH.....	92
Figure 21 Turnover numbers of 10-pNCA conversion to <i>p</i> -nitrophenolate by BM3 mutant N-D using as a cofactor either NADH or NBAH	94
Figure 22 Turnover numbers of 10-pNCA conversion to <i>p</i> -nitrophenolate by WT BM3 using as a cofactor either NADPH or NADH in 0.1 M and 1 M buffers	97
Figure 23 Strongly conserved residue cluster within the reductase domain of the CYP102A subfamily & consensus guided evolution approach utilized to generate new BM3 variants.....	106
Figure 24 Screening assay for the newly generated NTD1 variants performed from unpurified BM3 from bacterial cell lysates	114
Figure 25 Turnover numbers of 10-pNCA conversion to <i>p</i> -nitrophenolate by the NTD variants in harsh conditions	115
Figure 26 Turnover numbers of 10-pNCA conversion to <i>p</i> -nitrophenolate by the NTD variants at 4 °C with a fed batch of cofactor	117
Figure 27 Turnover numbers of 10-pNCA conversion to <i>p</i> -nitrophenolate by the variants NTD1 and NTD 235T at 4 °C and 30 °C.....	120
Figure 28 Experimental evolution methodology.....	1322
Figure 29 <i>B. megaterium</i> growth kinetics at various oleic acid concentrations.....	138
Figure 30 Domain architecture of the p450 BM3 cytochrome.....	138
Figure 31 Comparison of the pNP productivity of wild type BM3, DE and DE variants.....	140
Figure 32 Comparison of pNP productivity with wild type BM3 and DE in stringent conditions	141

Abbreviations

ADH : Alcohol dehydrogenase
AdR : Adrenodoxin reductase
Adx : Adrenodoxin
AIDA : Adhesin involved in diffuse adhesion translocation unit
AlkL : Outer membrane transporter from *Pseudomonas putida* GPo1
AtCPR : Cytochrome p450 reductase of *Arabidopsis thaliana*
BM-GDH-2 : Glucose dehydrogenase-2 from *Bacillus megaterium*
BNAH : N-benzyl-1,4-dihydronicotinamide
BTP : Bis-Tris propane
CO : Carbon monoxide
CPR : Cytochrome p450 reductase
CYP : Cytochrome p450
DCW : Dry cell weight
DMSO : Dimethyl sulfoxide
DSC : Differential scanning calorimetry
DSF : Differential scanning fluorimetry
EDTA : Ethylene diamine tetra acetic acid
FAD : Flavin adenine dinucleotide
FDH : Formate dehydrogenase
FdR : Ferredoxin reductase
Fdx : Ferredoxin
Fvx : Flavodoxin
FMN : Flavin mononucleotide
GDH : Glucose dehydrogenase
HEPES : Glycine, 4-(2-hydroxyethyl)-1-piperazineethanesulfonic acid
KBA : 11-keto- β -boswellic acid
kcat : Catalytic activity
Km : Michaelis-Menten binding constant
Ks : Dissociation constant of the Michaelis-Menten relation
LB-ADH : Alcohol dehydrogenase from *Lactobacillus brevis*
MOPS : 3-(N-morpholino) propanesulfonic acid
NADH : Nicotinamide adenine dinucleotide
NADPH : Nicotinamide adenine dinucleotide phosphate
nNOS : Nitric oxide synthase
NOR : Nitric oxide reductase
NTD : NTD variants containing the six NTD1 mutations
NTD1 : BM3 mutant T235A/R471A/E494K/S1024E/R966D/W1046S
NTD2 : BM3 mutant T235A/R471A/E494K/S1024E/R966D/W1046S/V978L
NTD3 : BM3 mutant T235A/R471A/E494K/S1024E/R966D/W1046S/S847G/S850R/E852P
NTD4 : BM3 mutant T235A/R471A/E494K/S1024E/R966D/W1046S/A769S
NTD5 : BM3 mutant T235A/R471A/E494K/S1024E/R966D/W1046S/A769S/S847G/S850R/E852P
NTD6 : BM3 mutant
T235A/R471A/E494K/S1024E/R966D/W1046S/A769S/S847G/S850R/E852P/V978L
NTD7 : BM3 mutant
T235A/R471A/E494K/S1024E/R966D/W1046S/A769S/S847G/S850K/E851A/E852S/V978L
N-D : BM3 mutant R966D/W1046S able to use NBAH and use NADH more efficiently
PBS : Phosphate buffered saline
PCNA : Proliferating cell nuclear antigen
PDH : Phosphite dehydrogenase
Pdr : Putidaredoxin reductase

Pdx : Putidaredoxin
PFCs : Perfluorocarboxylic acids
PHB : Poly(3-hydroxybutyrate)
pNCA : *p*-Nitrophenoxy fatty acid complex
pNP : *p*-Nitrophenolate
RE-ADH : Alcohol dehydrogenase from *Rhodococcus erythropolis*
ROS : Reactive oxygen species
Ru(LL)2PhenA : Ru(Bipyridine)2 5-acetamido-1,10-phenanthroline
SDC : Sodium diethyldithiocarbamate
SPION : Super paramagnetic iron oxide nanoparticle
T₅₀ : The temperature at which 50% of the enzyme's activity is lost in reference to a given reaction
T_m : The temperature at which 50% of CYPs in a sample loses its initial 450 nm absorption peak for a ferrous-CO assay, or in a broader sense the temperature at which 50% of CYPs in a sample loses their initial tertiary folding for other assays such as differential scanning calorimetry, circular dichroism or fluorimetry assays
TON : Maximum turnover number, defined as the amount of moles of product that a single enzyme can form. The units of TON are defined as mole of product per mole of enzyme and are dimensionless. Thus, TON provides a measure of specific yield which the enzyme can achieve
VD₃ : Vitamin D₃
WT : Wild type
W5F5 : solvent resistant BM3 mutant T235A/R471A/E494K/S1024E
Y-ADH : Alcohol dehydrogenase from *Saccharomyces cerevisiae*
Zn/CoIIIsep : Zinc dust/cobalt (III) sepulchrate

Avant-propos

Cette thèse est organisée en 5 chapitres. Elle est précédée d'une introduction sur la nature du sujet investigué dans le cadre de cette thèse, soit le cytochrome p450 BM3 aussi connue sous le nom de CYP102A1. Après un exposé des concepts fondamentaux associés à l'enzyme en question, le premier chapitre consiste en une synthèse de la littérature pertinente au cytochrome p450 BM3 en ce qui a trait aux travaux d'ingénierie moléculaire effectués pour son optimisation.

Au deuxième chapitre, l'article intitulé " Buffer formulation optimization for improved BM3 enzymatic reaction yield " est inséré. Celui-ci est soumis au journal *Biotechnology and Bioengineering*. J'ai effectué la totalité du travail technique et expérimental. Je suis l'auteur principal et le contributeur principal du travail intellectuel de cet article. Les coauteurs de l'article incluent Alain Garnier, Bruno Gaillet et Dominic Thibeault.

Au troisième chapitre, l'article intitulé " Optimisation of the P450BM3 cytochrome assisted by consensus-guided evolution " est inséré. Celui-ci sera soumis au journal *Applied Biochemistry and Biotechnology*. J'ai effectué la totalité du travail technique et expérimental. Je suis l'auteur principal et le contributeur principal du travail intellectuel de cet article. Les coauteurs de l'article incluent Alain Garnier et Bruno Gaillet.

Au quatrième chapitre, l'article intitulé " Oleic acid based experimental evolution of Bacillus megaterium yielding an enhanced BM3 variant " est inséré. Celui-ci sera soumis au journal *PNAS*. J'ai effectué la totalité du travail technique et expérimental. Je suis l'auteur principal et le contributeur principal du travail intellectuel de cet article. Les coauteurs de l'article incluent Alain Garnier et Bruno Gaillet.

Le cinquième chapitre conclue la thèse.

Introduction

Discovery

During the 1940s and until the mid 1950s endocrinologists were trying to elucidate the *in vitro* synthesis of the many different steroids found in mammals, pharmacologists were studying drug metabolism whereas toxicologists were inquiring into the central actors in the breakdown of xenobiotics compounds in the human body. Unbeknownst to each other, these three different branches of scientific discipline were looking for an enzyme involved in all of these activities. Their attention focused on a membrane bound enzyme, which could not be purified, that needed both atmospheric oxygen and nicotinamide adenine dinucleotide phosphate (NADPH) to carry out its reaction and acted by introducing hydroxyl groups onto saturated carbon-carbon bonds [1]. They were all looking for cytochrome p450 enzymes (CYP). CYPs were first isolated in 1955 when an enzyme residing within rabbit liver microsomes was found to oxidize xenobiotic compounds [2]. Three years later, this time in rat liver microsomes, the same type of oxidizing enzyme was reported and earned its current name p450 when, by chance, it was discovered that bubbling carbon monoxide (CO) into the microsome preparation resulted in an increase in absorbance which peaked at 450 nm [3]. Thus, the *pigment* observed at 450 nm was contracted to p450. That a hemoprotein absorbs light at 450 nm was unusual for the time as all other known heme-containing proteins, such as cytochrome b5 [4] or hemoglobin [5], absorbed light rather around 420 nm. By 1964, the p450 protein would be identified as an iron containing type-*b* hemoprotein and classified as a cytochrome, hence the name cytochrome p450 [6–10]. The identity of the fifth ligand coordinating the heme being a cysteine rather than a histidine residue is the underlying cause as to why CYPs absorb maximally at 450 nm rather than at 420 nm once reduced under CO gas [11]. Nowadays this particular cysteine residue has been shown to be conserved amongst most CYPs [12, 13].

Some 10 years after the discovery of CYPs anchored in liver microsomes [2, 3] the first soluble non-membrane bound CYP was discovered in 1965 in the bacterium *Pseudomonas putida* [14]. From a biotechnological perspective, this would be an important discovery, as soluble enzymes are much easier to handle than their membrane bound counterparts. This particular CYP was later named p450cam for its activity towards the substrate camphor and was also referred to as CYP101. It also informed that CYPs are parts of a multicomponent system where they necessitate other redox proteins for transporting electrons from cofactors, such as NADPH or nicotinamide adenine dinucleotide (NADH), to the CYP itself for them to execute their oxidative reaction [15]. In addition, in 1985, p450cam was the first CYP to have its crystal structure solved [16]. This particular work would be

key in understanding several mechanistic features of CYPs later on. The mid 1980s would see the discovery of the first soluble CYP naturally fused to its redox partner, thus forming a single polypeptide chain. The CYP would be named BM3 [17] as it came from *Bacillus megaterium* and was the third cytochrome identified within this bacterium [18]. BM3 would also be the second CYP whose crystal structure was solved partially at first [19], but with more parts being crystalized later, leading to its full three dimensional structure [20–22]. With the advent of sequencing technology, discovery of various CYPs blossomed as did the elucidation of the full electron transfer mechanism, from the cofactor, to the reductase and finally the oxidase. Soon after, domain architecture and cellular location of both CYPs and their respective redox partners would be used to classify these enzymes into the 10 different categories outlined in Figure 1, taken from the review of Cook & al. 2018 [23]. Beyond classes, CYPs are then divided into families, which are solely based on amino acid sequence homology. In the code by which CYPs are labelled they are first given the prefix "CYP" then a number is added to denote to which family it belongs, then a letter to denote the subfamily and finally a number for each distinct gene found within its subfamily [24]. For example, the work done in this particular thesis is with a type VIII CYP of the family 102, the first CYP identified within the subfamily A or CYP102A1. It is also often denoted simply as BM3. For members to be considered of the same family they are required to share amino acid sequences with a minimum sequence similarity of 40% whilst members of the same subfamily require sequence similarity greater than 55%.

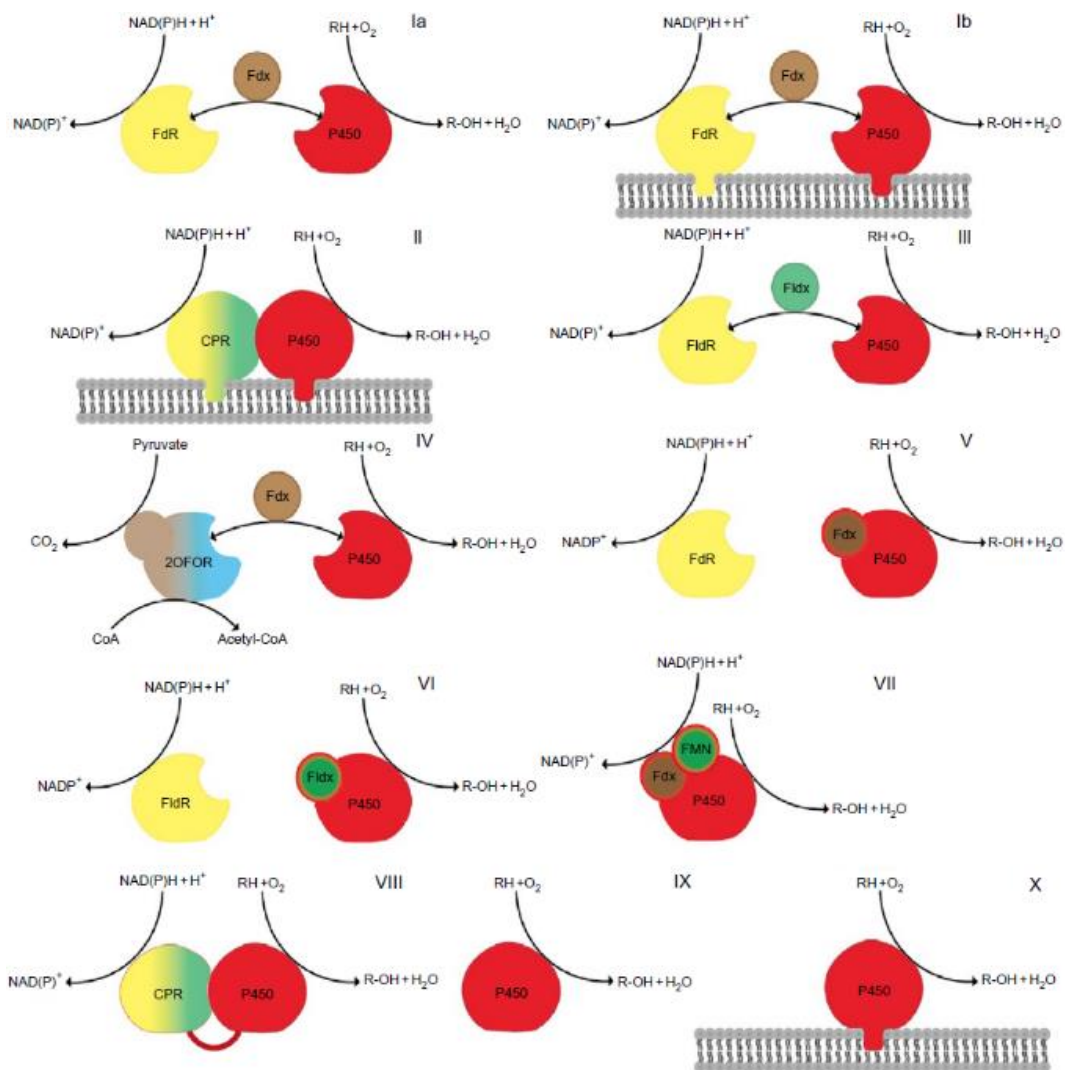


Figure 1: The 10 classes of CYPs labelled by their respective domain architecture, cellular localization and their respective redox partners, (edited from [23]).

Cytochrome p450 functions

The development and commercialisation of dideoxy DNA sequencing technology [25] in the 1980s would bring about the identification, as of 2014, of over 20 000 different CYPs [24]. CYPs have now been shown to be ubiquitous in all orders of life with some few exceptions, such as *Escherichia coli*, not having a single CYP encoded in its genome [26]. CYPs can perform an extensive array of oxidative reactions by introducing a single oxygen atom, which is why these enzymes are also dubbed monooxygenase, unto a wide range of substrates. In doing so, their function can be broadly divided into two endeavors: the production of useful metabolites and the breakdown of compounds.

On the production end, we are aware nowadays of the function of CYPs in producing hormones in mammals [27], fungi [28], plants and insects [29-30]. Apart from hormones, CYPs are almost always involved in the production of fatty acids, eicosanoids and sterols, many of whom are precursors to hormones [27–29]. In humans, CYPs have also been shown to participate in the metabolism of vitamin D and K [27]. For insects and plants, CYPs can further transform these metabolites into defensive compounds, that is, xenobiotics compounds against the would-be predators or herbivores, respectively [29]. Fungal and bacterial CYPs have been shown to participate in the production of similar compounds, namely antibiotics, to combat other microbial neighbours [31]. This ties closely into the second class by which CYPs functions are classified, that is, the breakdown of compounds where their role is to provide a protection against environmental hazards such as pollutants or xenobiotic compounds secreted by other organisms including antibiotics by microbes or natural pesticides by plants. Figure 2 illustrates some of these functions with the conversion of the hormone testosterone to 6 β -hydroxytestosterone by the human cytochrome CYP3A4 [32], the production of the antibiotic aurachin RE by the bacterial cytochrome CYP150A1 from *Rhodococcus erythropolis* [33], the breakdown of the carcinogen compound benzo[a]pyrene to either 3-OH-benzo[a]pyrene or benzo[a]pyrene-7,8-oxide [34, 35] by human cytochromes CYP1A1/CYP1B1 and the modification of a metabolite of the plant hormone gibberellin by CYP714A2 from *Arabidopsis thaliana* and CYP716D1 from *Stevia rebaudiana* to the natural sweetener steviol [36, 37], thought to act in plants in part as a feed deterrent towards insect [38].

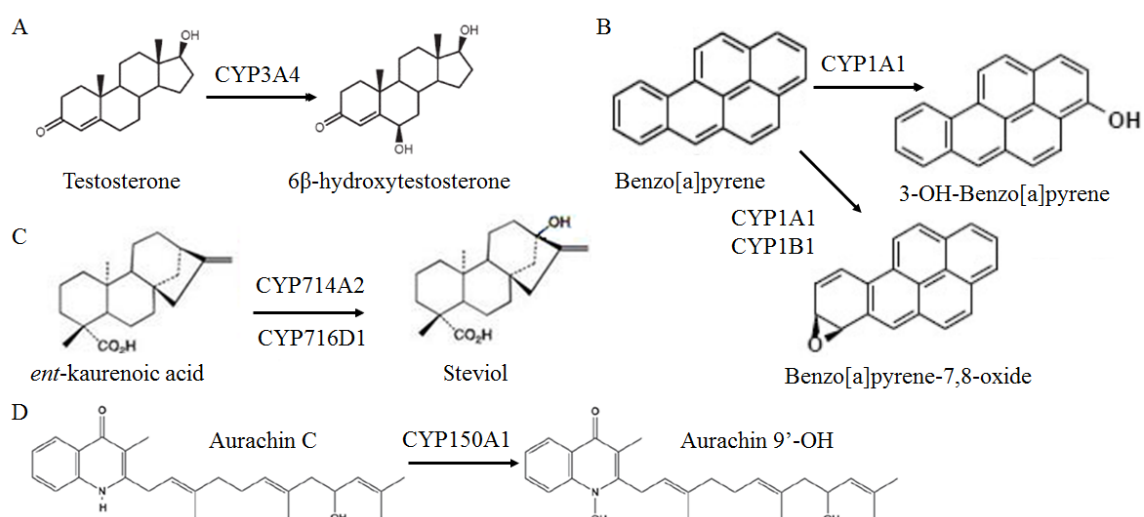


Figure 2: Key natural reactions of CYPs which highlight their function in nature. **A** Hormone metabolism in humans. **B** Xenobiotic compound breakdown in humans. **C** Insect repellent in plants. **D** Microbial defense in bacteria.

BM3 seems to have both functions. It is thought to protect *B. megaterium* from exogenous unsaturated fatty acids, which are toxic to that bacterium, by breaking them down. These fatty acids include oleic, linoleic and linolenic acid [39, 40]. Plants may use such fatty acids as a form of defense against *B. megaterium* which is found around the world typically living in the top soil just beside plant roots [41]. BM3 is also thought to be involved in the modification of branched fatty acids destined for the phospholipid cell membrane as well [42], possibly as a way to respond to variations in temperature [43]. What's more, these two last roles are not mutually exclusive since cell membrane fluidity is influenced by temperature

Cytochrome p450 BM3 oxidation

Catalytic cycle

CYPs are hemoproteins, implying that they possess a heme prosthetic group within their structure. A heme is a planar hydrophobic porphyrin ring consisting of four pyrrole subunits joined together by methine bridges where four nitrogen atoms protrudes inwards to coordinate a central reduced iron atom (Fe^{2+}) (Figure 3). In turn, the iron atom can coordinate its fifth bond with a cysteine residue thus forming an axial thiol ligand [16]. Unlike other CYPs however, other heme-containing proteins usually coordinate their fifth bond with a histidine residue [44]. The heme prosthetic group is central to the catalytic activity of CYPs as it allows them to coordinate atmospheric dioxygen which in turn allows them to catalyze the insertion of a single oxygen atom onto unactivated aliphatic or aromatic C-H bonds. What's more, CYPs do not exclusively have carbon as a target for oxygen insertion as they can also oxidize nitrogen and sulfur atoms [45–47]. The functional groups which decorate the porphyrin carbon backbone of the heme determine the class of heme. In the case of CYPs, a type b heme, also known as protoporphyrin IX, is found [9, 10]. Since BM3 is directly linked to its redox partner, that is the protein(s) whose role is to ferry the electrons provided by NADPH/NADH to CYPs, the protein is often described in two domains. The heme domain which contains the heme prosthetic group and the reductase domain charged with supplying electrons to the heme domain. As is the case for mammalian and plant reductase, which are not naturally fused to their respective CYPs, the BM3 reductase domain is sometimes referred to as CPR for cytochrome p450 reductase. The reductase domain itself contains two prosthetic groups, a flavin adenine dinucleotide (FAD) and a flavin mononucleotide (FMN). Thus, the CPR domain can be further subdivided into the FAD and the FMN domains. As outlined previously in Figure 1 however, the nature of these redox components is one of the main factors influencing the class in which a CYP belongs. These are often divided into two, sometimes even 3 components, compared to a CPR. Redox

components carrying a FAD prosthetic group include putidaredoxin reductase (Pdr), adrenodoxin reductase (AdR) and ferredoxin reductase (FdR) which are often paired with a corresponding redox component for instance an FMN prosthetic group such as flavodoxin (Fvx) and putidaredoxin (Pdx) or an iron-sulfur cluster such as adrenodoxin (Adx) and ferredoxin (Fdx). Prokaryotes, archaeoprokaryotes and fungus typically use such redox components rather than a CPR whereas the plant and animal kingdoms use both. Another noteworthy region of BM3, as for all CYPs naturally fused to a reductase, is the linker region that join the reductase to the oxidase domain. For BM3, it stretches roughly between the 450th and 476th amino acid of its sequence.

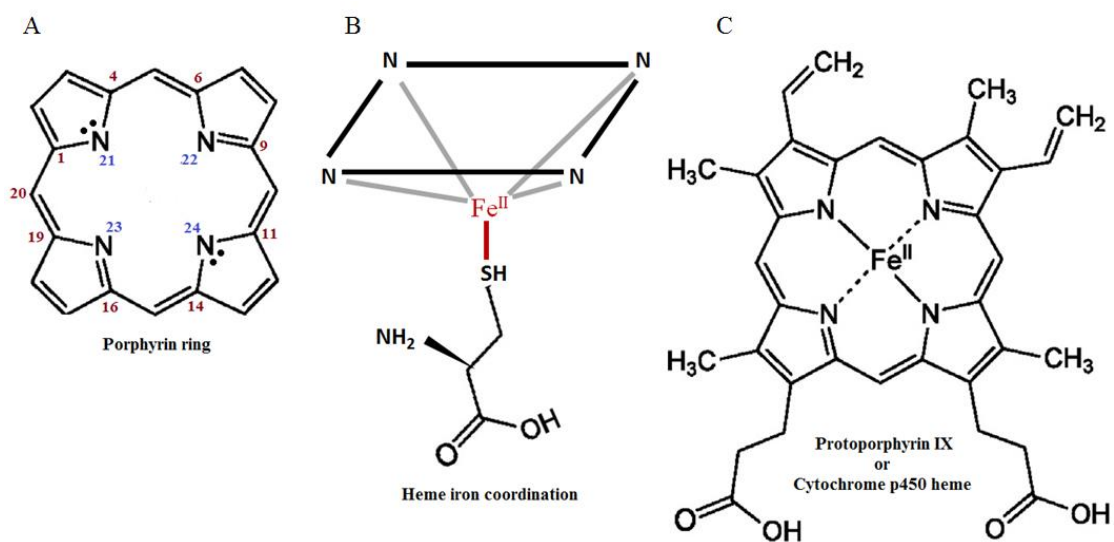


Figure 3: Illustrations of the heme prosthetic group. **A** Porphyrin ring with the four pyrrole subunits **B** whose nitrogen atoms directed inwards coordinates the central reduced iron atom with a cysteine residue. **C** Protoporphyrin IX which BM3 harbors at its heme domain.

Given the interest it garnered following its discovery, the catalytic cycle of BM3 has been extensively studied and is now well understood [48]. In addition, its crystal structure is the second ever resolved for CYPs [19] and, as of 2018, it now comprises close to 71 crystal structures in the RCSB protein data bank. The catalytic cycle of BM3 and the different states it can display is shown in Figure 4, edited from [23]. In the absence of substrate in the active site at the resting state (state 1), the iron of the heme coordinate a water molecule. Should a substrate enter the catalytic pocket of the heme domain (state 2) it displaces the water molecule and induce a conformational change in the shape of both the active site and the reductase domain bringing both FAD and FMN subdomains closer together facilitating the transport of the electrons from the cofactor NADPH to the heme [49, 50]. This conformational change also promotes the appropriation of an electron from NADPH which passes first through the FAD domain followed then by the FMN domain to finally reach the iron of

the heme domain. This electron reduces the iron from its ferric state (Fe^{3+}) to its ferrous state (Fe^{2+}) (State 3). At this point dioxygen can bind covalently to the heme iron reverting it to its ferric state (Fe^{3+}) and activating the oxygen (state 4) [50]. Following this, a second electron from NADPH is transferred thus forming the ferric peroxy complex (state 5). The protonation of the ferric peroxy complex ensues, yielding a hydroperoxy adduct (state 6). This hydroperoxy adduct then quickly protonates a second time resulting in the scission of the dioxygen which then leaves the active site with the protonating hydrogen thus triggering water loss. The electron pair remaining on the lone oxygen then pairs with the iron atom (now Fe^{4+}) and form a double bond with it [51] (state 7), thought to be the very last intermediate before hydroxylation of the product [52]. At this point, a hydrogen atom is abstracted from the substrate (state 8) leading to the generation of a radical rebound reaction where the radical substrate in turn combines with the oxygen and abstract the whole radical hydroxy adduct unto its radical carbon atom [53–59]. The substrate is then hydroxylated and water yet again coordinates itself with the iron of the heme. For reactions resulting in the epoxidation of an unsaturated bond the final hydrogen abstraction between state 7 and 8 does not occur, instead the state 7 intermediate reacts directly with the substrate's unsaturated bond to yield an epoxide [51].

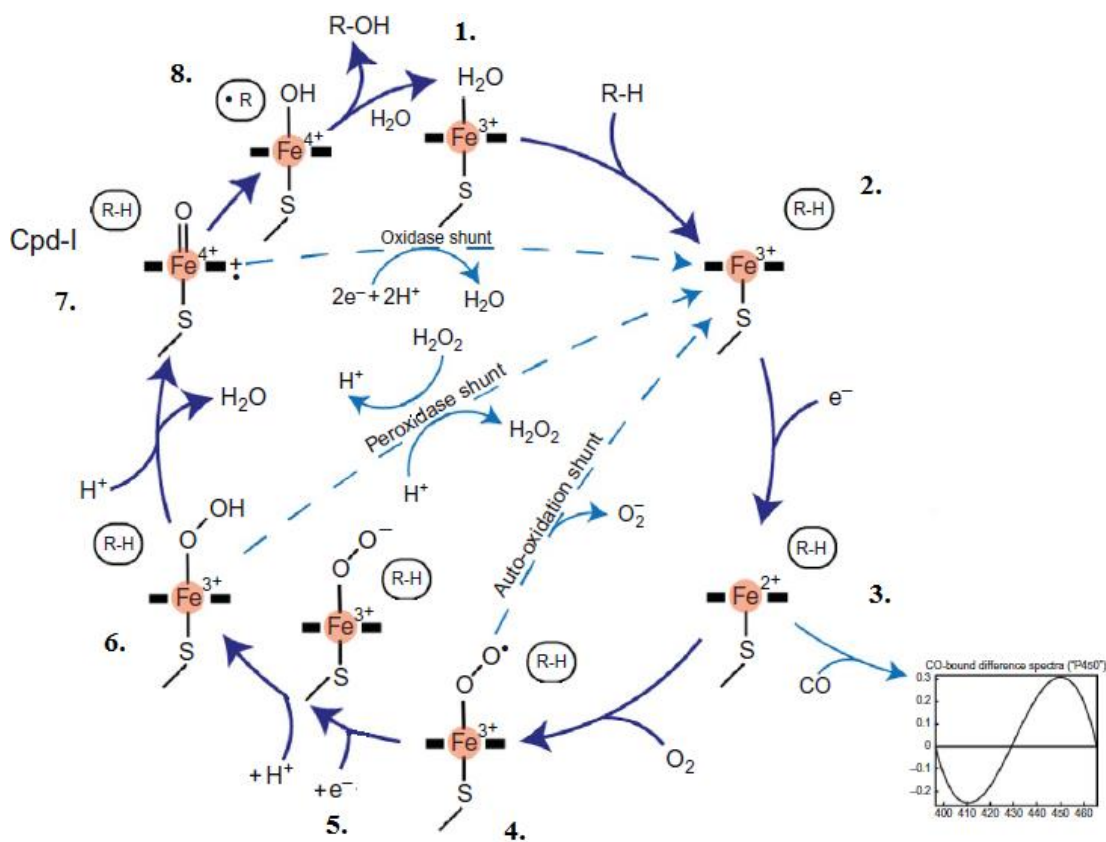


Figure 4: BM3 catalytic cycle. Each number around the figure denotes a state the catalytic pocket located within the heme domain goes through when BM3 inserts molecular dioxygen within a compound, edited from [23].

Uncoupling

The catalytic cycle of BM3, as that of all CYPs, can result in outcomes different than substrate hydroxylation. Indeed, states 4, 6 and 7 (figure 4) can all revert back to state 2 if they generate a superoxide anion, hydrogen peroxide or water, respectively. All of those outcomes ultimately prevent product formation in spite of the presence of all necessary reagents (NADPH, substrate, water and dioxygen). At state 4, should dioxygen binding be hindered, the following electron transfer may be too slow to prevent the loss of a superoxide anion. This phenomenon is called superoxide uncoupling. At state 6, if the substrate does not prevent the encroachment of a water molecule, the hydroperoxy adduct may collapse once protonated by water, to yield hydrogen peroxide. This in turn is called peroxide uncoupling. This particular event is interesting as it is reversible, such that hydrogen peroxide can also enter state 2 and then form the hydroperoxy adduct of state 6 where the catalytic cycle can continue its course and form product. This is commonly referred to in the literature as the peroxide shunt pathway. In nature, some CYPs preferentially use this pathway and are called peroxygenase. Finally, at state 7, if a substrate binds with no hydrogen atom positioned for abstraction, the oxygen atom can be reduced to water. This is called oxidase uncoupling. Hence, cofactor (NADPH) consumption is not necessarily coupled to product formation [60]. Any of these three pathways are termed uncoupling events. Should any of these events occur, it is relevant to notice that at least two of the accidental byproducts formed (hydrogen peroxide and superoxide anion/ O_2^-) are strong oxidants and may in fact damage the enzyme [61–63]. Furthermore, an uncoupling event result in NADPH waste. Conversely, the coupling efficiency is the molar ratio of hydroxylated substrate produced over cofactor oxidized. Ideally, this ratio would be equal to 1, but any cofactor oxidized through one of the uncoupling reactions described above would reduce the coupling ratio accordingly. The coupling efficiency of CYPs is usually higher for what is considered to be their natural substrates. For instance the coupling efficiency of BM3 towards myristic and palmitic acid can exceed 88 and 93 %, respectively [64]. Contrastingly, when using BM3 alongside non natural substrates, coupling usually decreases substantially as is the case with cyclooctane and cyclodecane where coupling efficiency only reaches 6 and 3 %, respectively. However, measures can be taken to raise coupling efficiency, with the use of decoy molecules for example whom tricks the catalytic site of the heme domain into hydroxylating non native substrates such as cyclooctane and cyclodecane up to a coupling efficiency of 81 and 44 %, respectively [65]. Similarly, when p450cam uses its natural substrate camphor or the non natural substrate norcamphor, hydroxylation reaches a coupling efficiency of 100 % with the former [66] and 12 % with the latter [67]. Point mutations to the active site can also increase coupling efficiency as was the case for p450cam T185F which raised

norcamphor coupling from 12 to 25 %. Thus, coupling ratios vary highly depending on the CYP and the substrate used but can be enhanced if necessary.

Kinetics of p450 BM3 oxidation

BM3 and other CYPs present some uncommon kinetic data derived from uncoupling events namely, coupling efficiency. A clear distinction must be made as well for another uncommon kinetic element present in CYPs and very similar to uncoupling that is, leakage. It is defined as the rate at which cofactors are used by the CYP in the absence of substrate (with units in mole of cofactor per mole of p450 per s or simply s^{-1}) [63]. Both coupling efficiency and leakage are highly important factors to assess as they are tied directly to the stability and the economical use of the enzyme should deleterious byproducts occur and cofactor be used wastefully. A more common kinetic element routinely used to assess the productivity of a CYP is that of maximum turnover number (TON) which is the maximum number of product mole that a mole of enzyme can form. There, TON units are of mole of product per mole of enzyme or dimensionless. Thus, TON provides a measure of specific yield the enzyme can achieve. The higher the TON value, the more product a given CYP quantity can generate, regardless of production rate. To a certain extent, TON data also gives indirectly information pertaining to the stability of the CYP in the reaction as an unstable enzyme allows a reduced yield. This unit of measurement is used mainly for free enzyme system, where a purified enzyme is used outside of a host cell. For whole-cell systems, where cells containing the biocatalytic enzyme are used to drive reactions forward, usually other units of measurement are used to characterize productivity, such as product mass per unit volume (g/L), product mass per unit volume and per unit time (g/L/s) and finally product mass per unit of dry cell weight (DCW) or wet cell weight (WCW), a dimensionless quantity, quite such as TON. Catalytic activity (k_{cat}) is often used to describe CYPs reaction rate and is defined as the molar quantity of product per unit mole of enzyme and time (s^{-1}). It describes the highest rate at which a given CYP can generate a given product or utilize a given reagent (a substrate or a cofactor). Both maximum turnover number and catalytic activity can be used interchangeably in the scientific literature about enzymatic systems, which is not be the case here, where a clear distinction is made between kinetics characteristics (k_{cat}) and productivity (TON). When comparing catalytic activities, the term relative activity is often used. This is a way to normalize data in relation to a reference value, when comparing the effect of reaction conditions for instance (organic solvent fraction, pH, temperature) or comparing different CYP mutants, usually against the wild type (WT) CYP. Finally, since BM3 has two active sites, the oxidase domain which bind substrates and generates products as well as the reductase domain which binds and consume cofactors, a k_{cat} can be observed for both domains.

CYP based assays

The unique feature of CYPs which first set them apart from other cytochromes was their unique absorption spectra, peaking at 450 nm when exposed to CO in the presence of a reducing agent. The nature of that peak would be explained in 1976 by Gunsalus et al. [11]. In what is oftentimes called the ferrous-CO assay, electrons are transferred to the iron atom of the heme by a reducing agent, most often sodium dithionate, thus reducing all the iron of the CYPs in solution into its ferrous form. In this state, due to the symmetry between the p orbital of the metal and the π orbital of the porphyrin, a metal to porphyrin charge-transfer can occur yielding a mercaptide complex between the now ferrous iron atom and the reduced thiol group of the cysteine ($\text{Fe}^{2+} - \text{S}^-$). This in turn generates the characteristic maximum absorption of CYPs at 450 nm (Figure 4, state 3). The technique by which the concentration of CYP in solution is assayed, the ferrous-CO assay, is largely performed as it was first described by Omura and Sato when they established that CYPs were in fact hemoproteins [9] and is still regularly cited for the purpose of describing the technique today. An advantageous feature of the assay is that it disregards the presence of any other protein in the sample thus the protein concentration assay for CYPs only detects CYPs.

In the same paper by Omura and Sato [9], the ferrous-CO assay highlights another feature intrinsic to CYPs that is characterised by a shift in the maximum absorption of the CO-CYP complex from 450 to 420 nm. It would later be determined by the same team that this shift in absorbance is associated with a loss in CYP activity or integrity [68]. Thus, a ferrous-CO assay can be used to verify CYP concentration and CYP integrity. It can also be used to assess CYP melting temperature or T_m which is the temperature at which 50 % of the initial absorption peak observed in CYPs at 450 nm is lost after a given incubation time. To evaluate this, CYP samples are incubated at several different temperatures for the same amount of time. From several points, a T_m can be established, which corresponds to the temperature at which the enzyme loses 50 % of its initial absorption at 450 nm. It is noteworthy to specify that T_m values are also used to describe the midpoint at which 50 % of the initial tertiary folding of a protein is lost at a given temperature for other techniques, namely for differential scanning calorimetry (DSC), circular dichroism or fluorimetry assays.

CYPs feature another key element which can be measured by spectrophotometry as well. The binding of substrates to the active site leads to the displacement of water as the sixth coordinating ligand to the heme iron (Figure 4 step 1). In turn, this change initiates a change from low spin to high

spin in the iron atom of the heme [69, 70]. High spin and low spin account for two possible classifications of spin states occurring in coordination atoms, in this case iron. The low spin state refers to the energy associated when the electrons pair up and fill all the lower energy orbitals of the iron, as is the case when water is present, whereas the high spin refers to the energy associated with electrons moving on to the outer orbitals of the iron when a substrate is present. In BM3, the change in spin state, in turn, increases the oxidation-reduction potential upsetting the thermodynamic balance within the enzyme towards reduction [71]. Binding of substrate compounds to the active site results in two types of characteristic spectral alterations in the UV-visible spectrum denoted as Type I and Type II [70, 72, 73]. Displacement of water as the sixth coordinating heme iron ligand results in an absorption peak at ~390 nm along with a dip at ~418 nm giving rise to the Type I shift in spectrum both are denoted in Figure 5A, edited from [74]. Type II spectral alterations are a result of direct coordination of a ligand to the heme iron which culminates in shift in the absorption spectrum from 430 to 455 nm, denoted in Figure 5B, however such complexes are usually inhibitory in nature and seldom lead to the generation of products. Thus, these spectral shifts can be used to evaluate the Michaelis constant K_m and the dissociation constant K_s for the substrate applied to the CYP in the samples investigated [75].

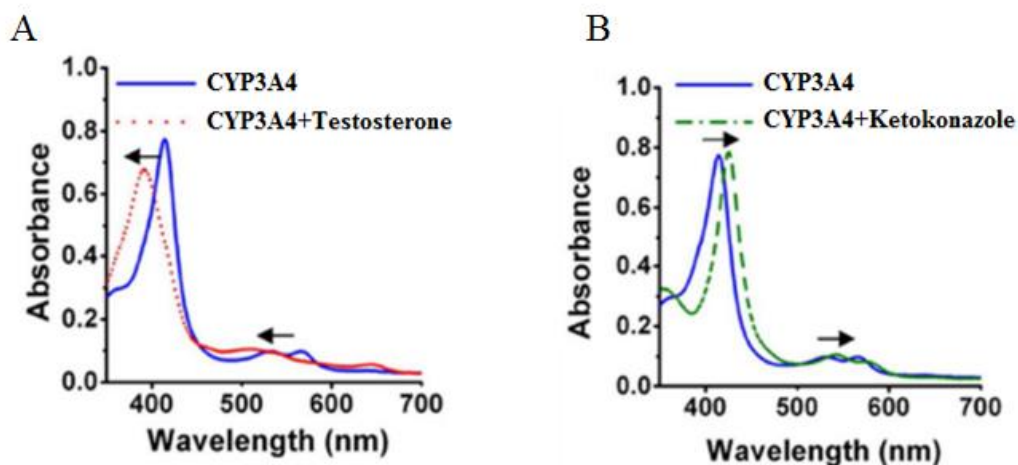


Figure 5: Examples with human CYP3A4 of the characteristic spectral alterations in the UV-visible spectrum seen in CYP's in the presence of a compound to the heme domain's active site. **A** Type I shift caused by the displacement of water at the heme domain by the natural substrate testosterone results in an absorption peak at ~390 nm along with a dip at ~418 nm. **B** Type II shift caused by the direct coordination of ketoconazole to the heme iron resulting in a shift in the absorption spectrum from 430 to 455 nm. Figure edited from [74].

Several assays have been developed over the years to allow a higher throughput of data than standard methods such as liquid or gas chromatography would allow, to monitor product formation and the parameters related to it (k_{cat} , K_m , TON, coupling efficiency). This typically translates in enzymatic reactions that can be monitored spectrophotometrically. A prominent assay in this regard is the *p*-nitrophenolate (pNP) assay where the hydroxylation of any variant of a *p*-nitrophenoxy fatty acid complex (pNCA) leads to the release of pNP which absorbs at 410 nm in deprotonated form in alkali conditions as well as the release of the corresponding fatty acid to which it was associated [76, 77]. For clarity pNCA is preceded by a number 6-, 8-, 10- or 12-pNCA to denote the length of the fatty acid present in the compound. Thus 12-pNCA is short for *p*-nitrophenoxy dodecanoic acid. Otherwise, the assay is typically referred to as the pNCA assay and its mechanism whereby CYPs releases pNP from pNCA can be seen in Figure 6. A number of other spectrophotometric assays exist as well including, but not limited to, 4-aminoantipyrine [78], *p*-nitrothiophenolate [79, 80], P450-Glo [81], benzyl-oxyresorufin O-dealkylation [82] and several coumarin based assays [83–87].

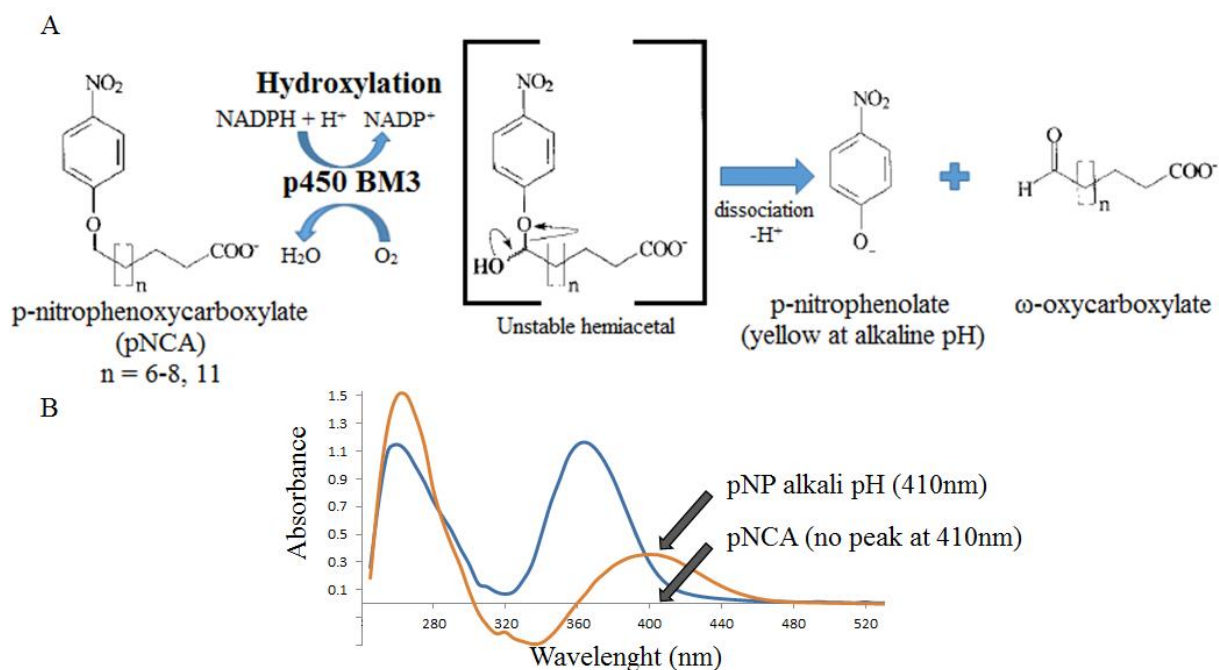


Figure 6: pNCA assay **A** mechanism and **B** comparison of the absorption spectra once pNP is released from pNCA at 410 nm. Figure 6A edited from [76].

For CYP fused to their redox partner, such as BM3, the use of nicotinamide-based compounds can easily be monitored by spectrophotometry as the absorption spectrum of the reduced form has a peak at 340 nm whereas the oxidised form does not (Figure 7) [88–90]. As such, assessing cofactor

consumption by the reductase domain is fairly straightforward and does not require more complex schemes as opposed to the substrates of the oxidase domain. Activity assays for the reductase thus implies measuring k_{cat} values using a nicotinamide-based compound or, a peroxide-based compound if the peroxide shunt pathway is to be used to supply electrons to the CYP. To evaluate CYP stability, both for the oxidase and reductase domains, activity assays using chromatography (LC/GC) or spectrophotometric techniques can be used to generate a T_{50} which represents the temperature at which 50% of the enzyme's activity is lost with respect to a reference state. This reference reaction can be used to test different parameters, such as buffer composition or enzyme mutation for instance, incubation time, pH, organic solvent content (v/v %), and cofactor or substrate concentration for instance.

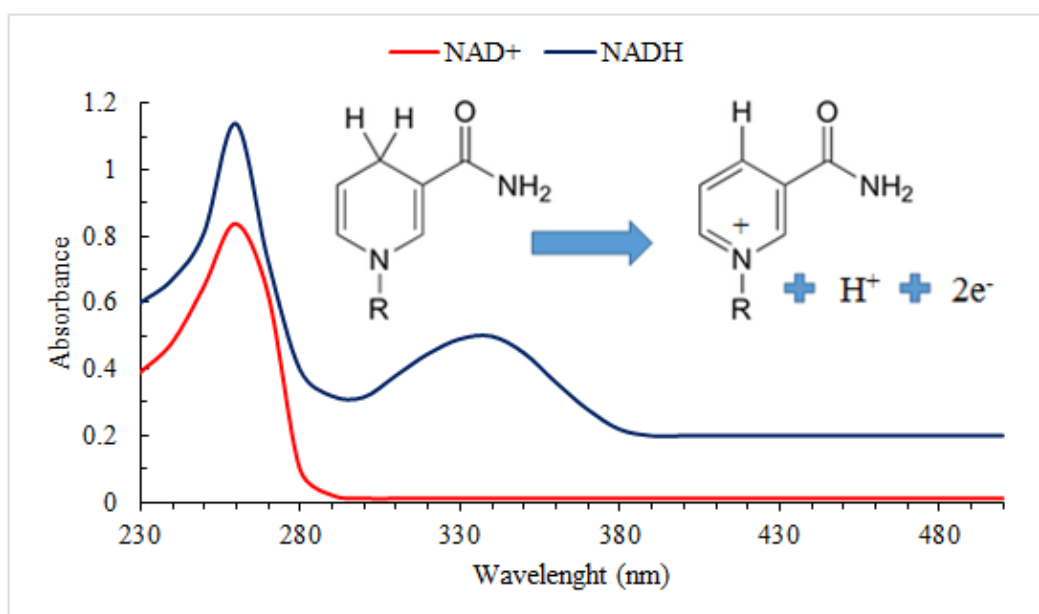


Figure 7: NADH absorption spectra for the reduced (blue line, top left) and the oxidized form NAD⁺ (red line, top right).

Functional groups added by oxidation

In terms of the net modification to the substrate, several outcomes can occur which depend on the particular CYP used and its own intrinsic regioselectivity. Once an oxygen atom is introduced the following rearrangements vary in the electronic environment around the modified C-H bond. This, in most cases, simply translates into the addition of a hydroxyl group to said C-H bond [61]. Including hydroxylation, Figure 8 lists the most common outcomes CYPs can convey. In addition, Figure 2 gives some more concrete examples, such as the hydroxylation of the hormone testosterone to 6 β -hydroxytestosterone [32] as well as the aromatic hydroxylation and epoxidation of the C=C alkene bonds of the carcinogen benzo[a]pyrene to either 3-OH-benzo[a]pyrene or benzo[a]pyrene-7,8-oxide

Industrial and commercial interest in p450 cytochromes

Medical

In regards to industrial and commercial interests, CYP based products offer a wide range of chemicals with an appeal for several different industries. For the medical industry, this interest manifests itself partly in the ability to produce eicosanoids and hormones, natural metabolites of human CYPs. In humans, fatty acid metabolism of arachidonic acid by CYPs leads to various eicosanoids such as prostaglandins, leukotrienes, lipoxins, resolvins and eoxins. These find many clinical uses in humans, fine tuning inflammation, anaphylaxis, leukocyte activation and vasoconstriction to name but a few [101–107]. In the case of hormones, gonadotropins, which regulates the secretion of sex hormones such as estrogen and progesterone, can be used to treat several diseases, including infertility and prostate disorders. In turn, estrogen and progesterone pills can be used as oral contraceptive or in hormone replacement therapy when hormonal disorders are observed. Steroids offer a wide range of applications as well as they are used to treat allergic, inflammatory, rhinitis, bronchial asthma and autoimmune conditions. In case of emergency, steroid injections may be given to treat acute asthma attack or shock. Furthermore, anabolic steroids can be used to increase muscle mass in patients suffering from muscular and other developmental disorders [108–110]. The catecholamines biosynthesis pathway also employs CYPs to generate other medically relevant molecules such as dopamine [111, 112], tryptophole [113], noradrenaline, adrenaline [111] and serotonin [114]. In the liver, CYPs are responsible for the breakdown of drugs, xenobiotics and antibiotics. Thus, the resulting metabolites can be used for the toxicity assessment of new drugs in preclinical assays and even in the improvement of already commercialized drugs, should their oxidized form prove more potent [115]. Furthermore, human CYP assay kits are now part of a key trial in which new drug compounds must pass in order to make sure they do not accumulate in the human body. It is therefore required to make sure that human CYPs are able to metabolize these new drug compounds [116]. Outside of humans CYPs, microbial CYPs offer the possibility to produce novel antibiotics such as griseofluvin by CYP GstF from *Penicillium aethiopicum* [117] or actinorhodin by CYP 107U1 from *Streptomyces coelicolor* [118].

It is estimated that plant species together can manufacture up to 200,000 compounds [119], among which 46,000 secondary metabolites are already identified [120]. Plants represent a veritable cornucopia of compounds for the markets. These include, to a large extent, various alkaloids, terpenoids, flavonoids, tannins and phenylpropanoids. In regards to medical applications, many compounds with a medicinal application have been identified in plants where their biosynthesis requires a CYP. For example vindoline, a synthetic intermediate to vinblastine used in chemotherapy

medication [121] in *Catharanthus roseus* formed by using both CYP71D12 & D351 [122, 123] or the depressant reticulín [124], which also serves as a precursor to several medicinal alkaloids including morphine [125] in *Papayer somniferum* formed using CYP80B3 [126], Table 1 further lists candidate molecules originating from CYP biosynthesis. The rationale for this potential is simple: whichever compound protects plants against pathogens, or even microbes against their peers, may well protect humans as well. [127–142]

Table 1. Commercially relevant biosynthesis products derived from various CYPs.

Application	Molecule	Use	CYP	Producing species	Reference
Medical	Griseofluvin	Antibiotic	GstF	Penicillium aethiopicum	[117]
	Actinorhodin	Antibiotic	107U1	Streptomyces coelicolor	[118]
	Artemisinin acid	Antimalarial agent	71AV1	Artemisia annua	[127]
	Berberamine	Cancer treatment	80A1	Berberis stolonifera	[128-131]
	Vindoline	Cancer treatment	71D12 & D351	Catharanthus roseus	[121-123]
	Oleanolic acid	Antiviral & cancer treatment	716A52	Panax ginseng	[132-133]
	Reticulin	Depressant	80B3	Papayer somniferum	[124, 126]
	Noscapine	Antitussive	82Y1 & 719A21	Papayer somniferum	[134-136]
Agriculture	Paclitaxel	Cancer treatment	725A1, 2 & 3	Taxus brevifolia	[137-139]
	Avenacins	Antimicrobial	51H10	Avena sativa	[140-142]
	Camalexin	Antifungal & antimicrobial	79B2 & 71B15	Arabidopsis thaliana	[148]
Fragrance	(+)-Nootkatone	Insect repellent	71AV8	Cichorium intybus	[161]
	(+)-Nootkatone	Perfume component	71AV8	Cichorium intybus	[161]
	Santalol	Perfume component	76F	Santalum album	[160]
	Glycyrrhizin	Flavoring agent	88D6 & 93E3	Glycyrrhiza uralensis	[165, 166]
Industry	6-iodo-4-hydroxytetralone				[173-174]
	3-hydroxyindanone				[174, 183]
	α -tocopherol	Intermediate chemical	102A1	Bacillus megaterium	[184]
	9-hydroxy-10-undecanoic acid				[185-191]

Agriculture

Both the agriculture and the horticulture industry have a stake in the many different products CYPs can generate. In regards to biosynthetic CYPs from plants the secondary metabolites they generate often lead to a compound whose role is that of a deterrent against insects and microbes. For instance, the cyanogenic glucosides linamarin and lotaustralin in either *Sorghum bicolor* [143] or *Manihot esculenta* [144], Table 1 lists further compounds in this regard. Plant hormones offer different applications on the other hand as they are of use in helping with stem elongation, seed germination, seed dormancy, stress resistance (to drought for example) and with ripening be it flower, fruit or vegetables [145–147]. It should be noted as well that plant hormones such as jasmonate and

salicylic acid are involved in the signalling pathways regulating camalexin production [148] in other words hormones can be used to indirectly promote plant defense against pathogens or insects. Insect hormones synthesized by CYPs can also offer some interesting products for the agriculture industry as juvenile (neotenin) [149] and moulting hormones (ecdysteroids) [150, 151] can be used as pest controls agents [152]. In addition, should the active site of the CYP be modified to induce a different template in oxidation localisation, structural analogs of these hormones could be used as pesticides as well [153]. In the raising of cattle for meat or dairy products, hormones can help with fertility [154, 155], growth [156] and lactation [157]. In fisheries growth hormones can be used to enhance yields, adjust the fertility and also switch the sex of the fish depending on the needs [158, 159].

Fragrance

The types of products which are of value to the food or perfume industry generated by CYPs find their origin exclusively in plant CYPs. The defensive compounds meant to deter pest often have for the human palate a pleasing aroma. Sandalwood oil whose main constituent is santalol is a staple in many perfumes and fragrances and is produced in *Santalum album* by CYP76F [160]. Besides its application as an insecticide, (+)-nootkatone produced by CYP71AV8 in *Cichorium intybus* [161] is largely used for the flavoring of foods and beverages as well as a fragrance. It is the main constituent of the aroma of grapefruit [162–164]. Yet another example would be that of glycyrrhizin the main compound contributing to the taste of licorice [165] in *Glycyrrhiza uralensis* by CYP88D6 & 93E3 [166].

Industry

Of the previous applications presented above, were CYP derived products present a commercial interest, all have in common that the metabolites are often directly related to the very function they present in nature. If we consider instead all the functional groups that can be added by the oxidation activity of CYPs we can begin to devise new synthetic routes to otherwise hard to synthesise existing or even non-existent chemicals. This is particularly true for the oxyfunctionalization of unactivated aliphatic or aromatic C-H bonds as this type of functionalization is difficult to achieve by traditional chemistry. Although oxidation processes of nonactivated C-H bonds by purely chemical means exist [167–169], it presents major disadvantages such as a lack in chemo-, site/regio-, and stereoselectivity [170, 171], which can outright prevent the synthesis of the desired product or lead to several undesired byproducts. Furthermore, even if the desired product is reached, chemical synthesis generates a large quantity of waste in terms of organic solvent [172] such

that the use of an enzymatically driven process can present itself not only as a greener more sustainable synthetic solution but also a more economical one. For example, 6-iodoindanone or 6-iodotetralone can be converted region- and stereo-selectively by p450 BM3 oxidative hydroxylation into, 6-iodo-4-hydroxytetralone. This compound is a precursor required for the synthesis of valuable intermediates which can themselves be further modified by chemical means into other valuable products [173, 174] (Figure 9).

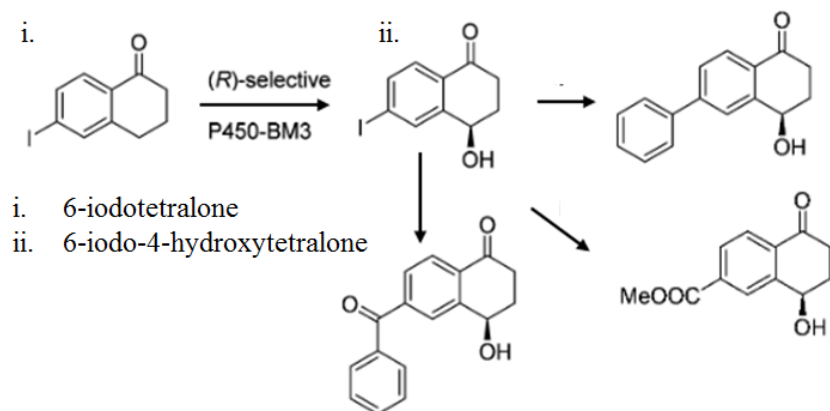


Figure 9: Example of the generation of valuable precursor chemicals by BM3 through the conversion of 6-iodotetralone (i) to 6-iodo-4-hydroxytetralone (ii). Subsequent products are produced through purely chemical means, figure edited from [173].

Glucoside incorporating 4-hydroxy-tetralones skeletons have been extensively used in Chinese folk medicine as antitumor as well as anti-inflammation drug [175–177]. The chemical compound 1-indanone, can yield many valuable intermediates required in the synthesis of other medicinal, agricultural and nutrition compounds [178–182]. For instance, following p450 BM3 hydroxylation of 1-indanone, the product 3-hydroxyindanone [174] can be obtained which finds large uses likewise as intermediates in the production of pharmaceuticals, namely tripartin, ligustrone C and tripartins [183]. Another example, again using p450 BM3 as a biocatalyst, is the production of α -tocopherol, a key precursor to both vitamin E and the antioxidant trolox, from pseudocumene and mesitylene [184]. To be clear, there again, the CYP reaction does not lead to the final compound but rather to an intermediate product in the synthesis steps which thereafter requires additional steps using standard chemical synthesis route. Finally, in a recent publication by the group of Dr Lionel Cheruzel from San José State University using a modified BM3 cytochrome, the synthon 9-hydroxy-10-undecanoic acid was produced [185] which is a precursor to malyngic, fulgidic and pinellic acids. These three oxidised lipids belong to a class of compounds known as oxylipins which are involved

in chemical defense against herbivores [186]. In this regard, malyngic acid already has shown promise as an insect repellent in agriculture [187, 188] or as a pharmaceutical agent [189–191]. The synthon 9-hydroxy-10-undecanoic acid can also serve as a precursor to generate (+)-mueggelone, phytoprostanes and 9,10-ketol octadecadineoic acid. The first, (+)-mueggelone, is a ten-membered lactone released by the marine cyanobacteria *Aphanizomenon flos-aquae* whose presence inhibits fish development [192]. Phytoprostanes encompass a large variety of compounds which act as botanical analogs to prostaglandins in the plant kingdom [193] and could be used to regulate both plant defense and plant growth in agriculture [194]. Finally, 9,10-ketol octadecadineoic acid can be used to induce flowering in horticulture [195, 196]. Figure 10 was taken from Dr Cheruzel’s publication [185] to illustrate this further.

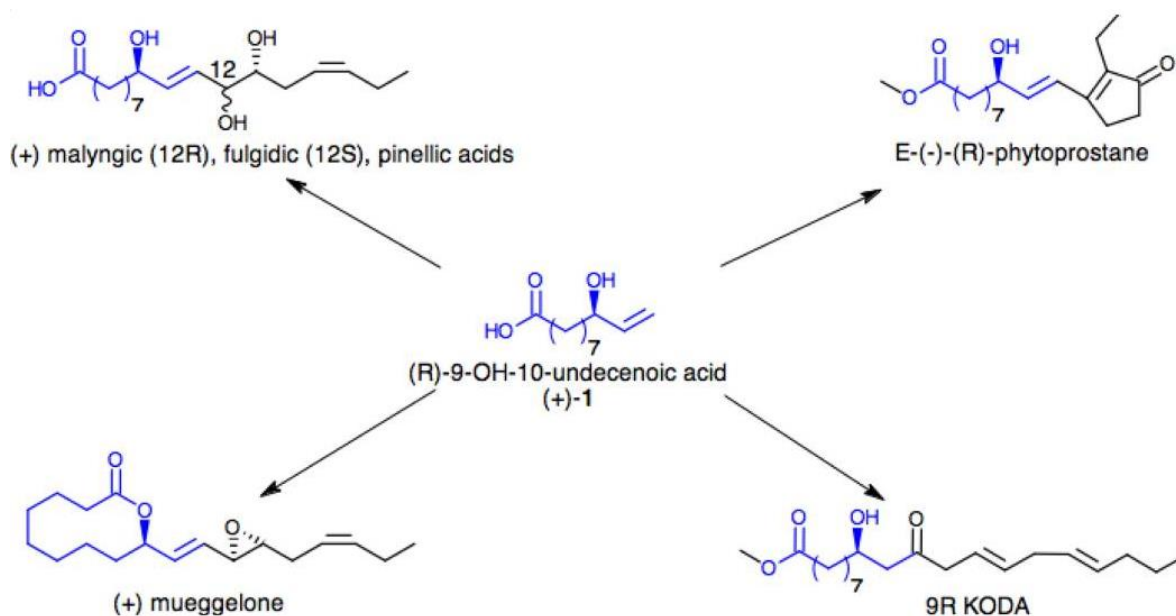


Figure 10: Example of the generation of valuable precursor chemicals by BM3 through the conversion of undecanoic acid to 9-hydroxy-10-undecanoic (center). Subsequent products are produced through purely chemical means.

1 Literature review - Cytochrome p450 BM3 biotechnology

1.1 Enzymatic process - Stability

In biotechnology, two strategies can be employed to produce valuable chemicals. One of these, is to produce these synthons through the use of growing or resting cell cultures. This particular strategy is often referred to in the literature as whole-cell bioconversion or simply as a fermentation where fermentation is defined as any microbial process by which a chemical modification to a substrate is made by an organism. The second strategy uses enzymes which are purified from cells and free from the cellular environment. The enzymes are directly exposed to the buffer solution in the reaction and the strategy is thus often referred to in the literature as free enzyme biocatalysis or, as is the case here in this work, as an enzymatic process or reaction. Table 2 offers a rough comparison of the generally accepted advantageous and disadvantageous features of each strategy. Enzymatic reactions using BM3 presents key advantageous features in that, unlike most other CYPs, BM3 is both soluble and naturally fused to its redox copartner. These two features stimulated the interest in using BM3 as a platform for the production of commercially relevant compounds. Furthermore, as pointed out by a 2012 review on BM3 by Wong et al. [48], the interest in BM3 began to widen in the nineties, whereas before, p450cam which is also soluble but not fused to its redox partners was arguably the most studied CYP. As a result, unlike most CYPs, BM3 has the distinction of having been extensively studied such that there is a considerable amount of literature on it. This translates for instance in having multiple crystals of its structure available, its catalytic cycle well understood, a large library of BM3 mutants tested as well as various approaches investigated to solve the other hurdles associated with the use of a CYP in a free enzyme system.

Table 2. Whole cell and free enzyme process factors to consider for each chemical production strategy.

Advantageous & disadvantageous features	Whole cell biotransformation	Free enzyme biocatalysis
Enzyme stability	+++ ^a	- ^a
Cofactor availability	++	-
Cascade reactions	++	+
Product formation rate	---	+++
Product recovery	---	+++
Secondary metabolites	- ^a	+ ^a
Overoxidation	--- ^b	- ^b
Substrate availability	--	--

^a Feature is negatively impacted furthermore by a process involving a CYP enzyme.

^b Disadvantageous feature unique to CYP enzymes.

One of these hurdles is that of stability: loss of the physical integrity of CYP enzymes and hence their activity, prevents a sizable quantity of products from being generated. Indeed, like most enzymes, CYPs, given enough time, eventually denature and hence lose their structure along with their activity, especially when exposed to harsher physical conditions such as extreme temperature, pH and organic solvent content. Thus, when using CYPs, the temperature range used as well as the buffer salt concentration must be restricted to preserve the integrity of the enzyme. Moreover, since substrates on which CYPs act are most often insoluble in water, they require an organic cosolvent to aid in their solubilisation in order to enable the CYP to gain access to these substrates. The problem with this, however, is that organic cosolvents are deleterious to the folding of most enzymes, including CYPs. Solubilisation can also be enhanced by increasing temperature but then again this would come at the cost of CYP stability. Issues of stability therefore also limit the amount of substrate which can be added to the reaction mixture. To remediate this impediment several strategies have been explored and reviewed in the following sub-sections. For several of these strategies values of TON are provided, all of whom are summarized into Table 3 at the end of section 1.5.3.

Table 3. TON data for various free enzyme strategies discussed in sections 1.5.1, 1.5.2 & 1.5.3.

CYP strategy	Immobilization	Electron source	Product	TON	Reference
CYP3A4	-	Cumene hydroperoxide	6 β -hydroxytestosterone	150	205
CYP102A1 4E10P	-	NADPH	Hydroxy methyl ibuprofen	330	215
	-		Hydroxy palmitic acid	838	
	-		Hydroxy myristic acid	774	
CYP102A1 PMO R2	-	NADPH	1-, 2-propanol	774	216-222
CYP119A1/Pdr/Pdx	-	NADH	Hydroxy lauric acid	9.2	261
CYP175A1-Fdr-Fdx	-	NADPH	Hydroxy β -carotene	0.238	264
CYP2C9/human CPR	+	NADPH	4-hydroxyflurbiprofen	363	290
	-	NADPH	4-hydroxyflurbiprofen	1600	
CYP101/Pdr/Pdx	+	NADH	5-exo hydroxycamphor	4500	293
CYP101/Pdr/Pdx	+	NADH	Hydroxy Camphor	48 316	294
CYP102A1		NADPH	Hydroxy lauric acid	548	
CYP102A1 ^{R966D/W1046S}	+	NADH	pNP	2983	295
		BNAH		2118	
CYP102A1 ^{R966D/W1046S}	+	NADH	pNP	1455	296
		BNAH		1025	
CYP102A1	+	NADPH	pNP	1800	297
heme domain CYP102A1 ^{F87A}	+	H ₂ O ₂	2-, 3-, 4-octanol/3-octanone	2.48	298
	-			1.2	
CYP102A1 variant 21B3	+	H ₂ O ₂	pNP	800	299
	-			470	
CYP102A1 variant M7/catalase	+	Zn dust/Co (III) sepiulchrate	hydroxy 3-phenoxytoluene	>2000	301
CYP102A1 variant m2-phasinPx2	+	NADPH	7-hydroxycoumarin	2218	304
CYP102A1	-	Light/EDTA/3,10-dimethyl-5-deazaflavin	Hydroxy lauric acid	698	360
heme domain CYP102A1	-	Light/SDC/Ru(LL)2PhenA	Hydroxy lauric acid	935	361-364
CYP102A1-PTDH	-	NADP ⁺ /phosphite	Hydroxy lauric acid	2250	309
CYP102A1 variant m2	+	Light/Triethanolamine/eosin Y	7-hydroxycoumarin	403	365
heme domain CYP102A1	-	Light/SDC/Ru(LL)2PhenA	pNP	230	366
heme domain CYP102A1 ^{Q403W}	-			430	
CYP152A2	-	indirectly H ₂ O ₂	Hydroxy myristic acid	200	369
CYP102A1 variant 21B3	-	H ₂ O ₂	pNP	430	200-202
	-		Hydroxy lauric acid	280	
	-		Hydroxy styrene	240	
CYP102A1 variant 9C1	-	H ₂ O ₂	desisopropyl, 5-, 4-hydroxy	180	371-372
CYP102A1	-	NADPH	propanolol	180	
CYP102A1	-	Zn dust/Co (III) sepiulchrate	Hydroxy Lauric acid	835	375
CYP102A1 variant M7/isocitrate dehydrogenase	-	NADPH	hydroxy 3-phenoxytoluene	2657	301
CYP2D6/CPR	-	NADPH	7-benzyloxy-4-N-ethylaminomethyl-coumarin	0.65	376
CYP101/Pdr/Pdx	-	NADH	hydroxycamphor & 2,5-diketocamphane	28 900	377
CYP102A1 ^{R47L/Y51F}	-	NADPH	Cyclohexanol	12 850	306
CYP102A1 ^{A74G/F87V/L188Q}	-	NADPH	2-, 3- 4-octanol & octanones	2200	
CYP102A1 ^{A74G/F87V/L188Q}	-	NADPH	Hydroxy myristic acid	3300	
CYP102A1 ^{A74G/F87V/L188Q/R966D/W1046S}	-	NADH	Hydroxy myristic acid	30 000	
154A8/FdR/FdX/GDH	-	NADPH	2-heptanol	2800	378
	-		2-octanol	3200	
	-		2-nonanol	4400	
	-		2-decanol	1700	

1.1.1 Point mutations

A classical strategy by which stability for industrially relevant enzyme can be enhanced is by adding stabilizing point mutations to the enzyme's sequence [197]. Where CYPs are concerned, there are few publications making use of this strategy and they mostly focus on one CYP, BM3. A common strategy to find such beneficial mutations is to conduct an error prone PCR experiment, where an error prone polymerase is used to create a large bank of enzyme variants, which are in turn tested and validated for enhanced stability or any other sought-after feature. Afterwards, the beneficial mutations can be pooled together in different combinations. One such experiment was conducted with BM3 where four stability enhancing mutations were discovered T235A, R471A, E494K and R1024E, yielding a new BM3 mutant named W5F5 harboring all four mutations [198]. This mutant showed increased resistance towards organic solvents while retaining its relative activity much better than the WT BM3. For instance, in comparison to activity without organic cosolvent, W5F5 could retain close to 100% of its initial activity in 12.5 % (v/v) ethanol whereas WT activity was entirely lost. Of these four mutations only T235A is on the oxidase domain whereas R471A and E494K are located on or in the vicinity of the linker region and R1024E is almost at the end of the reductase domain. It is noteworthy to add that the localization of these last three mutations being on or near the reductase domain in the W5F5 BM3 mutant is logical as it was demonstrated that for BM3 the reductase is the less stable of the two domains [199]. In a later paper, T235A, R471A, E494K and R1024E were added to four drug metabolising BM3 variants for whom original mutations were wholly localised to the oxidase domain's active site. The authors noted that at least in two of these new variants, removing T235A lead to a roughly 3-fold increase in activity whereas in the other two variants it did not lead to any alteration in activity. If anything, this highlights the importance of investigating combinatorial library carefully especially for mutations added close by other pre-existing mutations. In similar work the mutant 21B3 was further evolved through many rounds of error prone PCR towards a more stable variant dubbed 5H6 [200]. The mutant 21B3 was itself evolved from the BM3 F87A mutant created to better utilize hydrogen peroxide as an electron source [201, 202]. The melting temperature was assessed by a ferrous-CO assay and it was demonstrated that after 10 min incubation at different temperatures the T_m reached 43 °C for WT BM3, 46 °C for 21B3 and 61 °C for 5H6.

In a different work, P450sca-2 from *Streptomyces carbophilus* was utilized alongside the redox partners PdR and Pdx from *P. putida* to convert mevastatin to pravastatin using a mixture of error-prone PCR and iterative site saturation mutagenesis informed by a rational approach to the saturation sites selected. This lead to the creation of the P450sca-2 variant, R8-5C [203], which was

then further improved into the variant R8-5C III [204]. These variants were improved not on the basis of their stability but rather on their activity towards the conversion of mevastatin to pravastatin. In doing so, activity of WT P450sca-2, R8-5C and R8-5C variant III reached respectively 12.9, 53.0 and 377.5 mg/L after a 21-hour incubation period, a 29-fold improvement from WT to variant III. What's more, the coupling efficiency for R8-5C (36 %) and variant III (38 %) remains largely unaltered suggesting that these alterations neither hindered nor interfered with stability where coupling is concerned all the while providing enhanced productivity to the system. This is significant to stability in that mutations to the active site or more broadly to the oxidase domain can often have a deleterious effect on stability. In a different publication, using error prone PCR as well as site directed mutagenesis, human CYP3A4 was enhanced in its ability to use peroxides as an alternative cofactor source specifically hydrogen peroxide and cumene hydroxyperoxide [205]. In this work several variants with increased efficiency towards peroxide driven reactions were created including the T309V variant for whom hydroxylation of 7-benzyloxy-4-(trifluoromethyl) coumarin was enhanced 3-fold with cumene hydroxyperoxide as a cofactor. Another variant created in this works was that of T433S, which increased TON of testosterone to 6 β -hydroxytestosterone using cumene hydroxyperoxide roughly to 150 a 1.7-fold increase compared to WT CYP3A4. While stability increase is not explicitly demonstrated in this work, using a source of electrons such as hydrogen peroxide or cumene hydroxyperoxide necessitates increased stability towards such highly oxidative compounds.

Besides error prone PCR, another common strategy by which beneficial mutations are found is by rational design. Rather than using a randomized approach, rational design uses a knowledge-based scheme whereby beneficial mutations can be discovered and added to the enzyme's sequence. This strategy is easier to exploit when the target enzyme is well understood. A simple example of this, both the 21B3 and the 5H6 mutants were evolved from the BM3 mutant F87A, a mutation which serves to expand the substrate range of the enzyme and to better utilize hydrogen peroxide but, at the cost of impaired stability [198, 206]. Thus, armed with this information, a rational design approach would be to revert back this mutation to its original amino acid if one's goal is to stabilize the enzyme further. The work on the mutant 21B3 was further expanded in another paper reporting enzyme improvement by rational design with the aim to stabilize this particular BM3 variant [207]. In short, a computer simulation strategy named hybrid quantum mechanics/molecular mechanics calculation, which had seen success in describing intra- and inter- molecular electron transfer pathways in oxidoreductases in the past [208–211], was used to identify key residues around the coordination center of the heme iron of the BM3 variant 21B3. These residues would then be mutated to reduce

electron delocalization from oxidizable residues and possibly create in the process more stable mutants. Indeed, despite the fact that 21B3 had been evolved to efficiently catalyze reactions with hydrogen peroxide as a cofactor, it is still susceptible to hydrogen peroxide inactivation. Once several residues identified were screened for, the mutations W96A and F405L were shown to significantly enhance the stability of 21B3. In the presence of 3 mM hydrogen peroxide, the catalytic activity and the heme half-life for 21B3 lasted 0.38 min and 9.6 min respectively whereas it lasted 99 min and over 120 min for 21B3 W96A/F405L. This data also points out that oxidative activity is lost before heme destruction. In relative activity assays all 21B3 mutants lost over 50% of their activity in the presence of 3mM peroxide after 5-minute incubations unlike the 21B3 W96AA/F405L variant which kept almost 80% of its activity after 20 min incubation. In addition, both these mutations slightly enhanced activity towards 2,6-dimethoxyphenol from 96 min⁻¹ for 21B6 up to 116 min⁻¹ for the variant 21B3 W96AA/F405L. In another paper, using a different approach to rational design the authors compared the amino acid sequence of BM3 in *B. megaterium* ecotypes [212]. The paper identified that within the ecotypes of the BM3 sequences, most retained their activity towards their natural substrates but certain ecotypes showed enhanced stability of their oxidase domain (CO ferrous assay) or their reductase domain (reductase activity assay). Their result gives the oxidase domain of CYP102A1.1 (standard BM3) a T_m of 51 °C and a T_m of 55 °C for 4 other CYP102A1 ecotypes. On the other hand, the reductase domain of CYP102A1.1 was shown to have a T₅₀ of 45 °C whereas that of CYP102A1.5 a T₅₀ of 49 °C. The T₅₀ here is calculated from the reduction of ferricyanide catalyzed by reductase activity. None of the mutation are in critical or highly conserved regions in the BM3 sequence and are instead located towards the exterior of the enzyme. The papers thus identify some naturally occurring mutations amongst the BM3 ecotypes as stability enhancing mutations.

Again, in regards to a rational design strategy for CYPs, in a recent paper the electron transfer pathways and the effects of leakage in the reaction cycle of BM3 were investigated [63]. The authors generated BM3 mutants known to cause even more leakage and combined these deleterious mutations together. The results obtained highlighted the fact that there is indeed a strong relationship between leakage and stability. For example, every mutant created where leakage was enhanced also showed T_m values below that of wild type BM3. For instance, when mutations A82W/T268N/F393H were added to BM3, leakage was enhanced 50-fold and the T_m value of BM3 by ferrous-CO assay dropped from 55 °C to 40 °C. Using these same leakage prone mutants, the respective percentage of leakage event leading to the formation of hydrogen peroxide was assessed to be between 24 and 89 % compared to undetectable amounts for WT BM3. In these instances, the leakage assays were conducted in the absence of substrates for the oxidase domain but in the presence of NADPH. While

this paper produces the opposite of stability enhanced variants of BM3 it does leave a blueprint to follow to enhance the stability of CYPs which is to screen against leakage prone variants which could be done by identifying and modifying new amino acids sensitive to this phenomenon including those used by this research group in their papers on the subject [63, 213].

Using a different rational design strategy, in a different paper, the stability of wild type human CYP2B6 and dog CYP2B11 was enhanced by substituting a conserved amino acid residue differing in identity compared to the more stable and closely related rat CYP2B1 and rabbit 2B4, P334S [214]. This strategy would be applied in a similar fashion to the CYP102A subfamily from which BM3, also known as CYP102A1, comes from. Indeed, using rational design an interesting variant of BM3 named 4E10P was reported recently by the group of Dr Rudi Fasan [215]. By aligning the sequence of BM3's reductase with that of 15 other reductase domains sharing at least 38 % sequence identity, with 8 from the genus *Bacillus*, 14 strongly conserved residues conserved amongst most of these reductases but differing in BM3's sequence were identified and selected to test and generate stability enhanced BM3 mutants. This particular technique can also be described as consensus mutagenesis. From those 14 conserved, 12 BM3 reductase variants were constructed and fused to the BM3 oxidase variant named 4E10 (A82L/A328V) [216]. This particular variant was chosen because the two active site mutations it carries enables the enzyme to oxidize a wider range of non-native substrates such as the chromogenic substrate dimethyl ether [217]. What's more, by ferrous-CO assay it was demonstrated that these two active site mutations have little deleterious effects on the stability of the variant (T_m 54 °C) compared to wild type BM3 (T_m 55 °C). From the resulting 12 constructs generated the A82L/A328V/A584R/L685I/V760A/E853P BM3 variant, or 4E10P, displayed the greatest improvement stability. When it's T_{50} was assessed in dimethyl ether assays where the CYPs were incubated beforehand at 50 °C at increasing durations, a 50 % loss in activity for 4E10P required a 278 minutes preincubation whereas mutant 4E10 only required a 20 minutes period. The TON for the hydroxylation of methyl ibuprofen at 20 to 30 °C remained the same for most mutants presented in the study hovering at around 320-330 but a marked difference in TON was observed with reactions driven at 40 °C with 4E10 TON dropping to 58 while 4E10P TON reached roughly 290. For the hydroxylation of both palmitic and myristic acid 4E10 reached a TON of 462 and 645 respectively at 40 °C. However, for 4E10P, at the same temperature, TON for the hydroxylation of both palmitic and myristic acid reached roughly 838 and 774 respectively demonstrating that the new variant is indeed sturdier than the initial construct. In a series of publications [218, 217, 219–222], using a domain-based approach, the BM3 mutant PMO R2 was developed by optimizing separately the heme domain, the FMN domain and the FAD domain and then reunited afterwards. Optimization of each domain

involved a combination of random mutagenesis, site saturation mutagenesis identified rationally or through random mutagenesis and of sequence shuffling between variants, a strategy which is further discussed in section 1.5.1.3. This work led to bringing about a variant, PMO R2, which could achieve a TON of over 45 000 for propane hydroxylation to 2- and 1- propanol in a 9:1 ratio from the wild type BM3 enzyme which had no detectable activity towards propane. In regards to stability, there is much room for improvement over the amino acid sequence engineering of BM3 which has so far only been lightly explored.

1.1.2 Decoy molecules

A common strategy to widen the substrate range of an enzyme is to mutate key amino acids of the active site. Towards that end, several variants of BM3 have been generated over the years and have been extensively catalogued elsewhere [48]. Widening the substrate range usually implies augmenting the conformational stability of the active site through the mutation of amino acids. However, such mutations most often lead to enzyme variants which are more unstable [223–225]. For example, BM3 F87A mutation allows a much wider substrate range [76, 226–230] but at the cost of a lower overall stability [198, 206]. In this regard, the strategy of using decoy molecules to adapt the active site of the oxidase domain to a new substrate allows to circumvent this problem. The strategy goes as follows, a chemical compound possessing a carboxy group small enough to fit inside the catalytic pocket of the cytochrome and short enough not to be the target of hydroxylation by the CYP is added to the reaction mixture. The carboxy group, in turn, induce the CYP into starting its oxidative catalytic cycle. To the reaction is added a non-natural substrate which is then hydroxylated in the presence of the decoy molecule in the active site. As of yet, this strategy has been tested on CYP101A1 (p450_{cam}) from *P. putida* [231], CYP102A1 (BM3) from *B. megaterium* [204–213] as well as CYP152A1 (p450_{SP α}) and CYP152A2 (p450_{SP β}) from *Bacillus subtilis* [214–219]. The decoy molecules interact within a CYP with the amino acid(s) responsible for docking natural substrates through their carboxy group, thus in a way imitating the carboxy group of a fatty acid. For BM3 this tethering is believed to be facilitated by the amino acids Arg47 and Tyr51 [20]. The first test this of decoy molecule approach was conducted on p450_{SP α} and p450_{SP β} with the short fatty acids buta-, penta-, hexa-, hepta- and octanoic acid used as decoys [240]. A second decoy molecule tested for those same two CYPs were acetate anions which unlike the previous decoys are highly soluble, cheap and hardly usable as substrates for CYPs themselves [245]. To prevent possible hydroxylation of the aforementioned fatty acid decoys and to allow gas compound hydroxylation, perfluorocarboxylic acids (PFCs) instead of fatty acids were tested with BM3 with success [232]. The rationale for this

strategy being that the stable C-F chemical bonds could not be oxidized and thus the decoy molecule is not used as a substrate in the reaction [204–210]. In order to further mimic BM3 natural substrates and create hydrogen bridges observed from the crystal of BM3 complexed with N-palmitoyl glycine [246], later work on PFCs in the Watanabe lab would append amino acids to the new PFCs generations to that end [65, 236, 238, 239]. The breakthroughs of the Watanabe lab have important implications for the overall stability of CYPs as much of the past research on BM3 has focused on producing variants capable of acting on various substrates at the cost of stability since this almost always involved the generation of variants mutated in their active site. But decoy molecules dispense with this stability trade-off imposed to access to a wider substrate range. For substrate where the wild type BM3 enzyme shows no activity or very little activity the coupling efficiency in the presence of a decoy molecule is naturally higher. Of interest as well are the effects decoys have on BM3 variants mutated to accept new substrates. For example, with the BM3 KT2 variant (A191T/N239H/I259V/A276T/L353I) adding a PFC decoy to the reaction raised coupling efficiency on benzene substrates from 3 % to 10 %. On cyclohexane, coupling efficiency was raised from 19 % without decoy to 36 % with the use of a PFC decoy [237]. Finally on isophorone, coupling efficiency was raised from 4.4 % to 12 % [231]. Thus, the combination of an active site variant with that of a decoy can also be seen as a tool to augment coupling and thus indirectly, stability. The 10% coupling efficiency maximum reached with benzene would later be breached not by adding other mutations to the active sites but rather by fine tuning the PFC's length, C-F bond content and by adding an amino acid head to the compound to better mimic a substrate. Using benzene on wild type BM3 in the presence of an undecylic acid-L-phenylalanine or a Z-glycine-L-phenylalanine decoy enabled the reactions to reach a coupling efficiency of 45 % and 47 % respectively [238]. The 36 % coupling benchmark reached for cyclopropane would in turn be surpassed as well by screening for the best decoy molecule and by modifying the key amino acids involved in docking substrates in the oxidase domain of BM3. In this regard, the BM3 mutant R47L/Y51F was the best candidate to tether cyclohexane to the active site in effect raising coupling to 58 % [65]. In the case of propane, augmenting the pressure of propane gas from 8 kPa to 0.5 Mpa raised propane hydroxylation from 17 % [232] up to 48 % [233]. Thus, another feature to be fine-tuned rather than active sites modification are the physical conditions in which the reactions are run. Decoy molecules not only serve as a tool to bypass the use of unstable active site variants they can also be used to augment CYP coupling and, indirectly CYP stability.

1.1.3 Shuffle & fusion chimeras

A common strategy to enhance CYP stability is the generation of chimeras, a combination of sequences between various CYPs and their reductase components to generate a new CYP. There are two main avenues for this strategy, the first being the shuffling of sequences of CYPs whom are closely related to each another in order to produce more stable variants, shuffled chimeras (Figure 11A). For example, by DSC it was shown that the oxidase domain of CYP102A1, or BM3, has a T_m of 63 °C whereas the reductase had one of 48 °C [199]. One should thus expect the reductase domain of BM3 to be inactivated first. It would therefore follow that by changing the reductase to a more stable one there could be an overall enhancement in stability for the whole CYP. By monitoring fluorescence associated with flavin release when reductase denatures, it was demonstrated that the reductase of CYP102A1 (BM3) from *B. megaterium* ($T_m=49$ °C) is less stable than that of CYP102A3 from *B. subtilis* (T_m 59 °C). The fusion of the latter reductase to that the oxidase domain of BM3 yielded a chimera named A1MA3R which displayed higher thermal stability (T_{50} 56 °C) than either CYP102A1 (T_{50} 49 °C) or CYP102A3 (T_{50} 46 °C) in a 12-pNCA activity assay following incubations at elevated temperatures (23-60 °C) [247]. This last example is simple in that CYPs belonging to the same family were cut a single time and pasted together. More extensive cutting and pasting, or shuffling of sequences, can be applied when this approach is pushed further. The research group of Dr Frances Arnold from the Caltech institute attempted this very exercise creating somewhere around 3000 iterations combining the sequences of CYP102A1, A2 & A3 [248, 249]. In their first attempt, they were able to raise the enzyme stability, assessed by ferrous-CO assay, of CYP102A1 from $T_m=55$ °C to $T_m=62$ °C, for a properly folded variant named 22312333 which however lost its activity towards 12-pNCA. The second best properly folded variant, 32312333, which was active towards 12-pNCA reached a T_m of 56 °C. All variants in this work possessed either the F87A substitution in CYP102A1 or the corresponding substitution in CYP102A2 & 3, F88A [248]. In the following paper, sequence shuffling was investigated further and yielded even more interesting constructs. This time they were able to raise the stability, assessed by ferrous-CO assay, of CYP102A1 from $T_m=55$ °C to $T_m=63$ °C for a variant named 22313333 which showed a 9-fold improvement in relative activity towards 12-pNCA compared to BM3 using hydrogen peroxide as an electron source. Interestingly, several of the new chimeras created, including 22313333, showed activity towards verapamil and astemizole whereas all three CYP102A1-3 parents showed none [249]. These results highlight the finding that steric stability can affect activity both positively and negatively, a notion Arnold's group further reviews and discusses [250, 251]. The same strategy was explored solely in silico from a different lab with the same CYPs [252]. In work where the Urlacher lab characterised CYP102A7

from *Bacillus licheniformis* it was shown that this CYP retained 50 % of its activity after incubation in 26 % DMSO whereas CYP102A1 lost all of its activity in 15 % DMSO [253]. While not creating any chimera per se, it does highlight CYP102A7 as another interesting candidate for sequence shuffling within the CYP102A subfamily.

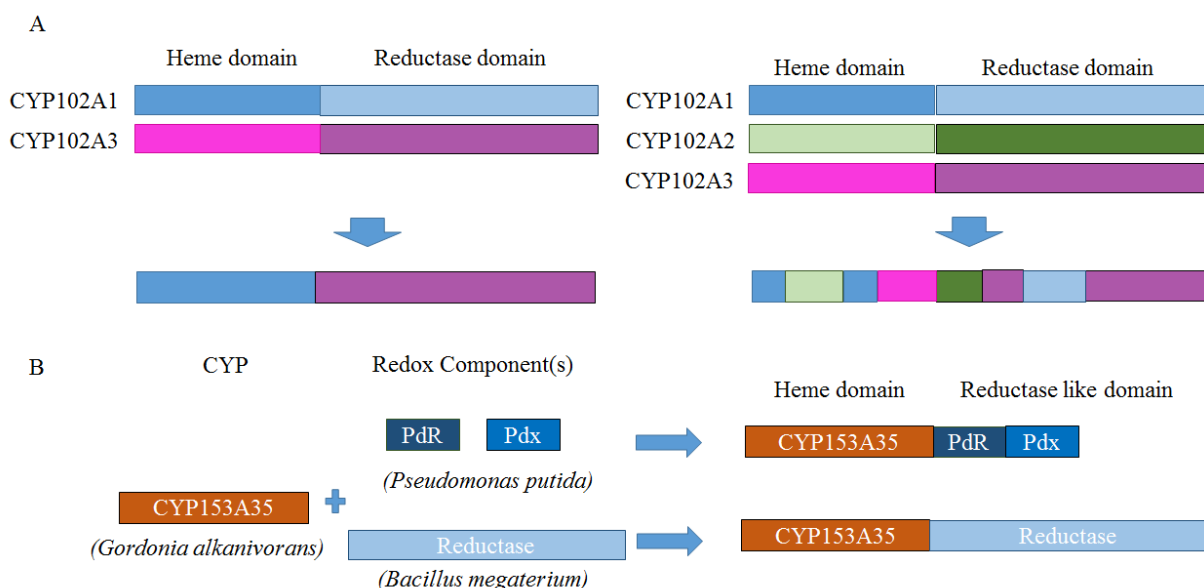


Figure 11: Examples of shuffled chimeras (A) with only the domains rearranged (left) or with fractions of homologous domains highly shuffled together into one complete CYP sequence (right). Examples of fusion chimeras with a CYP lacking a reductase partner fused with putidaredoxin components (right top) or a reductase (right bottom).

The second avenue to this strategy, fusion chimeras, is to express both an oxidase domain and reductase component(s) on the same strand, using either the CYPs natural redox partner(s) or some wholly foreign redox component (Figure 11B). This strategy is best suited for CYPs whom have not been well characterised to date, which implies that neither are their natural redox partners if they are even identified at all. In any case, many CYPs aren't well characterised and therefore their redox partners are still unknown. Hence, adding foreign redox partner is often the only choice available, whether fused or unfused, to be able to use the enzyme in a practical process. Again, most CYPs, unlike BM3, are not fused to their redox partners. This strategy can also double in making membrane bound CYPs soluble by replacing their anchoring domain with redox components. Alternatively, these less known CYPs can be of interest due to their activity profiles or, with extremophiles, due to their enhanced stability. In the former case for instance, attempts were made to combine BM3's oxidase with the reductase component of the rat nitric oxide synthase (nNOS) and reversibly, BM3's reductase with the oxidase of the rat nNOS. However, in both cases, this resulted

in lower stability and catalytic activity [254]. In another example of a fusion construct, the reductase of BM3 was fused to CYP153A35 from *Gordonia alkanivorans* and was compared to a mixture of CYP153A35, alongside Pdx and PdR from *P. putida* [255]. The CYP153A35-BM3 reductase fusion construct showed a coupling efficiency of 27.1% towards myristic acid and 23.7% towards palmitic acid whereas the CYP153A35/Pdx/PdR unfused mixture provided coupling efficiencies of 5% and 6%. These results are echoed in similar work [256] where CYP153A33 from *Marinobacter aquaeolei* was fused either to the BM3 reductase, to the Pfor reductase from *Rhodococcus ruber* or used unfused with Pdx and Pdr from *P. putida*. Coupling efficiencies reached their highest with a CYP153A33-BM3 reductase with a Gly-Gly-Ser spacer added to the linker region reaching 56 % for n-octane, 22 % for octanoic acid and 73% for dodecanoic acid. On the other hand, the CYP153A33, Pdx and Pdr reactions mixture generated couplings of only 16% for n-octane and 18% for dodecanoic acid.

There are a number of cases of fusion chimeras with CYP extracted from extremophiles. These are an interesting target as they are naturally more resilient to extreme pH, salinity, solvents or heat. The heat resistance feature of these CYP could be exploited to simplify the downstream processing of enzyme purification processes simply by heating at elevated temperatures the lysate of cells used for recombinant CYP production, since every other enzymes would precipitate with the exception of the extremophile CYP [257]. However, these kinds of CYPs have their own drawbacks. For one, their activity is usually quite low, for instance CYP119A1 from the extremophile *Sulfolobus acidocaldarius* [258] has a slow catalytic rate of 10.8 min⁻¹ with lauric acid [259] and of 0.59 min⁻¹ with styrene [260]. The stability of CYP119A1 is on the other hand substantial with the CYP retaining close to 80% of its original activity towards styrene epoxidation after a 90 minutes incubation period at 80 °C in comparison to a 25 °C incubation. Likewise, roughly 85 % of the original ferrous-CO spectra was retained in the same conditions. In fact, only at 90 °C did both stability metrics substantially dropped, both going under 25 % [260]. Concerning CYPs derived from extremophiles, a second drawback is that they are usually not well characterized such that both their natural redox partners and their natural substrates are often unidentified. This makes the generation of a functional fusion chimera between a CYP and redox partners more difficult to achieve. As an example, when CYP119A1 was used in conjunction with the redox partners Pdx and PdR of *Sulfolobus solfataricus* in the presence of NADH only about 0.5 % of the lauric acid substrate could be converted into products for a TON of 9.2 [261]. A similar problem could be observed when a sulfite reductase sharing 50% homology with BM3 was identified in *Geobacillus stearothermophilus* [262]. As when it was fused with the oxidase of BM3 the fusion construct retained all of its activity towards the hydroxylation of myristic and palmitic acid after incubation at 49 °C whereas CYP102A1 retained

only 5 %. Yet, the coupling efficiency of the chimera towards BM3's natural substrates was low, only reaching 10 % [263]. Success however was achieved when the extremophile CYP175A1 from *Thermus thermophilus* was fused to its own natural redox partners Fdx and FdR [264]. By ferrous-CO assay, CYP175A1 reached a T_m of 88 °C whereas in comparison, for the same assay, the oxidase of BM3 reaches a T_m of 57 °C [247]. The CYP175A1 fusion construct in terms of activity fared 9-fold better than its unfused counterparts. The hydroxylation rate of β -carotene could reach a maximum of 0.016 min⁻¹ and a TON of 0.238 for the CYP175A1 fusion construct after a 15 minutes reaction. Therefore, although the construct is stable and functional, product formation rates remained low as is typical for CYPs derived from extremophiles. To this day, several CYPs derived from extremophiles exist but have not yet been explored by way of fusion with foreign or native redox components. For instance, CYP119A2 from *Sulfolobus tokodaii* catalytically active at up to 80 °C [265], CYP213A2 from *Picrophilus torridus* with a T_m of 65 °C obtained by ferrous-CO [266], CYP154H1 from *Thermobifida Fusca* with a T_m of 67 °C obtained by circular dichroism [267] and a CYP from *Bacillus thermoglucosidasius* retaining 60% of its activity at 70 °C [268]. Furthermore, it's been clearly established for BM3 and flavocytochrome b2 from the yeast *Saccharomyces cerevisiae* [269, 270], that the length of the linker region affects electron transfer between the oxidase and the reductase domains, as such tinkering with the linker region's length and composition should be another element to investigate when creating fusion chimeras. The order in which the components are added is also a facet to investigate as was shown when the p450 components of *P. putida* were fused in this order, PdR-Pdx-p450cam, catalytic rates were 3 times higher than on a p450cam-PdR-Pdx fusion construct [271].

As there is much interest in the production of human CYP metabolites, several fusion approaches have been investigated for human or animal CYPs, as they are not naturally fused to the components of their reductase and to increase their solubility as these CYPs are mostly membrane bound [272]. In one such case, rat CYP 2E11 was fused with the BM3 reductase, the fused construct yielded a beneficial outcome in that it only produced a fifth of the hydrogen peroxide that 2E11 with its unfused rat reductase partner would in the presence of arachidonic acid and NADPH [273]. Contrastingly, the activity of the fused rat 2E11 towards arachidonic acid was greatly reduced reaching 0.22 min⁻¹ whereas the free-form 2E11 reached 3.7 min⁻¹ or about seventeen times faster. In terms of TON it's unspecified which approach would yield the greatest amount of product however. In a different case, the group of Dr Gianfranco Gilardi fused the human CYP2E1 to the BM3 reductase. In the process, they also excised the hydrophobic tail required for the anchoring in lipid membranes of human CYPs, the enzyme was found to be soluble and absent from lipid membranes

[274]. The fusion construct's activity reached 2.98 min^{-1} towards *p*-nitrophenol which remains in the range of what was observed for rabbit CYP2E1 reaching rates of 9.4 and 6.9 min^{-1} towards the same substrate [275, 276] whereas unfused human CYP2E1 could reach a rate of 2.0 min^{-1} in *E. coli* membrane preparations and 9.2 min^{-1} in microsomes [277, 278]. The effect this construct might have on stability are unclear, on one hand no more than 8 % NADPH consumed was used to produce *p*-nitrocatechol from *p*-nitrophenol [279]. On the other hand, this seems to be a normal feature for CYP2E1 rather than a result from the fusion of the CYP to the reductase domain of BM3, as the CYP2E1 has a prominent tendency for uncoupling and the generation of superoxide radicals in general [280–283] with a coupling percentage of 9 % for N-nitrosodimethylamine demethylation for example [281]. A similar attempt would be made again by the Gilardi lab this time by fusing CYP2C20 from *Macaca fascicularis*, a CYP which is closely related to human CYP2C8, with BM3's reductase [284]. The activity for the fusion construct compared to the unfused form of CYP2C20 was found to be almost identical for the substrate paclitaxel and half as fast for amodiaquine. The effect of the fusion on stability remained however unspecified. Again, from the same research group but in a different paper, human CYP 2C9, 2C19 and 3A4 were fused to the reductase domain of BM3 [285]. There as well, the activity of the chimeras was comparable with reconstituted and membrane preparations of the corresponding unfused human CYPs. The level of coupling attained for the generation of the products diclofenac, omeprazole and erythromycin was of 30, 20 and 15 % respectively with the CYP2C9, 2C19 and 3A4 fusion constructs. These coupling numbers are similar to that of CYP2C9 towards flurbiprofen reported to be 30% [286] as well as those reported for CYP3A4 towards testosterone at 16 % [287]. Further work from the Gilardi lab investigated the effects of various linker regions between human CYP3A4 and the reductase domain of BM3 where the characteristic 450 nm peak was monitored at 37°C incubations during 60 minutes by ferrous-CO assay. It was shown there that an unfused CYP3A4 retained only 10% of its original peak after 60 minutes, while both the CYP3A4-BM3 reductase and the CYPA4-5GLY-BM3 reductase fusion constructs retained 42% of their initial peak thus displaying higher conformational stability [288]. The 5GLY corresponds to 5 glycine residues added in the linker region to expand its length. On the other hand, leakage rates of the constructs were doubled in the absence of substrate compared to unfused CYP3A4. In addition, all fusion constructs NADPH consumption rates were compared to that of the unfused CYP3A4 which resulted in a 5-fold increase for CYP3A4-BM3 and the CYPA4-5GLY-BM3 reductase chimeras. But this rate increase did not hinder coupling as the CYPA4-5GLY-BM3 reductase showed the greatest coupling efficiency of all construct with 12.5% towards erythromycin N-demethylation [288] and 69.3% for testosterone 6β -hydroxylation [289], a marked

improvement from the coupling efficiency of testosterone reported for unfused CYP3A4 at 15.5% [287].

1.1.4 Immobilisation

A classical strategy chosen to enhance enzyme stability and yield consists in immobilizing the enzyme on a solid support. The microenvironment as well as the attachment of the enzyme to the solid support can enhance stability although often at the cost of some activity loss. Briefly, immobilization is accomplished by either covalent binding, affinity, adsorption or entrapment of the enzyme on a support. An additional benefit to immobilisation of an enzyme is that it can easily be separated from the reaction mixture and hence it greatly facilitates its reuse in subsequent enzymatic reactions and product purification. Enzyme immobilization can be combined with numerous other strategies for enzyme stabilization or even to modify the electron source used with it. Specifically, it is essential for electrode-based reduction strategies. To this day, several attempts to immobilize CYPs have been made with varying degrees of success.

In one case, CYP2C9 was immobilized in a self-assembled monolayer film on a gold surface where it could provide a TON of 363 for the hydroxylation of flurbiprofen to 4-hydroxyflurbiprofen. The free-form enzyme however exceeded the TON of the immobilised enzyme with a TON of 1600 [290]. In another case, the human CYPs 1A2, 2B4 and SCC were immobilized in multiple monolayers of amphiphilic films made out of glycerol and agarose which were deposited onto indium tin oxide/glass electrodes [291]. It was demonstrated by circular dichroism that when CYP3A4 was encased in 30 layers of these films it could retain its secondary structure at up to 150 °C whereas the free form lost its secondary structure at 60-70 °C.

In the group of Dr Teruyuki Nagamune from Japan, an unconventional technique to immobilize CYPs was crafted. Each of the three proliferating cell nuclear antigen (PCNA) sub units which assembles naturally into a trimer were fused to CYP101A1, Pdx and PdR from *P. putida* [261]. To further strengthen the trimer, cysteine residues were added to the PCNA subunits from *Sulfolobus solfataricus* to form additional disulfide bonds [292]. This construction would be immobilized when a phosphite dehydrogenase was added to the middle of a Y-PCNA-PDH-PCNA-Y construct where Y corresponds to either CYP101A1, Pd or PdR with Y identical in both ends. Production of the three PCNA fusion constructs altogether collectively formed a matrix of unending oligomerised PCNA

subunits in the process forming a protein based gel (Figure 12A) [293]. The system showed near perfect coupling with D-camphor reaching 99 % and could retain over 50 % of its ability to convert 1.5 mM of D-camphor for four consecutive cycles and then falling under 50 % at the fifth cycle at 25 °C. Using a rough estimation of their figures a TON of 4500 moles of 5-exo hydroxycamphor/moles of immobilized p450cam could be estimated for this immobilisation scheme. Difficulty in the diffusion of substrates towards the inside of the gel matrix was discussed as being a potential hindrance to the performance of this system and altering the fusion constructs towards that end could potentially enhance the yields of this approach significantly. In a second paper the PCNA immobilisation strategy was modified slightly dropping the gel matrix component and instead immobilizing the PCNA2 fragment on NHS-Mag sepharose magnetic beads through amine coupling with its surface (Figure 12B) [294]. Then adding PCNA1 fused to PdR as well as Pdx and PCNA3 fused to p450cam to assemble the trimer. By the same method, BM3 was immobilized as well, where it was fused with PCNA3 with PCNA1 unfused to any enzyme and PCNA2 immobilized on magnetic beads. A rough estimate from their figure gives a potential TON of up to 48 316 for D-camphor hydroxylation by immobilized p450cam and 548 for lauric acid hydroxylation by immobilized BM3 after 10 cycles of 20-minute reactions at 25 °C. Interestingly, for the reactions cycles where immobilized BM3 was used, lauric acid consumption showed no signs of slowing at the tenth cycle when compared to the initial cycle. Thus, had further reactions been driven past the tenth cycle a higher figure for TON could have been obtained.

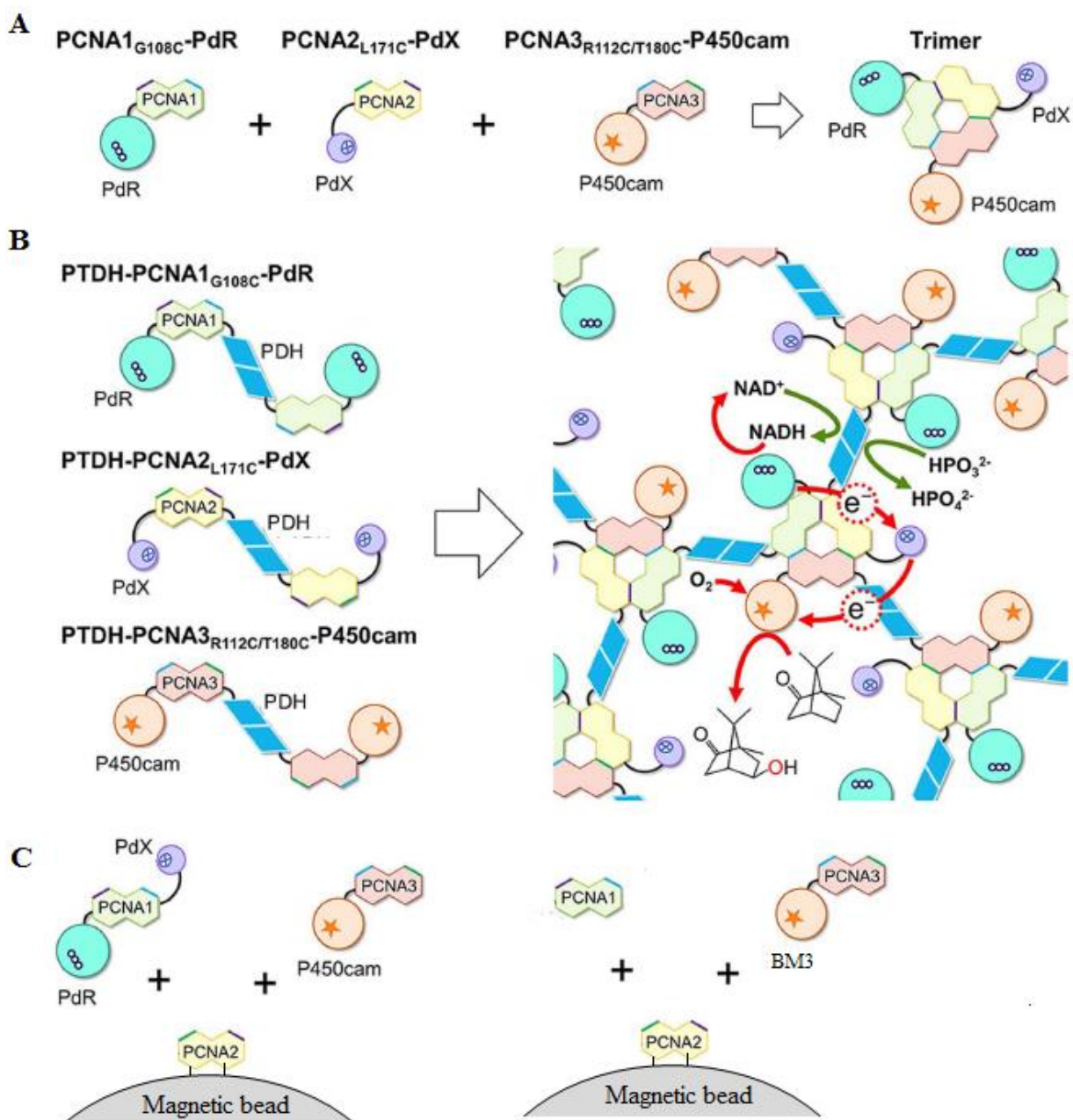


Figure 12: A. Assembly of the three PCNA fusion constructs to form a matrix of unending oligomerised PCNA subunits and in the process forming a protein based gel, edited from [293] B. Immobilization of the PCNA2 fragment through amine coupling with its surface on NHS-Mag sepharose magnetic beads with either p450cam (left) or BM3 (right), edited from [294].

In different work, magnetic nanoparticles were used to immobilize the R966D/W1046S BM3 mutant [295]. There, the immobilization of the mutant was performed using Ni_2^+ -functionalized magnetic nanoparticles which would first exploit the histidine tag located on the BM3 variant and then be further immobilized using glutaraldehyde to crosslink the CYP to the solid support. In this scheme, the immobilized enzyme retained 88 and 85 % of its initial activity towards NADH and the

biomimetic cofactor N-benzyl-1,4-dihydronicotinamide (BNAH, figure 13) respectively after 5 cycles of use with 350 μM of 10-pNCA substrate.

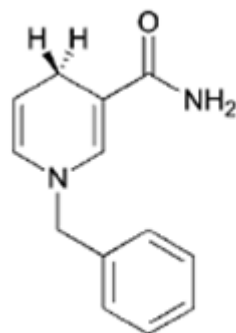


Figure 13: N-benzyl-1,4-dihydronicotinamide structure, edited from [296].

This tallied up to a TON for pNP production of 2983 using NADH and 2118 using BNAH as a cofactor. The storage stability of the immobilized CYP was explored as well with relative activity towards the cofactors NADH reaching 90% after 21 days and 41% after 28 days of storage at 4 °C. Contrarily, the free enzyme retained 31% of its initial activity towards NADH after 7 days and showed no activity towards 10-pNCA at that point. In later work, the same variant would then be immobilized on glutaraldehyde pre-activated super paramagnetic iron oxide nanoparticles (SPIONs) where storage stability would be further improved retaining 80% of its activity towards NADH after 1 month of storage at 4 °C [297]. However, after 5 reactions cycles with 350 μM of 10-pNCA, the SPION immobilized CYPs retained roughly 50 % of their initial activity for both NADH and BNAH. This would translate in a TON of 1455 and 1025 for pNP production using NADH and BNAH as cofactors, respectively. In other work by the team of Dr Vlada Urlacher from Düsseldorf University, BM3 was immobilised unto a tetraethoxy orthosilicate based sol-gel matrix. Here the immobilization brought forth a loss of 50% in activity for the enzyme when evaluated with a 10-pNCA assay [298]. Despite this, the immobilization did have a positive effect on the stability of BM3 as after 30 days immobilized BM3 retained 100% of its initial activity when stored at 4 °C and then 50 % when stored at 25 °C. On the other hand, in solution, BM3 kept 65 % of its initial activity when stored at 4 °C and 0% when stored at 25 °C after 30 days. With formate dehydrogenase present to recycle NADPH in the presence of the immobilized enzyme a TON of at least 1800 could be estimated from one of their figures. In later work by the same group, the heme domain of BM3 possessing the F87A mutation would be immobilised as well, this time using mesoporous molecular sieves of various pores sizes [299]. When both free and immobilized enzyme were fed octane and hydrogen peroxide, reaction rates reached

3.6 min⁻¹ and 7 min⁻¹ respectively. In addition, the immobilized BM3 CYP could hydroxylate 20 % of all octane in reaction whereas the free enzyme could only hydroxylate 9 %. It is interesting to note as well that in these octane conversion experiments, 10 μM of hydrogen peroxide were supplied to the reactions, a significant amount of a potent oxidative agent. In work done by a different research group, the 21B3 BM3 mutant would be immobilized this time using Ru(II)-diimine complexes decorated with aldehyde functional groups to facilitate the crosslinking and immobilization of the CYPs [300]. In this scheme, the 21B3 variant following immobilization could retain up to 95% of its initial activity towards 12-pNCA with hydrogen peroxide as a cofactor source when compared to the free form enzyme in solution. The same immobilized variant, 21B3, also yielded a TON of 800 towards 12-pNCA, up from 470 when compared to the enzyme in solution when using hydrogen peroxide as a source of cofactors.

In another publication, the BM3 variant M7 was immobilized unto a k-carrageenan support alongside catalase immobilized on DEAE-650S added to remove any hydrogen peroxide accidentally produced [301]. In this scheme, electrons were supplied by zinc dust/cobalt sepulchrate (Figure 14).

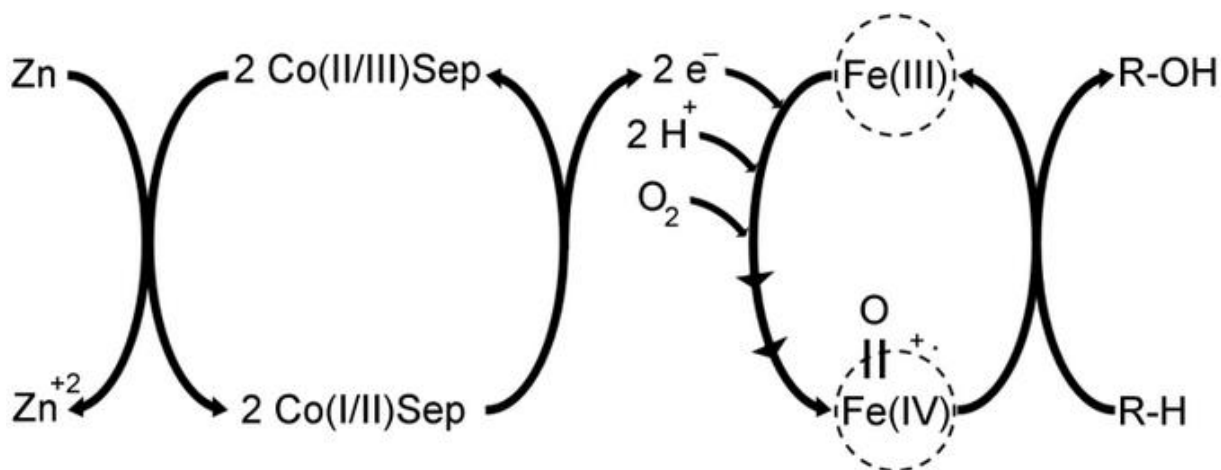


Figure 14: Zinc dust (Zn)/Cobalt sepulchrate (Co (II/III)Sep) scheme whereby electrons are transferred from the latter two chemicals to the catalytic heme of BM3 represented here by its iron center (Fe(III)/Fe(IV)). Figure taken from [302].

Using this scheme, the relative activity of immobilized BM3 M7 towards 12-pNCA after a 13-day storage time at 4 °C was of 50 % whereas the free BM3 M7 dropped under 30% of its initial activity after 7 days of storage. What's more, after a single hour of incubation at 60 °C the immobilized BM3 M7 variant could retain over 80% of its activity whereas in the same conditions free form BM3 M7 retained under 30% of its initial activity demonstrating that the immobilized

enzyme possesses enhanced thermostability. In terms of yields, this unique scheme could provide, at best, a TON of over 2000 for 3-phenoxytoluene hydroxylation with no information of TON for the free form enzyme. In different work, nitric oxide reductase (NOR) from *Aspergillus oryzae*, which is part of the cytochrome p450 family, was co-immobilized with the bacterial glucose dehydrogenase from *B. megaterium* within hyper porous ReSyn polymer microspheres [303]. Using this scheme following a 1-day incubation at 37 °C immobilized NOR retained a little over 95 % of its initial activity whereas the free form lost all of its initial activity after the same incubation period. After 4 days of incubation at the same temperature, immobilized NOR dropped to 40% of its initial activity demonstrating here again an immobilization approach that enhances CYP stability. In a different attempt to immobilize BM3 [304], the BM3 mutant m2 (Y51F/F87A), conferring a larger substrate spectrum to BM3, was fused to phasin P which enables the CYP to be immobilised unto poly (3-hydroxybutyrate) granules or P3HB granules (Figure 15). Those granules are produced naturally in some bacteria as an intracellular aliphatic carbon storage reserve and thus manifest themselves as granular inclusion bodies. Using vectors carrying the required genes, both the P3HB granules and the BM3 CYP were produced within *E. coli* cells. From a rough estimate of their figures a TON of at least 2218 moles of 7-hydroxycoumarin per moles of BM3 using NADPH as a cofactor could be assessed for this particular immobilization strategy. Although using PCNA subunits to immobilize p450cam can provide the highest TON for immobilization strategies at up to 48 000 with the substrate D-camphor, the substrate scope of p450cam is rather limited and the product output of BM3 with the same technique reaches a lackluster 548 for the substrate lauric acid. Otherwise for BM3, the R966D/W1046S mutant immobilized unto Ni₂₊-functionalized magnetic nanoparticles provided the highest turnover at 2983 using the low-cost cofactor NADH with the substrate 10-pNCA.

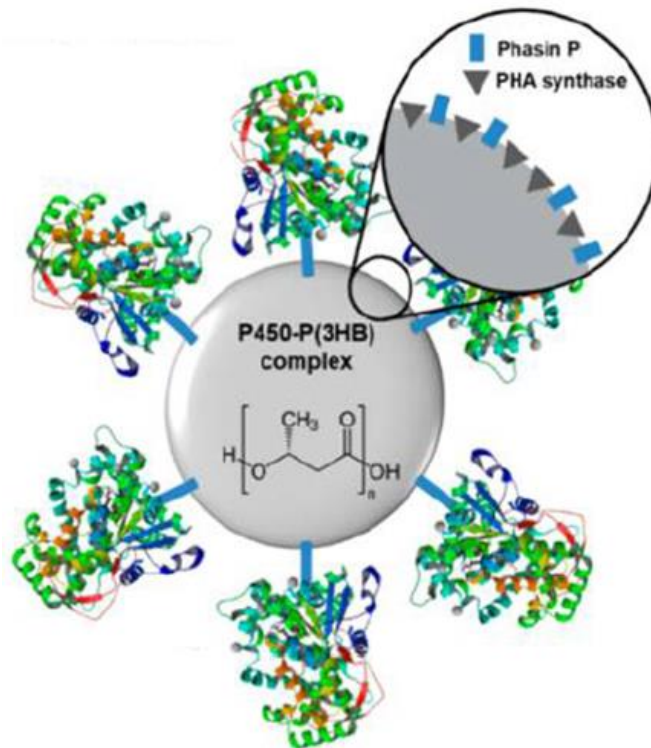


Figure 15: BM3m2 (Y51F/F87A) fused to phasin P and immobilised onto poly (3-hydroxybutyrate) granules. Figure taken from [304].

1.2 Enzymatic process - Electron source

The most conventional way by which CYP feed their reactions is by using the natural cofactor NADPH. Although most CYPs prefer the use of NADPH as a cofactor over NADH some CYP such as p450soy or p450cam favour the use of NADH over NADPH [305]. BM3 for instance uses with greater efficiency NADPH but it has also been shown to be able to use NADH [306]. Both NADPH and NADH tie into the second major hurdle to the application of BM3 in a free enzyme system, or any other CYP for that matter, in that they are expensive thus impose a limit of price in terms of which products are economically viable to produce. To compound this problem even further, these two cofactors, through uncoupling and leaking, are not always coupled to the successful generation of the desired product which in turn threatens the stability of the CYP. To bypass this problem, several strategies have been investigated and shall be further detailed below.

1.2.1 Nicotinamide reduction and recycling

An obvious solution to counter the high price of NADPH or NADH is to recycle them. To accomplish this an NADPH/NADH dehydrogenase enzyme can be added to the free enzyme system. The most common enzymes used to recycle NADPH in CYP based processes are glucose dehydrogenase (GDH), formate dehydrogenase (FDH), phosphite dehydrogenase (PDH) and alcohol dehydrogenase (ADH) whose corresponding acceptor substrates glucose, formate, phosphite and ethanol are inexpensive barely adding an extra cost to the whole process [307]. Additionally, several other NADPH dehydrogenase enzyme exists besides those [308]. Adding an enzyme to the system extends however the processing costs since an additional enzyme has to be produced and purified. To bypass this, the Nagamune lab fused with a spacer arm a PDH to a CYP and met some success with this strategy [293]. They also go on to point out that within the fused CYP-dehydrogenase construct the CYP is deactivated before the PDH implying that in terms of stability the bottleneck resides with the CYP. In similar work BM3 was fused to a PDH where phosphite was used in excessive amounts with very little NADP⁺ the authors were able to drive the hydroxylation of lauric acid, omeprazole and rosiglitazone forward similarly or slightly further than its free enzyme BM3/NADPH counterpart in terms of TON [309]. In any case, it could be argued that adding a second enzyme to a cell-free process invites a second enzyme liable to inactivation through stability issues. In this regard it is interesting to consider that besides CYPs, numerous other enzymes which garners industrial interest necessitate NADPH and that, as such, much work has already been done on the engineering of sturdy dehydrogenase enzymes. For instance, the PDH from *Pseudomonas stutzeri* was extensively mutated

generating a mutant named 12X with a half-life of 8440 minutes at 45 °C, the wild type enzyme on the other hand at the same incubation temperature had a half-life of 1.2 minutes [310]. In a different paper, NADPH PDH was extensively mutated in wholly different direction focusing on activity instead [311]. Where the wild type enzyme's rates of NAD⁺ and NADP⁺ reduction by gain of hydrogen were enhanced from 176 min⁻¹ and 85 min⁻¹ to 340 min⁻¹ and 130 min⁻¹, respectively. Attempts at enhancing the stability of NADPH/NADH dehydrogenases by immobilising them on solid supports have also been made. In one instance, two NADPH ADHs, Y-ADH from *S. cerevisiae* and LB-ADH from *Lactobacillus brevis*, had their residual activity improved 2 and 3.1 fold respectively following adsorptive immobilization on a hydrophobic surface [312]. In a different case, GDH from the hyperthermophilic bacteria *Aquifex aeolicus* was immobilized on a graphite electrode where it was shown it could retain 100 % of its activity following a pre incubation of 20 min at 50 °C [313]. While there seems to be highly stable dehydrogenase constructs and reliable immobilisation strategies available, the use of NADPH/NADH cofactors comes with another risk intrinsic to nicotinamide based compounds in that they themselves are not very stable. It's been plainly established that the nicotinamide based compounds NADPH and NADH are degraded more rapidly at increasing temperatures, in increasing phosphate buffers concentrations and at increasing acidic pH [314–318]. For example, at 30 °C in 50 mM TEA buffer at pH 7.2 the half-life of NADH is of 50 hours whereas that of NADPH is at 16.7 hours. Additionally, in the same conditions but at 40 °C NADH and NADPH's half-lives are at 12.5 hours and 3.75 hours, respectively [318]. In fact, below a pH of 6, above a temperature of 30 °C and above a phosphate buffer concentration of 0.2 M, nicotinamide based cofactor half-lives can drop significantly from hours to minutes [315, 317]. Fortunately, optimal pH for CYPs are usually between 7 and 8. However, many well-established p450 protocols [319] still use phosphate buffers today despite nicotinamide's sensitivity to them. In any case, care should be taken in formulating CYP reaction conditions in order to prevent nicotinamide compound degradation as well as enzyme inactivation.

A different strategy to bypass the high price of enzymes using NADPH and NADH is to use alternative low-cost nicotinamide analogues of these compounds. In the case of BM3, the R966D/W1046S mutations allows for a better utilisation of NADH [306] and the utilisation of the nicotinamide analogue BNAH [296]. In the case of BNAH, this strategy was tested with both BM3 and p450cam, where their ability to use 2 variants of BNAH, a structural analogue of NADPH only retaining it's nicotinamide ring unto which a benzyl group is added in place of a ribose (Figure 13) [296]. Furthermore, by using an organorhodium [296] or an osmium catalyst [320], BNAH has been shown itself to be recyclable. However, both of these catalysts are quite expensive. A combination of

sodium dithionite and sodium bicarbonate [321] has also been used successfully to recycle NBAH but with losses of cofactors reaching 20 to 65 % with each attempt to recycle NBA⁺ back to NBAH. An obvious alternative to using expensive organometallic catalysts or sodium dithionate/bicarbonate reduction is to enzymatically recycle the nicotinamide analogues. A task explored for many dehydrogenases met solely with failure [322] until a regeneration system using an NADH oxidase from *Lactobacillus pentosus* named LpNox was shown to be able to recycle both BNAH and methyl-1,4-dihydronicotinamide [323]. Despite this, it is noteworthy that in the work where a CYP was tested with two BNAH compounds, the authors point out [296] that the coupling efficiency when using these compounds was much lower than that of the natural cofactors NADPH and NADH. For this reason, should this strategy be used, it would be necessary to tailor CYPs for the use of these inexpensive cofactors to avert uncoupling, leakage and as a result, augment stability. Interestingly, in a different paper, when different nicotinamide analogues had their activity tested with various ene-reductases, each enzyme showed a different template of efficiency with the cofactors tested [324] demonstrating the need to not only tailor an enzyme to its cofactor but also the cofactor to its enzyme. Other examples in the literature exist where alternative nicotinamide analogs are further discussed [322, 325] or synthesized and tested though not with CYPs [324, 326–328]. Interestingly, cofactors including NADPH, NADH, FADH₂ and NBHA have all been successfully regenerated using pentamethylcyclopentadienyl rhodium bipyridine catalysts [296, 329] where it was also demonstrated that these catalyst remain catalytically between a pH range of 3.5 to 9.7 and well functional in temperatures as high as 69 °C with activities increasing as temperatures were themselves increased. The drawback of such catalyst however is in the time used for their preparation and the high cost required to acquire them. In any case, for biomimetic nicotinamide compounds to excel, CYPs should be tailor made to augment coupling efficiency, diminish leakage and augment yields.

1.2.2 Electrode driven reduction

A scheme envisioned by several research groups to solve the cofactor conundrum has been to immobilize CYPs of interest unto an electrode which could then transmit electrons to those now immobilized CYPs when an electric current is applied to the system [330, 331]. The express goal of such schemes is not limited to the production of a compound to an industrial scale but also as a form of disposable biosensor tool which can be used to detect substrates at concentrations in the micromole to the low nanomole range [332]. This second application finds its use in the detection of drugs in the medical and anti-doping industry. Unfortunately, adsorption of proteins directly to an electrode most often result in the denaturation of the CYP in part due to their inherent instability but also because

the immobilisation process can be harsh [333]. To avoid this, the most recent enzyme immobilization onto electrodes strategies are realised using a special layer or film between both components to keep the enzyme in its native state [334–336]. In this regard several films have been tested including, though not limited to, conductive polymers [337], surfactants [338–340], thiol self-assembled monolayers [341, 342], dendrimers [343], carbon nanofiber films [344] & microsome preparations [345]. A caveat to the immobilisation of enzymes in films on electrodes is that the subsequent evaluation on the amount of CYP immobilised cannot be as clearly and easily assessed as in solution. Thus, although data pertaining to establishing whether product formation was successful is fairly common, data in regards to TON and stability is scarce. Still, there are cases where glimpses of success can be observed, for example when CYP3A4 was immobilized unto a gold electrode within a poly-dimethyl diallyl ammoniumchloride film product formation rates of norverapamil never slowed down for 2 hours straight at 25°C [346]. It was demonstrated that the heme iron potential changes significantly from its state in solution when BM3 [71, 347] and CYP51B1 [348, 349] were immobilised on electrodes and embedded in a didodecyldimethylammonium bromide film. In the case of BM3 it has been suggested that this discrepancy is a result of partial heme dehydration caused by the hydrophobic nature of the film used [347, 350]. Given the catalytic cycle of CYPs reliance on the properties of the heme it is imperative for this strategy to function that these properties remain unaffected by the proximity of the electrode and the film used if any products are to be generated. Ultimately, the right film or layer has to maintain the same midpoint reduction potential of the $\text{Fe}^{3+}/\text{Fe}^{2+}$ heme iron located within the CYP in solution. Another important factor, that most likely tie into the one just outlined, is to modulate coupling efficiency. Indeed, enhancing the coupling efficiency of electrodes and CYPs in order to yield greater amount of products was clearly demonstrated when the Gilardi lab investigated the relationship between the two [339]. When they compared the coupling efficiency to the yields of products of various CYP3A4-reductase chimeras on glassy carbon and gold electrodes higher coupling clearly translated into a greater number of products.

In the instances where product formation is clearly demonstrated, some common threads seem to coalesce when using the electrode scheme. For instance, the presence of CYP reductase enzyme alongside CYPs generally aids in product formation [351–355]. In addition, for CYPs not naturally connected to a reductase, which is to say most CYPs, fusing a reductase also seems to enhance activity compared to an unfused system [330, 339, 354, 355]. This could possibly be explained by electrons being guided through tyrosine/tryptophan pathways located in reductase domains. Another thread is that of adding gold electrodes [339, 346] or gold nanoparticles to the

reaction [356–358] as they seem to aid altogether in product formation conceivably because gold acts as a good electron transfer relay by enhancing the electron transfer from the electrode to flavin functional groups [359]. While applying an electrical current to an electrode to drive CYP reactions forward is an interesting alternative to circumvent the expensive price of NADPH, one must first adopt an immobilisation strategy that keeps the enzyme stable and active at levels that competes with those observed in free enzyme reactions.

1.2.3 Light driven reduction

In this unique strategy, a low-cost chemical acts as an electron donor to a photosensitizer when reduced by light. In turn, those electrons are then transferred to a CYP to forward the oxidation reaction. The generic outline of this scheme can be seen in Figure 16. In this scheme, a low-cost chemical alongside light replaces the NADPH cofactor whereas the photosensitizer acts as a reductase domain would, ferrying electrons to the oxidase domain. It offers a potentially interesting feature with regards to the fine tuning of the cofactor present in solution. The cofactor could be added in large quantities in a batch reaction but with the availability of usable reduced cofactors fine-tuned by the quantity of light allowed to shine on the reaction. On the other hand, a common challenge with light driven reduction is that the purchase or the synthesis of the photosensitizers is expensive. While there are several instances where this scheme demonstratively works, in terms of TON in moles of product/moles of enzymes this strategy has not yet been able to surpass the yields of free enzyme NADPH systems.

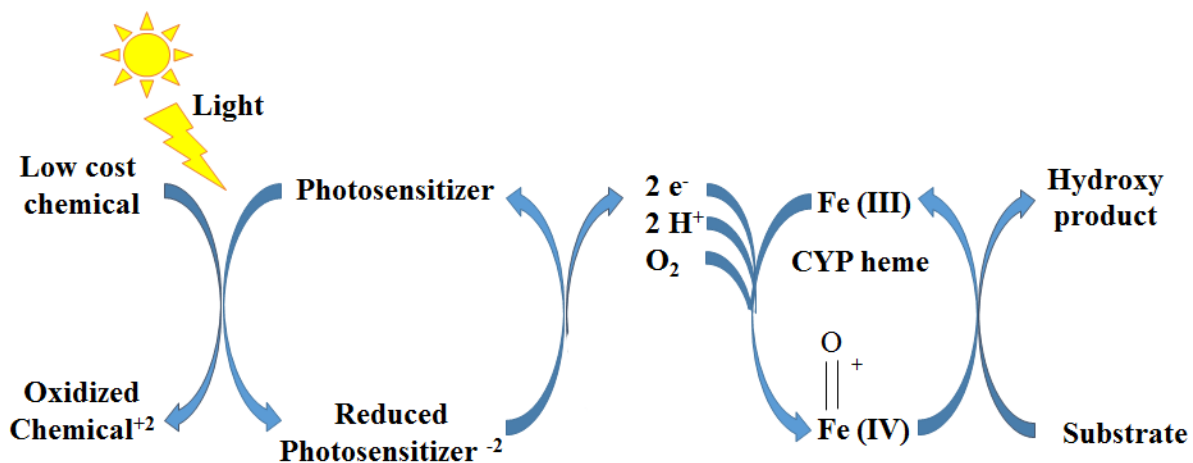


Figure 16: Light driven reduction generic outline.

In one of these light-driven strategies, ethylene diamine tetra acetic acid (EDTA) was used as the low-cost electron donor chemical and 3,10-dimethyl-5-deazaflavin was used as a photosensitizer to drive the BM3 reaction. A TON = 698 (molar basis) was reached with lauric acid [360]. The activity that could be observed for the hydroxylation of lauric acid was of 1.95 min^{-1} . In a similar case, where lauric acid was used with the low-cost electron donor chemical sodium diethyldithiocarbamate (SDC) and a Ru(Bipyridine)₂ 5-acetamido-1,10-phenanthroline (Ru(LL)₂PhenA) photosensitizer along with the heme domain of BM3, TON reached 935 and the activity reached 125 min^{-1} [361–364]. To compare, in recent work where BM3 was fused to a PTDH and reaction was driven with lauric acid, NADP⁺ and phosphite the TON for the BM3 fusion construct reached 2250 whereas the activity reached 480 min^{-1} [309]. In a different work, triethanolamine was used as the low-cost electron donor and eosin Y as a photosensitizer with the BM3 mutant m2 immobilized onto poly (3-hydroxybutyrate) granules in the presence of 7-ethoxycoumarin, this light driven strategy provided a TON of 403 [365]. In a previous work however, where the BM3m2 mutant was immobilized on the same support in the presence of 7-ethoxycoumarin and NADPH, the TON reached 2218 moles of product/moles of enzymes [304].

In another publication by the authors of the scheme using SDC/Ru(LL)₂PhenA the yields towards 16-pNCA were almost doubled from a TON of 230 to 430 moles of product/moles of enzymes by adding a single mutation Q403W to their BM3 heme domain-photosensitizer construct. This mutation was identified through rationale design by following crystallization of the BM3 heme domain-photosensitizer construct in closed and open conformation with N-palmitoylglycine [366]. Screening variants of the Ru(LL)₂PhenA photosensitizer also demonstrated that tailoring the photosensitizer, in addition to the CYP used, could improve this type of system with initial rates of reaction for 16-pNCA enhanced almost up three fold in the best case [367]. Thus, be it by point mutations to the heme domain or by fine tuning the photosensitizer, light driven systems can be improved in many ways, as these latter two publications highlight. The same group brought forth an interesting finding by showing that TON increased by 33% when catalase was added to the reaction system [362]. This means that peroxide, produced by the reaction cycle, is decomposed to water by catalase, which reduces the stress it induces on the enzyme, thus favoring TON. In that regard, it should be added that the photochemical processes between Ru(LL)₂PhenA and dioxygen are known to generate many reactive oxygen species such as hydrogen peroxide [368]. Ultimately, the issue of yield, which could be potentially related to enzyme stability and coupling efficiency, is of prime importance for this technology if it is to be considered competitive.

1.2.4 Peroxide driven reduction

As mentioned before, during a CYP's catalytic cycle uncoupling may result in the formation of either water, superoxide or hydrogen peroxide. What's different about the formation of hydrogen peroxide is that the reaction is reversible. This means that hydrogen peroxide in the presence of a substrate at the active site may supply electrons to the reaction and drive it forward through the peroxide shunt pathway (Figure 4). This phenomenon offers the possibility to use hydrogen peroxide instead of a nicotinamide cofactor to drive the oxidation reaction forward directly. There are two benefits in using this strategy, first hydrogen peroxide is extremely inexpensive as a cofactor source, and second no reductase is needed since hydrogen peroxide enters directly through the oxidase domain. This strategy opens up the variety of CYPs that could be used since most of them are not naturally fused to a reductase. On the other hand, using hydrogen peroxide conveys a great deal of problems as well. It is a strong oxidant and quickly inactivates most enzymes, including CYPs.

This strategy also requires monooxygenase CYPs to be somewhat engineered towards hydrogen peroxide use or else, the use of peroxygenase CYPs which naturally prefer using hydrogen peroxide over NADPH. In the latter case, the two peroxygenases CYP152A1 & 152A2 were investigated has a potential platform for the production of CYP metabolites [369]. In the strategy the authors employed, BNAH was used as a reducing agent to be added exogenously to the system where FMN would in turn reduce use BNAH to catalyze the conversion of dioxygen to hydrogen peroxide. In this way hydrogen peroxide concentrations remained low throughout the reaction and, as the authors noted, the percentage of conversion of myristic acid dropped from 100% (this strategy) to 40% when they added hydrogen peroxide directly to the reaction, underlining the deleterious effect of hydrogen peroxide on the enzyme. In this instance, a 100 % conversion translates to a TON of 200. It's also interesting to note that the highest kcat values were obtained when hydrogen peroxide was added exogenously going up to 200 min⁻¹ and 1200 min⁻¹ for CYP152A1 & 152A2, respectively, whereas the BNAH/FMN pathway only reached 35 min⁻¹ which is thought to be the result of the diffusion rate of dioxygen [370]. In a different approach where highly mutated variants of the BM3 oxidase mutant F87A were developed for the efficient use of hydrogen peroxide, the mutant 21B3 was developed following several rounds of error prone PCR [201, 202]. This mutant was shown to have much faster rates of peroxide driven hydroxylation towards the substrate 12-pNCA than its parent BM3 F87A rising from 23 min⁻¹ to 430 min⁻¹. The TON increased as well using this mutant, from 90 to 980 for 12-pNCA, from 70 to 280 for lauric acid and from 10 to 240 for styrene. Despite these significant improvements these TONs still fall short of more conventional nicotinamide based

strategies, for instance when compared to a recent publication where the BM3-PDH fusion lead to a TON of roughly 2250 with lauric acid and phosphite/NADP⁺ as substrates and cofactors [309].

Another notable feature of the work on the 21B3 mutant was that the authors reported it to be fully inactivated within 5 minutes in the presence of 10 mM hydrogen peroxide whereas, in a subsequent publication, this inactivation benchmark was bypassed by rather adding 1mM of hydrogen peroxide every 30 minutes to get the highest turnover possible [371]. This fed batch approach was performed with a different mutant, named 9C1, generated from the 21B3 variant. It was observed that after 180 minutes of reaction no more of the 9C1 CYP could be detected in solution. Thus, in order to obtain the highest yields with hydrogen peroxide, the latter must be kept to a minimal concentration although this comes at the cost of slower production rate. In the end, the 9C1 BM3 mutant was able to efficiently use of hydrogen peroxide as cofactor to reach a TON of 180 for with the substrate propranolol. Similarly, the TON from wild type BM3 using the propranolol substrate as well but with NADPH as a cofactor could reach, estimated from the information provided in a paper by the research group of Dr Gianfranco Gilardi, a TON of 180 [372]. As mentioned earlier under the point mutations chapter of section 1.5.1.1, the mutant 21B3 was optimized by error prone PCR towards the more stable variant named 5H6 [200], where it was demonstrated by ferrous-CO assay that after a 10 min incubation the T_m was of 43 °C for WT BM3, 46 °C for 21B3 and 61 °C for 5H6. This improved stability came at the cost of a decreased activity towards 12-pNCA in the presence of hydrogen peroxide going from 430 min⁻¹ for 21B3 to 220 min⁻¹ for 5H6. Although there is no data in terms of TONs provided by the authors, they do point out that 5H6 retained almost 100% of its activity after a 40 minutes incubation in the presence of 10mM of hydrogen peroxide, a marked improvement from 21B3 that lost all its activity in under 5 minutes. Therefore, despite showing decreased activity it is possible that 5H6's overall TON could be well above that of 21B3, given enough time and substrate, in a fed batch setting.

1.2.5 Zinc/cobalt (III) sepulchrate (Zn/CoIIIsep) reduction

A unique strategy devised by the research group of Dr Ulrich Schwaneberg was that of using a cheap affordable zinc dust to reduce cobalt (III) sepulchrate which would in turn supply BM3 with the electrons abstracted from the zinc dust and in the process regenerate cobalt (III) sepulchrate for further reduction cycles (Figure 14). This strategy was discussed in a previous section, where research on immobilisation strategies was reviewed. In this work, the variants R47F/F87A and R47Y/F87A were generated from the BM3 F87A variant [373]. In terms of activity, all 3 BM3 variants

demonstrated greater activity towards 12-pNCA using NADPH as a cofactor rather than Zn/CoIIIsep. For instance, F87A/R47F reached an activity of 117 min⁻¹ with NADPH and 19 min⁻¹ with Zn/CoIIIsep. In their following work a BM3 mutant further adapted to the Zn/CoIIIsep scheme was developed. The new BM3 variant, named M2 (R47F/F87A/M354S), reached an activity towards 12-pNCA of 124 min⁻¹ with NADPH and, more importantly, 64 min⁻¹ with Zn/CoIIIsep [374]. In terms of TON, using WT BM3 a TON of 835 could be obtained for hydroxy products of lauric acid when using the Zn/CoIIIsep strategy [375]. Again, to put in perspective, in other work where BM3 was fused to a PTDH and used alongside, NADP⁺ and phosphite TON reached 2250 for lauric acid hydroxy products [309]. Later on, the BM3 mutant M7 would be developed (F87A/V281G/M354S/R471C/A1011T/S1016G/Q1022R) where that particular mutant, once immobilized on DEAE650S, as mentioned earlier in the immobilisation review section (1.5.1.4), would provide a TON of over 2000 for 3-phenoxytoluene hydroxylation using the Zn/CoIIIsep strategy following a 5 day incubation [301]. However, when the authors compared the aforementioned strategy to one simply using NADPH recycled by an isocitrate dehydrogenase TONs there reached 2657 thus yielding comparable results for both strategies.

1.2.6 Enzymatic process - Biphasic systems

Amongst the factors currently preventing the application of CYPs in free enzyme biocatalytic processes is the lack of substrate availability for the often poorly hydrophilic substrates. This translates into slow reactions rates, poor product yields and inefficient cofactor utilisation as NADH or NADPH are very much soluble in aqueous solutions [263]. Low substrate availability for the CYPs increases the odds of cofactor leakage due to the absence of hydrophobic substrates inside the oxidase active site. An organic cosolvent can be used to mitigate this but it, in turn, also affects CYP stability, thus substrate availability and CYP stability are intimately linked. An alternative approach to increase substrate availability is to use a biphasic system where a water-immiscible organic phase serves as both a substrate reservoir and a product sink. Using this approach, what little amount of hydrophobic substrate the aqueous phase can hold, with or without a carrier solvent, is at least kept constant as it is being constantly replaced, as it is being used, by substrates solubilized in the organic phase. Several studies using free enzyme biocatalysis have experimented this approach and shall hereon be appraised. In one such study, the activity of the human CYP2D6 towards dextromethorphan in an aqueous solution was compared to that of several biphasic systems using as the organic phase: chloroform, dichloromethane, dichloroethane, di-butyl ether cyclohexane, pentane, hexane, isooctane, toluene and xylenes [376]. All halogenated and aromatic compounds almost immediately

destroyed CYP2D6 activity whereas the other compounds provided less than 50 % of the dextrophan product compared to the aqueous CYP2D6 reaction. However, the substrate used, dextrophan, is more hydrophilic than hydrophobic, thus subsequent testing was done with the more hydrophobic substrate 7-benzyloxy-4-N,N-diethylamino-methyl-coumarin in the presence of the least two damaging organic solvents, hexane and isooctane. In those instances, in the absence of an organic phase, no products could be detected, while in the presence of isooctane, the highest productivity was observed, where a final concentration of 7-benzyloxy-4-N-ethylaminomethyl-coumarin reached 0.13 μM and a TON 0.65.

In a study where a bacterial CYP was used instead of a human one, the hydroxylation activity of p450cam from *P. putida* towards camphor was chosen as a model CYP reaction [377]. There, the reaction conditions in an aqueous phase without an organic cosolvent were compared to that of a two-phase system of hexane/water with or without the anionic surfactant bis (2-ethylhexyl) sulfosuccinate sodium salt, which acted as a carrier solvent in the reactions. The scheme using the anionic surfactant proved the most productive of all three, with nearly 50-times more product generated in the surfactant/biphasic system than what could be achieved with the aqueous scheme totaling a TON of 28 900 which stands for both products hydroxycamphor and 2,5-diketocamphane, the latter coming from the hydroxylation of the former. The authors go on to demonstrate that uncoupling increases substantially with reactions using hydroxycamphor as a substrate suggesting that this secondary reaction might provide increased instability later on in the reaction. In another study, the hydroxylation of cyclohexane was explored in a cyclohexane/water biphasic reaction system with BM3 variants A74G/F87V/L188Q and R47L/Y51F where the latter double mutant showed greater productivity reaching a TON of 12 850 for cyclohexanol after 100 hours of reaction at 18 °C with the first 53 hours reaching volumetric production rate of 23.8 mg/L/h [306]. In the same work, a biphasic mixture of octane and water was also assessed with octane also acting as the targeted substrate but only with the BM3 variant A74G/F87V/L188Q as variant R47L/Y51F is not active towards octane. There 2-, 3-, 4-octanol as well as the corresponding octanones were generated as products. With all these products pooled together, TON for octane hydroxylation reached 2200. To be clear, in the latter 2 examples, both cyclohexane and octane served both as the water immiscible organic solvent and the substrate. Yet another biphasic system was assayed in this work using dodecane as the organic phase and myristic acid as the substrate with the BM3 variant A74G/F87V/L188Q. Here, the product profile diverged from what is typically obtained in aqueous reactions where a mixture of subterminally hydroxylated products are normally obtained from fatty acids. Indeed, the biphasic system yielded both mono- and dihydroxylated products reaching a TON of 3300 for all hydroxy

products with BM3 variant A74G/F87V/L188Q using the cofactor NADPH and 30 000 with BM3 variant A74G/F87V/L188Q/R966D/W1046S tailored to use the cofactor NADH more efficiently. In other work, when the hydroxylation of C7-C9 n-alkanes was attempted using CYP154A8 from *Nocardia farcinica* products generated in a wholly aqueous reaction tended to be overoxidized thus yielding diols instead of the desired S-(2)-alcohols [378]. On the other hand, experimentation with biphasic systems using C7-C9 n-alkanes as both substrates and immiscible organic phase to a 20 % (v/v) fraction of the reaction volume removed this problem. For these biphasic n-alkane/water schemes, the resulting TON calculated as moles of 2-alcohol per nmol of CYP154A8 was of 2800 for 2-heptanol, 3200 for 2-octanol, 4400 2-nonanol and 1700 2-decanol. Roughly 5-10 % of products were that of the corresponding 3-alcohols and 5-15 % of the other products were that of corresponding ketones, the results of overoxidation. While this biphasic system seems to stir overoxidation away from the generation of diols, ketones are produced, thus a biphasic system does not fully prevent the overoxidation of products either. Interestingly, while a biphasic system mitigates some of the impracticalities of free enzyme biocatalysis, it can expose CYPs to secondary reactions by overoxidation of the product which can complicate downstream processing of the desired products.

1.3 Whole-cell process

As discussed earlier, the chemicals which can be manufactured through biotechnology can be produced using, broadly speaking, one of two strategies: a whole-cell biotransformation and free enzyme biocatalysis. Free enzyme biocatalysis, relies on enzymes overproduced, removed and often purified from a recombinant microorganism to catalyze the enzymatic reaction(s) in solution. Whole-cell biotransformation consists of a culture of microorganisms which transforms either a feedstock or an exogenous substrate to the desired chemical compound. In this regard, the whole-cell strategy can be further subdivided into two other categories. The first, uses growing cells within a medium, where they produce, from the feedstock or from an exogenous substrate added to the culture, the desired product. The second, uses resting cells centrifuged and resuspended in a reaction buffer, exogenous substrates are then supplied to those cells where the desired enzymatic reactions take place. The former subdivision, the growing cells, usually transcribes into a more productive scheme albeit at the cost of a more intensive process of purification of the product whereas the latter, resting cells, possesses the opposite drawback and benefit. Each strategy of free enzyme biocatalysis and whole-cell biotransformation bears their own benefits and obstacles, all of whom were outlined previously in Table 2 under section 1.5.1. Briefly, a whole cell process lends itself well to the overexpression of more than one recombinant enzyme and as such are prime candidates when considering several enzymes to generate a multistep reaction on a substrate. Furthermore, the cofactor machinery of the cell can be used to circumvent the expensive cofactor conundrum of free enzyme biocatalysis. Thus, compared to free enzyme biocatalysis, whole cell processes are seen as somewhat mitigating the cofactor problem associated with the latter. However, a whole-cell process is typically slower than a free enzyme process, this is mainly due to the barrier of the cell membrane which imposes its own diffusion rate between the substrate and the cell. Similarly, this same cell membrane also imposes another diffusion rate between the product and the cell which complicates its purification downstream and exposes the product to further modifications due to the plethora of other enzymes whom may react with the product. The cellular environment of the cell also offers a major benefit to the recombinant enzyme used in that it provides a much more robust environment than a free enzyme process would. Yet, when it comes to CYP based whole-cell strategies a distinction from the traditional advantages and drawbacks must be made especially in regards to stability. While enzymes are usually thought of as safe and stable in a whole-cell process [379], this is less true for CYP based process. Indeed, when the stability of a CYP153A/BM3 reductase fusion construct was followed throughout the whole-cell biotransformation of dodecanoic acid methyl ester to its hydroxy products, roughly 16 % of the initial concentration of CYPs were lost after a 30-hour incubation period [256].

Inversely, following 28-hour of incubation, hydrogen peroxide concentration increased from 20 μM to 240 μM . That said, the relationship between CYP stability and hydrogen peroxide has been clearly established with regards to productivity, as adding an enzymatic component protecting CYPs from hydrogen peroxide, such as a catalase for instance has been shown to mitigate CYP deactivation [380]. In a another publication, the CYP153A/BM3 reductase fusion construct was further assessed where both stability and density were monitored during the biotransformation of dodecanoic acid to ω -OH-dodecanoic acid in a 1-L bioreactor [381]. There, while cell density remained constant throughout the bioconversion, 50 % of the correctly folded enzyme was lost after only 2 hours, thus the loss of functional CYPs could not be attributed to cell death. In 100-ml flask reactions, the bioconversion of dodecanoic acid to ω -OH-dodecanoic saw this product further oxidized to its corresponding α,ω -dicarboxylic acid. In fact, after 1-hour, all of the substrate was converted to product but after 4 hours close to 18 % of products was the α,ω -dicarboxylic acid. While the formation of secondary products is undesirable, it is to be expected in a whole-cell process. CYPs however, add an additional layer to this inconvenience in that they may overoxidise their products. The last two publications using the CYP153A/BM3 reductase fusion construct are seminal in that they highlight several limitations intrinsic to a CYP based whole-cell process as well as limitations common to a whole-cell processes. Specifically, these are: the limited stability of CYPs within the cell due to hydrogen peroxide production, the overoxidation of products by CYPs, the need for additional cofactors besides the endogenous sources, carrier solvent or permeabilization agent limitations in regards to enzyme folding/cell toxicity and enzyme inhibition by either substrate or product.

The importance of stabilizing CYPs in whole-cell system was also highlighted when human CYP3A4 was co-expressed with the human molecular chaperone HDJ-1 in *E. coli* which increased catalytic activity and CYP3A4 intracellular concentration respectively 15 and 3.3-fold [382]. In a different publication, *S. cerevisiae* cells overexpressing the type III membrane protein ICE2p alongside CYP71D55 from *Hyoscyamus muticus* and the CPR of *A. thaliana* (AtCPR) were found to enhanced (+)-valencene hydroxylation to trans-nootkatol by up to 50% compared to strains using the native promoter of ICE2p after 72 hours fermentations, reaching 30 mg/L [383]. This seems to be in part a result in the stabilization of CPRs over time by IC2P has at the 24 hours timepoint in fermentations overexpressing ICE2P the reductase activity, compared to the strains using the native ICE2P promoter, improved by a factor of 2.94 fold for constructs expressing CYP71D55 and AtCPR in *Saccharomyces cerevisiae*. Furthermore, a similar effect was found when CYP71D13 from *Mentha piperita* with AtCPR as well as CYP2D6 with human CPR were used alongside ICE2P overexpression thus enhancing reductase activity after 24 hours by 3.73-fold and 3.3-fold respectively. Immunoblot

analysis also confirmed that strains overexpressing ICE2P retained higher content of both CYP and CPR after 48- and 72-hour fermentations.

Interestingly, a screen aiming to identify genes whose overexpression benefited whole-cell CYP reactions in the yeast *Pichia pastoris* expressing CYP71D55 from *H. muticus* identified the homologous recombination DNA repair gene RAD52 as a candidate. It had, when overexpressed, a remarkably positive effect on the bioconversion of (+)-valencene to trans-nootkatol where it led to an increase in productivity of 39.9 mg/L to 62 mg/L corresponding to an increase of 55 % [384]. The authors go on to argue that the beneficial relationship between RAD52 and CYP71D55 might be attributed to the stabilizing effects of efficient homologous recombination following damage by oxidative species which are known to occur during CYP reactions. It may well be that oxidative byproducts generated in CYP reactions not only threaten CYP stability but also the integrity of other cell centric processes such as genome integrity.

To this day, several whole-cell articles about CYPs have been written and attempt to deal in one way or another with these challenges or, more broadly, to enhance the productivity of their cell cultures despite these aforementioned challenges. Progress in tackling whole-cell biotransformation technology in the context of CYPs is further discussed below. At the very end of chapter 1.5.4, all product output data mentioned in this same chapter is summarized within Table 4.

1.3.1 Permeability

Cells can somewhat shield enzymes from organic solvents and are generally considered as being a more potent vehicle of stability than a free enzyme system [379], thus it enables exogenous insoluble substrates and their accompanying organic cosolvent to be added at a concentration higher than what a free enzyme process would allow [385]. Regardless of the latter benefit, substrate availability remains an issue for whole-cell biotransformation, that is typically tied to slower reaction rates which stems from the difficulty substrates encounter in passing the cell membrane [386]. Compounded to that problem is that of difficult product recovery which can be attributed as well to the permeability of the membrane effectively retaining products inside the cell and complicating downstream processing associated with product recovery. In one such example, the bioconversion of oleanolic to queretaroic acid was attempted in *E. coli* cells expressing CYPmoxA from *Nonomuraea reticatena* but hindered by the permeability of the membrane as only 3.3 % of the oleanolic acid

substrate applied to the system could be converted, unlike the free enzyme reaction where 17 % of the initial 200 $\mu\text{g/mL}$ of oleanolic acid could be converted to product [387]. When faced with such a problem, it can be a viable alternative to switch instead to a free enzyme system as is the case in the aforementioned example, otherwise, strategies to pass the cell envelope can be explored and implemented.

In the context of CYPs, apart from substrates and products, decoy molecule permeability has been investigated for travel through the cell membrane. When PFC9, pelargonic acid saturated with fluorine atoms, was supplied to *E. coli* cells expressing BM3 in the presence of benzene, a substrate for which wild type BM3 has little activity unless in the presence of a decoy molecule, a marginal increase in productivity was observed going from 40 μM without PFC9 up to 60 μM of phenol in the presence of decoys in 5 hour reactions [239]. This implied that the fluorinated decoy PFC9, despite being largely similar to a fatty acid for which cells have membrane transporters, could not readily enter the cells. Adding a phenylalanine moiety to the carboxy side of PFC9 yielded the decoy PFC9-Phe for which 190 μM of phenol could be produced by the cells after a 5-hour incubation with the cells. Removing the fluoride from the PFC9-Phe decoy yielded the compound C9-Phe for which 790 μM of phenol was produced in the same incubation conditions thus implying that the fluorination was largely at fault for the poor permeability of the original decoy PFC9. After testing several variations of amino acids and alkane chain combinations the decoy compound C7-Pro-Phe was found to pass the cell envelope best and gave a turnover of 3810 μM of phenol after a 5-hour incubation period converting 38 % of the initial 10 mM of benzene supplied to the whole-cell reaction. Similarly, the same permeability problem was encountered when the conversion of isophorone to 4-hydroxyisophorone was attempted with *E. coli* cells expressing either the CYP101A1 variant WFAL or the BM3 variant RLYFIP with either of the decoy molecules PFC9 and PFC10 having no effect whatsoever on product turnover [231].

To bypass a cell's membrane, a common strategy is to use chemicals which permeabilize the lipid bilayer of the membrane without wholly disrupting the cell. In one such case, CYP105A1 from *Streptomyces griseolus* was expressed in *E. coli* cells with the substrate abietic acid where CTAB, Polymyxin B, toluene, Tween 20 and EDTA were tested as permeabilizing agents [388]. There, the absence of any permeabilizing agents yielded 30 μM of the product 15-hydroxyabietic acid whereas the best agent, polymyxin B provided a yield of 95 μM following a 24 hours incubation period. In a similar case, this time using CTAB to permeabilize the cell envelope, the whole-cell conversion in *E.*

E. coli cells expressing CYPsb21 from *Sebekia benihana* raised the turnover of cyclosporine A to γ -hydroxy-*N*-methyl-L-Leu4-Cyclosporine A from 0 % without CTAB to 45.4 % of an initial 100 μ M of cyclosporin A after a 12 hours of incubation period [389].

In a similar case, 2-hydroxypropyl- β -cyclodextrin was used both as a solubilizing and permeabilizing agent to aid in the conversion of the substrate (+)- α -longipinene to 12-hydroxy- α -longipinene in a whole-cell process using *E. coli* cells and CYP264B1 from *Sorangium cellulosum*. Use of this permeabilizing agent effectively raised product turnover from 21 to 37.2 mg/L [390]. Yet in another comparable case, this time using the yeast *Schizosaccharomyces pombe* in which the human CYP21 was expressed to convert 17- α -hydroxy-progesterone to 11-deoxycortisol, the permeabilization agents triton x-100, CTAB and Tween 80 were tested [391]. There, compared to the control reactions lacking a permeabilization agent, triton x-100 had no effect on productivity, CTAB destroyed the biocatalysts and tween 80 improved by 50 % product turnover. In the end, this particular biotransformation could boast a turnover just under 225 μ M of 11-Deoxycortisol following a 10-hour incubation period. In a following publication also using fission yeast, Triton X-100 was tested as a permeabilization agent and was found to be best suited at a concentration of 0.3 % v/v. There, it was found that for the hydroxylation of testosterone by human CYP3A4, product volumetric production rate reached 0.45 mM/day for untreated cells and 3.77 mM/day for Triton X-100 permeabilized cells, an 8.4 fold improvement [392].

A different strategy by which the cell envelope can be crossed in whole-cell processes is to express a transporter whom is able to transport the substrate and/or the product across the cell envelope. Where CYPs are concerned, transporters capable of transporting fatty acid like substrates are the most common. For example, when the fusion construct of the CYP153A G307A from *Marinobacter aquaeolei* and the BM3 reductase domain were used in *E. coli* cells to convert methyl dodecanoate to ω -hydroxy methyl dodecanoate the outer membrane transport system (AlkL) from *P. putida* GPo1 was co-expressed in the cells as well [256]. Compared to a system lacking the AlkL transporter product output was improved three-fold at up to 4 g/L. The AlkL transporter was also described in another publication where it was used to facilitate the transport of (S)-limonene into *E. coli*'s cytoplasm where it could be hydroxylated by CYP153A6 from *Mycobacterium sp.* HXN-1500 to (S)-perrilyl alcohol [393]. The addition of the AlkL transporter in this instance raised productivity of (S)-perrilyl alcohol from 2.88 g/L to 5.96 g/L increasing turnover of product by a two-fold factor. In another similar example, BM3 was co-expressed in *E. coli* cells with the alkane transporter from

Pseudomonas oleovorans in order to facilitate the efficient conversion of pentadecanoic acid to 12-, 13-, and 14-hydroxypentadecanoic. There, the presence of the transporter roughly doubled product output up to 1 mM [394]. What's more, the transporter also displayed its versatility by transporting as well C12 to C18 fatty acids into the cells.

Moving away from transporters but staying in cell engineering strategies to bypass the limitations of the cells to take up substrates, CYP105D1 from *Streptomyces griseus* was appended at its amino acid terminus the secretory signal of *E. coli*'s alkaline phosphatase targeting it to the periplasmic space within *E. coli* cells [395, 396]. In the periplasmic space, CYP105D1 displayed an activity of 0.067 min^{-1} in erythromycin N-demethylation and of 0.072 min^{-1} in benzo[α]pyrene 3-hydroxylation whereas, in comparison, when the same CYP was targeted to the cytoplasmic space, activity slowed to 0.058 and 0.056 min^{-1} , respectively. This particular strategy is beneficial in that it limits the thickness of cell barrier substrate and product need to cross. However, it is also limited to gram-negative bacteria such as *E. coli*.

1.3.2 Cell surface display

The strategy to express CYPs to the periplasmic space has been pushed further where instead CYPs are sent to the outer membrane on the surface of the cells facing towards the buffer where the substrates are located. While not strictly speaking a permeabilization strategy, cell surface display tries to address the same issue of substrate availability. This was first attempted with the redox partner of CYP11A1, Adx, when it was expressed to the outer membrane of *E. coli* through the signal peptide and the translocation unit of the adhesin involved in diffuse (AIDA), to anchor it to the outer membrane [397]. Then, CYP11A1, AdR, NADPH, glucose and GDH were supplied exogenously to the reaction mixture along with the substrate cholesterol to yield pregnenolone with the activity of the system reaching 0.0035 min^{-1} (on a CYP11A1 molar basis), but being in the same range as detergent permeabilized whole-cell CYP11A1 assays. The authors also go on to clearly demonstrate that, on the outer membrane, Adx dimerizes and recruits both CYP11A1 and AdR to its side. In other work, BM3 was expressed on the surface of *E. coli* using the ice-nucleation protein from *Pseudomonas syringae*, there again with an external source of cofactor, NADPH, being added to the reaction [398]. Comparison between surface displayed BM3 and purified BM3 favored the latter with activities for NADPH consumption in the presence of the substrates lauric acid, arachidonic acid and 12-pNCA going up to 650, 2100 and 2700 min^{-1} , respectively, corresponding to 3.1, 1.45 and 4.29-fold greater activities than on cell surface displayed BM3. Furthermore, purified BM3 and cell surface

BM3 displayed an activity of 110 min⁻¹ and 72 min⁻¹ respectively for 12-pNCA. No coupling or TON data is explored in this study and although the kinetic data would suggest that coupling efficiency is greater in the cell surface strategy for BM3 with 12-pNCA it is unclear as to whether or not this would translate into greater productivity for the cell surface stratagem. In a separate work, the human CYP3A4 was expressed to the cell surface of *E. coli* through a fusion with AIDA [399]. Reactions were initiated in the presence of exogenously supplied recombinant human CPR, NADPH, glucose, GDH and the substrate testosterone. The conversion of testosterone to 6 β -hydroxytestosterone was conducted successfully in CYP3A4 cell surface preparations however only reaching roughly a tenth of the products generated by purified CYP3A4. In another comparable publication by the same group, CYP106A2 from *B. megaterium* was expressed to the surface of *E. coli* cells again using AIDA as an anchor with the objective to hydroxylate 11-deoxycorticosterone, imipramine and abietic acid to their respective products 15 β -hydroxy-deoxycorticosterone, desipramine and 12-hydroxy-abietic acid [400]. Relying again on external cofactors, reactions were supplied with NADPH, NADP⁺, glucose and GDH. They then demonstrated by HPLC that they were indeed capable of synthesising the three aforementioned products but did not provide clear kinetic or productivity data otherwise. In other work by the same group, human CYP1A2 and CPR were co-expressed to the cell surface of *E. coli* using AIDA yet again to convert, along with exogenously supplied NADPH, 7-ethoxyresorufin to 320 nM resorufin in 40 hours with cells set at an OD₅₇₈ of 40 in the reaction [401].

This strategy shuffles the benefits and drawbacks of a whole-cell approach. On one hand access of the substrate to the biocatalyst is no longer a problem and the difficulty in extracting the products from the cells is largely non-existent if the products are never trapped within the cells. What's more since the reaction takes place outside the cell both substrate and product are unlikely to enter metabolic pathways thereby adding unwanted secondary metabolites to the reaction. On the other hand, the protective qualities of whole-cell reactions as well as the cofactor regeneration apparatus are no longer in play when this strategy is used. Yet it should be noted that the membrane environment to which CYPs are here constricted to could somewhat reproduce the microenvironment that make immobilized enzymes more stable.

1.3.3 Cofactor regeneration

The host cell's metabolism enables whichever reactions taking place within it to utilize the natural cofactor generation pathways present [379]. In normal conditions, there is ample reserve of cofactors within a cell to supply its requirements. However, once modified genetically to overproduce

a given molecule that requires such cofactors, it may well induce a shortage of the latter, which then becomes a limiting step of the process. This phenomenon is also contradictory with what is assumed to be a given and natural benefit as to the electron source of a whole cell system as highlighted in Table 2. Nevertheless, to overcome this problem, a dehydrogenase enzyme is commonly engineered into the host strain to accommodate the energy demands of this recombinant process [402–405].

In work where the BM3 variant F87V was used to convert 1-hexene to 1,2-epoxyhexane in resting *B. subtilis* cells, the BA-GDH from *Bacillus amyloliquefaciens* was added to the scheme as it is able to recycle both NADH and NADPH [406]. The consequence of the co-expression of both BM3 F87V & BA-GDH was a 53% increase in product specific synthesis rate, from 0.96 $\mu\text{moles/gDCW/min}$ (when BM3 F87V was expressed without BA-GDH) up to 1.47 $\mu\text{moles/gDCW/min}$ with BA-GDH. In other work by the same group, the BM3 variant F87V was used to convert n-octane to 2- & 3-hexanol, there again using BA-GDH to recycle cofactors in resting *B. subtilis* cells. Here, the authors go on to establish that BA-GDH possesses increased pH, temperature and organic solvent tolerance when compared to BS-GDH from *B. subtilis* [407]. As they tested their whole-cell system a comparison in yield was made with the system lacking BA-GDH, roughly providing half the output of what the other cell process co-expressing BA-GDH could provide, which tallied roughly at 2000 μM of both 2- & 3-hexanol after a 3-hour incubation at 30 °C. Other papers report similar findings in whole-cell CYP schemes where the addition of a dehydrogenase increases product turnover. In one case for instance, co-expressing CYPsb21 and GDH A in *E. coli* cells increased product turnover of cyclosporine A to γ -hydroxy-*N*-methyl-L-Leu4-Cyclosporine from 45.4 % to 53.5 % of an initial 100 μM of cyclosporin A subsequent to a 12 hour incubation period [389]. When CYP105A1 from *S. griseolus* was co-expressed with LB-ADH in *E. coli* cells, this provided a net increase of 5 and 10 % in total production and formation rate of the product 15-hydroxyabietic from abietic acid compared to cells only expressing CYP105A1 [388]. In the first two cases described with the BM3 mutant F87V product specific synthesis rate and product output doubled as a result of adding a dehydrogenase to recycle NADH and NADPH. However, in the last two cases, although the overexpression of a dehydrogenase, GDH A and LB-ADH, had a positive effect on the whole-cell process, the effect was limited only enhancing product turnover by 8.1 and 5 % respectively. Thus, there is much variability on the intensity in which the whole-cell process is enhanced by adding a recycling enzyme suggesting that each case is unique and that cofactor reserves within cells may or may not be the main bottleneck of the process.

In different work, 2-propanol was used both as a solvent to dissolve abietic acid but also as a substrate for LB-ADH. An added benefit to alcohols as substrates for ADH enzymes resides in their ability to freely diffuse in and out of cell membranes but, on the other hand, adding too much of such solvents eventually becomes deleterious to the cells as well. In this respect, another avenue explored to accommodate the energy demands of the cells is to add the dehydrogenase's own substrate to the reaction mixture. For example, a clear relationship was established between, on one end, increasing concentrations of glycerol present in whole-cell *E. coli* reaction mixtures using a glycerol dehydrogenase and, on the other end, the amount of camphor p450cam could convert to 5-exo-hydroxycamphor achieving either 20 or 75 % camphor hydroxylation with an added 5 % or 10 % (v/v) of exogenous glycerol in reactions mixtures containing 3 gDCW/L and 2 mM of camphor [408]. In this regard, strain engineering can be used to further bolster the ability of the cells to generate cofactors by allowing dehydrogenase substrates such as glycerol or glucose to pass through the cell envelope more effectively by adding a protein dedicated to facilitate transport across cell membranes. Such a strategy was attempted in *E. coli* cells with the glucose facilitator from *Zymomonas mobilis*, glucose dehydrogenase-2 from *B. megaterium* (BM-GDH-2) and the BM3 variant QM in the hydroxylation of α -pinene to α -pinene oxide, verbenol & myrtenol [409]. Interestingly, BM-GDH-2 is also able to regenerate both NADH and NADPH. When compared to the host strain only expressing BM3 variant QM, the strain expressing all three aforementioned components, showed nine times higher initial α -pinene oxide formation rate and roughly a 9.6-fold higher yield of total products, at 32 mg/gDCW. Although this specific strategy was not attempted with glycerol in a CYP whole-cell process, such a facilitator exists in nature for glycerol as well, dubbed glpF, in the commonly used microbe *E. coli* [410–412]. In addition, unlike 2-propanol, glycerol is not toxic to the cells but its diffusion in and across the cell membrane is limited.

In an innovative strategy, the alkane-oxidizing NADH dependent CYP153A from *Polaromonas hydrogenivorans* sp. JS666 was used for the selective oxidation of n-octane to 1-octanol in recombinant *P. putida* strain KT2440 with the unique NAD⁺-reducing hydrogenase from *Ralstonia eutropha* H16 that oxidizes H₂ which, unlike other dehydrogenase substrates such as glycerol and 2-propanol, diffuse effectively across cell membranes and is not cytotoxic to cells [413]. This system was able to provide a productivity towards the conversion of n-octane to 1-octanol of 101 mg/L after 24 hours. Furthermore, if all secondary products were included to 1-octanol production (2-octanol, octanal and octanoic acid), a productivity of 165 mg/L could be reached after 24 hours. In this study however, no comparisons were made to a system expressing a more traditional dehydrogenase or simply without a dehydrogenase co expressed at all. In another unique scheme to supply cofactors to

a whole-cell system a combination of light, eosin Y, which acts as a photosensitizer binding specifically to the heme domain of both bacterial and human CYPs, and triethanolamine whose role is that of an electron donor, were supplied to the cytoplasm of *E. coli*. When photosensitized under light illumination, eosin Y uses triethanolamine as a sacrificial electron donor to drive the reaction forward. This provides an inexpensive source of cofactors through light and triethanolamine and forgoes the necessity of redox partners, a feature particularly useful for CYPs whose redox partners are unidentified. This particular strategy was exploited successfully with the BM3 variant m2 in *E. coli* cells where a TON of 16 for the conversion of 7-ethoxycoumarin to 7-hydroxycoumarin could be observed [414]. In another innovative example, two dehydrogenases were used, RE-ADH from *R. erythropolis* and LB-ADH, to recycle NADH and NADPH respectively [415]. In that particular instance, the BM3 mutant 19A12, a mutant with 18 substitutions to the oxidase domain of BM3 which was originally developed for the oxidation of short chain alkanes [220], was paired with LB-ADH. Another 19A12 mutant, this time harbouring additional mutations R966D/W1046S to its reductase domain in order to utilise NADH more efficiently [306], was paired with both LB-ADH and RE-ADH. Finally, yet another pairing used in this work was with wild type BM3 and LB-ADH. There, after 24-hour reactions, the titers for conversion of cyclooctane to cyclooctanone were measured with WT, 19A12 and 19A12^{R966D/W1046S} reaching, 169, 481 and 640 mg/L respectively. This would suggest that the ability to use both cofactors instead of a single one has significant effect on product output. Of note in this work as well is that both dehydrogenase used, LB-ADH and RE-ADH, not only recycle their respective cofactor but also further oxidise cyclooctanol to cyclooctanone following the hydroxylation of cyclooctane to cyclooctanol by BM3. On this particular topic, it is interesting to note that several papers which explore whole-cell CYP reactions use an ADH not only to supply cofactors but also to help assist in the synthesis of products in cascade or multistep reactions [415–418].

Besides co-expressing a dehydrogenase alongside a CYP, strains can be further engineered to enhance the energy pool available to the CYPs inside the cells. In one such case, four *E. coli* genes were knocked out, namely two NADH dehydrogenases to skew the energy pool away from NADH and towards NADPH through the native transhydrogenase gene which can catalyze the conversion of NADP⁺/NADH to NADPH/NAD⁺ in either direction [419]. The two other genes knocked out in that work were *adhE* and *ldh* whose elimination lead to the removal of two fermentation pathways, ethanol and lactate. This was accomplished with the goal of redirecting the energy demands of the cell away from these metabolic pathways and towards the engineered CYP pathway for propanol production using the BM3 variant *PMoR2*. Taken together, all these genetic modifications resulted in about a two-fold increase in product per glucose yield (0.98±0.21).

1.3.4 Cascade reactions

Cascade reactions are reactions whereby multiple catalytic steps are required by enzymes to obtain the desired product. In this respect, whole-cell reactions lend themselves better to this endeavor. This is because whole-cell system enables the user to avoid the arduous work required to individually produce and purify each required enzyme. In the context of cascade reactions CYPs possess an interesting feature, which is their ability to oxidize not only their substrates but also some of their products, sometimes more than once. While this feature can lead to undesired secondary metabolites it can also be exploited. For instance, in resting *E. coli* cells where the BM3 variant A82F/A328F sequentially oxidized cyclohexane to cyclohexanol to cyclohexanone to 2-hydroxycyclohexanone. Thereafter 3 different butanediol dehydrogenases were tested to stereoselectively convert 2-hydroxycyclohexanone to either (S,S)-, (R,R)- or (R,S)-cyclohexanediol [420]. In similar work, in resting *E. coli* cells the BM3 variant 19A12 and CM1 were used to convert cyclooctane to cyclooctanol and then using two alcohol dehydrogenases, RE-ADH and LB-ADH, to both regenerate NADH/NADPH and to convert cyclooctanol to cyclooctanone [415]. This provided a TON of 24363 for cyclooctanone. The same group also used this very strategy of a whole-cell double-oxidation cascade with integrated cofactor regeneration in resting *E. coli* cells to convert n-heptane using BM3 variant 19A12 and CM1 alongside the same two dehydrogenases to yield different distributions of isomers of heptanol and heptanone as products [416]. Yet another similar strategy was devised when CYP154A8 from *Nocardia farcinica* was expressed in resting *P. putida* cells alongside LB-ADH which not only supported cofactor regeneration but also oxidized stereoselectively the unwanted (R)-2-octanol to 2-octanone leaving behind the desired product (S)-2-octanol [417]. This strategy lead to an impressive TON of 10 300 for (S)-2-octanol. Finally, a comparable strategy was devised when triacylglycerols were converted first to their three corresponding carboxylic acids by the *Thermomyces lanuginosus* lipase Tll and then subjected to the fatty acid decarboxylation activity of CYP152L1 from *Jeotgalicoccus* yielding the corresponding 1-alkene of each carboxylic acid [418]. Using resting *E. coli* cells, this strategy generated up to 0.69 mM or 126 mg/L of 1-tridecene using triacylglycerols as a substrate.

1.3.5 Biphasic systems

The use of a two-phase water/water-immiscible organic solvent system, or a biphasic system, has already been explored and explained previously in the context of an enzymatic process at section 1.5.3. There, the water-immiscible organic phase acts as a sort of reservoir for both substrates and

products which, in turn, selectively accumulate in this phase thereby facilitating product removal. This latter benefit is especially important in whole-cell systems as this facilitates the heavy processing work tied to the purification of the products which is a key drawback in general for whole-cell biotransformations. What's more, the products of CYPs are often more hydrophilic, polar and reactive than their often-insoluble substrate counterparts and are thus sometimes toxic to bacteria. An example of this, was when 5 % (v/v) n-octane was used both as a an organic phase and a substrate source to produce octanoic acid in *E. coli* cells [421]. There, it was established that increased concentrations in the aqueous phase of the water soluble product octanoic acid, was toxic to *E. coli* cells, as most short chain fatty acids are [422]. On the other hand, both long- and medium-chained fatty acids are not toxic to *E. coli* cells [423], however aliphatic hydrocarbons once oxyfunctionalized become toxic to cells [424], as is the case for octanoic acid. Therefore, the continuous extraction of such products to the water-immiscible layer of a biphasic system can be beneficial to the whole-cell bioconversion process in regards to cell toxicity. Where CYPs are concerned, this strategy was employed with CYP153A from *Marinobacter aquaeleoi* in *E. coli* cells, where the substrates lauric acid and methyl laurate were used both as hydrophobic layer of the biphasic system and as the substrate source with yields of 1.2 g/L and 4.0 g/L for ω -hydroxy lauric acid and ω -hydroxy methyl laurate respectively [256]. In different work, utilizing BM3, the comparison of the efficiency by which *E. coli* cells achieve the bioconversion of 4-hexylbenzoic acid to its products, ω -1 & to ω -2 hydroxybenzoic acid, was made between a whole-cell reaction using a biphasic hexadecane/water system and a reaction lacking one. For the former, when using the biphasic system, activities were enhanced by a factor of 2 going from 2.1 min⁻¹ to 4.1 min⁻¹. This translated in the conversion of an initial concentration of 5 mM of hexylbenzoic acid to its hydroxycounterparts to 3 mM (60%) for a whole-cell system without a biphasic system and of 4.3 mM (86%) for the biphasic system after a 4 hour incubation period [425]. In a more unique publication [426], the monooxygenase p450pyr from *Sphingomonas sp.* HXN-200 harbouring the I83H mutation was selected for the sufoxidation of five substrates in an aqueous/ionic liquid biphasic system using resting *E. coli* cells. A total of 4 ionic liquids were tested to establish their toxicity towards the *E. coli* cells with only trihexyltetradecylphosphonium bis(trifluoromethylsulfonyl)imide demonstrating no apparent toxic effect on the cells. Indeed, growth rate of the cells with and without this ionic liquid were almost identical. The greatest productivity for the five reactions assessed in this work could be attributed to the biphasic scheme were the conversion of the substrates thioanisole, 4-fluorothioanisole, ethyl phenyl sulfide, 4-methylthioanisole and *p*-methylthioanisole to its corresponding products provided an increase from 9.4 to 20 mM for (R)-phenyl methyl sulfoxide, 1.9 to 9.9 mM for (R)-4-fluorophenyl methyl sulfoxide, 5.4 to 16 mM for

(R)-ethyl phenyl sulfoxide, 4.2 to 22 mM for (R)-methyl *p*-tolyl sulfoxide and 5.7 to 24 mM for (R)-methyl *p*-methoxyphenyl sulfoxide, roughly a 2 to 5-fold increase.

While it does not seem a complex task at first glance, the choice and amount of immiscible solvent is not clearly defined nor are general guidelines for the proper use of a biphasic system for whole-cell process clearly established [405]. For example, when a biphasic system using isooctane as the hydrophobic layer in a whole-cell *E. coli* process for the bioconversion of camphor by CYP101A1 no products could be detected in the hydrophobic layer as it had transformed into a gel over time effectively preventing extraction [408]. Be that as it may, two publications lay out a set of criteria by which to guide the choice of the organic phase to be used in the biphasic whole-cell process. In one of these two publications, in order to mitigate problems of microbial toxicity associated to terpenoid substrates [427], several hydrophobic solvents were tested in a biphasic whole-cell process using BM3 variant QM in *E. coli* cells to convert α -pinene to α -pinene oxide, *trans*-verbenol & myrtenol [409, 428]. Organic layers of n-Decane, dodecane, corn oil, olive oil, oleic acid, diisononyl phthalate, and butyl stearate to 17 % (v/v) were tested, all of whom met the criteria of low water solubility, chemical stability, thermal stability and high flashpoints. Low water solubility ensures that the organic layer does not destroy the cell, the CYP or that it be metabolised by either of those thus generating unwanted metabolites later in the product purification procedure. Chemical and thermal stability ensures as well the generation of unwanted metabolites. A high flashpoint was selected as a safety precaution criterium. Organic solvents were evaluated for their ability to react with CYPs and consume NADPH as a cofactor thereby producing unwanted metabolites. In this regard, the organic solvent diisononyl phthalate proved the least reactive with NADPH as this reaction activity was roughly of 0. Partition of the products of the reaction were investigated as well in the 17 % (v/v) diisononyl phthalate biphasic system where the products verbenol and myrtenol showed similar partition coefficients, 77.5 and 74.3, thus highly favouring the organic phase. The third substrate, α -pinene oxide, showed only trace amounts in the aqueous phase by GC-MS analysis suggesting that mostly all of α -pinene oxide migrated to the organic phase. The toxic effects of diisononyl phthalate were investigated as well by measuring the specific glucose consumption in *E. coli* cells. At 5 % (v/v) diisononyl phthalate, glucose consumption dropped to 42.5 % of the original rate whereas at 50 % (v/v) of diisononyl phthalate the rate dropped to 20 % of the original consumption rate, revealing that although the organic solvent phase decreased the vitality of cells to an extent, those same cells could handle very high content of diisononyl phthalate as an organic phase. In the end, the system was able to yield 32 mg/gDCW of all three products combined together. The other publication where criteria for a good hydrophobic solvent for a biphasic system were tested utilised the yeast *Yarrowia lipolytica*

to co-express either human CYPs 2D6 or 3A4 with the human CPR in order to produce respectively 1-hydroxybulfuralol or 6 β -hydroxyprogesterone [429]. There, a total of 10 water immiscible organic solvents were tested. Initially, two of those, toluene and 1-octanol were chosen for their good solvent properties. They in fact demonstrated the highest solubility of progesterone. They, however, also displayed a level of toxicity too high to the cells. Next, the solvents bisethyl hexyl phthalate and dibutyl phthalate were chosen for their inert nature to avoid the risk of reacting either with the cell's own metabolism pathways or the CYPs themselves, generating unwanted metabolites in the process. The final 6 solvents, 1-decanol, 1-dodecanol, methyl laureate, ethyl oleate, n-decane and n-dodecane were added to the lot of solvents to be tested with the possible caveat that they may represent a potential carbon source or feedstock for *Y. lipolytica* thereby possibly producing unwanted metabolites. These last 8 solvents did not present any obvious toxic effect on the cells but nevertheless, both n-decane and n-dodecane would not be selected from the list of solvents as their ability to dissolve progesterone was considered too weak. Finally, product formation rate for each of the last 6 solvents was compared relative to a whole-cell system lacking a hydrophobic layer with the substrate ethyl oleate improving the activity by a factor of 10 % on average. However, when productivity was compared between a whole-cell process in an aqueous phase and a biphasic system using ethyl oleate as the immiscible phase, the latter generated after a 96 hours incubation period, roughly 230 μ M of hydroxyprogesterone, a 4.6-fold improvement in product output compared to process lacking an immiscible phase.

Thus, guidelines to consider in choosing the right solvent for a biphasic system may include low water solubility, chemical and thermal stability, high flashpoints, solvent power, cell and CYP toxicity, whether or not it can be accidentally used as a substrate by either the CYP or the cell, and finally activity or yield in the presence of the solvent.

1.3.6 Alternative microorganisms

For a whole-cell process selecting the adequate host cell is essential for a productive and efficient biotransformation. All organisms have their intrinsic strengths and weaknesses with eukaryotic organisms typically favored when covalent post-translational modifications are essential [430]. In regards to CYPs, several human, animal and plant CYPs are of industrial interest and although there is evidence for covalent post-translational modifications (glycosylations, phosphorylations, nitration or ubiquitination) [431], there is exhaustive evidence that these CYPs can perform their catalytic roles flawlessly in bacterial systems particularly in *E. coli* without these post-translational modifications.

All CYPs considered, the choice host of production, be it for free enzyme biocatalysis or for whole-cell bioconversion, has been *E. coli*. This bacterium offers a set of beneficial features that usually makes it the default host cell before considering other hosts, these features include fast growth kinetics, high cell density cultures, inexpensive simple culture media, the wealth of knowledge associated to this particular bacterium, quick plasmid transformation procedures as well as the large libraries of *E. coli* plasmids and mutants [432]. Where CYPs are concerned *E. coli* has the rare distinction of lacking any CYPs naturally encoded in its genome [26] this facilitates performing a ferrous-CO assay as no other indigenous CYPs can be detected. In addition, this means that no unwanted secondary products can be generated by a native CYP. What's more, there is evidence that native Fvx and FdR from *E. coli* can support p450 activity [433]. Beyond *E. coli* several other host cells have been explored as possible platforms for CYP based whole-cell bioconversions.

Amongst those is the bacterium from which BM3 originated, *B. megaterium*, discovered a little over 130 years ago and heavily studied since the 1960s. This bacterium, much like *E. coli*, shares the distinction of being well researched as well as having being firmly established in many industrial biotechnological processes [434–436]. In a fairly recent paper, CYP105A1 from *S. griseolus* was used in a whole-cell *B. megaterium* process to produce the 3-cyclohexyl-hydroxy derivatives from the hypoglycemic drugs glibenclamide and glimepiride. In this work, according to the research group of Dr Rita Bernhardt from Saarland University in Germany, a group specialized in whole-cell processes, the choice of the host cell was first based on the fact that it is nowadays a well-established gram-positive production platform [437]. In contrast to *E. coli*, a gram-positive bacterium such as *B. megaterium* lacks the additional outer membrane characteristic of a gram-negative bacteria. Furthermore, there is clear evidence that the outer membrane of *E. coli* impedes on the intake of hydrophobic substrates [438] thus one less membrane reduces the substrate availability problem associated with whole-cell processes. In addition, the low intrinsic protease activity, the simple cultivation media requirements and, unlike *E. coli*, the ability of *B. megaterium* to stably replicate and maintain recombinant plasmids for a long time even without the selective pressure of antibiotics makes it an ideal feature for long incubations in whole-cell processes [434]. In the best conditions, the authors were able to convert 25 mg of glimepiride in 3.5 hours and 25 mg of glibenclamide in 12 hours to their respective hydroxy products. The initial scheme of production included the Fdx Etp1 and the FdR Arh1 from the fission yeast *S. pombe*. Interestingly, control whole-cell reactions lacking these redox partners yielded the same amount of products, suggesting that *B. megaterium*'s own endogenous redox components were both compatible and sufficient to drive these reactions forward. In another publication where *B. megaterium* was chosen as a host strain, the native CYP106A2 [439]

was used for the bioconversion of 11-keto- β -boswellic acid (KBA) to 15 α -hydroxy-KBA since boswellic acids in general have been shown to be commercially relevant to the pharmaceutical industry [440]. The decision for this particular host strain was mainly informed by the more permeable nature of gram-positive bacteria. Here, once bioconversion reactions relied on recombinantly expressed rather than endogenously induced CYP106A2, volumetric productivity increased 15-fold to 560.7 mg/L/day of 15 α -hydroxy-KBA. As *B. megaterium*'s genome encodes several different CYPs [434–436], the bacterium was used in two subsequent publications by the Bernhardt group as a host cell for whole-cell bioconversion processes to establish the hydroxylase activity on hormones and vitamin D₃ (VD₃) respectively for CYP106A2 [441] and CYP109E1^{I85A} [442]. For CYP106A2, using dehydroepiandrosterone as a substrate resulted in a volumetric yield of 438.4 mg/L and a reaction rate of 103 mg/L/h for the generation of the products 7 α - & 7 β -OH-dehydroepiandrosterone. On the other hand, for the production of 25-OH-VD₃ through CYP109E1^{I85A}, production rates of 45 mg/L/day could be reached in a whole-cell process.

In other work yet again by the Bernhardt group, *B. megaterium* was chosen as a host cell for its the carbon and energy storage-serving poly(3-hydroxybutyrate) (PHB) granules. These PHB granules were shown to be able to store and accumulate the highly hydrophobic substrate cholesterol which was fed to the cells. In addition, when human CYP11A1, which targets cholesterol for side cleavage (Figure 17), and its redox partner AdR were recombinantly expressed in *B. megaterium* both accumulated to the surface of the phospholipid/protein monolayer of the PHB granules [443]. To validate the beneficial effects of the PHB granules, yields were compared with a *B. megaterium* mutant strain lacking the PHB-producing polymerase subunit PhaC with the net result of a decrease in productivity of pregnenolone from cholesterol by CYP11A1 in the host cell from 22 mg/gDCW to 2.5 mg/gDCW after a 48-hour bioconversion. Again, by the Bernhardt group, the same PHB strategy would be further explored, this time using the human mitochondrial CYP27A1 to convert cholesterol, 7-dehydrocholesterol and VD₃ to 113 mg/L of 27-hydroxycholesterol, 80.8 mg/L of 25-hydroxy VD₃ and 122 mg/L of 25-, 26- or 27- hydroxy-7-dehydrocholesterol after an incubation period of 48 hours [444]. Yet another noteworthy element of interest in this work was that CYP27A1 was shown to localise to the PHB granules.

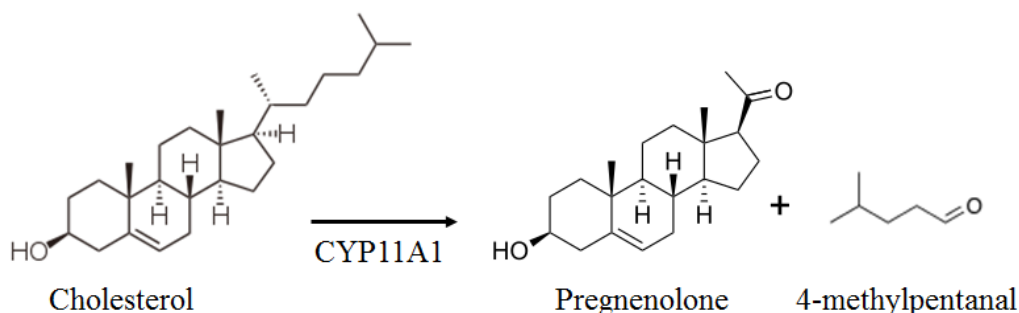


Figure 17: Cholesterol side cleavage by human CYP11A1 yielding the two products pregnenolone and 4-methylpentanal.

Staying within the *Bacillus* genus, another host cell explored as a potential candidate for a CYP based whole-cell system has been the gram-positive organic solvent-tolerant *B. subtilis* 3C5N which was developed as a whole-cell biocatalyst for the epoxidation of the toxic alkene, 1-hexene into a valuable intermediate for chemical synthesis, 1,2-epoxyhexane [406]. In this work, given the particular toxicity of the substrate, several other host cells were compared in regards to their viability against the substrate 1-hexene. The bacterial strains *E. coli* DH5 α , *B. subtilis* 168, *B. subtilis* 3C5N, *B. subtilis* GRSW2-B1, and *Pseudomonas putida* F1, were tested where 5 ml of cell suspensions for each strain with an initial cell density set to roughly 108 cfu/ml were incubated at 37 °C with increasing concentrations of the substrate 1-hexene for 12 hours. There the *B. subtilis* strain 3C5N was shown to be the most resistant strain, being able to withstand the highest 1-hexene concentration, 1 M, most likely due to its high level of tolerance towards organic solvents and a somewhat hydrophobic cell surface. In the end, the 3C5N strain expressing BM3 F87V could convert 1-hexene to 1,2-epoxyhexane at a yield of 2.2 mg/gDCW. In a following paper by the same group, the rationale for choosing *B. subtilis* for the whole bioconversion of hexane to 2- and 3-hexanol by BM3 F87V was yet again informed by the resistance of that host strain to the toxicity of both the aforementioned substrate and its resulting products [407]. There, 2- and 3-hexanol product concentration would reach 0.204 mg/L.

Another bacterial candidate that has been investigated as a potential production platform and selected for evaluation due to its increased tolerance towards organic solvents is the gram-negative bacterium *P. putida*. On the basis of this feature, *P. putida* was used as a host strain in the bioconversion of (S)-limonene to (S)-perillyl alcohol by CYP153A6 from *Mycobacterium* strain HXN-1500. However, the bacterium's own endogenous enzymes proved problematic as up to 26 % of the total amount of oxidized terpenes were that of the side products perillyl aldehyde and perillic acid [393]. For this reason, the *E. coli* strain W3110 was selected instead, mainly due to the fact that

it was not reported has having any enzymes acting on metabolites of limonene. In the end, 8 % of the total amount of products from strain W3110 corresponded to the unwanted side product perillyl aldehyde, with no traces of perillic acid produced. Comparing the two host cells, *P. putida* and *E. coli* showed a productivity towards (S)-perillyl alcohol synthesis of 4.37 and 5.96 g/L respectively. As seen here, while stability features are appealing for a whole-cell process, in addition to the knowledge base and tools available for well-established organisms such as *E. coli*, undesired side reactions tipped the balance in favour of the latter for the selection of a host strain. In a similar publication, which was discussed earlier, CYP154A8 from *Nocardia farcinica* was used in the bioconversion of n-octane to (S)-2-octanol in both *P. putida* and *E. coli* cells [417]. Here again, *P. putida* was chosen on the basis of its increased resistance towards organic solvents, more specifically the permeabilizing agent methyl- β -cyclodextrin, for which it provided greater productivity towards n-octane conversion to (S)-2-octanol compared to *E. coli* by a factor of 1.8. In a different paper, also previously discussed for its cofactor regeneration strategy, *P. putida* was selected as a host strain in part for its established resilience towards organic solvents for the whole-cell conversion of n-octane to 1-octanol [413]. There, using CYP135A from *Polaromonas* JS666, it was able to produce 101 mg/L of 1-octanol after a 24-hour incubation period. Here again, several side products were detected, 2-octanol, octanal and octanoic acid which, taken together, accounted for 64 mg/L of side products, or 38.8 % of all oxidised products, after the same 24-hour incubation period. Here as well, as the alternative organism chosen in place of *E. coli* is less studied and understood, deleting any endogenous enzymes responsible for these secondary products would require some additional research.

A criteria from which an organism can be selected in regards to CYPs can arise from the necessity of having compatible redox components in a host strain genetically close to the bacterium from which the recombinant CYP is taken, for instance CYP105A1 from *S. griseolus* was used alongside *B. megaterium*'s own endogenous redox components to generate products from glibenclamide and glimepiride [437]. This is particularly relevant for actinomycetes as of to date several of the new CYPs discovered are within that particular order [445–448]. In the next two publications to be discussed, the gram-positive host bacterium *S. lividans*, was selected in part due to the fact that amongst the *Streptomyces* genus it is one of the most researched and established as a host for recombinant protein expression [449, 450]. In the first publication, compatibility of the cellular environment between the recombinant CYP and that of the host strain was the reason for which the common host strain *E. coli* was discarded as a host cell in favor of a genetically closer one to that of the recombinant CYP. Indeed, when both CYP105A1 and B1 from *S. griseolus* were expressed in *E. coli*, only low levels of these enzymes could be detected, which prompted the research group to search

for the genetically closest well developed expression host strain available, *S. lividans* [451]. Interestingly, although expression levels of both CYPs were even lower in *S. lividans*, which is attributed to the use of a low-copy number expression plasmid, product output of 7-hydroxycoumarin from 7-ethoxycoumarin was 2 to 3-fold higher than that of the recombinant *E. coli* strain. This may be a result of greater cooperativity between the cellular environment, notably the native redox machinery of *S. lividans* and that of the CYPs from *S. griseolus*. Another explanation, as the authors go on to suggest, may reside in the ability of *S. lividans* to withstand prolonged contact with both the 7-ethoxycoumarin substrate and the product 7-hydroxycoumarin. In the second publication, the host bacterium *S. lividans* was selected on the basis that its redox components would be compatible with those of CYP105D1 from *S. griseus* and CYP107B1 from *Streptomyces erythraeus* [452]. This proved an effective choice only for CYP107B1, which was able to use the endogenous redox components of *S. lividans* to convert 27.6 mg/L of 7-ethoxycoumarin to 7-hydroxycoumarin in 6 hours. Another actinomycete investigated as a potential platform for a CYP based whole-cell process is *R. erythropolis* [453]. The *Rhodococcus* genus is known for its heightened solvent tolerance as well as its great catabolic range, shown to be capable of oxidizing a variety of hydrophobic compounds [454, 455]. Unsurprisingly, it possesses numerous CYPs [456]. This makes it an interesting host organism to investigate new CYP specific substrates and products. It is also naturally equipped with sterols/steroids transporters [457], a key feature as cell permeability is a known bottleneck in whole-cell processes. In addition, although the use of *Rhodococcus* strains has been limited in the past, due to the fact that it would completely breakdown steroid compounds [456], the triple deletion mutant strain RG9 of *R. erythropolis* can no longer catabolise most sterol like compounds [458], making this particular host cell ideal for sterol or steroid CYP based whole-cell bioconversion. In any case, *R. erythropolis* strain RG9 was used to biotransform norandrostenedione to 16 β -OH-norandrostenedione in a whole-cell process using the BM3 variant M02 [453]. Whole-cell bioconversion yielded roughly 350 mg/L of products after 20-hour incubation with no new products detected after 22 hours.

Apart from bacteria, yeast have also been a platform investigated for whole-cell bioconversion using CYPs as biocatalysts. When it comes to expressing eukaryotic CYPs, yeast comes equipped with their own CPR redox partner which is more likely to be compatible with eukaryotic CYPs. Should the system lack CPR the possibility to co-overexpress the redox component remains an option. In addition, as the vast majority of eukaryotic CYPs are membrane bound, yeast, unlike bacteria, provide a more suitable environment for the production of these membrane bound enzymes as they come equipped with inner organelles which includes the endoplasmic reticulum and

the mitochondria where they can anchor [459, 460]. One particular yeast system explored is *P. pastoris*, one of the most popular heterologous protein expression systems, due to the host cell's ability to produce high levels of functional soluble or membrane bound proteins [461, 462]. This yeast host cell platform is particularly well suited for long & large-scale whole-cell bioconversion as it uses integrative plasmids thereby allowing transformants to stably integrate the heterologous genes into the genome ensuring maximal stability of the CYP/CPR genes over time. In addition, cell densities can reach over 100g/L of DCW and over 400 g/L of WCW and protein expression yield reaching 14.8 to 30 g/L have been reported in large-volume fermentations [463, 464]. Another useful feature of *P. pastoris* is that it is a eukaryotic organism closer genetically than any bacteria to CYPs originating from other eukaryotes, humans for instance. On this basis, *P. pastoris* is an ideal choice as an expression host for eukaryotic CYP based whole-cell processes. In one case, human CYP17 α was expressed in *P. pastoris* for the whole-cell bioconversion of progesterone to 17-OH- and 16-OH-progesterone. The system fully converted 1 μ M of progesterone in under 20 minutes, thus reaching a volumetric yield of 314 μ g/L, [465]. In another *P. pastoris* whole-cell system, (+)-valencene was converted to *trans*-nootkatone at up to 58 mg/L using CYP71D55 from *H. muticus* following a 24 hours incubation period [384].

Arguably, the most popular yeast, *S. cerevisiae*, carries the most comprehensive dataset available of all yeasts with its physiology, metabolism and genetics well understood with many tools and strains available for biotransformation projects [464, 466]. In this respect, the *S. cerevisiae* strain WAT11, containing chromosomally integrated *A. thaliana* CPR, was chosen for the whole-cell bioconversion of hydroxylate ferulic acid to 5-OH-ferulic acid using CYP84 from *A. thaliana* [467]. The optimal bioconversion yield obtained with this system was of 1.6 mg/L or 0.6 mg/gDCW of product. A yeast similar to *S. cerevisiae*, in that it has also been extensively studied, is *S. pombe* also known as fission yeast. This intensive characterization can be attributed to the numerous key properties this yeast shares with higher eukaryotes. Indeed, for this fission yeast, the protein folding quality control mechanism is closer to mammalian cells than for the budding *S. cerevisiae*, making its pairing with eukaryotic CYPs potentially more efficient. However, in regards to industrial applications, the fission yeast expression system is underdeveloped and does not have the same track record of recombinant protein expression and chemical production than *S. cerevisiae* [464, 468]. Nevertheless, it has been the target of whole-cell bioconversion using CYPs as the cellular biocatalyst. The rationale of eukaryotic compatibility motivated the use of *S. pombe* as a host cell to express human mitochondrial CYP11B2 [469] and 11B1 [470]. There, both CYPs were found to localize to the yeast's mitochondrial membrane where they could efficiently use the endogenous Adx and AdR homologues

therein located. For CYP11B2, bioconversion of 11-deoxycortisol to cortisol reached 1.01 $\mu\text{g/L}$ after a 24-hour incubation period whereas, for the conversion of the same substrate, using CYP11B1, conversion reached 72.9 mg/L and 219 mg/L of products following a 24-hour and a 72-hour bioconversion period, respectively. Likewise, several functional human CYPs and CPRs have now been successfully expressed in fission yeast including CYP3A4 [471], CYP2B6 [472], CYP2D6 [473], CYP4Z1 [474] and CYP21 [391]. Yeast being closely related to moulds, CYP509C12 from the mold *Rhizopus oryzae* and its associated reductase was successfully expressed in fission yeast where it biotransformed progesterone into 11 α -hydroxyprogesterone in a whole-cell process within the first 6 hours of incubation up to a titer of 9.43 mg/L [475]. The compatibility of human CYPs with both their natural CPR partner and foreign eukaryotic CPRs was tested extensively in whole-cell biocatalytic conversion in fission yeast [476]. There, it was found that while CYP3A4 preferred exclusively its natural redox partner human CPR, CYP17 and 21 could use with equal efficiency fission yeast CPR or the *Ammi majus* weed CPR. Surprisingly, CYP2D6 displayed its highest efficiency when coexpressed with fission yeast CPR rather than human CPR. On the whole, *S. pombe* has been established as a platform for human or higher eukaryotic CYPs. Case and point, it has been used for example as a screening tool to identify substrates and inhibitors for the membrane bound human CYP4Z1, a CYP that is overexpressed in breast and ovarian cancer cells but otherwise undetectable in non-senescent cells [392].

The yeast *Y. lipolytica* has become over the years an increasingly popular recombinant protein expression platform due its ability to produce high molecular weight proteins in high amounts and to achieve high cell densities [464]. Where CYPs are concerned however it is known to be able to catabolize a wide variety of hydrophobic substrates such as alkanes and to absorb efficiently such compounds through a variety of methods such as the secretion of emulsifying agents, modifications of cell surface properties in order to bind hydrophobic substrates and by using some substrate specific transporters for fatty acids, triglycerides and alkanes [477, 478]. In a case study the fungal CYP53B1 from *Rhodotorula minuta* was tested in a whole-cell bioconversion assay, *Y. lipolytica* cells were used as a production host for para-hydroxybenzoic acid by using benzoic acid as a substrate [479]. There, the product accumulated to 1.6 g/L after 214 hours in *Y. lipolytica*. In a latter publication, due to the facility with which *Y. lipolytica* uptakes hydrophobic compounds and its natural resistance to hydrophobic solvents, it was selected as a whole-cell production platform of 6 β -hydroxyprogesterone using human CYP3A4 along with human CPR [429]. In the best of conditions here, product output of 6 β -hydroxyprogesterone reached roughly 76 mg/L in 90 hours. Whole-cell systems expressing CYPs where different host cells are compared are scarce yet, for yeast, one publication of this sort

has been released. Using a broad-range yeast vector to express either BM3 or CYP505A1 from *Fusarium oxysporum* the productivity of the CYPs was explored with the substrate 4-hexylbenzoic acid in the yeasts *S. cerevisiae*, *Kluyveromyces marxianus*, *Arxula adeninivorans* and two strains of *Y. lipolytica* [480]. Interestingly, both yeast strains of *Y. lipolytica* displayed no activity for BM3 whereas for CYP505A1, no detectable activity could be found for *S. cerevisiae* following 24-hour incubations. The best productivity achieved with BM3 was with *S. cerevisiae* reaching roughly 7.5 $\mu\text{mol/gDCW}$ of ω 2-OH-benzoic acid product whereas with CYP505A1 an even greater productivity of approximately 30 $\mu\text{mol/gDCW}$ of the same product was obtained in *A. adeninivorans*. The CYP of fungal origin, CYP505A1, performed the best out of the two CYP used in yeast hosts and implying that a more native environment may be more beneficent to the CYP expressed. What's more important in the comparison of these yeasts is that productivity was highly influenced by the choice of the host strains with the other strains reaching roughly a third or a tenth of productivity with BM3 or CYP505A1 respectively. For whole-cell reactions using resting cells of *A. adeninivorans* expressing CYP505A1 a space time yield of 1.3 $\mu\text{mol/h/gDCW}$ of ω 2-OH-benzoic acid was reached whereas for growing cells a space time yield of 6.1 $\mu\text{mol/h/gDCW}$ could be obtained with the same product. This might be attributed to the endogenous CYPs being expressed and produced in much greater numbers in growing cells rather than resting cells in *A. adeninivorans* as the authors found wild type CYPs were expressed in this yeast.

Beyond *E. coli*, the choice of a host cell can generally be seen as a way to mitigate problems of permeability, compatibility in regards to cellular environment, compatibility between CYPs and endogenous redox components as well as cell viability with regards to toxic decoy molecules, substrates, products or permeabilization agents. Furthermore, since whole-cell biotransformation is more easily scalable than free enzyme processes, plasmid or recombinant DNA stability, enzyme and cell densities are other key elements which can inform on which organism to choose from. While well-established organisms offer safety in the wealth of knowledge and precedents they hold (*E. coli*, *S. cerevisiae*) less common production platforms can offer significant advantages but are accompanied with less extensive biotechnological tools and knowledge base (*P. putida*, *Y. lipolytica*).

Table 4. Product outputs for various whole cell strategies discussed in chapter 1.5.4

Host cell	CYP Strategy ^a	Product	Product Yields			Incubation period (h)	Publication
			TON (mol/mol CYP)	mg/gDCW	mg/L		
<i>S. cerevisiae</i>	CYP71D55/AtCPR/CE2P	trans-nookatol		30		72	383
<i>P. pastoris</i>	CYP71D55/RAD52	trans-nookatol		62			385
<i>E. coli</i>	CYPmoxA	Hydroxy oleanoic acid		0.0066			387
Free enzyme				0.034			
<i>E. coli</i>	CYP102A1/C7-Pro-Phe	Phenol		359		5	239
<i>E. coli</i>	CYP105A1/polymyxin B	15-hydroxyabietic acid		30.3		24	388
<i>E. coli</i>	CYPsb21/CTAB	γ -hydroxy-N-methyl-L-Leu4-Cyclosporine A		0.0454		12	389
<i>E. coli</i>	CYP264B1/2-hydroxypropyl- β -cyclodextrin	12-hydroxy- α -longipinene		37.2			390
<i>S. pombe</i>	CYP21/ tween 80	11-deoxycortisol		78			391
<i>S. pombe</i>	CYP3A4/Triton X-100	Hydroxy testosterone		1147		24	392
<i>E. coli</i>	CYP153A ^{G307A} -BM3 reductase/alkL	ω -hydroxy methyl dodecanoate		4000			256
<i>E. coli</i>	CYP153A6/alkL	(S)-perril alcohol		5960			393
<i>E. coli</i>	CYP102A1/alkane transporter	12-, 13-, & 14-hydroxypentadecanoic		258			394
<i>E. coli</i>	CYP102A1 CMT ^{NADH} /RE-ADH	Hepanol and Heptanone isomers	2930	76	656	48	416
<i>E. coli</i>	CYP102A1 19A12/LB-ADH			8	54		
<i>E. coli</i>	CYP102A1 19A12/LB-ADH	Cyclooctanone	24363	481			415
<i>E. coli</i>	CYP102A1 19A12 ^{NADH} /LB-ADH		8461	640			
<i>P. putida</i>	CYP154A8/Fdr/Ykum/LB-ADH	(S)-2-octanol	10 300	150	1800	48	417
<i>E. coli</i>	CYP152L1/Ttl	1-tridecene			126		418
<i>B. subtilis</i>	CYP102A1 F87V/BA-GDH	1,2-epoxyhexane		2.2 ^b			406
<i>B. subtilis</i>	CYP102A1 F87V/BA-GDH	2- & 3-hexanol		204		3	407
<i>E. coli</i>	CYP105A1/LB-ADH	15-hydroxyabietic		91.6			388
<i>E. coli</i>	CYP101/GlyDH	5-exo-hydroxycamphor		84.1 ^b	252		408
<i>E. coli</i>	CYP102A1 QM	α -pinene oxide, verbenol & myrtenol		32			409
<i>P. putida</i>	CYP153A/H ² Dehydrogenase	1-octanol & secondary products		165		24	413

<i>E. coli</i>	CYP102A1 m2/Eosin Y, TEOA, light	7-hydroxycoumarin	16	3.65			414
<i>E. coli</i>	CYP153A/BM3 reductase/ biphasic	ω -hydroxy lauric acid		1200		30	256
		ω -hydroxy methyl laurate		4000		28	
<i>E. coli</i>	CYP102A1	ω -1 & ω -2 hydroxy benzoic acid		594		4	425
		(R)-phenyl methyl sulfoxide		304 ^b	3044 ^b		
		(R)-4-fluorophenyl methyl sulfoxide		169 ^b	1687 ^b		
		(R)-ethyl phenyl sulfoxide		250 ^b	2500 ^b		426
		(R)-methyl p-tolyl sulfoxide		359 ^b	3591 ^b		
<i>E. coli</i>	p450pyr ^{J83H} /GDH/[P6,6,6,14][NTF2]	(R)-methyl p-methoxyphenyl sulfoxide		442 ^b	4422 ^b		
		3-cyclohexyl-hydroxy glibenclamide		25	12		
		3-cyclohexyl-hydroxy glimpiride		25	3.5		437
<i>B. megaterium</i>	CYP105A1						
<i>B. megaterium</i>	CYP106A2	15 α -hydroxy-boswellic acid		560	24		439
<i>B. megaterium</i>	CYP106A2	7 α - & 7 β -OH dehydroepiandrosterone		438	4.25		441
<i>B. megaterium</i>	CYP109E1	25-hydroxy vitamin D ₃		45	24		442
<i>B. megaterium</i>	CYP11A1	Pregnenolone	22				442
<i>B. megaterium</i>	CYP27A1	27-hydroxycholesterol		113	48		
		25-hydroxy VD ₃		80.8	48		444
		25- & 26/27- hydroxy-7- dehydrocholesterol		112	48		
<i>S. lividans</i>	CYP107B1	7-hydroxycoumarin		27.6	6		452
<i>R. erythropolis</i>	CYP102A1 M02	16 β -OH-norandrostenedione		350	20		453
<i>P. pastoris</i>	CYP17 α	16-OH-progesterone		3.16	0.333		465
<i>S. cerevisiae</i>	CYP84	5-OH-fenflurite	0.6	1.6			467
<i>S. pombe</i>	CYP11B1	Corticosterone		209 ^b	72		470
<i>S. pombe</i>	CYP509C12	Progesterone		9.43	6		475
<i>Y. lipolytica</i>	CYP53B1	para-hydroxybenzoic acid		1600	214		479
<i>Y. lipolytica</i>	CYP3A4	6 β -hydroxyprogesterone		76	90		429

^a Strategy denotes the key components of the whole cell system starting with the identity of the CYP used, mutations or variant of the CYP followed by components added to the system (other enzymes, biphasic buffer, membrane permeabilizer).

1.4 Objectives

CYP enzymes offer the possibility of generating a massive array of different valuable products however the application of large scale enzymatic processes is limited by their short operational stability, their catalytic efficiency and their reliance on the expensive cofactor NADPH [481, 197, 482, 272, 483]. Additionally, most CYP based reactions necessitates the addition of an organic cosolvent as most CYP substrate are insoluble [484], this further compounds to the problem of operational stability as such solvents are deleterious to the stability of CYPs. To facilitate the development of CYP based biocatalytic processes commercially they must reach an economically viable threshold. That is, a point at which producing a given mass of product per CYP biocatalyst quantity per unit of time is profitable. To that end, the CYP enzyme BM3 from *B. megaterium* was selected for this work because unlike most CYPs, it is soluble and therefore not bound to any membrane, thus simplifying its purification procedure. Also, it is naturally fused to its redox partner, is the most researched CYP to date and consequently, it offers a large library of mutants with most of the mutations at the oxidase domain enabling it to accommodate one of the largest substrate range of CYP enzymes. Furthermore, the performance of BM3 can be easily followed spectrophotometrically with a model reaction using 10-pNCA easing investigation into this particular CYP's use (Figure 6). Likewise, nicotinamide compound use (NADPH, NADH, BNAH) can also be monitored spectrophotometrically (Figure 7). Thus, the general objective of this thesis was to improve the relevant properties of the BM3 enzyme for an industrial application. To achieve this, several limitations had to be contended with. Specifically, the three main limitations associated with CYPs, operational stability, catalytic efficiency and their reliance on the expensive cofactor NADPH. Consequently, contending with these three limitations were split into two specific objectives for this thesis. In the process this also enabled us to expand our comprehension of the fundamentals of stability of the BM3 enzyme.

The first objective was to overcome the dependence of BM3 on the expensive cofactor NADPH. This was first addressed by mutating BM3, using two mutations from the literature, so that it could better utilize the cofactor NADH and accept the biomimetic cofactor BNAH [306]. This generated the BM3 mutant named ND. This objective was then moreover grappled with by tailoring the reaction conditions so that they would most importantly ensure the stability of the cofactors themselves.

The second objective was to address the operational stability and the catalytic efficiency of the biocatalyst BM3 with the use of the alternative cofactors NADH and BNAH. To this end the N-D mutant was mutated to augment its stability towards organic cosolvents using four mutations published in the literature [198] thus generating a new BM3 mutant dubbed NTD1. Consensus mutagenesis was then applied to NTD1 to further enhance the operational stability and catalytic efficiency of NTD1 with the alternative low-cost cofactors NADH and BNAH. This yielded two new mutants dubbed NTD5 and NTD6. The enhanced product output these mutants provided could also be further enhanced by using a fed batch approach to avoid leakage events which ultimately affect the operational stability of BM3. Alternatively, using fundamental science associated with *B. megaterium*'s own natural metabolism, experimental evolution was applied to the bacterium and devised in a way to force the evolution of the genomically encoded wild type BM3 towards a highly productive variant. The experiment in question generated a new more productive variant named DE and could be used to quickly discover new point mutations enhancing activity and/or stability.

2 Buffer formulation optimization for improved BM3 enzymatic reaction yield.

Authors: Thierry Vincent^a, Bruno Gaillet^a, Dominic Thibeault^b & Alain Garnier^{a*}

Affiliation:

^a Department of chemical engineering, Université Laval, Québec, Québec, Canada, G1V 0A6

^b Oleotek, Thetford Mines, Québec, Canada, G6G 0A5

* corresponding author: Alain Garnier; email: alain.garnier@gch.ulaval.ca; telephone +1 418 656

[2303](#)

Résumé

Le cytochrome p450 CYP102A1 de *Bacillus megaterium* est une monooxygénase qui est mieux connue sous le nom de BM3. C'est une enzyme possédant un groupement prosthétique hémique capable de catalyser l'hydroxylation de plusieurs substrats différents. Plusieurs de ces substrats présentent un intérêt commercial pour l'industrie pharmaceutique et de chimie fine. Au contraire de la majorité des autres cytochromes p450, BM3 est soluble et fusionné à son partenaire redox naturel qui lui fournit les électrons nécessaires issus du NADPH pour catalyser ses réactions enzymatiques. Cependant, l'usage industriel de cette enzyme est limité par son instabilité ainsi que par les coûts élevés de son cofacteur, le NADPH.

Dans cet ouvrage, nous explorons les effets de la recette des tampons et de la température sur la stabilité de l'enzyme BM3 sauvage et son mutant R966D/W1046S ainsi que sur la stabilité des cofacteurs contenant un groupe nicotinamide NADPH, NADH et le cofacteur biomimétique N-benzyle-1,4-dihydronicotinamide. Nous démontrons ici que la stabilité du cofacteur est plus importante que celle de l'enzyme pour en augmenter la productivité. Nous démontrons également que les basses températures augmentent le couplage des réactions d'oxydoréduction se faisant, augmentant le ratio molaire de *p*-nitrophénolate produit à partir du 10-pNCA par cofacteur oxydé. Globalement, la réaction optimisée mène à une augmentation de la production totale de produit d'un facteur de 2 à 2.6 lorsque l'enzyme BM3 sauvage ou le mutant R966D/W1046S fut utilisé, respectivement, avec l'un des trois cofacteurs susmentionnés.

Abstract

The p450 cytochrome monooxygenase CYP102A1 from *Bacillus megaterium*, better known as BM3, is a heme-thiolate enzyme that catalyzes the hydroxylation of numerous substrates. Many of the resulting products are of commercial interest to the pharmaceutical and fine chemical industries. Unlike most other p450 cytochromes, BM3 is both soluble and fused to its natural redox partner, which supplies the necessary electrons from NADPH to drive its reaction forward. However, the industrial use of this enzyme is limited by its poor stability and its expensive cofactor.

In this work, we explore the effects of buffer formulation and temperature on the stability of wildtype and BM3 mutant R966D/W1046S as well as on the stability of nicotinamide cofactors NADPH, NADH and the biomimetic cofactor N-benzyl-1,4-dihydronicotinamide. We demonstrate that cofactor stability is more important to increase product yield than that of the enzyme. We also demonstrate that low temperatures enhance oxydo-reduction reactions coupling thus resulting in an increase in the molar ratio of *p*-nitrophenolate produced from 10-*p*NCA per oxidised cofactor. Overall, the optimized reaction conditions lead to a 2 to 2.6-fold increase in total product output when wildtype BM3 or R966D/W1046S mutant is used with either of these three aforementioned cofactors.

Keywords: BM3, nicotinamide, NADPH, NADH, NBAH, bioprocess engineering, biocatalysis.

2.1 Introduction

In the field of white biotechnology, p450 cytochrome enzymes continue to attract a substantial amount of interest. This is mainly due to their ability to hydroxylate saturated C-H bonds, which is a difficult reaction to carry out by traditional chemistry. In addition, many p450 can act upon a wide variety of substrates [61], many of whom are of industrial interest [62, 485]. Reactions are driven forward pending the transfer of electrons by a redox partner from the oxidation of NADPH to NADP⁺ to the active oxygenation site of the p450. Electrons can also be supplied by NADH, with p450cam for example favouring this nicotinamide compound over NADPH [486].

Unlike most other p450 enzymes, the cytochrome from *Bacillus megaterium*, known as CYP102A1 or simply BM3, is a soluble enzyme fused with its redox partner into a single polypeptide [17]. Two prosthetic groups found within the reductase domain, flavin mononucleotide and flavin dinucleotide, channel the electrons liberated by the oxidation of NADPH towards the monooxygenase heme domain. The scope of substrates that BM3 can naturally act upon can be further enhanced by mutating its active site to accept new substrates. There is in fact nowadays a large number of BM3 mutants tailored to accept different substrates [48]. Additionally, instead of mutations to the active site, decoy molecules can be used to allow BM3 to accept an even larger variety of non-native substrates [232, 237]. Nevertheless, most substrates are essentially non-polar and this impedes their access to p450 enzymes as they are marginally soluble in water. This can be alleviated by adding an organic cosolvent to the aqueous reaction phase, albeit at a low concentration to avoid enzyme deactivation [198, 487–489]. As a result, the necessity for an organic cosolvent limits the stability and the product yield achievable by p450 enzymes and are therefore a principal hurdle to their industrial application. Unsurprisingly, the issue of cytochrome p450 stability has been identified repeatedly across reviews tackling the application of cytochrome p450 biotechnology as one of the main hurdles preventing their industrial implementation [197, 272, 481–483]. Another obstacle to the application of p450 is their dependence on the expensive nicotinamide cofactors, NADPH and NADH, required to drive the reaction forward. To this effect, it was reported [306] that the R966D/W1046S BM3 mutant (N-D mutant) enabled the enzyme to use NADH with greater efficiency, and it was later shown that these same two mutations also allowed the enzyme to use N-benzyl-1,4-dihydronicotinamide (NBAH) [296], in place of NADPH/NADH, an even less expensive cofactor analog.

As NBAH seemingly improves the cofactor situation, we decided to focus our work on p450 BM3's stability by using differential scanning fluorimetry (DSF) to screen buffer formulations for maximum conservation of BM3 integrity and, by extension, increasing its product output. To that end, sodium citrate, tris, bis-tris propane (BTP), phosphate buffered saline (PBS), glycine, 4-(2-hydroxyethyl)-1-piperazineethanesulfonic acid (HEPES), potassium acetate and 3-(N-morpholino) propanesulfonic acid (MOPS) buffers were tested on the BM3 N-D mutant. However, despite identifying buffer formulations best preserving the structural integrity of BM3, we noticed that these formulations were deleterious to the stability of all three nicotinamide compounds (NADPH, NADH and NBAH) and thus hindered the overall yield of the reactions. As BM3 can cause the release of fluorescent *p*-nitrophenolate (pNP) from the *p*-nitrophenoxydecanoic acid (10-pNCA) substrate [76], we decided to use this substrate to monitor spectrophotometrically the turnover number (TON, defined as the molar ratio of overall pNP produced per BM3 present) and kinetics allowing greater throughput to test several buffers. In this work, we demonstrate the steps taken to enhance nicotinamide stability in our buffer formulations lead to an increase in TON for all three nicotinamide compounds (NADPH, NADH and NBAH) for both wild type (WT) and BM3 N-D mutant.

2.2 Material and Methods

Chemicals

Both DH5 α and BL21 (DE3) *Escherichia coli* strains were purchased from Thermo Fisher Scientific. The pET16B vector was obtained from Novagen. Restriction, phosphatase and ligase enzymes were purchased from New England Biolabs whereas the Pfu polymerase, the deoxynucleotides and the accompanying PCR buffer were purchased from Bio Basic. DNA primers were purchased from IDT technologies. For DSF the SYPROTM orange protein gel stain (5000X concentrate in dimethyl sulfoxide) was bought from Thermo Fisher Scientific. The substrates *p*-nitrophenoxydecanoic acid and N-benzyl-1,4-dihydronicotinamide were synthesized by Oleotek as described in the referenced citations [490, 491]. Both NADH and NADPH were purchased from p212121. Else, chemicals for bacterial cell cultures, buffers and organic solvents were acquired from Bioshop Canada.

Cloning, expression & purification

The BM3 gene sequence was obtained by PCR using genomic DNA extracted from *Bacillus megaterium* (ATCC 14581) as a template and using forward primer P450-BM3-AS2, ATGACAATTAAGAAATGCCTCAGCC, reverse primer P450-BM3-AAS2, ACACGTCTTTTGGTATCGG and *pfu* polymerase. In order to subclone the BM3 gene into the pET16B vector, the PCR product previously obtained was further amplified with forward primer P450-BM3-AS1, CGACTAGTATGACAATTAAGAAATGCCTCAGCCA, and reverse primer P450-BM3-AAS1, ATGGATCCTTACCCAGCCCACACGTCTTT. The PCR product was then subcloned into a pET16B vector using *SpeI/BamHI* restriction sites. This cloning strategy added an octahistidine tag (GHHHHHHHH) followed by a spacer (SSGHHTSM) at the N-terminus. To generate the W1046S mutant, a PCR amplicon was first generated from the pET16B vector containing WT BM3 gene with forward primer *SpeI*pet16b, CCATCATACTAGTATGACAATTAAGAAATGCCTCAGC, and reverse primer *BamHI*pet16b, ATGGATCCTTACCCAGCGCTCACGTCTT, containing the W1046S mutation. The resulting PCR product was then subcloned into pET16B using *SpeI/BamHI* restriction sites.

The mutant R966D/W1046S or N-D was generated by introducing the R966D mutation on the W1046S mutant by DpnI site directed mutagenesis using forward primer 1678, GCGTCTTATAACGGTCATCCGCTG and reverse primer RCR966D, ATTTGGCATATCAGAAAAAGCGGTAT. To do so, 100 ng of plasmid, 10 nmoles of

deoxynucleotides, 10 pmoles of each primer and 5 units of Pfu polymerase were added to a 50 μ l PCR reaction tube. To generate a megaprimer, 20 cycles of PCR with an elongation time of 2 minutes were performed, after which 30 cycles with a 20-minute elongation time was completed to allow full plasmid amplification. To the resulting PCR reactions, 10 units of DpnI restriction enzymes were added and the reactions were incubated 1 h at 37 °C. The PCR products were then transformed by a standard heat shock protocol into DH5a cells and then sent for sequencing.

The BM3 sequence and N-terminal octahistidine tag containing pET16B was transformed into BL21 cells by heat shock on Luria-Bertani plates containing 100 μ g/ml ampicillin. A single colony was then picked and grown overnight at 37 °C in 100 ml of Luria-Bertani broth containing 100 μ g/ml ampicillin. Using a 2.5 % inoculum (20 ml), the cells from the pre-culture were then grown at 37 °C in 0.9 L of modified Terrific Broth (MTB, 24 g tryptone, 48 g yeast extract, 10 g NaCl per liter, pH 7.5) containing 100 μ g/ml of ampicillin. When the culture reached an OD₆₀₀ of 0.5-0.6, isopropyl β -D-1-thiogalactopyranoside was added to a final concentration of 1 mM. After which, 150 ml of MTB and 50 ml of 50 % (v/v) of 0.48 micron filtered glycerol was added. Following this, the incubation temperature was immediately lowered to 28 °C. Cells were grown for 10 hours and pelleted by a 10 min centrifugation at 4500 g after which they were stored at -80 °C. For the enzyme isolation and purification, frozen cells were thawed on ice, resuspended in 80 ml of lysis buffer (100 mM NaCl, 25 mM tris-HCl pH 8 with 1 mM phenylmethylsulfonyl fluoride) and lysed by sonication with 4x15-s bursts separated by 30 s pauses. Sonication and every following step was performed on ice or at 4°C. Sonicated cells were centrifuged at 26 200 g for 30 min. After which, the recombinant proteins were purified by applying the supernatant onto a Ni-sepharose 6 fast flow resin (GE healthcare) packed in a homemade chromatography column. The column was first washed with 200 ml running buffer (40 mM NaH₂PO₄, 500 mM NaCl, pH 7.4), followed successively by 100 ml of running buffer with 10 mM, 20 mM and 50 ml of 40 mM histidine running buffer. Enzymes were eluted with a 160 mM histidine running buffer, the eluate dissolved in 1 volume of glycerol yielding a 50% glycerol enzyme solution, stored at -80 °C. Concentrations of p450 enzymes were measured by CO difference spectroscopy applying a 91 mM⁻¹cm⁻¹ extinction coefficient to the 450 nm absorption peak, as described in Omura & Sato 1964 [9].

Differential scanning fluorimetry

In order to study the effect of buffer formulation on enzymatic stability, DSF was used. The SYPRO orange dye (5000X), for whom fluorescence increases when binding to hydrophobic regions of a protein, was used to monitor protein unfolding. As a sample is heated in a qPCR chamber, the enzyme unfolds and hydrophobic surfaces exposition increases, as well as fluorescence. The effect of solvent composition on the protein unfolding temperature, and thus protein stability, can hence be studied in multiwell plates. This technique allows a higher throughput than differential scanning calorimetry (DSC), circular dichroism and the CO difference spectroscopy used for p450 enzymes.

DSF assays were performed in 96-well WHT/CLR hard shell PCR plates (Bio-Rad), 50 μ l/well, sealed with microseal C film (Bio-Rad) on a Bio-rad CFX96[™] real time system C1000 Touch[™] thermal cycler (Bio-Rad). For every experiment, a final concentration of 750 nM and 2X diluted with DMSO was used for the N-D mutant and the 5000X SYPRO[®] orange dye (Thermo Fisher Scientific), respectively. Prior to the experiment, the 96-well plate was centrifuged 1 min at 80 g. The qPCR was programmed as such: Lid, 105 °C; Volume, 50 μ L; Step 1, 15 °C, 31 s; Step 2, 15 °C, 30 s; Step 3, absorption read using All channels; Step 4, back to step 2, 80 cycles, + 1 °C/cycle at up to 95 °C. Hence, temperature started at 15 °C and stopped at 95°C. The All channels function of the qPCR from Biorad searches for a fluorescence signal in every channel integrated in the device including the excitation and emission wavelengths of SYPRO orange between 450-490 nm and 560-580 nm respectively. The inflection point of the melting curve, T_m , also represents the point where dye fluorescence reached 50% of its maximum fluorescence, which was then used as an indication of enzyme folding and stability. For the study of pH effect, 100 mM PBS was used, for the study of buffer effect, final concentrations of 50, 100, 150, 300, 750 and when possible 1000 mM, pH 7 were used and finally, for the experiments on solvent effect, a 1000 mM PBS, pH 7 was used. The means for each sample set were calculated from four experimental replicates for which the standard deviations were all less than 3 %.

Nicotinamide stability assays

Degradation kinetics of the nicotinamide compounds were followed at 340 nm for both NADH and NADPH and at 355 nm for NBAH. The final concentration of nicotinamide compounds was set at 300 μ M with 5 % (v/v) methanol and 5 % (v/v) glycerol in a final volume of 300 μ L, in the dark. The assays were initiated by adding 280 μ l of buffer on 20 μ l of 4.5 mM NADPH/NADH dissolved in water or 285 μ l of buffer on 15 μ l of 6.0 mM NBAH dissolved in methanol.

Measurements were taken every 5 minutes for 8 hours on a Synergy H1 plate reader (BioTek) at 25 °C. The standard deviation and mean for each sample set were calculated from three replicates.

Activity assays with 10-pNCA

For TON measurements, final concentrations of 100 nM enzyme, 600 μ M 10-pNCA and 1500 μ M cofactor (NADPH, NADH or NBAH) were used, in a 0.1M or 1 M buffer (different buffers), at pH 7 or 8, always with 5 % MeOH (v/v), in the dark. The reactions were all performed overnight, as it was determined to be sufficient to reach final concentration values, in a final volume of 2 ml at 4 or 25 °C. Assays were initiated by adding 40 μ l of 75 mM cofactor stock solution. Following overnight reactions, 1 ml of reaction sample was transferred to a 1 cm cuvette. Afterwards, in order to reveal pNP, 150 μ L of 10 N NaOH was added to the 1 ml reaction sample. This was then followed by the addition of 850 μ L of MeOH, to fully dissolve the remaining organic substrates (10-pNCA and NBAH) to a final volume of 2 ml in the cuvette. The absorbance of pNP was then measured at 410 nm in a Genesys 10S UV-Vis spectrophotometer (Thermo Fisher Scientific) and the concentration was determined from a calibration curve. TONs were calculated by dividing the final concentration of pNP by the concentration of enzymes. The standard deviation and mean for each sample were calculated from 3 replicates of two independent experiments.

Likewise, for kinetics measurements, final concentrations of 100 nM enzyme, 300 μ M 10-pNCA and 300 μ M cofactor (NADH or NBAH) were used in a dual buffer of 10 mM PBS/100 mM BTP buffer, pH 8, 5 % MeOH (v/v). The reactions were all performed in a final volume of 300 μ l in 96 well plates. Assays were initiated by adding 100 μ l of 900 μ M cofactor stock solution (NADH or NBAH) to 200 μ l of reaction mixture containing both enzyme and 10-pNCA. Leakage kinetics were monitored in the absence of 10-pNCA where methanol was added in place of the substrate to a final concentration of 5 % MeOH (v/v). To monitor pNP release and cofactor consumption of NBAH or NADH measurements were made at 410 nm, 355 nm and 340 nm, respectively. Measurements of the absorbance of pNP and cofactors were made in a Synergy H1 hybrid multi-mode reader (BioTek) every 6 s for 2 min with the first measure taken at $t = 6$ s. The concentrations of pNP, NBAH or NADH were determined from a calibration curve. The standard deviation and mean for each sample were calculated from 3 replicates of two independent experiments.

2.3 Results

Differential scanning fluorimetry

As can be seen on Figure 18, when testing the effect of pH, a maximum T_m was obtained at pH 7 for the BM3 N-D mutant in 100 mM PBS buffer. Figure 18 also shows that BM3 N-D tolerates alkaline conditions much better than acidic ones, as T_m drops quickly below pH 6.5 while it decreases progressively above 7.0. Common enzyme buffers at increasing concentrations were tested at the optimal pH of 7 (Table 5). For every buffer tested, with the exception of the acetate buffer, an increase in concentration translated into an increase in T_m , and therefore stability, for the N-D mutant. The citrate buffer offered the highest T_m at 55.5 °C, followed by BTP and PBS both with a T_m at 53 °C in 1 M buffers. The denaturation temperature of N-D in the presence of increasing concentrations of organic cosolvents was also compared (Table 6). Amongst those tested, dimethyl sulfoxide (DMSO) and methanol had the least deleterious effect on BM3, with T_m of 49 and 45 °C, respectively, at 7.5% (v/v) cosolvent in 1 M PBS buffer, pH 7. The same conditions for both of these cosolvents were tested in citrate as well as in BTP buffers. As shown in Table 7, the BTP buffer provided the highest stability for BM3 when used with either DMSO ($T_m = 53$ °C) or methanol ($T_m = 48$ °C) at 7.5% (v/v) cosolvent, while for the citrate buffer, only the T_m for methanol could equal that of BTP buffer also reaching 48 °C.

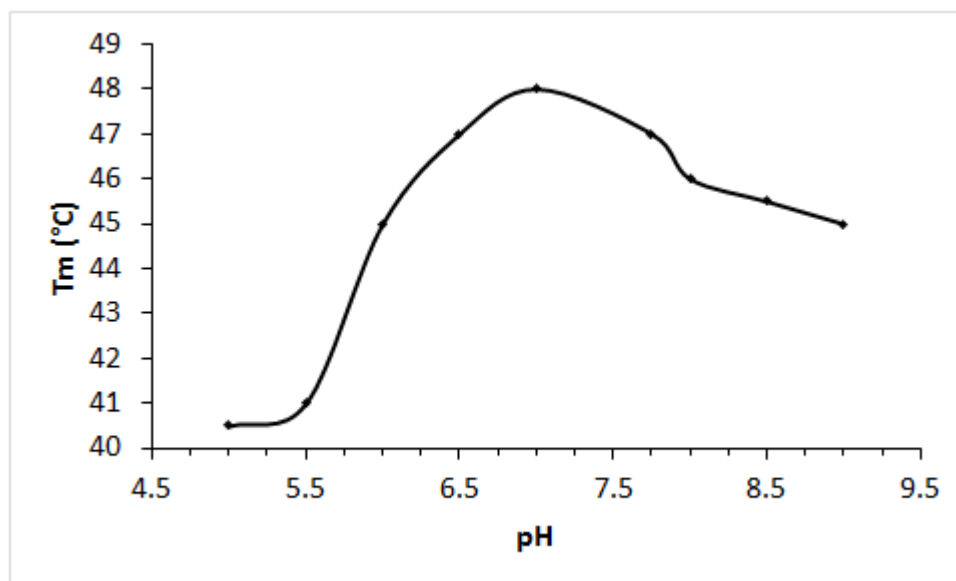


Figure 18: Melting temperature of BM3 N-D mutant for different pH. Conditions: 750 nM enzymes, 2X SYPRO orange and 100 mM phosphate buffer.

Table 5. Effect of common buffers at increasing concentrations on the denaturation temperature of BM3 N-D, ranked in decreasing order of T_m . Conditions: 750 nM enzymes, 2X SYPRO orange, pH 7.

Buffer	Buffer concentration mM					
	50	100	150	300	750	1000
Melting temperature °C						
Sodium Citrate	47	47.5	48	49	52.5	55.5
BTP	46	46	46	46	53	53
PBS	47	48	49	49	51	53
Glycine	46	46.5	47	47	49	49
HEPES	47	47	47	48	49	
Tris	47	47	47	47	47.5	
Potassium acetate	46	46	46	46	46	46
MOPS	45	45	45	45	45.5	46

Table 6. Tolerance of the N-D mutant towards organic cosolvents at increasing concentrations in regards to melting temperature with the ideal buffer at the top and the worst at the bottom of the table. Conditions: 750nM enzymes and 2X SYPRO orange.

Solvent	PBS buffer 1M pH7, Cosolvent % (v/v)					
	0	2.5	3	4	5	7.5
Melting temperature °C						
DMSO	53	51	51	50	50	49
Methanol	53	51	50	49	48	45
1-Heptanol	53	50	50	47	46	46
Ethyl Acetate	53	48	46	46	47	45
Acetonitrile	53	49	48	47	45	40
Ethanol	53	48	46	45	43.5	39
Methyl Ethyl Ketone	53	46	46	43	43	36
Ethylene glycol	53	44	44	43	41	40
Chloroform	53	45.5	42	40	41.5	36.6
Isopropanol	53	46	44	41	39	32
tert Butanol	53	45	43	40	38	31
3-Pentanol	53	43.8	43.8	40.3	37.3	36.5
n-butanol	53	37	37	38.5	36.5	33.3
Acetyl acetone	53	37	35.3	33.5	33	31

Table 7. Exploration of optimal cosolvent/buffer combination in regards to melting temperature. Conditions: 750nM enzymes and 2X SYPRO orange.

% cosolvent (v/v)	1M Citrate buffer pH7		1M BTP buffer pH7		1M PBS buffer pH7	
	DMSO	MeOH	DMSO	MeOH	DMSO	MeOH
0	55.5	55.5	53	53	53	53
2.5	53	53	53	52.5	51	51
3	52.5	52	53	51.5	51	50
4	52	52	53	51	50	49
5	52	50	53	50	50	48
7.5	50	48	53	48	49	45

Cofactor stability

NADPH, NADH and NBAH stability was evaluated by monitoring their oxidation at 340 nm for NADPH and NADH, and 355 nm for NBAH over 8 hours in the absence of substrate and enzyme, in different buffers at pH 7. A first-order degradation rate constant, k_d , was calculated from these data according to eqn [1] where C_{rc} and C_{rc0} are the reduced cofactor concentration at time t and at time 0, respectively. As displayed in Figure 19, the citrate and the PBS buffers were the least efficient in preserving the reduced form of nicotinamide, either at 0.1 or 1 M. On the other hand, both tris and BTP 0.1 M buffers consistently prevented NADH and NBAH degradation, while NADPH was best preserved in 1 M tris and BTP.

$$C_{rc} = C_{rc0} \cdot e^{-k_d t} \quad [1]$$

Maximum conversion of 10-pNCA to pNP by BM3

With an excess of cofactor, the TON of 10-pNCA to pNP was evaluated using either WT or N-D BM3, in various buffers (Fig. 20a). Reactions with WT BM3 at pH 8 consistently provided higher TONs for all three buffers tested for either NADPH or NADH when compared to reactions conducted at pH 7 (Fig. 20a). As demonstrated by DSF (Fig. 18) the T_m of BM3 is at its highest at pH 7. This seems to imply that cofactor stability has more impact on TON than enzyme stability

within the pH range 7 to 8 since a more alkaline pH favours nicotinamide stability (Lowry 1961, Wu 1986). With respect to buffers, WT BM3 TON using NADPH was larger with 0.1 M tris compared to 0.1 M PBS or 0.1 M BTP (Fig. 20a). We demonstrated by DSF that 0.1 M tris, $T_m = 47\text{ }^\circ\text{C}$, provided less stability to BM3 than 0.1 M PBS, $T_m = 48\text{ }^\circ\text{C}$ (Table 5) whereas, with respect to nicotinamide compound stability, both tris and BTP buffers offered the highest protection with PBS not being as efficient. Therefore, parameters promoting nicotinamide stability over enzyme stability also promote greater TON. At a lower temperature, which favours both enzyme and cofactor stability, reactions were driven even further generating higher TONs than at room temperature (Fig. 20b). With the optimisation of these 3 parameters (buffer, pH & temperature) compounded WT BM3 TON improved 1.9 and 2.6-fold for NADPH and NADH, respectively, when compared to the initial condition using 0.1 M tris pH 7 at $25\text{ }^\circ\text{C}$ (Fig. 20b). The optimisation is even more impressive if it is compared with the same conditions but in the 0.1 M PBS buffer of Figure 20a improving TONs by a factor of 2.23 and 3.24 for NADPH and NADH, respectively (Fig. 20a).

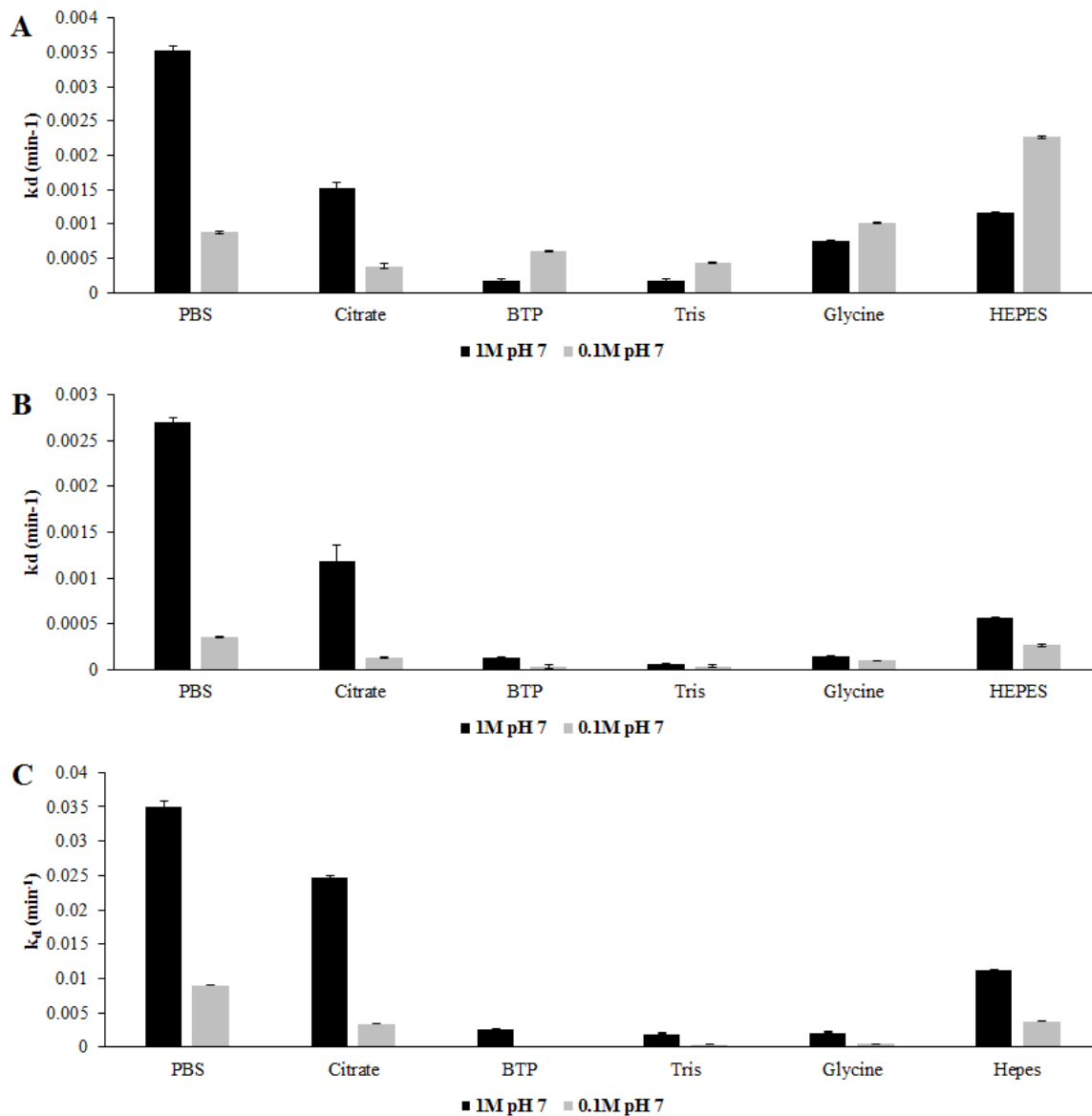


Figure 19: Cofactor degradation rates at 25° C in buffers at both 1M and 0.1M concentrations. NADPH (a), NADH (b), NBAH (c). The standard deviation and mean for each sample set were calculated from three replicates.

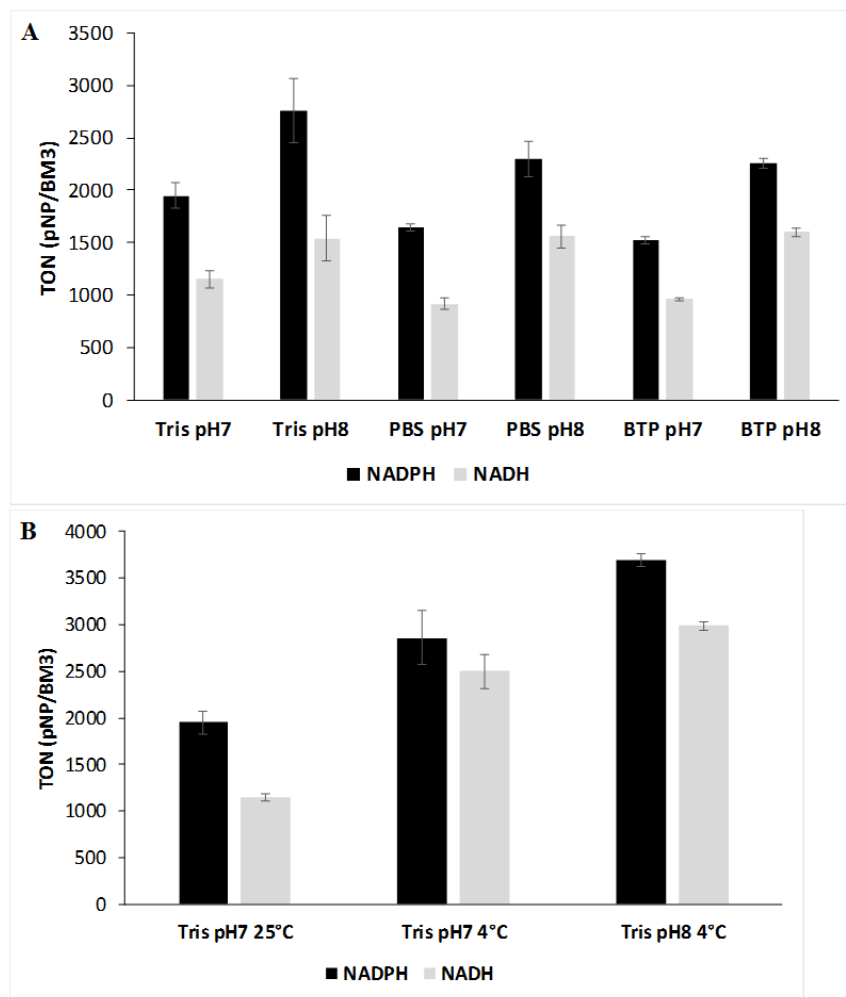


Figure 20: Turnover numbers of 10-pNCA conversion to *p*-nitrophenolate by wild type BM3 using as a cofactor either NADPH or NADH. a) In 0.1M buffers ideal to preserve nicotinamide integrity (Tris & BTP) or demonstrating great ability to prevent enzyme unfolding (PBS & BTP) at both pH 7 & 8 with all reactions driven at 25°C. b) In 0.1M Tris buffer at 4°C. The standard deviation and mean for each sample were calculated from 3 replicates of two independent experiments.

For the BM3 N-D mutant, reactions using NABH or NADH were improved at higher pH, when using either BTP or PBS buffers (Fig. 21a) but not when using tris. In this particular instance, PBS provided the best TONs for both NADH and NBAH. The TONs of N-D mutant with NBAH in decreasing phosphate concentrations at pH 8, with and without BTP is presented in Figure 21b. There, when using the NBAH cofactor, a combination of 0.1 M BTP with 0.01 M PBS mildly improved TONs when compared to the 0.1 M PBS buffer at pH 8, 25 °C. At 4 °C, with the BTP/PBS buffer, both NBAH and NADH TONs are improved, 2.2-fold and 2.5-fold, respectively when compared to the initial condition of 0.1 M BTP pH 7 at 25 °C (Fig. 21c). These latter findings demonstrate that fine tuning buffer composition, pH and temperature to nicotinamide stability leads to enhanced TON

of the main p450 BM3 reaction. With both WT BM3 (Fig. 20b) and BM3 mutant N-D (Fig. 21c) we observed a higher TON when lower temperatures were used. However, enzymatic reactions driven at lower temperatures typically incur a loss in reaction rate which prompted us to investigate the reaction kinetics. There, as shown in Table 8, we found that when using either NADH or NDAH cofactors for the BM3 N-D mutant, only turnover frequency for the reductase was affected in this manner in both the presence ($k_{cofactor}$) and in the absence ($k_{leakage}$) of 10-pNCA substrates. In contrast to this, the turnover frequency for the oxidase domain (k_{pNP}) increased at 4 °C. Correspondingly, coupling was enhanced as well at 4 °C, and therefore, the cofactor is used more efficiently at a lower temperature.

Table 8. Kinetics of BM3 mutant R966D/W1046S in dual buffer 10 mM PBS/100 mM BTP pH 8 at both 4 and 25 °C.

Kinetic parameter	NADH	NADH	NDAH	NDAH
Temperature (°C)	4	25	4	25
k_{pNP} (min ⁻¹)	202 ± 3.8	68.9 ± 3.8	48.9 ± 3.8	26.7 ± 6.7
$k_{cofactor}$ (min ⁻¹)	440 ± 58	500 ± 87	204 ± 24	267 ± 29
<i>Coupling</i> (%)	45.9	13.8	24	10
$k_{leakage}$ (min ⁻¹)	88 ± 8	486 ± 61	204 ± 20	1035 ± 153

K_{pNP} , $k_{cofactor}$ and $k_{leakage}$ are the turnover frequencies respectively for the production pNP from the substrate 10-pNCA in the presence of cofactors, the consumption of cofactors in the presence of 10-pNCA and the consumption of cofactors in the absence of substrate at the oxidase domain. The data for the catalytic constants was extracted from the slope obtained between t = 6 sec and t = 18 sec.

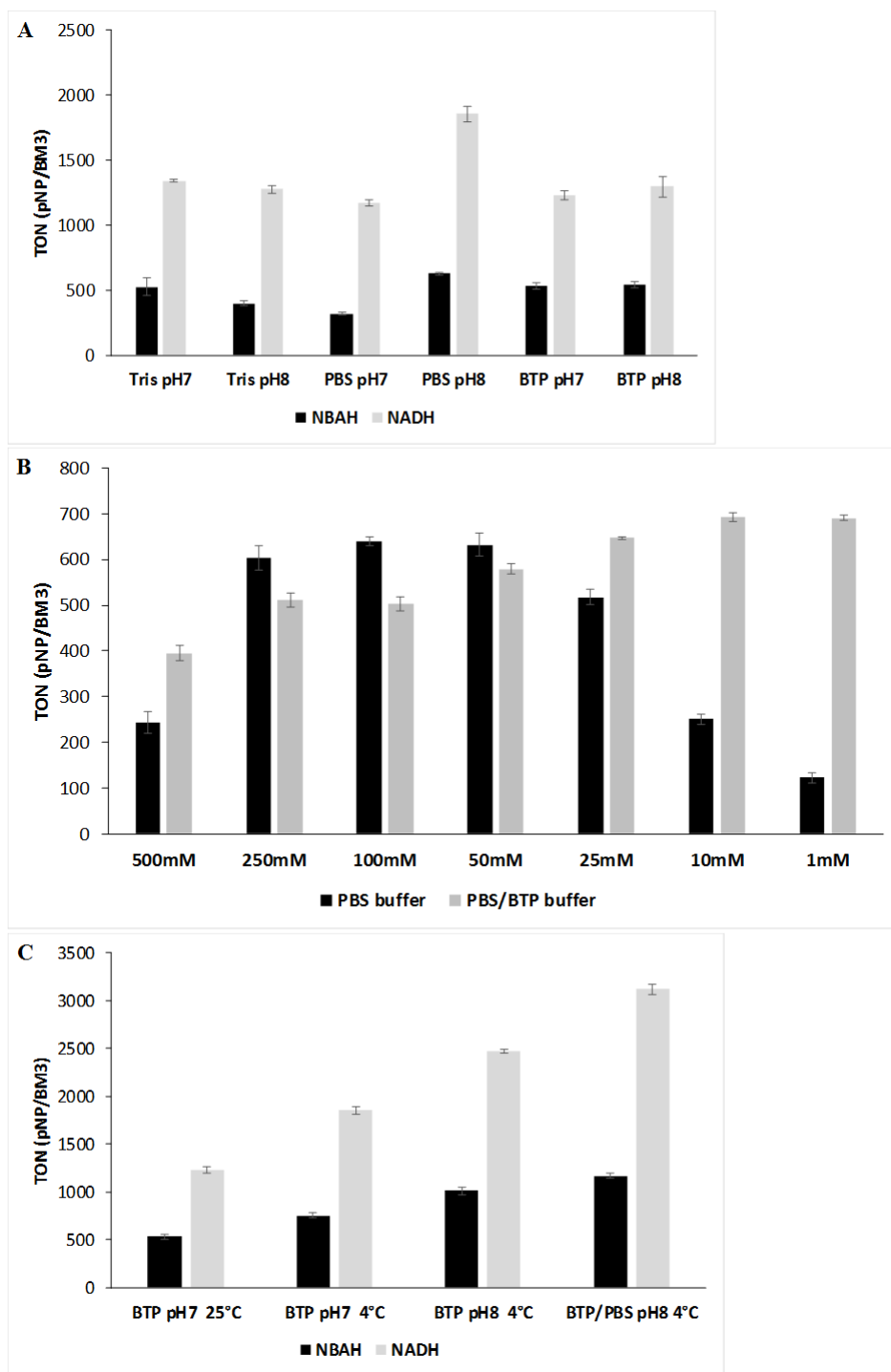


Figure 21: Turnover numbers of 10-pNCA conversion to *p*-nitrophenolate by BM3 mutant N-D using as a cofactor either NADH or NBAH. a: In 0.1M buffers ideal to preserve nicotinamide integrity (Tris & BTP) or demonstrating great ability to prevent enzyme unfolding (PBS & BTP) at both pH7 & 8 with all reactions driven at 25°C. b: In PBS buffers at increasing concentrations with and without a fixed concentration of 0.1M BTP buffer at 25°C. c: In 0.1M BTP and in 0.1M BTP/0.01M PBS buffer at 4°C. The standard deviation and mean for each sample were calculated from 3 replicates of two independent experiments.

2.4 Discussion

Through the heme contained within p450 cytochromes, their concentration can be measured by light absorption at 450 nm when the iron atom of the heme binds to carbon monoxide. This effect can also be used to evaluate the integrity of its monooxygenase domain. However, the reductase domain integrity is not monitored by this assay. In addition, it was demonstrated by DSC that BM3 has a T_m of 63 °C and 48 °C for its monooxygenase and reductase domains, respectively [199], thus suggesting that heat inactivation of the reductase domain of BM3 precedes that of the monooxygenase. Unlike DSC, DSF monitors the overall integrity of the enzyme and therefore can not indicate precisely where unfolding occurs within the protein. However, DSC is not well suited for the large-scale screening of multiple samples to establish an ideal buffer unlike DSF which is also inexpensive. Thus, we chose this technique over the p450 ferrous-CO and the DSC assay to screen for optimal reaction conditions.

Although our results (Fig. 18) suggest that p450 conformational stability is optimal at pH 7, exactly how and why this is remains elusive. Increasing charge repulsion within the folded enzyme and the loss of salt bridges as a result of local changes in charge distribution are factors to consider. Colloidal stabilization, which is highly dependent on pH, has been touted as a factor enhancing protein stability as well [492, 493]. Interestingly, DSF has been shown to be able to detect additional inflection points where protein-protein complexes are found [494]. However, no additional inflection points were found in our data despite the fact that it was demonstrated that BM3 functions best in pairs rather than individually [49, 495].

As shown in Table 5, increasing buffer concentrations enhance BM3's stability. Molecular crowding resulting in an excluded solvent effect might explain why increased concentration of buffer salts better protects the enzyme's conformational stability in the face of increasing temperatures. The high buffer salt concentration would exclude water and organic cosolvent access to the enzyme itself thereby enhancing its stability. Yet this would not explain why some buffers are more effective than others at stabilizing BM3. Rather, ligand binding of the buffers unto the enzyme might best explain the stabilizing effect of buffer salts such as PBS, citrate and BTP (Table 5). Various reviews [496, 497] have presented this claim as well, yet the exact mechanism by which a ligand/buffer stabilizes a protein is rarely established. In the case of BM3, the PBS buffer might bind inside the reductase active site where the 3 phosphates of NADPH would normally bind.

Whilst the exact interaction between buffers as stabilizing ligand molecules and proteins is not a thoroughly investigated field there are numerous instances where a positive effect on the T_m of a specific protein has been reported due to the usage of a specific buffer. This includes BTP, citrate, tris, HEPES and acetate buffers [498]. In this work, PBS, citrate and BTP buffers provided the best stabilization effects on BM3 (Table 5). There is limited data on the use of buffers more expensive than the common tris, citrate and PBS buffers as is the case with BTP. In one publication, 252 soluble proteins were tested by DSF against 28 different formulations [499]. Of the buffer tested, three repeatedly proved better at improving protein stability, namely citrate, bis-tris methane and N-(2-Acetamido) iminodiacetic acid buffers. The authors highlighted that despite the fact that several different buffers have been available for many years, buffers typically used in science are most often the least expensive ones, such as the citrate buffer, thus potentially overlooking better formulations.

The compatibility of organic cosolvent for BM3 has been investigated before. In one study, relative activity was investigated with WT BM3 as well as other mutants, including the w5f5 mutant optimized for increased organic cosolvent tolerance, in the presence of increasing organic cosolvent concentrations of tetrahydrofuran, dimethylformamide, acetonitrile, acetone, ethanol and DMSO [198]. They reported that 70% of activity was retained when the reaction was driven in a solution of 10% (v/v) DMSO whereas the other solvents allowed to retain only 5% of the enzyme activity at the same concentration. In another study, relative activity was studied, for several BM3 mutants built upon the w5f5 mutant, in the presence of increasing concentration of isopropanol, acetonitrile, DMSO and methanol with the latter two outperforming the other cosolvents [489]. This correlates with our own results (Table 6) where both methanol and DMSO display the highest enzyme melting temperatures of all organic cosolvents tested.

A weakness of DSF resides in its incapacity to inform on the ability of the buffers therein screened to drive reactions forward successfully, i.e. enzyme activity per se. As a result, when performing a p450 reaction in 1M PBS buffer, pH 7, 5% DMSO, it can be observed that, although enzyme stability is favoured in these conditions, nicotinamide compounds are quickly degraded and thus TON are extremely low (data not shown). Based on these findings, we therefore included in our work the investigation of conditions that would prevent nicotinamide loss in order to ultimately enhance TONs. We thus took a closer look at the relationship between factors affecting nicotinamide loss and TONs, such as buffer, pH and temperature.

It has been established that several buffers including PBS and citrate do not protect NADPH and NADH from degradation [315, 500]. Furthermore, it was shown that the rate of hydrolysis of the nicotinamide-ribose bond of NAD⁺ can be enhanced 3 to 4 folds in 0.1M PBS or citrate buffers, pH 7.5 when compared to either unbuffered reaction or tris and acetate buffers at the same concentration and pH [501]. In a different study, NADH and NADPH were shown to have half-lives of 27 and 13 hours, respectively, in 0.1M PBS buffer, pH 7, 25 °C, but half-lives of 330 and 31 hours, respectively, in tris buffer under the same conditions, thus showing the preserving qualities of tris over phosphate [502]. This is in agreement with our results (Fig. 19) where citrate and PBS buffers were by far the worst candidates in preserving the integrity of all three nicotinamide compounds tested (NADPH, NADH and NBAH) unlike tris and BTP. Nevertheless, the 0.1 M PBS buffer remains commonly used in p450 protocols [503–506]. In addition, to this day, several publications routinely use this buffer. Be that as it may, enhanced stability of NADPH and NADH in 0.1M tris and BTP, pH 7, also translated into higher p450 TONs when compared to 0.1M PBS, pH 7 (Fig. 20a). This demonstrates, at least for buffers, that taking into consideration nicotinamide as well as enzyme stability translates into higher TONs. Interestingly, although almost all cofactor degradation rates are significantly lowered in the less concentrated 0.1 M buffers this is not the case with NADPH when used with BTP or tris (Fig. 19a). This nevertheless does not translate into higher reaction yields when 1 M instead of 0.1 M Tris or BTP buffer is used, at either pH 7 or 8, despite the fact that both 1 M buffers enhance NADPH stability compared to 0.1 M (Fig. 22). The nature of this discrepancy is otherwise unclear to us.

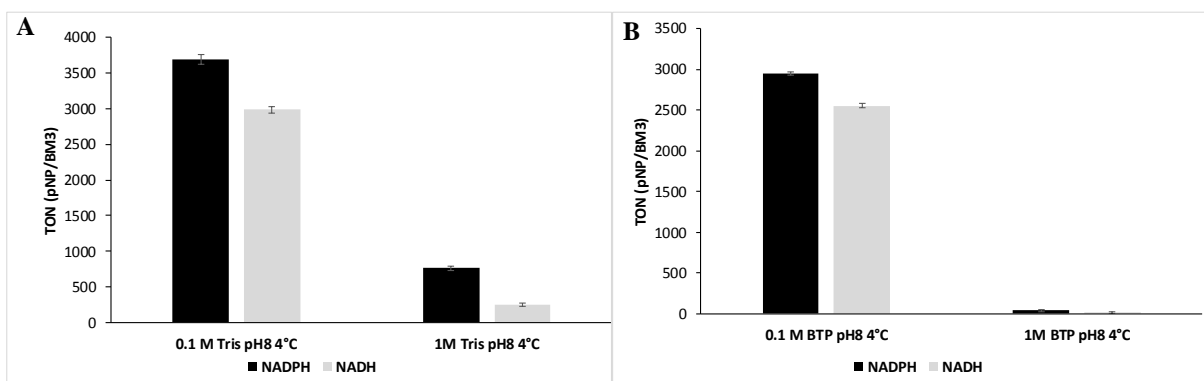


Figure 22: Turnover numbers of 10-pNCA conversion to *p*-nitrophenolate by WT BM3 using as a cofactor either NADPH or NADH in 0.1 M and 1 M a: Tris buffer b: BTP buffer at 4 °C pH 8. The standard deviation and mean for each sample were calculated from 3 replicates of two independent experiments.

The main mechanism behind the degradation of NADPH and NADH is that of a general acid catalysis [502, 507]. Indeed, it was confirmed that the relationship between pH and the degradation of those compounds can be averted by increasing pH [317, 502]. Here again, as can be seen in Figure 20a, prioritizing nicotinamide stability, with a pH of 8, translated into enhanced TONs. High temperatures have also been shown to accelerate NADH and NADPH degradation [317]. Here again, simply lowering temperatures from 25°C to 4°C and increasing pH from 7 to 8 improved TONs for the WT enzyme 1.9 to 2.6-fold for both NADPH and NADH cofactors, which translates into a TON of 3691 and 2984 respectively (Fig. 20b). However, lowering the reaction temperature prevents the use of DMSO which offers the highest protection for p450 (Table 6) as it is solid below 19 °C. Thus, in these conditions, the second-best co-solvent, methanol, was selected.

For the BM3 N-D mutant in the presence of either NBAH or NADH, increasing pH from 7 to 8 only slightly increased TONs in PBS and BTP buffers while it decreased with the tris buffer (Fig. 21a). Another surprising result was that, at pH 8, PBS provided considerably higher TON values for NADH despite being the most deleterious buffer for the stability of all nicotinamide compounds (Fig. 19). We theorized that as both NADH and NBAH miss either 1 or 3 phosphate groups compared to NADPH, the use of PBS can act as a decoy molecule inside the reductase's active site thereby promoting the correct use of both electron donors. PBS buffers at decreasing concentrations, with or without 0.1 M BTP, were prepared to assess if a lower concentration of PBS could be used not so much as a buffer but as a ligand or a decoy molecule in order to enhance TONs even further (Fig. 21b). BTP was chosen as it was the second-best buffer following PBS (Fig. 21a). When comparing the TONs of the 0.1M PBS buffer to the dual 0.1M BTP / 0.01 M PBS buffer, TONs were improved by about 8% from 639 to 693 moles of pNP/moles of p450 for the latter case (Fig. 21b) (this increase was significant within a $\alpha = 0.05$ significance level). Contrastingly, when the dual BTP/PBS buffer was used at pH 8, 4°C, TONs were increased 1.15-fold when compared to BTP alone for NBAH and 1.26-fold for NADH (Fig. 21c). Here again, as was the case for WT BM3, lowering temperatures from 25°C to 4°C and increasing pH from 7 to 8 improved TONs for BM3 mutant N-D by a factor of 2 for both NBAH and NADH demonstrating that favoring nicotinamide stability first and then enzyme stability can significantly improve TON. Overall, compared to the initial conditions, 0.1M BTP, pH 7, 25°C, dual BTP/PBS buffer at 4°C, pH 8 raised TONs 2.2-fold up to 1170 for NBAH and 2.5-fold for NADH up to a total of 3117.

The coupling of the CYP enzyme redox reactions are measured using the rate at which product is generated divided by the rate at which cofactor is consumed to evaluate the ratio of product formed to that of cofactor consumed, on a molar basis. It is a measure of how effective a cytochrome is at using a cofactor to drive a reaction successfully on a given substrate. Failure to catalyze the reaction correctly can lead amongst other things to the generation of hydrogen peroxide or superoxides, strong oxidants which are deleterious to the enzyme. Buffers such as BTP have been described to have the ability to act as free radical scavengers [508] which may be one of the features which makes it a superior buffer for BM3, particularly when using an alternative cofactor such as NBAH given its low coupling at 25 °C with the N-D mutant (Table 8). It's also interesting to note that coupling percentage from Table 8 is at its highest at 4 °C and that yields are likewise enhanced when temperature is lowered (Fig. 21c) an effect we surmise stems in part from the slower activity of the reductase observed at lower temperatures. This would suggest that a greater coupling efficiency at a lower temperature is another factor besides nicotinamide and enzyme stability which can help drive reactions further. In addition to increased coupling efficiency, leakage towards either cofactors was hindered when the temperature was lowered which may also contribute to the overall better product output observed at 4 °C. We did not however investigate if the addition of phosphate to the buffer composition when using NBAH or NADH increased coupling, and thus TON, by acting as a ligand inside the reductase's active site. Although there is no other published data to which the coupling efficiency obtained here can be compared, our results in regards to TON falls in the same range as to what was obtained with the BM3 N-D mutant when it was first used with NBAH [296] achieving a TON of 312 in a 20 mM PBS buffer, pH 7.4, close to our own result of 533 in 0.1 M BTP pH 7 at 25 °C. In terms of buffer composition, much remains to be investigated. Good's buffers as well as many other buffers could still be tested to improve BM3's performance. In this regard, organic cosolvents mixtures, namely methanol or ethylene glycol, could be further explored at temperatures below 0 °C as a mean to enhance BM3's product output. A major pathway to the degradation of nicotinamide compounds not yet discussed is the nucleophilic addition at the C-4 position of the pyridine ring of nicotinamide to form a 1,4-dihydropyridine structure, a reaction which has been shown to occur with substrates harboring nucleophilic moieties [509]. We have not yet established how the substrate 10-pNCA and its products, pNP and ω -oxycarboxylate, influence nicotinamide stability in this regard nor how some buffers might act as nucleophiles in this type of pathway to nicotinamide degradation. A different factor that could also influence TONs is that of competitive inhibition by the product ω -oxycarboxylate released when using 10- or 12-pNCA, a factor which could be prevented with the use of a biphasic system.

2.5 Conclusion

Our work demonstrates that, in terms of total yield, or TON, a 2 to 2.6-fold improvement in the performance of p450 BM3 reactions can be gained by simply improving the buffer system with the cofactor stability in mind. This effect was observed for NADPH, NADH and NBAH with both WT and N-D BM3. Furthermore, by the same strategy we also demonstrated that product yields for the N-D mutant using NADH (TON = 3117 for pNP/BM3 Fig. 21c) can compete with that of WT BM3 using its natural cofactor NADPH (TON = 3691 pNP/BM3 Fig. 20b). This is an important step as NADPH cost is one of the main factor that holds back the commercial use of this soluble enzyme for the production of valuable chemicals given that NADPH is generally ten times the price of NADH. In addition, NADH just like NADPH can be regenerated enzymatically. The chemical analog NBAH, which can be regenerated chemically [296], can be purchased and synthesized for a tenth to a hundredth of the price of NADH. As such, although the best TON obtained with NBAH (TON = 1170 pNP/BM3 Fig. 21c) is roughly a third of that obtained with NADH (TON = 3117 pNP/BM3 Fig. 21c) using NBAH would be still be more cost effective than using NADH. Furthermore, the N-D mutant could be evolved further to better accommodate NBAH.

3 Optimisation of the p450BM3 cytochrome assisted by consensus-guided evolution

Authors: Thierry Vincent^a, Bruno Gaillet^a & Alain Garnier^{a*}

Affiliation:

^a Department of chemical engineering, Université Laval, Québec, Québec, Canada, G1V 0A6

* corresponding author: Alain Garnier; email: alain.garnier@gch.ulaval.ca; telephone +1 418 656

[2303](#)

Résumé

Les cytochromes p450 ont attiré beaucoup d'intérêt au courant des dernières années dû à leur capacité d'insérer un atome d'oxygène dans un lien carbone-hydrogène saturé, un exploit difficile à accomplir en chimie traditionnelle. La plupart des activités dans ce domaine ont été centrées sur l'enzyme bactérienne CYP102A1 ou BM3 de *Bacillus megaterium*, comme elle s'est montrée capable d'hydroxyler/agir sur une large variété de substrats menant ainsi à la production de pharmaceutique, d'hormones et de produits chimiques fins attrayants pour l'industrie. En outre, au contraire des autres cytochromes, BM3 est soluble et naturellement fusionné à sa réductase facilitant ainsi son usage. L'utilisation industrielle de BM3 est néanmoins entravée par son instabilité et la nécessité qu'elle entraîne d'utiliser le NADPH, cofacteur hautement dispendieux. Dans cet ouvrage, nous avons ajouté plusieurs mutations au mutant BM3 R966D/W1046S, qui améliorent le rendement spécifique de l'enzyme quand les cofacteurs peu coûteux NADH et N-benzyle-1,4-dihydronicotinamide (NBAH) sont utilisés au lieu du NADPH. Soit les mutations A769S, S847G, S850R, E852P et V978L, toutes localisées sur le domaine réductase de BM3 afin de laisser intact le site actif du domaine oxydase. Pour les réactions utilisant le NBAH et le nouveau mutant nommé NTD5, ceci a mené à une augmentation du rendement spécifique de l'enzyme d'un facteur 5.2 comparativement au mutant R966D/W1046S. Pour les réactions utilisant le NADH et le nouveau mutant nommé NTD6, ceci a mené à une augmentation du rendement spécifique de l'enzyme d'un facteur 2.3 comparativement au mutant R966D/W1046S. Nous avons démontré également que les réactions effectuées avec le NADH combiné au mutant NTD6 surpassent le rendement spécifique possible avec l'enzyme sauvage BM3 utilisant le NADPH tout en gardant son habileté à utiliser ce dernier cofacteur avec un plus grand rendement spécifique.

Abstract

P450 cytochrome enzymes have attracted much interest over the years as they are able to insert oxygen into saturated carbon-hydrogen bonds, a difficult feat to accomplish by traditional chemistry. Much of the activity in this field has centered on the bacterial enzyme CYP102A1, or BM3, from *Bacillus megaterium*, as it has shown itself capable of hydroxylating/acting upon a wide range of substrates, thereby producing industrially relevant pharmaceuticals, fine chemicals and hormones. In addition, unlike most cytochromes, BM3 is both soluble and fused to its natural redox partner, thus facilitating its use. The industrial use of BM3 is however stifled by its instability and its requirement for the expensive NADPH cofactor. In this work, we added several mutations to the BM3 mutant R966D/W1046S that enhanced the turnover number achievable when the inexpensive cofactors NADH and NBAH were used in place of NADPH. These new mutations, A769S, S847G, S850R, E852P and V978L, are all localized on the reductase domain of BM3 thus leaving the oxidase domain intact. For NBAH-driven reactions by a new mutant named NTD5, this led to a 5.24-fold increase in total product output when compared to the BM3 mutant R966D/W1046S. For reactions driven by NADH with another new mutant named NTD6, this enhanced total product output by as much as 2.3 fold when compared to the BM3 mutant R966D/W1046S. We also demonstrated that reactions driven by NADH with the NTD6 mutant not only surpassed total product output achievable by wild type BM3 with NADPH but also retained the ability to use this latter cofactor with greater total product output as well.

3.1 Introduction

Cytochrome p450 enzymes (CYPs) belong to a family of heme-thiolate enzymes that bear the capacity to insert, from molecular dioxygen, a single oxygen atom into a saturated carbon-hydrogen bond, resulting in the hydroxylation of the targeted substrate [510]. Such reactions are difficult to perform when using purely chemical methods, as it is a multi-step process that leads to the formation of undesired side products and toxic chemicals. As such, CYPs offer interesting alternative synthesis routes. The substrate range of CYPs is wide, allowing them to participate in the synthesis/metabolism of hormones [511], lipids [101, 102], antibiotics [512–514], vitamins [515–517] or the breakdown of xenobiotics such as herbicides [518–520], insecticides [521, 522] and drugs [523–526]. Although this large substrate compatibility is dispersed across the CYPs of many different species, one in particular, CYP102A1 or simply BM3, has shown to be able to accommodate a broad substrate range if used with a decoy molecule [232, 240], with modifications to its active site [82, 218, 226, 527, 528] or simply by combining both strategies [237]. Moreover, unlike most CYPs, BM3 has two distinct advantages, it is a soluble enzyme and is naturally fused to its redox partner [529] making it catalytically self-sufficient. BM3 also boasts the highest turnover frequency ever reported for a CYP (17 000 min⁻¹ for arachidonic acid [530]).

The reaction cycle of wildtype BM3 normally necessitates electrons from nicotinamide adenine dinucleotide phosphate (NADPH) which are transported through the reductase domain all the way to the oxidase domain's active site. There, electrons can reduce dioxygen and the reaction cycle can either go towards the proper hydroxylation of the substrate [50] or, should the reaction fail to hydroxylate the substrate, go towards the generation of either water, peroxide or a superoxide anion [60]. Both these outcomes are referred to as coupling and uncoupling events respectively, the former being expressed as the percentage of electrons from the cofactor actually used to hydroxylate the substrate. Similarly, should the oxidase's active site lack its substrate, the reductase may still oxidize NADPH and shuttle electrons towards the oxidase, an event described as leakage and resulting in the generation of either peroxide, superoxide or water [63]. These side reactions are especially important to consider as they expose the enzyme to reactive oxygen species (ROS) which can in turn lead to the formation of various protein radicals [531], and hence decreased enzyme stability [63]. Accordingly, for CYPs, there is also evidence that protein radicals, heme adducts and the loss of the heme itself can occur as a result of the faulty transfer of the electrons from NADPH across the reductase, towards the oxidase's active site [532, 533]. The high price of the cofactor NADPH remains a major hurdle in propelling forward an economically viable free enzyme process but it can be bypassed by using

alternative low-cost cofactors such as nicotine adenine dinucleotide (NADH) [306] or N-benzyl-1,4-dihydronicotinamide (NBAH) [296] with the R966D/W1046S BM3 mutant (termed N-D mutant in this work). The change in electron source however causes an increase in both uncoupling and leakage when compared to NADPH (unpublished data). It is therefore imperative to limit uncoupling, leakage, proteins radicals and heme adducts within BM3 in order to make an economically viable enzymatic process with low-cost cofactors such as NADH or NBAH.

The stability of CYPs has been singled out in numerous reviews as the main hurdle when considering its applicability process [197, 272, 481–483]. In the case of alkane hydroxylation for instance, this issue strongly manifests itself by the necessity to use an organic co-solvent to improve the substrate solubility in the aqueous reaction phase. Indeed, increasing organic solvent concentration rapidly leads to CYP denaturation and deactivation. Very few avenues are available to alleviate this effect. In one case, by screening libraries generated by both error prone-PCR and site saturation mutagenesis, a mutant of BM3 containing four mutations (T235A/R471A/E494K/S1024E) was created [198]. Named W5F5, the mutant was described as being able to retain its relative activity more efficiently than BM3 in reactions driven at increasing concentrations of organic cosolvents with *p*-nitrophenoxydodecanoic acid (12-pNCA) used as a substrate and supplied with NADPH. For instance, when assessing the relative activity between reaction driven in 0 and 25 % (v/v) DMSO, wild type BM3 retained less than 45 % of its activity whereas the W5F5 mutant retained 100 % of its activity. Furthermore, compared to BM3, W5F5 was shown to have a greater turnover frequency towards those same substrates going from 114 to 286 min⁻¹ and from 49 to 294 min⁻¹ in reactions performed in 0 % and 25 % (v/v) DMSO, respectively. In another publication, these same mutations were applied to the BM3 drug-metabolizing mutants M01, M02, M05, and M11 [489]. There, the mutants were shown to better retain their turnover frequencies in increasing organic cosolvent concentrations than their original counterparts. In this work, our first objective was to combine the N-D BM3 mutations with the stabilizing mutations of the W5F5 mutant, cited above, to obtain variants that are both more stable and capable of using more affordable cofactors. The combination of these two sets of mutations generated the mutant NTD1 (Table 10). Another notable effort in improving the stability of BM3 was to replace the reductase domain of BM3 with the more thermostable reductase domain of CYP102A3 of *Bacillus subtilis*, thus generating the A1MA3R chimera [247]. This BM3 chimera was shown to be significantly more thermostable than wildtype BM3 but its turnover number in term of substrate utilisation was 30% inferior to BM3 using NADPH as cofactor. In a similar strategy, a library of chimeras of BM3 and CYP102A2 was created

where the p450 cytochromes displayed both a wider substrate range and increased thermostability [534].

In the work presented here, rather than generating chimeras between CYP102A1 (BM3), CYP102A2 and CYP102A3 we opted to create, from NTD1, several new variants by consensus guided evolution using these same CYPs. As CYP102A1, CYP102A2 and CYP102A3 are closely related, they share a similarity of amino acid sequence of 61 %. Consensus guided evolution was chosen as a technique by which to enhance enzyme performance as it is a much less work-intensive process than directed evolution and because it can rely on existing data in regards to the relative stability of CYP102A1, A2 & A3. In the reductase domain, several clusters of amino acids are highly conserved such as those implicated (or nearby those implicated), in the anchoring of either one of the two flavin prosthetic groups. For instance, located in the flavin adenine dinucleotide/NADPH-binding domain of BM3, the amino acids V849, A853 and W854, whom were shown to interact with the adenine group of NADPH [22] (Figure 23A). We decided to explore the discrepancies between CYP102A1, A2 and A3 sequences in such strongly conserved regions. Thus, our second objective was to create, from NTD1, through a consensus guided approach, variants that brought forth enhanced stability and yield all whilst retaining the ability to utilize alternative cofactors such as NADH or NBAH. To do so, we opted to copy the amino acids mismatches in some of these strongly conserved areas (Figure 23B) within the reductase region and generated in the process a small library of 12 variants derived from NTD1.



		V849	A853	W854		
A						
CYP102A1 (BM3)	839	EKQASI	TVSVV VS GE AW SG	YGEYKGIASNYLAELQE		873
CYP102A2		PRQASI	TVGV V RGP AW SG	RGEYRGVASNDLAERQA		
CYP102A3		ANIVSM	TVGV V KAS AW SG	RGEYRGVASNYLAELNT		
CYP102A4		QDRLSI	TVGV V NAP AW SG	EGTYEGVASNYLAQRHN		
CYP102A5		HNRLSI	TVGV V NAP AW SG	EGTYEGVASNYLAQRHN		
B						
CYP102A1 (BM3)	839	EKQASITVSVV S GE AW SGYGEYKGIASNYLAELQE				873
			S TV VV AW SG GEY G ASNYLAEL			
CYP102A3			ANIVSMTVGVV K AS AW SGRGEYRGVASNYLAELNT			
			S TVGVV K AS AW SG GEY G ASNYLAEL			
CYP102A1 variant			EKQASITVGVV K AS AW SGYGEYKGIASNYLAELQE			

Figure 23: A. Strongly conserved residue cluster within the reductase domain of the CYP102A subfamily. B. Consensus guided evolution approach utilized to generate new BM3 variants.

To evaluate the performance of the created variants, we followed spectrophotometrically *p*-nitrophenolate (pNP) release from the hydroxylation of *p*-nitrophenoxydecanoic acid (10-pNCA) by BM3 [76] which enabled us to measure the turnover number (TON), defined in this work as the overall molar ratio of pNP produced per BM3 present, as well as the reaction rates of each BM3 variant of interest. We therefore describe new BM3 mutants that display an increase in both TON, turnover frequency and thermotolerance when used with the more affordable cofactors NBAH and NADH but also with NADPH. Moreover, as all of the mutants in this work display a propensity for leakage when used with NBAH or NADH we used a fed batch approach to mitigate these, to further enhance TON.

3.2 Methods

Chemicals

Escherichia coli bacterial strains used in this work, DH5 α and B121, were acquired from Thermo Fisher Scientific. The restriction enzyme DpnI was purchased from New England Biolabs whilst the Pfu polymerase, the deoxynucleotides and the PCR buffer were purchased from Bio Basic. The vector pET16B was obtained from Novagen. All DNA primers were purchased from IDT technologies. NADH and NADPH were purchased from p212121. Both *p*-nitrophenoxydecanoic acid [490] and N-benzyl-1,4-dihydronicotinamide [491] were synthesized by Oleotek using the protocols in the afore referred work. Organic solvents and all other chemicals were purchased from Bioshop Canada.

Cloning, expression & purification

The cloning of both the wild type BM3 and the N-D mutant into the pET16B vector was achieved and described in previous work (Chapter 2). Briefly, the wild type BM3 sequence was inserted into pET16B by PCR using an amplified genomic DNA template from *Bacillus megaterium* (ATCC 14581) followed by restriction-based cloning using *SpeI/BamHI* restriction sites. Cloning in the pET16B added an octahistidine tag (GHHHHHHHH) which was followed by a spacer at the N-terminus (SSGHHTSM). Similarly, for the generation of the W1046S mutation, the whole DNA sequence of BM3 was amplified and reinserted with the new mutation using the *SpeI/BamHI* restriction sites. Subsequently, to generate the N-D mutant, the R966D mutation was inserted to the W1046S BM3 mutant by DpnI site directed mutagenesis. The addition of the T235A, R471A, E494K & S1024E mutations unto the N-D mutant, thus generating the NTD1 mutant, was performed by TOP Gene Technologies Inc. Subsequently, the prefix NTD was used to describe every mutant generated by consensus guided evolution as they were all created by using NTD1 as a parent mutant. Additional mutations added thereafter to the NTD mutants were performed by DpnI site directed mutagenesis. Table 9 lists the primers used for the generation of all mutants created in this work whereas Table 10 describes the combination of primers and the template used to generate these same mutants.

Table 9. Nucleotide sequence of each primer used in this work.

Primer name	Primer sequence
A21purple1	CAAGCAAGCATCACGGTCGGCGTTGTCAGAGGACCAGCGTGGAGCGGACGT
A23purple1	TTCTCCATATCCGCTCCACGCGCTTGCTTTGACAACGCCGACCGTGATGCTTGCTTG
A21purple4	ATGCTTGAAGTCTTAAAAATACGAGGCGTGTGAA
A21purple5	GCACTGGCTTCTAAAACGGTCTGCCCGCCGATAAAG
A21purple6	GAGGTTCAAGAAGCTGCTACGCGCACACAGCTTCGC
A21Green1	TCCGTATTTGGATGCGGCGATCATAACTGGGCTTCTACGTATCAATATGTGCCTCGTT TTATCGATGAAACGCTTGCCGC
A21Green2.2	ATTGTAACGGCGTCTTATAACGGTAAACCG
21AEE-QD1	CACGTCTTTTTCGTACATGCCTGTATCTTGTAGCTGCTG
A21EE-QD2	CACGTCTTTTTCGTATCGGCCTTTATCTTGTAGCTGCTG
A21EE-QD3	CACGTCTTTTTCGTACATGCCTGTATCTTGTAGGTGCTCGAGCCATAAGCG
A21A-D	TGCTTCAACGTCAGGTGCCAT
A21V-L	GTTCAAGCACTTAATGGAACAAGAC
RCV978L	TCAATTTCTTGCCGCTTGTCCATTAGGTGCTGAACGTATGT
BamHIp16b	ATGGATCCTTACCCAGCGCTCACGTCTT
A235T	TGAACAAAGCGATGATTTATTAACGCATATGCTAAACGG
RCR966D	ATTTGGCATATCAGAAAAAGCGGTAT
R966D	ATACCGCTTTTCTGACATGCCAAAT
Sp16b	CCATCATACTAGTATGACAATTAAGAAAATGCCTCAGC
1678	GCGTCTTATAACGGTCATCCGCCTG

The PCR reactions used for mutagenesis of the NTD sequences were performed with 100 ng of plasmid, 10 nmol of deoxynucleotides (Bio Basic), 10 pmol of each primer and 5 units of *Pfu* polymerase (Bio Basic), all of which were added to a 50 µl PCR reaction tube. To generate a megaprimer, 20 cycles of PCR with an elongation time of 2 minutes followed by 30 cycles with a 20-minute elongation time was performed. DpnI (NEB) restriction enzymes, 10 units, were added to the ensuing PCR reactions which were then incubated 1 hour at 37 °C. The edited plasmids were then inserted by a standard heat shock protocol into DH5α competent cells and sent for sequencing.

The production of every different BM3 mutants in this work was achieved by transforming through heat shock the *E. coli* strain BL21 (DE3) with the pET16B expression plasmid on Luria-Bertani (LB) plates containing 100 µg/ml ampicillin. A single colony was then selected and grown overnight at 37 °C in 100 ml of LB medium with 100 µg/ml of ampicillin. The pre-culture would then be centrifuged at 2550 g for 10 minutes and resuspended in 100 ml of fresh LB broth. A 2.5 %

inoculum (22.5 ml) of pre-culture was added to 0.9 L of modified Terrific Broth (MTB, 24 g/L tryptone, 48 g/L yeast extract, 10 g/L NaCl, pH 7.6) containing 100 µg/ml of ampicillin and grown at 37 °C. Once the culture reached an OD₆₀₀ of 0.6, 150 ml of MTB, pH 8, 50 ml of 50 % (v/v) 0.48 µm filtered glycerol, 200 µl of ampicillin at 100 mg/ml and 1.2 ml of 1M isopropyl β-D-1-thioglycopyranoside (IPTG) were added to the culture. Afterwards, the incubation temperature was promptly set to 28 °C. Cells were incubated for 5-8 hours and were thereafter pelleted by a 10 min centrifugation at 2550 g and stored at -80 °C. For the purification, the cells were first thawed on ice, resuspended in 20 ml of lysis buffer (100 mM NaCl, 25 mM Tris-HCl, 1 mM phenylmethylsulfonyl fluoride, pH 8) and then lysed by sonication using 4 x 15 s bursts with 30 s pauses. Sonication and every subsequent step were either performed on ice or at 4°C. Afterwards, sonicated cells were centrifuged at 26 200 g for 35 minutes. The supernatant was passed on 25 ml of a Ni sepharose™ 6 Fast Flow resin (GE Healthcare) packed in a homemade chromatography column, prepared by rinsing it with 200 ml running buffer (40 mM NaH₂PO₄, 500 mM NaCl, pH 7.4) before and after the supernatant solution was applied to the column. After which, the column was successively washed with running buffers of increasing histidine concentration beginning with 100 ml at 10 mM, 100 ml at 20 mM and then 50 ml at 40 mM. Enzymes were then eluted from the column by applying a running buffer with 160 mM histidine. The eluate was mixed to 1 volume of glycerol yielding a 50% glycerol enzyme solution and stored at -80 °C. CO difference spectroscopy was used to measure the concentrations of p450 enzymes by using an extinction coefficient of 91 mM⁻¹cm⁻¹ for the 450nm absorption peak as described by Omura & Sato 1964 [9].

Activity assays with 10-pNCA

Fresh NADPH and NADH cofactor stocks were prepared in Milli-Q water, NBAH and 10-pNCA were prepared in methanol. All assays were prepared in a final volume of 1.5 ml with 100 nM of BM3, pH 8 and were incubated overnight in darkness. Assays where NBAH was employed utilized a dual buffer of 10 mM PBS/100 mM Bis-Tris propane (BTP) whereas assays using either NADH or NADPH both employed a 100 mM Tris buffer. The enzymatic reactions determining TON in harsher conditions (experiments shown in Figure 25, panel A and B) were performed in the presence of 15 % methanol (v/v) at 4 °C or in the presence of 5% methanol (v/v) at 30 °C, with 600 µM 10-pNCA and 1500 µM cofactor (NADH or NBAH). For the assays performed at 30 °C, prior to the initiation of the reactions, buffers were preincubated 1 hour at 30 °C. Otherwise, before adding the cofactor to the reactions, 45 µl of 20 mM 10-pNCA was added to the reaction mixture after which the reactions were initiated by adding 30 µl of a 75 mM stock cofactor solution to the reaction mixture. The cofactor preincubation assays shown in Figure 25, panel C and D were similarly prepared but with the p450

enzymes first incubated in absence of 10-pNCA with 250 μM NADH without any methanol or 250 μM NBAH with 0.3 % methanol (v/v), both for 30 minutes at 4 °C. Following this, 10-pNCA and cofactors were added to a final concentration of 600 μM and 1500 μM , respectively. In the cofactor pre-incubation assays, final methanol concentration reached 5.3 % and 5 % (v/v) for NBAH and NADH, respectively.

The fed batch assays investigating TON with the NBAH cofactor (experiments shown in Figure 25A), were achieved using 600 μM 10-pNCA and 1500 μM NBAH in 5% methanol (v/v). Before adding NBAH to the reaction, 45 μl of 20 mM 10-pNCA was added to the reaction mixture after which the reactions were initiated by adding 5 μl of a 75 mM stock cofactor solution every 5 min, for 30 min. The enzymatic reactions determining TON shown in Figure 26, panel B and C were performed using 1 mM 10-pNCA and 3 mM cofactor (NADH or NADPH) in 5% methanol (v/v). Prior to the addition of either cofactor to the reaction, 37.5 μl of 40 mM 10-pNCA was added. The reactions were then initiated by supplying 10 μl of a 75 mM cofactor solution (NADH/NADPH) to the reaction mixture every 5 minutes a total of 6 times for a final cofactor concentration of 3 mM. For the absorbance measurements, 1ml reaction mixture was mixed with 150 μl , 10 N NaOH and 850 μl methanol in a 2 ml microtube. A 1 ml volume of this mixture was added to a 1 cm wide cuvette from which the absorbance of *p*-nitrophenolate was measured at 410 nm in a Genesys 10S UV-Vis spectrophotometer (Thermo Fisher Scientific) and the concentration determined from a calibration curve. If the absorbance level leaved the range of the calibration curve, the samples would then be further diluted in methanol. The standard deviation and mean for each sample set were calculated from two independent experiments each with three biological replicates.

Likewise, for kinetic measurements, the dual BTP buffer and the Tris buffer in 5% methanol (v/v), pH 8 were used with NBAH and NADH, respectively, with a 100 nM enzyme concentration, and lower substrate concentrations, 300 μM 10-pNCA and 300 μM cofactor (NADH or NBAH), 25 °C. The reactions were all performed in a final volume of 300 μl in 96 well plates and measured using a Synergy H1 hybrid multi-mode plate reader (BioTek). Once reactions were initiated by the addition of 100 μl of 900 μM cofactor stock solution (NBAH or NADH) to 200 μl of reaction solution containing both 10-pNCA and p450 enzyme, absorbance measurements were performed every 6 s for 2 min. The release of pNP from 10-pNCA and the consumption of NBAH or NADH were measured at 355 nm, 340 nm and 410 nm respectively. To monitor leakage, methanol was added to the mixture in place of 10-pNCA thus keeping methanol concentration at 5 % (v/v). The concentrations of pNP,

NBAH or NADH were established from a calibration curve. The standard deviation and mean for each sample set were calculated from three experimental replicates.

Library screening

The screening of the mutant library was performed from the lysates of *E. coli* B121 strains. Every mutant was transformed into a B121 strain and grown at 37 °C in 100 ml of LB broth to an OD of 3.0 after which they were induced with the addition of 100 µl, 1 M IPTG. Cells were grown for 3 hours at 28°C and centrifuged at 2840 g at 4 °C in 50 ml tubes for 10 minutes. Cell pellets were resuspended in 15 ml of lysis buffer (100 mM NaCl, 25 mM Tris-HCl, 1 mM phenylmethylsulfonyl fluoride, pH 8) and lysed by sonication using 4 x 15 s bursts separated by 30 s pauses, always on ice. A total of 4 ml of each sample was then further centrifuged 2 min at 10 390 g, 4 °C, and then put back on ice. Concentration of p450 enzymes was assessed by the CO difference spectroscopy method in each sample. The screening assays themselves were performed as described for kinetic measurements at 25°C but only with NBAH and with measures taken every 15 seconds for 30 minutes. The TON achieved for each member of the library was measured at the end of that 30-minute assay. The standard deviation and mean for each sample set were calculated from three experimental replicates.

3.3 Results

BM3 mutant library construction and selection

The N-D mutant (R966D/W1046S) was first modified by adding the four mutations of W5F5 (T235A/R471A/E494K/S1024E) which have been shown to increase BM3's stability [198]. This variant was named NTD1 (Table 10 lists the mutants cited or constructed in this work). Starting from and including NTD1, a library of 12 mutants was created (Table 10) based on a consensus approach between CYP102A1 (BM3), CYP102A2 and CYP102A3, the latter two from *B. subtilis*, in highly conserved amino acid clusters in the reductase sequence (Figure 23), and screened from cell lysates for yield. The TON value for each variant tested can be seen in Figure 24. In light of the positive results obtained with NTD2, 3 and 4, combination of their mutations was introduced in variants NTD5 and NTD6 (Table 10). Mutations comprised in NTD3 and NTD4 were combined into NTD1, yielding NTD5, while NTD6 resulted from the combination of NTD5 and NTD2 mutations. Although most variants generated in our library added amino acids present on the sequence of both CYP102A2 and A3, two of the three mutations brought forth on NTD3 were present solely on CYP102A2 and not A3. Therefore, from NTD6 another variant was generated, NTD7, where two mutations were adjusted to those found on the sequence of CYP102A3 instead. Mutants N-D, NTD1-7 were produced, purified and further tested. All of the TONs of figure 24 are significantly lower than those of figures 25-27 which we presume is due to the fact that in figure 24 unpurified cell lysates are used whereas for figures 25-27 purified BM3 enzymes are used.

Table 10. Mutations carried by every BM3 mutant in this work and primer used in their creation.

BM3 Mutant	Parent mutant	Added mutations	Primers used to generate mutant	Reference
N-D	WT BM3	R966D, W1046S	SpeIpet16b + BamHIpet16b, 1678 + RCR966D	Maurer et al. 2005, Ref. 41
W5F5	WT BM3	T235A, R471A, E494K, S1024E	n/a	Wong et al. 2004
NTD1	N-D	T235A, R471A, E494K, S1024E	n/a	
NTD 235T	NTD1	A235T	A235 + RC1678	
NTD5	NTD3	A769S, S847G, S850R, E852P	A21purple5 + BamHIpet16b	First reported here
NTD6	NTD5	V978L, A769S, S847G, S850R, E852P	1678 + RCV978L	
NTD7	NTD6	V978L, A769S, S847G, S850K, G851A, E852S	1678 + A23purple1	
Library				
NTD2		V978L	1678 + RCV978L	
NTD3		S847G, S850R, E852P	A21purple1 + BamHIpet16b	
NTD4		A769S	A21purple5 + BamHIpet16b	
NTDa		P808E	A21purple4 + BamHIpet16b	
NTDb		K572H, T576S, K580Y, A583R	A21Green + RCR966D	
NTDc	NTD1	A534S, H539K	A21Green2.2 + RCR966D	First reported here
NTDd		E1036Q, E1037D, K1038T, R1040M	R966D + 21AEE-QD1	
NTDe		E1036Q, E1037D, R1040M	R966D + 21AEE-QD2	
NTDf		Q1033E, Q1034H, E1036Q, E1037D, K1038T, R1040M	R966D + 21AEE-QD3	
NTDg		L755V, D757E, P758A, V759A	A21purple6 + RCR966D	
NTDh		A1008D	1678 + A21A-D	

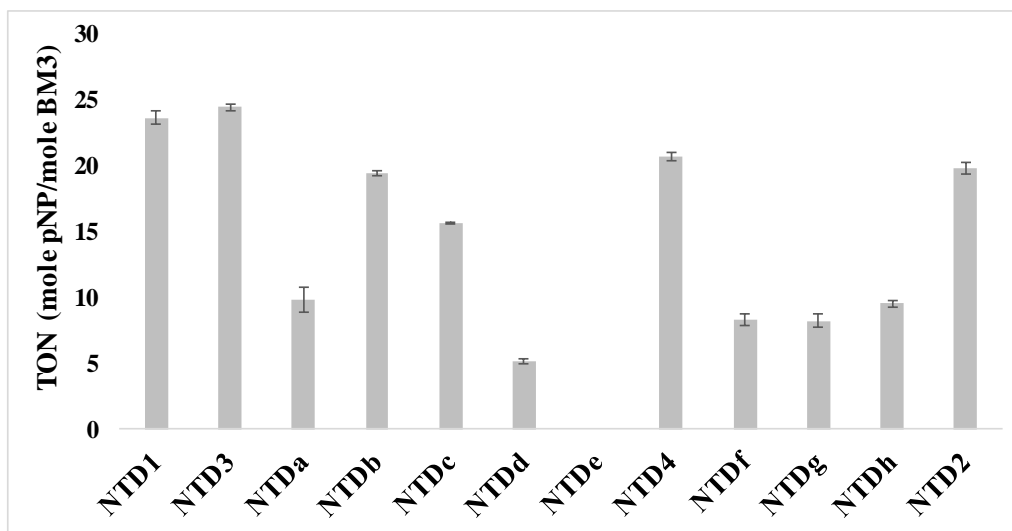


Figure 24: Screening assay for the newly generated NTD1 variants where turnover numbers for the conversion of 300 μ M 10-pNCA to *p*-nitrophenolate by the newly generated NTD1 variants using 300 μ M NBAH and 100 nM of unpurified BM3 from bacterial cell lysates with all reactions driven at 25°C were evaluated. The standard deviation and mean for each sample set were calculated from three experimental replicates.

BM3 mutant stability assessment

At this point, focus was directed at establishing the stability of the newly created mutants in harsh conditions. The TONs obtained in assays at either 30 °C (black bars) or in 15 % methanol (v/v) (grey bars) are shown at figure 25, panels A and B. These assays were performed with either NBAH (Fig. 25A) or NADH (Fig. 25B). With respect to the N-D mutant, on NBAH at 30 °C, TON increased by 1.53-fold for NTD1 and by 5.24 and 5.45-fold for NTD5 and NTD6, respectively. High methanol concentration, 15% (v/v), entirely inhibited the formation of product for the N-D mutant with NBAH (Fig. 25A). All the other mutants used in high methanol concentration (15% v/v) provided some level of production, with mutants NTD5 and NTD6 having the highest TON at 802 and 834, respectively. When using NADH at 30 °C, in regard to the N-D mutant, TON increased by 1.39-fold for NTD1 and by 2.27-fold and 2.30-fold for NTD5 and NTD6, respectively. With a high methanol concentration of 15%, when compared to the N-D mutant, TON increased by 4.06-fold for both NTD1 and NTD5 with the highest product output observed for NTD4 reaching a TON of 2275, a 4.40-fold increase. There however, the NTD6 mutant showed the lowest TON at 1679, less effective than all other mutants created, with the exception of mutant N-D which reached a TON of 517. Apart from thermal and organic solvent tolerance, resilience towards leakage was evaluated as well with NBAH and NADH (Fig. 25C and D, respectively) both preincubated in the presence of 250 μ M of either cofactor, a total of 30 min at 4 °C with mutants N-D, NTD1, NTD5 and NTD6, the latter two having

been chosen because of their superior TON values when tested at higher temperature or higher organic solvent concentration (Fig. 25A-B).

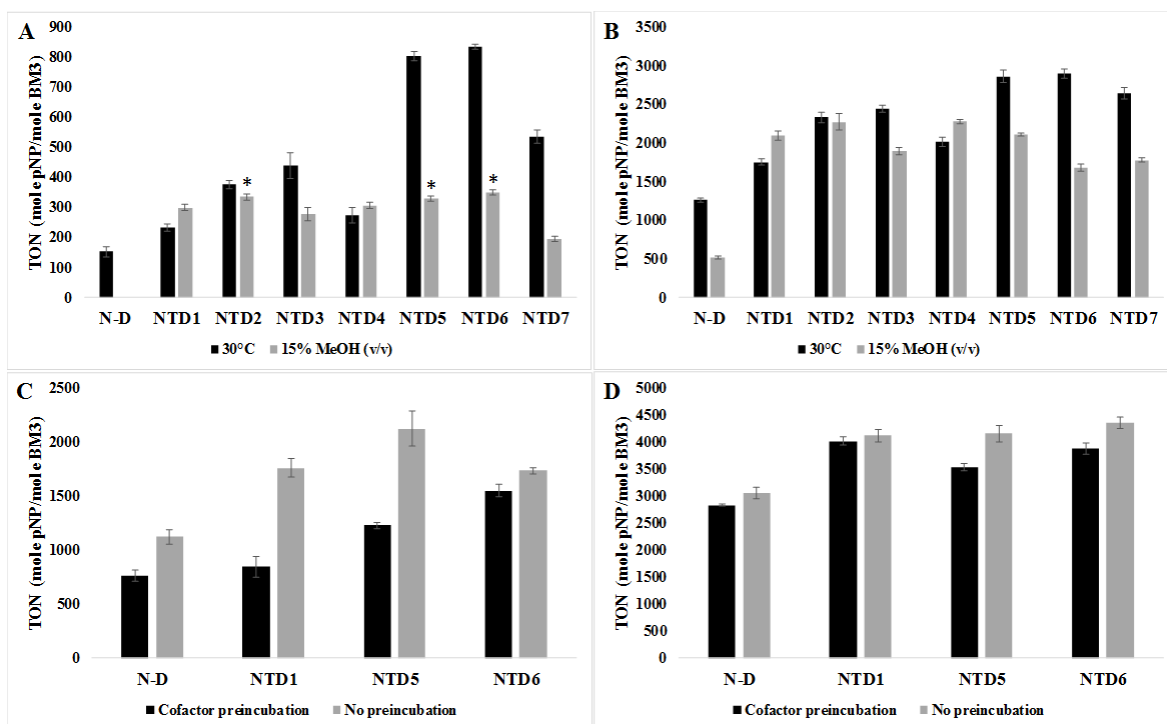


Figure 25: Turnover numbers of 10-pNCA conversion to *p*-nitrophenolate by the NTD variants identified in the library screening assay for different harsh conditions and cofactors. (a) and (c): NBAH; (b) and (d): NADH; (a) and (b): either at 30 °C or in 15 % methanol (v/v) at 4 °C; (c) and (d): either with or without the preincubation of the cofactor. The standard deviation and mean for each sample set were calculated from two independent experiments each with three biological replicates. The star above NTD2, NTD5 and NTD6 is used to specify that, using an unpaired t-test with an alpha of 0.05, these mutants are statistically different from NTD1.

When reaction mixtures were preincubated with NBAH, NTD5 retained the highest TON reaching 1225, a 1.61- and 1.45-fold greater product output than N-D and NTD1, respectively. Likewise, NTD5 also provided the highest TON when reactions were achieved without NBAH preincubation reaching 2120, a 1.89- and 1.21-fold increase when compared to N-D and NTD1, respectively. Compared to reactions when enzymes were not preincubated solely with cofactors, preincubation with NBAH caused a downturn in product output, out of a third for N-D and a half for both NTD1 and NTD5. In contrast, when mixtures were preincubated with NADH, overall TON were minimally affected, maintaining a global value that never failed below 89% of their initial product output. The highest yielding mutant without NADH preincubation, NTD6, reached a TON of 4344, a 1.42-fold and 1.06-fold increase from N-D and NTD1, respectively. However, when NADH was

preincubated with the BM3 variants, NTD1 displayed the highest TON reaching 4006, a 1.42- and 1.03-fold increase when compared to N-D and NTD5, respectively.

BM3 TON optimization

To avoid the detrimental effects of leakage observed in the preincubation assay, reactions were performed at 4 °C in a fed batch mode, where 250 μM NBAH (Fig. 26, panel A) or 500 μM NADH/NADPH (Fig. 26, panels B and C) of cofactor were added to the reaction mixtures every 5 minutes. With respect to reactions initiated with the entirety of cofactor added initially to the reaction mixture (batch mode, Fig. 25 panel C), the fed batch approach provided only marginal improvement for NBAH, with NTD1, increasing its TON by a factor of 1.09, while other mutants were not significantly impacted (Fig. 26, panel A). Also for NBAH, comparing mutants in fed batch, the most productive mutant, NTD5 which reached a TON of 2233 improved TON by a factor of 2.02 and 1.17-fold when compared to N-D and NTD1 respectively.

For NADH and NADPH, higher substrate concentrations were used, given the less deleterious effect of cofactors and higher TON observed in the preincubation assay (Figure 25, panel D). Indeed, for NADH and NADPH, 1mM 10-pNCA instead of 600 μM and a total of 3 mM cofactor, supplied in 500 μM every 5 min for 30 minutes, instead of 1.5 mM were used. With respect to NADH, when comparisons were made between TON obtained when the cofactor was initially fully added to the reaction mixture (Fig. 25, panel D) and fed batch reactions (Fig. 26, panel B), the resulting effect was far more appreciable than for NBAH. Indeed, increases in TON by 1.31, 1.70 and 1.66 fold, for mutants N-D, NTD1 and NTD6 respectively were observed, with the latter reaching the highest TON amongst all mutants tested, 7225 +/- 81.6, significantly higher (At a level $p = 0.05$) than the TON obtained with the N-D mutant, 4006 +/- 119 (with 6 experimental replicates). We have also investigated the effect of fed batch feeding on TON with the more expensive cofactor, NADPH (Fig. 26, panel C). The transition from wild type BM3 to the N-D mutant lowered the yields achievable with NADPH going from 4903 to 3958 pNP/BM3 a 19.3 % reduction in TON between the two. Nevertheless, using fed batch, the TON of the NTD1 mutant increased 1.31 and 1.62-fold, in comparison to the BM3 wild type enzyme and the BM3 N-D mutant respectively going up to a TON of 6429. Of all mutants considered however, the most productive mutant for NADPH driven fed batch reactions was NTD6, increasing TON by a factor of 1.35 and 1.67 compared to wildtype BM3 and the N-D mutant, respectively, reaching a TON of 6641.

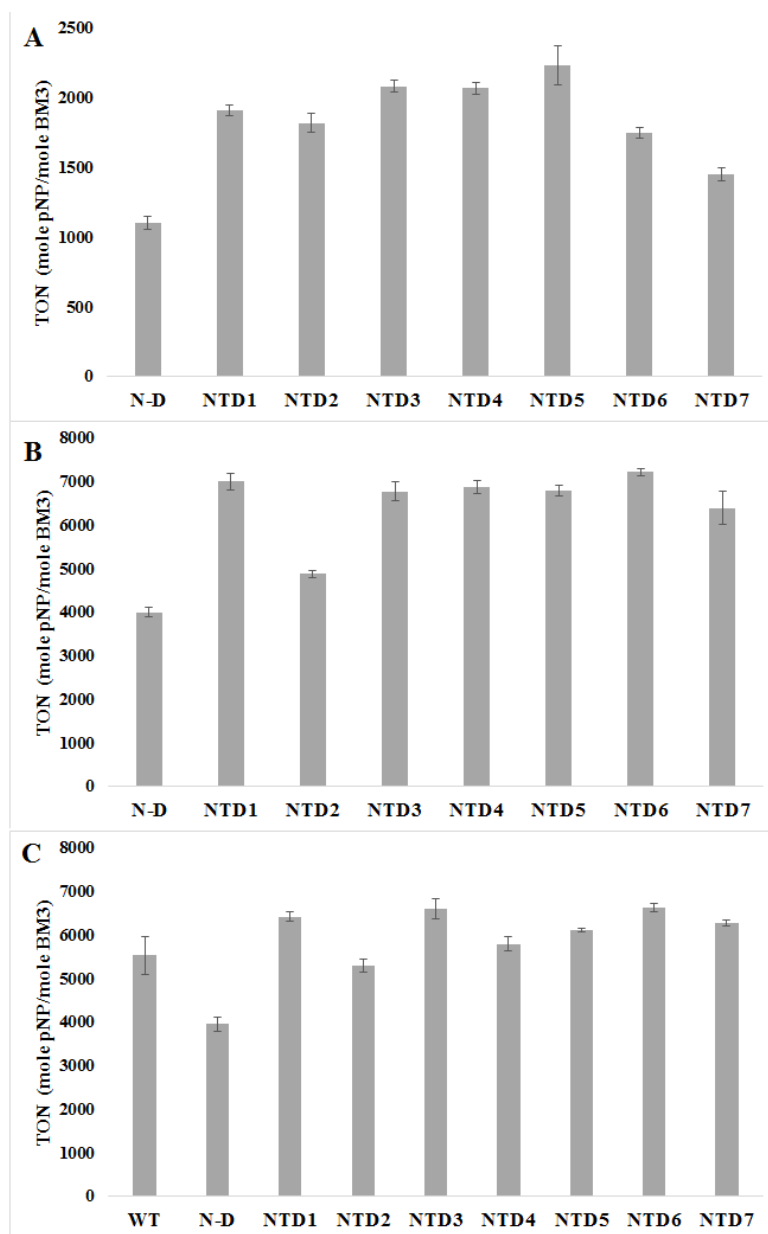


Figure 26: Turnover numbers of 10-pNCA conversion to *p*-nitrophenolate by the NTD variants at 4 °C with a fed batch of a) NBAH, b) NADH and c) NADPH. The standard deviation and mean for each sample set were calculated from two independent experiments each with three biological replicates.

BM3 mutant kinetics

In addition to TONs, the kinetics of the various NTD mutants were assessed by monitoring the activity of the oxidase domain towards 10-pNCA and that of the reductase domain with both NBAH and NADH, in the presence or in the absence of 10-pNCA. The kinetics of a number of mutants used shared some similarities for both cofactors (Tables 3 & 4). For instance, cofactor

consumption rates and leakage rates were at their highest with NTD5 and N-D, respectively, regardless of the cofactor used. The same trend could be observed for the rate of pNP release, which was at its highest with NTD5 when used with either cofactors. As for coupling, NTD2 showed the highest coupling ratio with both cofactors, 21.3 % and 26.5 % for NBAH and NADH, respectively. On a mutant-specific basis however, for NBAH, the successive mutations performed on the wildtype BM3 brought about a gradual increase of coupling ratio, parallel to the increase in TON, from 10 % to 12.8 % and 13.7 % for N-D, NTD1 and NTD5, respectively (Table 11). Meanwhile for NADH, transition between the various mutants followed the same trend, increased the coupling ratio progressively from 8.4% (WT BM3), 13.8 % (N-D), 19.6 % (NTD1) and then finally to 26 % with the most productive mutant NTD6 (Table 12 and Figure 26, panel B).

Table 11. Kinetics of promising BM3 mutants in dual buffer 10 mM PBS/100 mM BTP pH 8, 25 °C.

NBAH								
Mutant	WT	N-D	NTD1	NTD2	NTD3	NTD4	NTD5	NTD6
k_{pNP} (min ⁻¹)	0	26.7 ± 6.7	113 ± 12	71.1 ± 14	91.1 ± 3.8	64.4 ± 14	127 ± 6.7	107 ± 6.7
k_{NBAH} (min ⁻¹)	0	267 ± 29	884 ± 120	333 ± 29	786 ± 94	412 ± 36	928 ± 68	780 ± 60
Coupling ratio (%)	0	10.0	12.8	21.3	11.6	15.6	13.7	13.7
$k_{leakage}$ (min ⁻¹)	0	1035 ± 153	274 ± 34	601 ± 88	343 ± 52	280 ± 71	264 ± 50	425 ± 38

Table 12. Kinetics of promising BM3 mutants in 100 mM Tris pH 8, 25 °C.

NADH								
Mutant	WT	N-D	NTD1	NTD2	NTD3	NTD4	NTD5	NTD6
k_{pNP} (min ⁻¹)	2.07 ± 0.43	68.9 ± 3.8	171 ± 10	198 ± 3.8	244 ± 7.7	136 ± 3.8	273 ± 12	244 ± 14
k_{NADH} (min ⁻¹)	24.7 ± 3.3	500 ± 87	875 ± 37	745 ± 53	972 ± 73	898 ± 42	1264 ± 153	940 ± 120
Coupling ratio (%)	8.4	13.8	19.6	26.5	25.1	15.1	21.6	26.0
$k_{leakage}$ (min ⁻¹)	23.5 ± 8.4	486 ± 61	185 ± 29	60.2 ± 8.0	222 ± 14	129 ± 24	148 ± 8.0	139 ± 37

K_{pNP} , $k_{cofactor}$ and $k_{leakage}$ are the turnover frequencies for, respectively, the production pNP from the substrate 10-pNCA in the presence of cofactors, the consumption of cofactors in the presence of 10-pNCA and the consumption of cofactors in the absence of substrate at the oxidase domain. Data for the catalytic constants were extracted from the slope of concentration with respect to time, obtained between $t = 6$ s and 18 s. The standard deviation and mean for each sample set were calculated from three experimental replicates.

3.4 Discussion

In this work, we improved product turnover in terms of TONs by transitioning from the BM3 mutant N-D to the NTD1 mutant using either NBAH (Fig. 25A) or NADH (Fig. 25B) as cofactors in our reactions. These resulting enhancements echo those observed previously where relative activities were compared at increasing organic cosolvent concentrations between wild type BM3 and W5F5 [198]. The same can be said about the mutants M01, M02, M05 and M11 unto which were added the four W5F5 mutations, there again when relative activities were compared to increasing organic cosolvent concentrations the same stabilizing effect was observed [489]. With the drug metabolizing M01-11 mutants set however, the authors reported that when the W5F5 mutation T235A, the only mutation located on the oxidase domain, was removed and the other three were kept, relative activities were retained even better. These results were appealing to our work as we preferred to generate high yield BM3 variants with an unmodified oxidase domain. In light of this particular work, we generated from the mutant NTD1 a variant where the mutation T235A was reverted to its original amino acid threonine thus creating mutant NTD 235T. However, when NTD 235T was used with either NBAH or NADH (Figure 27) it underperformed with regards to TON when compared to NTD1. This discrepancy could be attributed to the very different substrate assay and oxidase domain that were used. Moreover, we believe this also highlights the limit of what can be learned from relative activities assays as, although they can be informative in regards to the initial rates and stabilities of the enzymes, they do not necessarily inform as to which enzyme possesses the highest TON. From what was known of W5F5, although we expected to obtain higher TONs with NTD1 compared to N-D at 30 °C or with 15 % methanol (v/v) (Fig. 25, panels A and B), we were not certain that this would lead to an increase in TONs, especially in the case where cofactors were preincubated, as it had never been tested before (Fig. 25, panels C and D). Interestingly, for the biomimetic cofactor NBAH, although NTD5 provided overall the highest TONs and higher coupling efficiency when compared to both N-D and NTD1, it did not necessarily present the greatest coupling efficiency overall, but did possess the slowest leakage rate (Table 11). Thus, for NBAH, the central issue to its efficiency may center on either limiting leakage as much as possible or handling the damage to the enzyme that may result from leakage events as best as possible. For NADH, the mutants which provided overall the best TONs, NTD6, also presented the second highest coupling percentage (26 %), alongside NTD2 which reached 26.5 % (Table 12). The coupling efficiency of NTD2 came as a surprise as it noticeably underperformed with NADH (Figure 26, panel B) compared to every mutant except N-D. What's more, with the exception of WT BM3, it also displayed the lowest leakage rate for NADH and greater stability than NTD1 with regards to heat and solvents (Figure, panels A and B). This discrepancy in

product turnover for NTD2 could be attributed to its incapacity to efficiently use the high electron flux supplied by the reductase when 1 mM NADH was used in these assays, even though it was provided using fed batch, in comparison to the other mutants generated in this work.

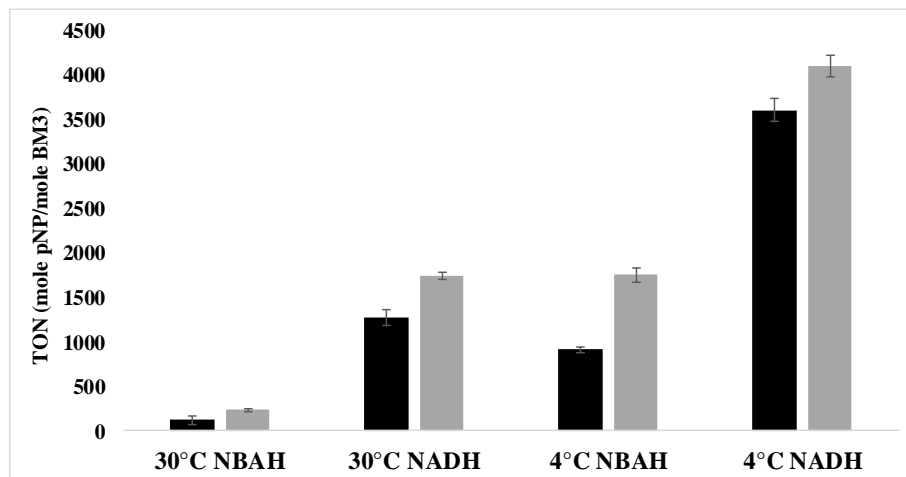


Figure 27: Turnover numbers of 10-pNCA conversion to *p*-nitrophenolate by the variants NTD 235T (black) and NTD1 (grey) at 4 °C and 30 °C. The standard deviation and mean for each sample set were calculated from two independent experiments each with three biological replicates.

In order to enhance TON even further, a fed batch of NBAH, NADH or NADPH at 4 °C (Fig. 26) was applied to the mutant reactions with the hope of bypassing the damage associated to leakage, to which batch reactions are more likely to be susceptible. Indeed, in batch, the reactions are initiated at high cofactor concentration (1500 μ M, Figure 25, panels C and D) which favors its waste in futile reaction, among which peroxide production. In contrast, fed-batch reaction, where cofactor is fed continuously and therefore the actual cofactor concentration is lower, is less likely to suffer from leakage damage. There, NTD1 outperformed N-D with every cofactor. In turn, for NBAH, NTD5 provided the highest possible TON reaching 2233 while, for NADH or NADPH, NTD6 provided the highest TONs going up to 7225 and 6641, respectively.

The consensus guided approach utilized in this work to generate NTD1 variants provided some interesting hits in our initial screen (Figure 2), in particular with NTD2-4. Furthermore, the pooling of some of these mutations (Table 10), NTD5 & NTD6 specifically, further enhanced the properties of NTD1 particularly in regards to heat tolerance, cofactor preincubation and TON in NBAH assays. In this regard, the NTD7 mutant only outperformed NTD1 in heat tolerance assays but otherwise could not compete with NTD1 in terms of TON in the cofactor fed batch reactions at

4°C for all three cofactors tested (Fig. 26). Similarly, in a recent paper where a consensus guided approach was also used to enhance BM3 stability, the latter was achieved, with the BM3 variants M, P and O retaining most of their original TON for the oxidation of ibuprofen methyl ester at 20 °C compared to a harsher temperature of 40 °C [215]. Product output of these 3 variants generated comparable TON values compared to the parent variant 3E10 at 20 °C not hindering productivity neither enhancing it. Thus, in the aforementioned case as well as for that of NTD7, unlike NTD5 & NTD6, these particular mutants fell short of our own secondary objectives which is to not only just enhance stability but also the productivity of the enzyme.

It is noteworthy to consider that all the mutations present on NTD1 through NTD6, except for T235A, are located either on the linker region or the reductase domain. In regards to the linker region, which is estimated as being between amino acids 460-475 [535], R471A is the only amino acid located within it and substitutes an arginine to an alanine. Interestingly, based on the ratios of the amino acid composition of linker regions found across proteins, alanine is generally preferred over arginine [536]. Although the linker region does not directly control either domains of BM3 it does play a central role in coordinating the heme and reductase domain [537]. A few amino acids farther, A493 interacts through hydrogen bonds with the flavin mononucleotide (FMN) prosthetic group while E494 protrudes towards the heme domain interacting with that domain through solvent molecules [21]. These two mutations, R471A and E494A account for half of the mutations associated with W5F5. Next A769, mutated to a serine residue in NTD4-7, is located within the flavin adenine dinucleotide (FAD) connecting domain close by to C773 a strongly conserved residue within the CYP102A thought to promote disulfide bonding both within the enzyme and between enzymes to form dimers [22, 495]. Further down the sequence S847 interacts with the FAD isoalloxazine ring whereas E852 with the FAD adenine base. In addition to S850, these three residues are substituted in the NTD variants 3, 5, 6 and 7. Even further down the sequence V978 which is located close to N976 whom interacts through a hydrogen bond with the adenine of NADPH [22]. Similarly, R966, replaced by aspartic acid in the N-D mutant, is thought to interact with the phosphate group next to the adenine moiety of NADPH, nearby N976. Interestingly, the mutation of V978 to leucine is absent in NTD5 but present in NTD6 with the former performing best on NBAH while the latter shows higher TON on NADH. Hence, it may well be that further tailoring the enzyme cofactor binding pocket for greater product output would strain further the efficient use of one cofactor at the cost of the other.

All of these mutations account for most of the additional mutations added unto NTD1 and identified as having beneficial effects overall on TONs for either NBAH or NADH. As these beneficial mutations are located on the linker region, near the FAD/FMN binding sites and near the binding pocket of the nicotinamide-based compounds, it may be that they positively contribute to TONs by handling with lesser damaging outcomes electrons from leakage prone cofactors such as NADH and NBAH throughout the reductase and unto the heme. Reactions driven in mild conditions, such as 4 °C, only leave events of uncoupling and leakage as a potential source from which the enzyme can sustain damage. As demonstrated when cofactors were preincubated at 4 °C with 250 μ M of either NBAH or NADH, the BM3 enzymes saw their yields crippled (Fig. 25, panels C and D). In such assays, the artificial cofactor NBAH proved the most deleterious, nearly halving the TON of N-D, NTD1 and NTD5 (Fig. 25, panel C). Given the propensity of the enzymes to leak with either NBAH or NADH (Table 11 and 12), we surmised that reactions driven at 4 °C with an initial high concentration of cofactors (e.g. 1500 μ M) may be the main factor leading to enzyme inactivation through leakage or uncoupling events (Fig. 25, panels C and D). We thus devised a fed batch approach to counter this (Fig. 26). We expected this to enhance significantly product output for reactions using the NBAH biomimetic cofactor, given its sensitivity observed in the cofactor preincubation assay, but when this strategy was employed, TON either remained similar, as for N-D and NTD6, or lightly enhanced by 5 to 9 %, as was the case for NTD5 and NTD1 going up from a TON of 2120 to 2233 and of 1758 to 1913, respectively. Inversely, the reactions driven with the cofactor NADH benefited much more from this strategy increasing the TON by more than 1.6-fold for NTD1, 5 and 6 mutants. However, using a dehydrogenase to initiate reactions with a small and limited supply of oxidized cofactors (NAD^+ or NADP^+) rather than a fed batch of reduced cofactors (NADH or NADPH), would likely limit leakage events more efficiently and resulted in greater yields for NADH or NADPH. The fed batch approach had little effect in increasing product output for NBAH (Fig. 25, panel C, Fig. 26, panel A), despite kinetic data pointing to leakage rates that are several folds greater than for what was observed with NADH (Table 11 & 12). Given the generally low coupling efficiency of BM3 variants used in this work for NBAH (Table 11), tailoring the reductase active site may be the most relevant facet to explore in order to increase yield significantly with this particular cofactor.

In any case, the greatest TON observed was with the biomimetic cofactor NBAH, with the NTD5 mutant (2233, Fig. 26, panel A). This is interesting, considering other TONs reported in the literature for alternative approaches to the expensive NADPH cofactor. For example, using a combination of zinc dust as an electron source and cobalt (III) sepulchrate as a mediator, a TON of 936 was reported for the M5 BM3 mutant with the substrate 12-pNCA [373]. With the same electron

source, an even greater TON of 2837 could be achieved with the immobilised M9 BM3 mutant whilst using 2-phenoxyltoluene as a substrate [301]. In a different strategy where a photosensitizer was attached to the BM3 heme domain through a non-native cysteine residue and reactions driven forward by electrons supplied by the reduction of sodium diethyldithiocarbamate through light, a TON of 935 [364] and 120 [538] could be achieved with lauric acid and 16-pNCA as substrates, respectively. This brings NBAH as a competitive contender in the approaches to bypass the dependence to NADPH.

The largest TON achieved in our work was of 7225 for NADH and 6641 for NADPH, with the NTD6 mutant.. These TON represent a 1.8- and 1.2-fold improvement compared to those obtained with the N-D mutant for NADH and the WT enzyme for NADPH, respectively. However, according to a publication analysing the cost of enzyme based biocatalytic processes [539], a free enzyme system dedicated to the production of pharmaceuticals on an industrial scale necessitates a productivity of 100-250 kg product/kg free enzyme. Converted to a mass basis, the best TON observed in this work, for NTD6 with NADH, translates to 8.31 kg pNP/kg BM3. Therefore, it follows that much more work into the engineering of a stable and productive BM3 variant must be accomplished before this technology reaches a economically viable industrial-scale process stage. In all cases, a TON of 45 800 has been reported for the BM3 mutant p450_{PMO}R2 which was optimised for its ability to hydroxylate propane to propanol with the use of the cofactor NADPH through several oxidase domain mutations [220, 221], or 23 kg propanol/kg BM3. This bridges the gap by a fourth of the required productivity of the biocatalyst for pharmaceuticals produced in a free enzyme process. Unlike the p450_{PMO}R2 mutant however, both NTD5 and NTD6 have not had their oxidase domain significantly modified, with the exception of a single mutation, T235A, which is not in the active site, leaving it open to further customisation for any given substrate. In addition, our work has led to the usability of three different cofactors, with greater TON and stability than WT BM3 for NADPH or mutant N-D for NADH/NBAH.

3.5 Conclusion

By adding the W5F5 mutations [198] onto the N-D mutant [306], to widen nicotinamide cofactor range, we have generated a mutant, NTD1, which harbor not only increased organic solvent tolerance, as expected, but also greater productivity, increasing TON by a factor of 1.73 for NBAH and 1.75 for NADH compared to the N-D mutant. We have also generated several different mutants from NTD1 derived from our consensus guided approach (NTD2-7) which displayed greater thermostability and leakage tolerance towards NBAH or NADH, without compromising productivity. For the former cofactor, NBAH, the mutant NTD5 displayed the highest TON of all mutants in this work reaching 2233, a 2.0-fold improvement from the parent mutant N-D. On the other hand, the NTD6 mutant displayed the highest TON for NADH reaching 7225, a 1.8-fold improvement compared to the N-D mutant as well as reaching 6641, a 1.2-fold improvement compared to WT BM3 on NADPH. For both NBAH and NADH, these values represent, to our knowledge, the highest TON ever reported in the literature. What's more, with the exception of the T235A mutation, the oxidase domain of the NTD mutants of this work remain unaltered, permitting mutations widening the substrate range of the enzyme to be added as desired. Lastly, as to the consensus guided evolution strategy we devised in this work, there remains several key areas to explore within the reductase domain to enhance yield and stability in order to tailor more accurately the efficient use of the low-cost cofactors NBAH and NADH. Notably, amino acids in the vicinity of FAD, FMN and the nicotinamide binding domain.

4 Oleic acid based experimental evolution of *Bacillus megaterium* yielding an enhanced BM3 variant

Authors: Thierry Vincent^a, Bruno Gaillet^a & Alain Garnier^{a*}

Affiliation:

^a Department of chemical engineering, Université Laval, Québec, Québec, Canada, G1V 0A6

* Corresponding author: Alain Garnier; email: alain.garnier@gch.ulaval.ca; telephone +1 418 656

[2303](#)

Résumé

Au contraire des autres cytochromes p450 monooxygénases, CYP102A1 de *Bacillus megaterium*, aussi communément connu sous le nom de BM3, est soluble et attachée à sa réductase naturellement, formant une seule chaîne polypeptidique. Comme les autres monooxygénases, BM3 peut catalyser l'insertion d'oxygène dans un lien carbone-hydrogène saturé pouvant ainsi générer une large variété de produits commercialement utiles dans l'industrie pharmaceutique et de chimie fine. Néanmoins, la basse stabilité de l'enzyme endigue son implémentation dans des procédés industriels biocatalytiques due au coût important qui serait associé à l'enzyme.

Dans cet ouvrage, nous avons cherché à améliorer le rendement spécifique de l'enzyme en usant d'une approche dite d'évolution expérimentale, non encore tentée pour améliorer cette enzyme. En exploitant le métabolisme propre de *B. megaterium* envers l'acide oléique, nous avons accéléré l'évolution d'une nouvelle variante de BM3 engendrant ainsi la substitution de 34 acides aminés. Cette nouvelle variante, nommée DE, augmenta la résistance au cosolvant organique, le rendement spécifique de l'enzyme et améliora la versatilité dans l'utilisation des cofacteurs nicotinamides NADPH et NADH. Globalement, la conversion du substrat 10-pNCA en son produit, le *p*-nitrophenolate, par la variante DE mena à une augmentation du rendement spécifique d'un facteur de 1.23 et de 1.76 en utilisant le NADPH ou le NADH, respectivement, comme source de cofacteur, comparativement à l'enzyme sauvage BM3.

Abstract

Unlike most other p450 cytochromes monooxygenases, CYP102A1 from *Bacillus megaterium*, also commonly known as BM3, is both soluble and attached with its redox partners forming a single polypeptide chain. Like other monooxygenases, it can catalyze the insertion of oxygen onto the carbon-hydrogen bond which can result in a wide variety of commercially relevant products in the pharmaceutical and fine chemical industries. However, the relatively poor stability of the enzyme holds back the implementation of a BM3-based biocatalytic industrial process due to the important enzyme cost it would prompt.

In this work, we sought to enhance BM3's total specific product output by using experimental evolution, an approach not yet attempted to improve this enzyme. By exploiting *B. megaterium*'s own metabolism towards oleic acid we pressed the evolution of a new variant of BM3, containing 34 new amino acid substitutions. This new variant, dubbed DE, showed increased organic cosolvent tolerance, increased product output and increased versatility in the use of either nicotinamide cofactors NADPH and NADH. Altogether, the conversion of the substrate 10-pNCA to its product *p*-nitrophenolate by the DE variant led to an increase in output of 1.23 and 1.76-fold when using respectively NADPH or NADH as a source of cofactors, compared to wild type BM3.

Keywords: BM3, consensus guided evolution, turnover number, protein engineering, bioprocess engineering & N-benzyl-1,4-dihydronicotinamide

4.1 Introduction

In the last decades cytochrome p450 (CYP) enzymes have garnered much attention in the fields of biotechnology and chemistry, mainly due to their unique ability to insert a single oxygen atom into inactivated aliphatic C-H bonds [170, 540, 541]. Although the oxyfunctionalization of saturated aliphatic C-H bonds by purely chemical means exist [167–169], such synthetic pathways present major disadvantages which includes reaction conditions requiring large quantities of organic solvents [172] as well as reactions lacking in chemo-, regio-, and stereospecificity [170, 171]. This leads to much harmful waste chemicals to be disposed of in the environment and low yield reactions producing a mixture of racemic products or otherwise undesirable side products. In that respect CYP enzymes present an interesting biocatalytic alternative as they open many new potentially lucrative synthesis routes to valuable chemicals [542]. Additionally, the multiple oxidative biosynthetic and catabolic pathways in which these heme-containing enzymes are involved lead to the production of a great variety of commercially relevant metabolites [510, 543–545] with some already produced and marketed using CYP based processes [23]. The CYP which has garnered the most interest to date is that of the gram-positive bacteria *Bacillus megaterium* dubbed CYP102A1 or BM3 as it was the first CYP enzyme discovered to be both soluble and fully fused into a single polypeptide to its protein redox partners [17]. Accordingly, BM3 can be subdivided into two catalytically active domains, the oxidase domain which inserts oxygen unto inactivated aliphatic C-H bonds using atmospheric dioxygen and the reductase domain which supply electrons to the oxidase domain through its consumption of NADPH [546]. In addition, it has to date the highest catalytic activity ever reported for a CYP reaching $17\,000\text{ min}^{-1}$ for arachidonic acid hydroxylation [530]. Yet the wild type BM3 enzyme is limited in substrates to medium or long-chain fatty acids [547] or fatty acid like compounds as substrates [548–551]. As a result, over the years, BM3 has expanded its library of oxidase active site mutants in order to expand its substrate range as well as its substrate chemo-, regio-, and stereospecificity for certain substrates [48]. In more recent years, the introduction of decoy molecules has further expanded the scope of substrates which could be targeted by BM3 by tricking the active site into adding oxygen unto non-native substrates [65, 232–234, 237–239].

Although much work has focused on expanding BM3 substrate range to great success, much more engineering is required to generate more stable and productive BM3 enzymes, as this has been identified as the main bottleneck preventing the industrial application of these biocatalysts. Indeed, reviews on the state of CYP biotechnology identify the operational stability of these enzymes as being the main hurdle holding back their practical implementation in biocatalytic industrial processes [197,

272, 481–483]. To this end, several publications have reported work focused on stabilizing point mutations to the structure of BM3. Directed evolution has been used several times to unearth stabilizing point mutations from libraries of BM3 variants generated by error prone PCR. In an early publication, the oxidase domain of BM3 harbouring the F87A mutation, which can act as a peroxygenase [202], was subjected to successive rounds of directed evolution to generate the 21B3 mutant which displayed greater productivity in hydrogen peroxide driven biocatalysis than its parent, towards the substrates 12-NCA, lauric acid and styrene [201]. The 21B3 mutant would then later be further optimized, again by directed evolution, towards a more stable variant dubbed 5H6 [200]. In different work the whole BM3 sequence was targeted for directed evolution rather than just the oxidase domain where four stabilizing mutations were added to the amino acid sequence of BM3 thus generating the BM3 mutant w5f5 which was shown to be more resistant to organic solvents [198]. It's been reported that the reductase domain of BM3 is less stable than its oxidase domain [199]. Interestingly, of the four mutations located on the w5f5 BM3 mutant, three were located outside of the oxidase domain [198]. Accordingly, this same disparity of domain stability would be further explored later with the aim of enhancing the overall stability of BM3 through domain swapping of the more stable reductase domain of CYP102A3 from *Bacillus subtilis* to that of CYP102A1 from *B. megaterium*, yielding a more stable chimera A1MA3R compared to both CYP102A1 and CYP102A3 [247]. Yet, another strategy besides fusion constructs and directed evolution that has been explored to enhance BM3's productivity is that of consensus mutagenesis. By aligning the reductase sequence of BM3 with that of other reductase domains sharing at least 38 % of amino acid sequence identity, several BM3 variants strongly conserved in key locations were explored and retained on the BM3 sequence thus generating more stable [215] or more productive variants (Chapter 3). A similar approach was also utilized to enhance BM3's operational productivity when CYP102A1 ecotypes had their respective domains compared in regards to their stability with some of these ecotypes displaying greater stability for either domain, thanks to but a few amino acids substitutions [212]. Experimental evolution, is typically used to study evolutionary processes in organisms which are forced to adapt to new environmental conditions through natural selection [552, 553]. Research into BM3 revealed that the enzyme may have a role in protecting *B. megaterium* from exogenous unsaturated fatty acids by breaking them down, as it was shown that fatty acids such as oleic, linoleic and arachidonic acid both induce BM3 expression and promote cell death [39, 40]. To date an experimental evolution approach has never been explored as a technique to enhance BM3' productivity. Correspondingly, in this work, selective pressure was applied to *B. megaterium* to generate more productive variants of BM3 by supplying cultures of this bacteria with increasing concentrations of oleic acid starting with concentrations at which the bacteria barely survived.

4.2 Materials & Methods

Chemicals

Most chemicals used in this work was purchased from either Bioshop Canada, Gold Biotechnology, Sigma Aldrich, Thermo Fisher Scientific or p212121. Else, the Pfu polymerase was purchased from Bio Basic, DNA primers were acquired from IDT technologies, *p*-nitrophenoxydecanoic acid was purchased from TCI Chemicals and N-benzyl-1,4-dihydronicotinamide was synthesized by Oleotek as described in [491]. The *B. megaterium* strain used in this work, *B. megaterium* de Bary (ATCC[®] 14581[™]), was obtained from ATCC as was the pBR322 vector. The *Escherichia coli* DH5 α and BL21 (DE3) strains were both acquired from Thermo Fischer Scientific. The pET16B vector was acquired from Novagen whereas the restriction enzymes *SpeI*, *BamHI*, and *DpnI* were acquired from New England Biolabs.

Bacillus megaterium transformation

Prior to the transformation procedure, *B. megaterium* cells were grown at 30 °C in 25 ml lysogeny broth (LB) medium (10 g/L tryptone, 5 g/L yeast extract, 5 g/L NaCl, adjusted to pH 7 with HCl) in a 250 ml shake flask at 210 rpm until cells reached an optical density at 600 nm of 1. The cells were then centrifuged at 3000 g for 10 min, resuspended into 1.5 ml fresh LB medium and then kept on ice. Following this, 475 μ l of *B. megaterium* cell suspension was mixed with 15 μ l of pBR322 vector DNA in 0.1 cm gapped electroporation cuvette (Bio-Rad) and incubated on ice for 30 min. The resuspendend cells were then subjected to a single electric pulse (1000 V, 50 μ F, 200 Ω) using the Bio-Rad Gene Pulser Xcell[™]. The electroporated cells were then transferred to a 1.5 ml microtube and incubated 1 hour at 37 °C on a heating block, plated on LB agar plates containing 15 μ g/ml tetracycline and incubated overnight at 30 °C.

Experimental evolution cultures of Bacillus megaterium

Every culture following the initial *B. megaterium* transformation contained 15 μ g/ml tetracycline, were grown at 30 °C and stirred at 210 rpm with the exception of the 20 L bioreactor culture where cultures were stirred at 150 rpm. Plated cells were grown at 30 °C. Unless stated otherwise, all centrifugation steps were performed at 3000 g for 10 min at room temperature. Oleic acid was dissolved in dimethyl sulfoxide (DMSO) to generate a stock solution of 158.5 μ M which was used to prepare cultures containing up to 5 μ M of oleic acid. A stock solution of oleic acid in DMSO of 20 mM was used to prepare cultures whose oleic acid concentration was set to be between

10 μM and 300 μM . These stock solutions were selected to ensure that DMSO concentration in cultures remained below 5 % (v/v) so as to not interfere with bacterial growth.

To establish the maximum oleic acid concentration *B. megaterium* could handle, plated transformants were first grown in a 25 ml preculture of LB medium without oleic acid in a 250 ml shake flask for 10 hours. Subsequently, cells were centrifuged, resuspended in 25 ml of fresh LB medium and 250 μl of these resuspended cells were added to 25 ml of LB medium in 250 ml shake flask containing concentrations of Oleic acid ranging from 0 μM to 100 μM . These cultures were then incubated for 6 hours and their optical density at 600 nm measured every hour.

For clarity and to better describe the procedure utilised for the experimental evolution of *B. megaterium*, Figure 28 was added. The experiment was initiated by incubating a single colony of *B. megaterium* harbouring the pBR322 vector in a 25 ml preculture of LB medium without oleic acid in a 250 ml shake flask for 10 hours. Cultured cells were then centrifuged, resuspended in fresh LB medium and poured inside a bioreactor (20 L working volume, 30 L head-space volume) containing 19.5 L of LB medium and 2.5 μM of Oleic acid. Cells were grown for 12 hours at 150 rpm with pH maintained at 7 with phosphoric acid. Compressed sterile air was sparged to keep dissolved oxygen from falling below 20 %. These latter tasks encompass step 1 described within figure 28. At the end of the incubation, 25 ml of cultured cells were harvested and used to streak LB agar plates containing 0, 2.5 and 5 μM oleic acid for overnight incubation. Afterwards the same 25 ml was mixed with 25 ml of glycerol and stored at -80 $^{\circ}\text{C}$ in a 50 ml falcon tube. An isolated colony grown on LB agar plates containing 5 μM of oleic acid was then grown further for 8 hours in a 50 ml preculture of LB medium with 5 μM oleic acid in a 500 ml shake flask. Cells were then centrifuged and resuspended in 50 ml of fresh LB. Following this 8.5 ml was added to four 2 L shake flasks containing 850 ml of LB medium with either 5, 10, 20 or 30 μM of oleic acid. Cells were incubated for 8 hours. This would conclude step 2 and begin step 3 in figure 28. By the end of the incubation, 25 ml of cultured cells were harvested and used to streak LB agar plates containing 30, 40 and 50 μM of oleic acid for overnight incubation. Afterwards the same 25 ml was mixed with 25 ml of glycerol and stored at -80 $^{\circ}\text{C}$ in a conical 50 ml tube. Following this, an isolated colony grown on LB agar plates with 50 μM of oleic acid was then further grown for 8 hours in a 50 ml preculture of LB medium with 50 μM oleic acid in a 500 ml shake flask. Cells were then centrifuged and resuspended in 50 ml of fresh LB. Following this 8.5 ml was added to four 2 L shake flasks containing 850 ml of LB medium with either 50, 100, 200 or 300 μM of oleic acid. Cells were incubated for 8 hours. Finally, 25 ml of the 300 μM

oleic acid culture was mixed with 25 ml of glycerol and stored at $-80\text{ }^{\circ}\text{C}$ in a conical 50 ml tube. Another 10 ml fraction was centrifuged in a conical 15 ml tube at 8000 g for 10 min at $4\text{ }^{\circ}\text{C}$ and stored at $-20\text{ }^{\circ}\text{C}$ for later genomic DNA extraction.

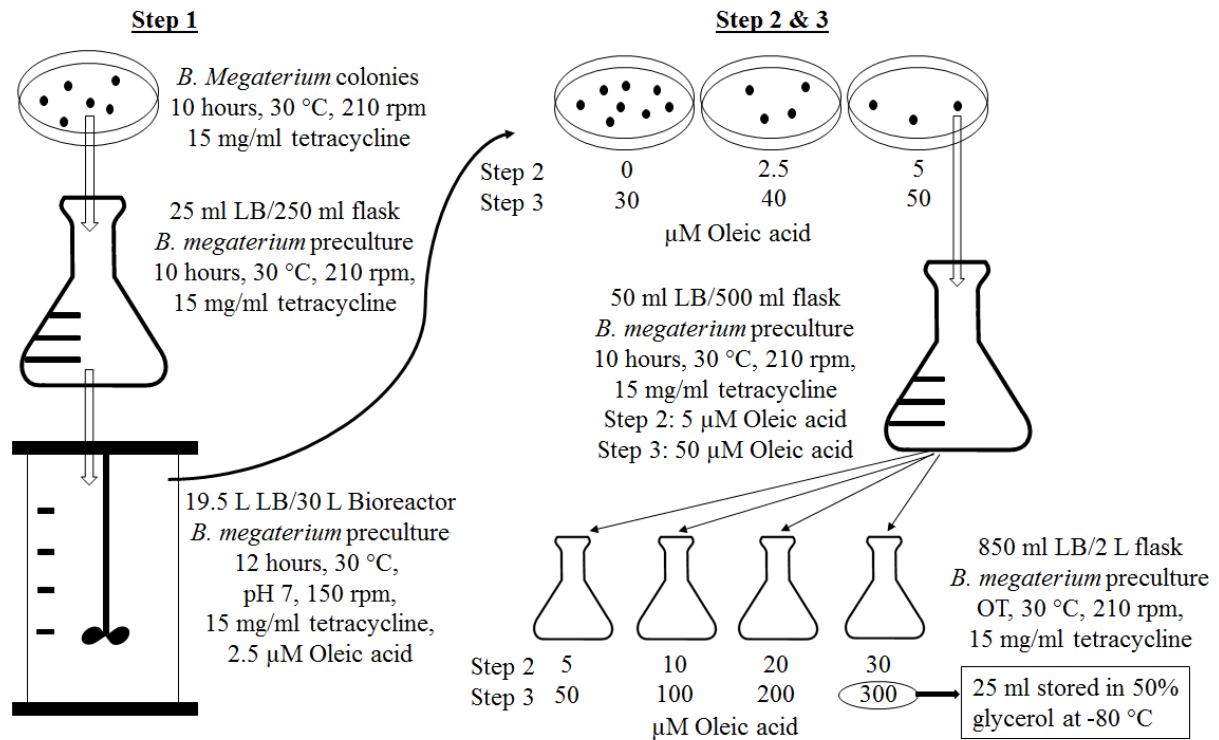


Figure 28: Experimental evolution methodology

Genomic DNA extraction

Following experimental evolution procedures, cell pellet obtained from the centrifuged 10 ml fraction was thawed on ice while CTAB lysis buffer solution for genomic DNA extraction (2% w/v CTAB, 20 mM EDTA, 100 mM Tris-HCl, 1.4 M NaCl, pH 8) was incubated in a $65\text{ }^{\circ}\text{C}$ bath to dissolve all CTAB crystals. Once ready, 400 μl of CTAB solution was used to resuspend the pellet. The mixture was then transferred to a 2 ml microtube and incubated at $65\text{ }^{\circ}\text{C}$ for 30 min. Following this, 200 μl of phenol was added to the CTAB cell pellet mixture after which 200 μl of a 96/4 solution of chloroform and isoamyl alcohol was added to the mixture and gently shaken. The preparation was then centrifuged at 10000 g for 2 min. Then, 375 μl of aqueous phase at the top was removed and

transferred to a 2 ml microtube. Thereafter, 375 μ l of a 96/4 solution of chloroform and isoamyl alcohol was added to the sample, gently shaken and centrifuged at 10000 g for 2 min. Then, 350 μ l of aqueous phase at the top was removed and transferred to a new 2 ml microtube to which 350 μ l of isopropanol was added. The sample was then gently inverted and incubated 10 min at room temperature. Following this, the sample was centrifuged at 10000 g for 10 min after which the supernatant was removed. In place, 750 μ l of ice cold 70 % ethanol was added and allowed to incubate for 2 minutes at room temperature. The sample was then centrifuged at 10000 g for 5 min. Ethanol was then removed and the microtube was opened and allowed to dry. Once dry, 100 μ l of milli-Q water was added to the microtube.

Cloning, expression & purification

The new BM3 gene sequence generated by experimental evolution was obtained by PCR from the genomic DNA extracted from the *B. megaterium* variant which had evolved to tolerate oleic acid. This genomic DNA served as a template for the forward primer 5UTR, CATTGAAAGCGGTCTGGCAAACGAGAGA, and the reverse primer 3UTR2, CATGTGAAGGTGGCGGTGATGGA and the *pfu* polymerase to generate PCR products to send for sequencing and for cloning procedures. The PCR program for this amplification went as such: 95 $^{\circ}$ C, 5 min / 95 $^{\circ}$ C, 1 min / 60 $^{\circ}$ C, 1 min / 72 $^{\circ}$ C, 4 min, last three steps repeated 29 times followed by 72 $^{\circ}$ C, 10 min. The WT BM3 gene sequence was similarly obtained from the genomic DNA extracted from unevolved WT *B. megaterium* 14581 cultured in the absence of oleic acid. The genomic DNA therein acquired served as a template for the forward primer P450-BM3-AS2, ATGACAATTAAGAAATGCCTCAGCC, reverse primer P450-BM3-AAS2, ACACGTCTTTTGCGTATCGG and *pfu* polymerase. The PCR program for this amplification went as such: 95 $^{\circ}$ C, 5 min / 95 $^{\circ}$ C, 1 min / 60 $^{\circ}$ C, 1 min / 72 $^{\circ}$ C, 3.5 min, last three steps repeated 29 times followed by 72 $^{\circ}$ C, 10 min.

In order to subclone the BM3 gene into the pET16B vector, both evolved and WT PCR products were further amplified using the forward primer P450-BM3-AS1, CGACTAGTATGACAATTAAGAAATGCCTCAGCCA, and the reverse primer P450-BM3-AAS1, ATGGATCCTTACCCAGCCCACACGTCTTT. The PCR products were then subcloned into a pET16B vector using *SpeI/BamHI* restriction sites. As a result, the BM3 enzyme integrated into the vector would now have an octahistidine tag (GHHHHHHHH) as well as a spacer (SSGHHTSM) added to the N-terminus of their sequence. Backcross mutations added to the evolved BM3 variant in

relation to its WT parent were performed by DpnI (NEB) site directed mutagenesis. The forward primer I26V/T28A, TTATTAACACAGATAAACCGGTTCAAGCTTTGATGAAAATTGCGGATGA, and the forward primer I127V/T135A were used with the reverse primer RC1230, GTTGCTTCATGAAGAGCGAACTGCTGACCGATACACGCAC, to generate the corresponding mutations by megaprimer PCR.

The PCR reactions used for mutagenesis of the DE sequence were performed with 100 ng of plasmid, 10 nmoles of deoxynucleotides (Bio Basic), 10 pmoles of each primer and 5 units of Pfu polymerase (Bio Basic) all of which were added in a 50 μ l PCR reaction tube. To bring about a megaprimer, 20 cycles of PCR with an elongation time of 1.5 min/cycle were carried out followed by 30 cycles with a 20min/cycle elongation time to allow full plasmid amplification. Afterwards, 10 units of DpnI restriction enzymes were added to the resulting PCR reactions which were then incubated at 37 °C for 1 h. The PCR reactions were then inserted into *E. coli* DH5a competent cells through a standard heat shock protocol and then sent for sequencing.

The production of the different recombinant BM3 enzymes was accomplished first by transforming the pET16B vector by heat shock into *E. coli* strain BL21 (DE3) on LB plates containing 100 μ g/ml ampicillin. A single colony was then picked and grown overnight at 37 °C in 100 ml of LB medium with 100 μ g/ml of ampicillin. The pre-culture medium would then be replaced by centrifuging it 10 min at 8000 g and resuspending the pellet obtained in 100 ml of fresh LB medium. An inoculum of 22,5 ml of pre-culture would then be added to 0.9 L of modified Terrific Broth (24 g/L Tryptone, 48 g/L yeast extract, 10 g/L NaCl, pH 7.6) containing 100 μ g/ml of ampicillin and grown at 37 °C. When the culture reached an $OD_{600} = 0.6$, induction was initiated by supplementing the culture with 1.1 ml of 1M isopropyl β -D-1-thiogalactopyranoside (IPTG) to a final concentration of 1 mM. In addition, 150 ml of modified Terrific Broth pH 8, 50 ml of 50 % (v/v) 0.48 micron filtered glycerol and 200 μ l of 100 mg/ml of ampicillin would be added to the culture, after which the induction temperature was immediately set to 28 °C. Cells were incubated for 5-8 hours and were thereafter pelleted by centrifugation at 8000 g for 10 min after which they were stored at -80 °C. For purification, centrifuged cells were first thawed on ice, then resuspended in 20 ml of 100 mM lysis buffer (NaCl, 25 mM Tris-HCl pH 8 with 1 mM phenylmethylsulfonyl fluoride) and lysed by sonication using 4 x 15s bursts separated by 30 s pauses. Sonication and every following step would then be performed on ice or at 4°C. When sonication was complete, the suspension was clarified by centrifugation at 10,000 g, 35 min. The BM3 enzyme was purified by feeding the clarified supernatant

onto 25 ml of Ni sepharose 6 fast flow resin (GE Healthcare) packed in a homemade chromatography column. The packed column was first washed with 200 ml of running buffer (40 mM NaH₂PO₄, 500 mM NaCl, pH 7.4). Then, the column was further washed three times with 100 ml of three different washing buffers identical in composition and pH to the running buffer but with histidine added to the solution. The first washing buffer contained 10 mM histidine, the second 20 mM histidine and the third 40 mM of histidine. The enzyme was eluted from the column with an elution buffer, again identical to the running buffer but also containing 160 mM histidine. The eluate obtained was mixed to 1 volume of glycerol yielding a 50% glycerol enzyme solution which would then be stored at -80 °C. In order to measure the p450 concentration, the CO difference spectroscopy method was used with an extinction coefficient of 91 mM⁻¹cm⁻¹ to generate the characteristic 450 nm absorption peak of CYP enzymes [9].

Activity assays with 10-pNCA

To establish the maximum turnover number (TON) the BM3 variants could generate, the spectrophotometric activity assay developed for BM3 based on the release of *p*-nitrophenolate (pNP) from *p*-nitrophenoxycarboxylic acids was used [76]. All enzymatic assays were performed overnight with 100 nM enzyme, 600 μM *p*-nitrophenoxydecanoic acid (10-pNCA) and 1500 μM of either NADPH or NADH in a 100 mM Bis-Tris propane buffer with 5 % (v/v) methanol, in a total volume of 1.5 ml, pH 8, 4 °C, in darkness. Buffer solutions were always preincubated at 4 °C prior to the reaction to ensure the correct temperature would be maintained from the very beginning of the experiment. Noteworthy, 10-pNCA was added before the cofactor (45 μl of 20 mM 10-pNCA and 30 μl of a 75 mM cofactor stock solution).

Reactions aimed at investigating thermal stability were preincubated at 37 °C for 10 minutes after which reactions were initiated as described above, once 10-pNCA and then NADPH was added, the samples were transferred to a 25 °C bath, in darkness. Likewise, the organic solvent tolerance reactions were preincubated for 10 minutes in a 100 mM Bis-Tris propane buffer but with 10 % (v/v) methanol at 4 °C, in darkness. Reactions were initiated by the addition of 10-pNCA followed by NADPH and also performed at 4 °C, in darkness.

After an overnight incubation, 1 ml of each reaction solution was mixed with 150 μl of 10 N NaOH in a 2 ml microtube and 850 μl of methanol was added to the mixture up to a final volume of 2 ml. After this, 1 ml of this mixture was added to a 1 cm width cuvette to detect the absorbance of

p-nitrophenolate measured at 410 nm in a Genesys 10S UV-Vis spectrophotometer (Thermo Fisher Scientific) and pNP concentration was determined from a calibration curve. To maintain pNP concentration within the range of the calibration, samples could be diluted further in methanol. The standard deviation and mean for each sample set were calculated from three independent experiments each with three biological replicates. The units of TON in this work are defined as moles of pNP per mole of CYP enzyme or more simply, pNP/CYP.

Similarly, for kinetic measurements, the 100 mM Bis-Tris propane buffer, 5 % (v/v) methanol, pH 8 was used at a temperature of 25 °C. Concentrations of 100 nM (BM3) and 300 μM (10-pNCA/NADPH) were used. Reactions were performed in a final volume of 300 μl in 96 well plates. To initiate the reactions, 100 μl of 900 μM NADPH stock solution was added to 200 μl of reaction mixture containing both the enzyme and 10-pNCA. To monitor both pNP production and NADPH utilization, absorbance measurements were made at 410 nm and 340 nm, respectively using a Synergy H1 hybrid multi-mode reader (BioTek) every 5 s for 5 min with the first measure taken at $t = 30$ s. The concentrations of both pNP and NADH (or NADPH) were obtained from a calibration curve. Again, the standard deviation and mean for each sample set were calculated from three experimental replicates. The units for the enzymatic activity towards the release of pNP or the consumption of NADPH are defined as moles of pNP or NADPH per moles of CYP per minute which is shortened here to min^{-1} . Coupling ratio is defined as the ratio between CYP pNP production rate and NADPH consumption rate and is expressed as percentage.

4.3 Results

To establish the concentration of oleic acid to be used in the experimental evolution of *B. megaterium*'s BM3 enzyme, several cultures were grown using different concentrations ranging from 0.05 to 100 μM . From these preliminary assays, the initial concentration of 2.5 μM oleic acid was selected to conduct the experimental evolution experiment, as it was the highest concentration tolerated by the bacterium, significantly slowing its growth without arresting it (Figure 29). After several rounds of growth on both solid and liquid media at increasing oleic acid concentration up to a final concentration of 300 μM , the BM3 gene from the evolved *B. megaterium* strain was extracted and sent for sequencing. The resulting sequence accumulated over 170 nucleotide substitutions and a total of 34 mutations in the amino acid sequence compared to WT BM3. Of these 34 amino acid substitutions, 5 were located in the heme domain, another 5 were located inside the linker region and finally, the remaining 24 were all located in the reductase domain (Figure 30, Table 13). Specifically, the flavin mononucleotide (FMN), flavin adenine dinucleotide (FAD) and NADPH subdomains of the reductase harboured respectively 6, 11 and 7 substitutions, all of which are recorded in Table 13. For simplicity, this new BM3 variant was named DE. The amino acid sequence of DE was aligned against the first 9 members of the CYP102A subfamily as well as two other members of the CYP102 family, CYP102D1 and CYP102F1 (Table 14). It shows that, for 9 of the 34 amino acid substitutions, experimental evolution led to substitutions of amino acids that originally differed in wildtype *B. megaterium* compared to the other microorganisms, to amino acids that were more similar to what was found in these other family members. Also, 4 of these substitutions took effect on amino acids that were consensual among the different species and lead to amino acids that were not.

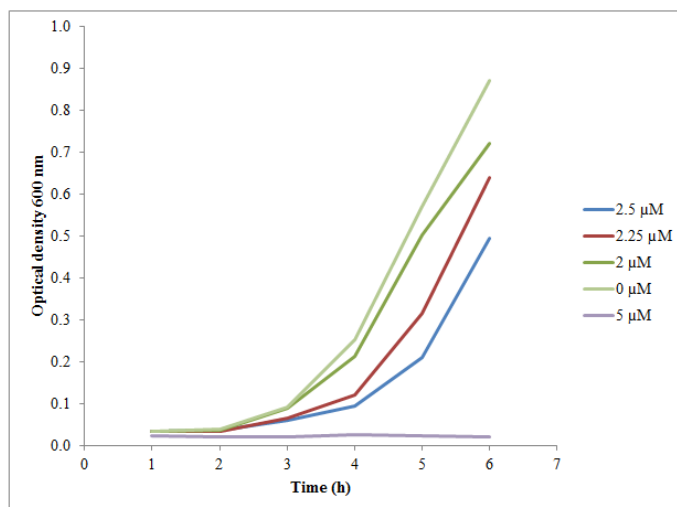


Figure 29: *B. megaterium* growth kinetics at various oleic acid concentrations to determine the maximum tolerable concentration for *B. megaterium* to set up an experimental evolution experiment. A range of concentrations between 0.05 and 100 μM oleic acid was assayed. For clarity, only a few key growth curves are displayed in the figure, between 0 and 5 μM oleic acid.

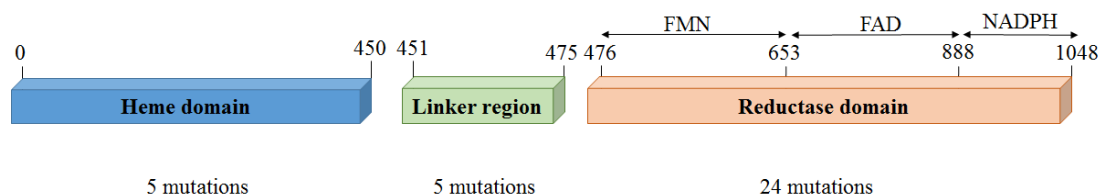


Figure 30: Domain architecture of the p450 BM3 cytochrome. Subdomains of the reductase domain are denoted as well above the arrows.

Table 13. Amino acid substitutions accumulated by p450 BM3 DE compared to its parent sequence p450 BM3.

Domains	Mutations
Heme domain	T1P, V26I, A28T, V127I & A135T
Linker region	K452Q, P463R, V470E, K473T & A474V
FMN subdomain	Q546E, L589F, D599E, V624L, D637E & K639A
FAD subdomain	G660R, T664A, Q674K, T715A, A716T, A741G, A782V, K813E, I824M, E870N & I881V
NADPH subdomain	E889G, D895G, E947K, E954N, M967V, A1008D & D1019E

Table 14. Sequence alignment of new evolved DE mutant compared to members of the CYP102 family.

Organism	p450 Cytochrome	Mutations towards consensus								Mutations leaving consensus				
		A28T	V470E	T664A	T715A	A741G	E887G	M967V	A1008D	D1019E	Q546E	K639A	D893G	E947K
Bacillus megaterium	CYP102A1 WT	A	V	T	T	A	E	M	A	D	Q	K	D	E
	CYP102A1 DE	T	E	A	A	G	G	V	D	E	E	A	G	K
Bacillus subtilis	CYP102A2	S	Q	A	L	G	R	K	D	A	Q	K	D	D
	CYP102A3	S	A	G	L	D	G	V	D	A	G		D	E
Bacillus anthracis	CYP102A4	S	E	A	L	D	N	L	D	E	Q	K	N	T
Bacillus cereus	CYP102A5	S	E	A	L	D	N	L	D	E	Q	K	D	T
Bradyrhizobium diazoefficiens	CYP102A6	H	R	M	A	G	G	A	D	E	Q	A	D	D
Bacillus licheniformis	CYP102A7	S	G	A	F	E	G	L	A	I	E	T	D	D
Bacillus thuringiensis	CYP102A8	S	E	A	L	D	N	L	D	E	Q	K	N	T
Bacillus weihenstephanensis	CYP102A9	S	E	A	L	D	N	L	D	E	Q	K	N	T
Streptomyces avermitilis	CYP102D1	Y	Q	L	L	G	T	V	A	K	R	P	D	Q
Actinosynnema pretiosum	CYP102F1	F	V	A	V	G	S	H	A		H	R	D	E
Consensus		PUsc, S/T	E	A	Hsc, A/L	G	G	Hsc	D	E	Q	K	D	NCsc
Secondary consensus						NCsc	Hsc							

Following purification of the BM3 DE mutant, this new CYP was then further characterized and compared to its parent WT BM3. To assess the productivity of DE, a 10-pNCA assay was conducted with either NADPH (Figure 31, panel A) or NADH (Figure 31, panel B) as a source of cofactor. Using NADPH as a cofactor, the DE mutant proved more productive than its WT parent with a TON of 6060 pNP/CYP compared to 4918 for the WT, a 23 % increase. Similarly, with NADH, the DE mutant proved more productive than its WT parent with a TON of 2316 pNP/CYP compared to 1313 for WT, an increase of 76 %. The activity of both WT and DE BM3 were monitored with the 10-pNCA assay using NADPH, where it was determined to be of 147 and 256 min⁻¹, respectively, a 74 % increase in rate for the mutant. In regard to the consumption rate of NADPH, WT BM3 displayed an activity of 192 min⁻¹ whereas the DE variant reached 588 min⁻¹. Taken together these data translate to a coupling percentage of 76.6 % for WT BM3 and 43.5 % for the DE variant (Table 15). A total of two new mutants were created from the DE variant where, in each case, two closely located amino acid substitutions located on the heme domain were backcrossed to their original amino acids identity to investigate their importance in DE's performance. These two new variants, named DE 26/28 and DE 127/135 are thus essentially the same as the DE variant minus substitutions at amino acids 26 and 28 or 127 and 135, respectively, which were reverse-mutated to share again the same amino acid as WT BM3. Their productivity was assessed in the presence of either NADPH or NADH as a cofactor source (Figure 31). In the case of variant DE 26/28, compared to the DE variant, it displayed a 15.2 % lower TON, 5140 pNP/CYP, and a 5.9 % lower TON, 2179 pNP/CYP in the presence of either NADPH or NADH, respectively. In the case of the DE 127/135 mutant in the presence of NADPH, the observed TON was almost identical to that of the DE variant reaching 6033 pNP/CYP. Contrastingly, in the presence of NADH the DE 127/135 mutant displayed

a 21 % decrease in TON compared to the DE variant, with a value of 1830 pNP/CYP. The thermal tolerance of the new BM3 variant DE was investigated and compared to that of WT BM3 by preincubating both CYPs for 10 minutes at 37 °C prior to the initiation of the reaction with NADPH and its completion at 25 °C (Figure 32). There, WT BM3 displayed greater stability than its DE counterpart, reaching a TON of 1620 pNP/CYP whereas DE reached only 1400 pNP/CYP. Conversely, when organic solvent tolerance was assessed by preincubating both CYPs for 10 minutes at 4 °C in the presence of 10 % (v/v) methanol prior to the initiation of the reaction with NADPH, the DE mutant displayed the greatest turnover reaching 2625 pNP/CYP whereas WT BM3 reached only 1961 pNP/CYP, a 34% increase in TON for the DE variant compared to WT.

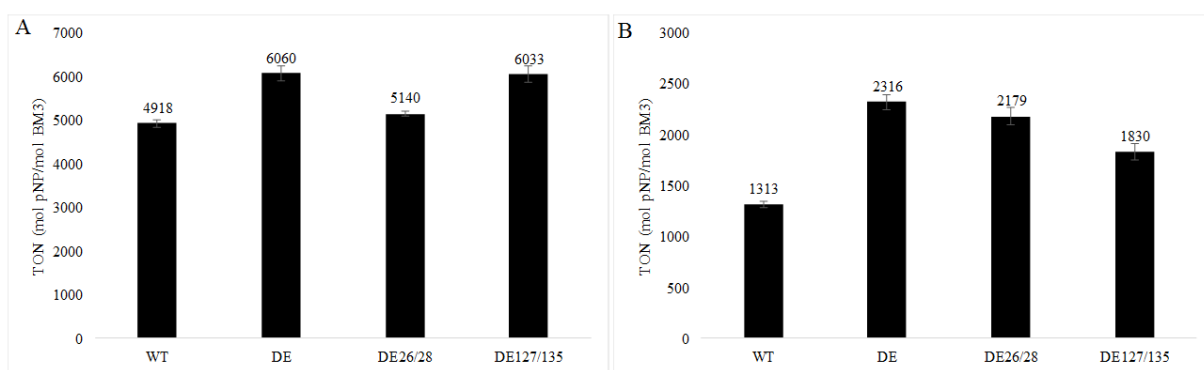


Figure 31: Comparison of the pNP productivity of wild type BM3, DE, DE I26V/T28A and DE I127V/T135A mutants using as cofactors either A. NADPH or B. NADH. The standard deviation and mean for each sample set were calculated from three independent experiments each with three biological replicates.

Table 15. Kinetic data for pNP production using NADPH as a cofactor for both wild type BM3 and the DE mutant.

BM3	WT	DE
10-pNCA min ⁻¹	147	256
NADPH min ⁻¹	192	588
Coupling %	76.6	43.5

The standard deviation and mean for each sample set were calculated from three experimental replicates.

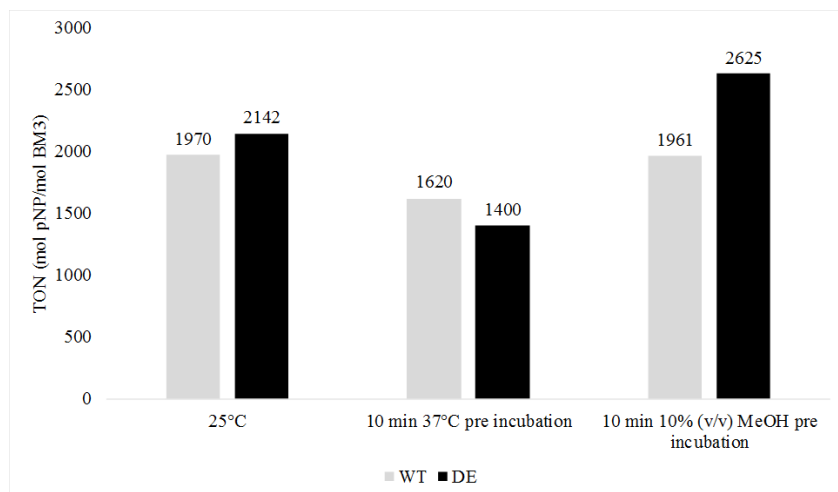


Figure 32: Comparison of the pNP productivity between wild type BM3 and the DE mutant in stringent conditions with a high thermal preincubation (2 leftmost columns) or organic cosolvent concentration (methanol, 2 rightmost columns) using NADPH as a cofactor. After preincubations, thermal stressed reactions were incubated at 25 °C and organic solvent stressed reactions were both incubated and preincubated at 4 °C. The standard deviation and mean for each sample set were calculated from three independent experiments each with three biological replicates.

4.4 Discussion

Much of the early work characterizing BM3 within *B. megaterium* lead us to postulate that growing this particular bacterium in the presence of a tolerable amount of any of the unsaturated fatty acids oleic, linoleic or arachidonic would apply a selective pressure on the BM3 gene to either enhance the productivity of the CYP or its expression or both. This first hypothesis was informed by the fact that the protein repressor BM3R1 which controls BM3 expression [554] can have its repression lifted in the presence of unsaturated fatty acids, possibly as an adaptive response to metabolize these same fatty acids which are toxic to *B. megaterium* [40]. Furthermore, cultures of this bacterium, which had either been treated with nafenopin to induce BM3 expression or lacking the BM3R1 repressor altogether, displayed increased resistance against unsaturated fatty acid toxicity [39]. In an extensive review on BM3 [48], the authors surmise with respect to this information that part of the natural role of BM3 could be to detoxify such xenobiotic lipids. Interestingly, only 4 % of the fatty acid content of *B. megaterium* is unsaturated, mainly 5-hexa and 5-octadecenoic acid [555]. Thus, BM3 could have other roles in *B. megaterium* such as modulating membrane fluidity as branched fatty acids, all of whom are a natural substrate for BM3, comprise 80 % of *B. megaterium*'s cell wall [42]. In any case, these early findings inspired the experimental evolution approach used here where cultures were laced with increasing concentrations of oleic acid generating in the process a variant of *B. megaterium* which could tolerate 300 μM of oleic acid, up from an initial maximum tolerable concentration of 2.5 μM .

The experimental evolution of BM3 generated a highly mutated sequence accumulating 34 mutations in total, of which only 5 were located inside the oxidase domain. In this regard Table 13 details the nature and the location of these mutations. Given the heme domain is considered to end at amino acid S450, this would make the heme domain span for 42.9 % of the whole BM3 sequence. Yet, only 14.7 % of mutations affected that domain leading to suppose that the oxidase domain is not the most critical region for *B. megaterium* resistance to fatty acids. The few amino acids located on the heme domain prompted us to investigate whether these mutations were helpful in the performance of the new mutant, particularly V26I as it sits directly inside the heme catalytic pocket, a location far more critical to the enzyme's activity than other positions located further away. What's more, the A28T and T82A mutations are themselves relatively close to the catalytic pocket as well. As denoted in Figure 31 however, these oxidase domain mutations affect TONs only slightly negatively for both DE26/28 and DE127/128 backcross mutants. On the other hand, taken together, the linker region and the reductase domain span 57.1 % of the whole BM3 sequence. Yet, mutations hosted within this area

account for 29 of the 34 new mutations identified or 85.3 % of all new mutations. This skewed distribution may be a response to the fact that the reductase domain is being more critical to BM3 stability than the heme domain. Our data in regard to stability does not, however, fully support this hypothesis as, despite the new DE variant showing increased organic solvent resistance, it has less thermal tolerance than its WT BM3 parent (Figure 32). Also, modifications to the reductase domain had some lasting effect on the versatility of the reductase. In the course of this work, several other DE variants were tested with N-benzyl-1,4-dihydronicotinamide, a cheap source of cofactors. The DE variants tested included DE W1048A, W0148S, R966D W1048S and R966D V967M W1048S. Still, none of these DE mutants could utilize the cofactor in the presence of 10-pNCA, unlike the same mutations group on WT BM3, and thus generated no products (unpublished data).

Our initial hypothesis was that, through experimental evolution, oleic acid would enhance BM3 activity and productivity in *B. megaterium*. This was proved correct when we were able to confirm that the evolved BM3 sequence (DE) mutant displayed enhanced productivity in terms of TON (Figure 31) and activity towards both substrate and cofactor when compared to WT (Table 14). However, the lower coupling ratio observed in DE compared to WT was surprising (Table 15), as we expected that evolution would further reduce uncoupling events. It can be assumed that for *B. megaterium* optimising the metabolic activity towards oleic acid as quickly as possible offered a greater competitive advantage over enhancing the ratios of the activities of both oxidase and reductase domains. It's also possible that this is only the case with the substrate 10-pNCA but not with oleic acid although we did not investigate activity with this substrate. In any case, the objective of this work, to generate an improved scaffold of BM3 with minimal work, was successful.

In regards to the BM3 DE amino acid sequence identity, we found the mechanism by which the mutated amino acids enhanced productivity and whether all of these substitutions were beneficial to the overall performance of the enzyme. In that regard, we verified whether the similarity between the new DE mutant and other members of the CYP102 family reached a consensus for some of the new mutations. A total of 10 CYPs, 8 of whom belonged to the CYP102A subfamily, were selected and compared to both WT and evolved DE BM3 (CYP102A1) in regards to their amino acid sequence identity (Table 14). Noteworthy, an amino acid identity of at least 40 % is required to classify CYPs within the same family and 55 % within the same subfamily [556]. Of the 34 substitutions present in BM3 DE sequence, 9 replaced the WT amino acid by one similar to those found on the other members of the CYP102 family (9 leftmost columns of Table 14). This could in part explain the enhanced

properties of the new sequence. However, this aspect was not further explored through mutants bearing these substitutions on the wild type sequence. Conversely, 4 mutations replaced a WT amino acid similar to the ones in other CYP102 family members with a new dissimilar one (4 rightmost columns of Table 14). This would have been another interesting feature to investigate as to whether these particular mutations helped or hindered the DE or the BM3 CYP. It is also of interest to consider that of all of the 29 amino acid substitutions located in the linker region or reductase domain, with the exception of M967V, none are located near residues identified as being potentially involved in FAD, FMN or NADPH binding [22]. In recent work [557], it's been observed that there can be extensive interactions between the key residues of an active site and more distant residues within an enzyme's structure greatly influencing which substitutions an enzyme can tolerate. This distribution of substitutions on the reductase domain again confirms that it was the most critical portion of BM3 for its resistance to fatty acid as these site mutations can be found in our work as well as in naturally evolved CYPs. Regardless, the sequence generated by this technique showed increased TON and activity, as was predicted when the experiment was designed. What's more, sequences generated from this technique could serve as a platform to discover new productivity enhancing mutations and in the process generate improved BM3 variants.

4.5 Conclusion

We have developed here a technique by which new improved BM3 variants can be generated with minimal work comparatively to consensus guided evolution or directed evolution by error prone PCR. In the process we have also created the BM3 DE variant, which shows increases product output compared to the WT sequence with either NADPH or NADH as a cofactor by 23 % and 76 %, respectively. The usefulness of this technique to the engineering of more productive variants of BM3 can manifest itself in different ways once the experimental evolution is complete and the new sequence is identified. On one hand, the sequence could be mined for beneficial mutations that could be later added in different combinations unto the wild type BM3 sequence. On the other hand, the new sequence could be seamlessly inserted back into *B. megaterium*'s genome in place of the WT BM3 sequence and the experiment repeated further to generate a second-generation variant even further improved.

General conclusion

Since the discovery in the mid-1980s of the first soluble CYP naturally fused to its redox partner, better known as BM3, this particular CYP has been extensively studied and characterized. The enzyme has proven itself quite flexible in its substrate scope being able to hydroxylate a variety of commercially relevant compounds. It can, furthermore, be fine-tuned to act upon very specific substrates with great efficiency as was the case with the BM3 mutant PMO R2, which can achieve a TON of over 45 000 for propane hydroxylation to 2- and 1- propanol [218, 217, 219–222]. Conversely, the wild type BM3 enzyme has no detectable activity towards propane. However, BM3 and CYPs in general still have some operational limitations which hamper their implementation as commercially sound biocatalytic routes to employ in the manufacture of valuable chemical compounds [197, 272, 481–483]. As such, to this day attempt to tame the enzyme for industrial applications in either a whole cell or an enzymatic approach is an ongoing process. This thesis has reviewed the hurdles inherent to both an enzymatic and a whole cell process in chapter 1.5 and through the articles inserted into this thesis sought to address those inherent to an enzymatic process.

One of these problems is associated to the natural cofactor of BM3, NADPH, which is highly expensive. In the paper inserted in chapter 2, NADPH and the alternative cofactors NADH and NBAH use were explored using the BM3 mutant R966D/W1046S which we named N-D. By tailoring reaction conditions to maximize the nicotinamide-based compounds (NADPH, NADH, NBAH) stability first and then BM3's stability second, the performance of the reactions, in terms of total yield, or TON, could be improved by a factor of 2 to 2.6-fold. To achieve this, temperatures were lowered to 4 °C as it promoted nicotinamide compound stability. However, we discovered that temperature also had a positive effect on another problem associated to CYPs, catalytic efficiency. CYP enzymes are not wholly efficient in the use of their substrates to generate the desired product sometimes consuming a cofactor but producing water, hydrogen peroxide or a superoxide anion instead. In this phenomenon, called an uncoupling event, a cofactor is wasted and both hydrogen peroxide and a superoxide anion can damage the enzyme. This problem of catalytic efficiency goes further, cofactors can also be consumed in the absence of substrate to the oxidase domain leading a phenomenon dubbed a leakage event whose consequences are similar to that of an uncoupling event. For both NADH and NBAH, when temperatures were lowered to 4 °C oxidase activity was raised, reductase activity was slowed, coupling efficiency was enhanced and leakage rates were slowed down. Besides cofactor stability, enhancing the catalytic efficiency most likely ties as well into the

enhanced TONs observed at 4 °C in this work (Table 8). Interestingly, we also demonstrate that product yields for the N-D mutant using NADH (TON = 3117 for pNP/BM3 Fig. 21c) can compete with that of WT BM3 using its natural cofactor NADPH (TON = 3691 pNP/BM3 Fig. 20b). Going back to the problem associated with the price of the cofactors, although the best TON obtained with NADH (TON = 3117 pNP/BM3 Fig. 21c) is roughly three times that of the highest TON obtained with NBAH (TON = 1170 pNP/BM3 Fig. 21c) using NBAH it is important to note that it would still be more cost effective to use NADH as it costs somewhere between a tenth to a hundredth of the price of NADH and can be recycled as well.

Yet one more problem associated with the use of BM3, is its operational stability. On the one hand, CYP substrates are most often insoluble in aqueous media, their solubility can therefore be achieved by adding an organic cosolvent and by raising the temperature both of which are deleterious to the operational stability of the enzyme. In addition, the undesired products of uncoupling and leakage events further strain this problem. The paper inserted into chapter 3, sought to address this first by combining the mutations of the W5F5 mutant evolved for solvent resistance [198] onto the N-D mutant developed to accept a wider nicotinamide cofactor range [306] thus generating a mutant named NTD1 which displayed increased organic solvent tolerance and greater productivity widening TON by a factor of 1.73 and 1.75 for NBAH and NADH respectively. Subsequently, new mutants derived from NTD1 were generated using a consensus guided approach using CYP102A2 and A3 as template reference. In that particular work new mutations were limited to the linker region and the reductase domain leaving the oxidase domain untouched.

The CYP102A2 and A3 were selected as templates for the reductase as it was shown that their domain although sharing much sequence identity with CYP102A1 (BM3) both display higher reductase stability but lower oxidase stability [199, 247]. This was also done to fine-tune the catalytic efficiency in regards the alternative cofactors used (NADH, NBAH) which are highly dependent on the architecture of the reductase. The mutants thus generated (NTD2-7) displayed greater thermostability and leakage tolerance towards NBAH and NADH, without jeopardizing productivity. For instance, the mutant NTD5 displayed the highest TON of all mutants when using the cofactor NBAH at up to a TON of 2233, roughly a 2.0-fold improvement from the parent mutant N-D. For both cofactors NADH and NADPH, the NTD6 mutant displayed the highest TON of all mutants at up to 7225 for NADH, a 1.8-fold improvement from the parent mutant N-D and reached a TON at up

to 6641 for NADPH, a 1.2-fold improvement compared to WT BM3. These values are significant as they represent, to our knowledge, the highest TON ever reported in the literature for NBAH and NADH. Furthermore, with the exception of the T235A mutation, the oxidase domain of the NTD mutants of this work remains unaltered, allowing mutations widening the substrate scope of the enzyme to be added as desired. Of importance as well, the total product output of reactions driven with NADH now outperforms those driven with the natural cofactor NADPH. This work did not, however, fully explore the consensus guided evolution strategy possible between CYP102A1, A2 & A3 leaving several key areas to explore within the reductase domain to potentially enhance yield, stability and catalytic efficiency with the low-cost cofactors NADH and NBAH.

The last paper inserted into this thesis at chapter 4 took a detour in fundamental science before steering back into engineering. From information relating directly to the biological role of BM3 within *B. megaterium* we used its predicted natural metabolism to implement an experimental evolution approach to the bacterium and devised it in a way to force the evolution of the genomically encoded wild type BM3 towards a more productive mutant. Indeed, the experiment resulted in the generation of a new BM3 variant dubbed DE which displayed greater TON than its wild type counterpart reaching 6060 for NADPH and 2316 for NADH a 1.23 and 1.76-fold improvement respectively. On the fundamental side, this validated the predicted protection role of BM3 towards unsaturated fatty acid metabolism (English et al., 1994; Palmer et al., 1998). On the engineering side, this provided us with a new technique to evolve and enhance BM3. The technique can be used to mine for beneficial mutations that could later be tested in different combinations onto the wild type BM3 template it could serve as the basis entry data for machine learning once a few sequences have been generated and validated. In addition, whichever new sequence is generated, it could be seamlessly inserted back into the *B. megaterium* genome in place of the WT BM3 sequence simply to once more repeat the experiment in order to generate enhanced second-generation variants. Although, this particular work somewhat improved the operational stability of the enzyme the main goal of this particular work was to offer an alternative tool or approach to solve the problems of operational stability and catalytic efficiency. An avenue not explored but considered within this thesis work was to replace the WT BM3 sequence with that of R966D/W1046S to perhaps explore the evolution of a mutant suited for the use of the nicotinamide cofactor NBAH.

The overall work of this thesis sought to curtail the overarching problems holding back BM3 enzymatic processes. One of these problems was the highly prohibitive cost of the cofactor NADPH.

We circumvented this particular problem by using the low-cost biomimetic NBAH cofactor. However, several molecules potentially acting as a biomimetic cofactor to NADPH could be synthesized and tested for BM3 compatibility, stability and its potential to be recycled chemically or enzymatically. In regards to further enhancing operational stability and catalytic efficiency, as we've discovered a beneficial relationship between low temperature driven reactions and both TON and coupling ratio improvements, another interesting avenue to explore would be that of enzymatic reactions driven below the freezing point of water with freezing-point depression agents such as glycerol, ethylene glycol, propylene glycol and even antifreeze proteins. Furthermore, as outlined previously, several mutations remain to be investigated using either a using a consensus guided approach or an experimental evolution approach. In conclusion, our work here in this thesis as provided new technical insights and new high-performance mutants (NTD5, NTD6 and DE) to enhance the performance of BM3 based enzymatic bioprocesses with low cost cofactors (NADH, NBAH) as well as a new technique by which new mutations, and therefore new mutants, can be identified to further enhance BM3. Ultimately this narrows the gap presently precluding the use of BM3 as a competitive biocatalyst in the chemical industry.

References

1. Estabrook, R. W. (2005). Steroid hydroxylations: A paradigm for cytochrome P450 catalyzed mammalian monooxygenation reactions. *Biochemical and Biophysical Research Communications*, 338(1), 290–298. <https://doi.org/10.1016/j.bbrc.2005.08.168>
2. Brodie, B. B., Axelrod, J., Cooper, J. R., Gaudette, L., La Du, B. N., Mitoma, C., & Udenfriend, S. (1955). Detoxication of drugs and other foreign compounds by liver microsomes. *Science (New York, N.Y.)*, 121(3147), 603–604.
3. Klingenberg, M. (2003). Pigments of rat liver microsomes. *Archives of Biochemistry and Biophysics*, 409(1), 2–6.
4. Chance, B., & Pappenheimer, A. M. (1954). Kinetic and spectrophotometric studies of cytochrome b5 in midgut homogenates of cecropia. *The Journal of Biological Chemistry*, 209(2), 931–943.
5. Lemberg, R., Legge, J. W., & Lockwood, W. H. (1941). Coupled oxidation of ascorbic acid and haemoglobin. *Biochemical Journal*, 35(3), 339–352.
6. Omura, T., & Sato, R. (1962). A new cytochrome in liver microsomes. *The Journal of Biological Chemistry*, 237, 1375–1376.
7. Nishibayashi, H., Omura, T., & Sato, R. (1963). A flavoprotein oxidizing NADPH isolated from liver microsomes. *Biochimica Et Biophysica Acta*, 67, 520–522.
8. Omura, T., & Sato, R. (1963). Fractional solubilization of haemoproteins and partial purification of carbon monoxide-binding cytochrome from liver microsomes. *Biochimica Et Biophysica Acta*, 71, 224–226.
9. Omura, T., & Sato, R. (1964). THE CARBON MONOXIDE-BINDING PIGMENT OF LIVER MICROSOMES. I. EVIDENCE FOR ITS HEMOPROTEIN NATURE. *The Journal of Biological Chemistry*, 239, 2370–2378.

10. Omura, T., & Sato, R. (1964). THE CARBON MONOXIDE-BINDING PIGMENT OF LIVER MICROSOMES. II. SOLUBILIZATION, PURIFICATION, AND PROPERTIES. *The Journal of Biological Chemistry*, 239, 2379–2385.
11. Hanson, L. K., Eaton, W. A., Sligar, S. G., Gunsalus, I. C., Gouterman, M., & Connell, C. R. (1976). Letter: Origin of the anomalous Soret spectra of carboxycytochrome P-450. *Journal of the American Chemical Society*, 98(9), 2672–2674.
12. Rupasinghe, S., Schuler, M. A., Kagawa, N., Yuan, H., Lei, L., Zhao, B., ... Lamb, D. C. (2006). The cytochrome P450 gene family CYP157 does not contain EXXR in the K-helix reducing the absolute conserved P450 residues to a single cysteine. *FEBS letters*, 580(27), 6338–6342. <https://doi.org/10.1016/j.febslet.2006.10.043>
13. Oezguen, N., Kumar, S., Hindupur, A., Braun, W., Muralidhara, B. K., & Halpert, J. R. (2008). Identification and analysis of conserved sequence motifs in cytochrome P450 family 2. Functional and structural role of a motif 187RFDYKD192 in CYP2B enzymes. *The Journal of Biological Chemistry*, 283(31), 21808–21816. <https://doi.org/10.1074/jbc.M708582200>
14. Hedegaard, J., & Gunsalus, I. C. (1965). Mixed function oxidation. IV. An induced methylene hydroxylase in camphor oxidation. *The Journal of Biological Chemistry*, 240(10), 4038–4043.
15. Katagiri, M., Ganguli, B. N., & Gunsalus, I. C. (1968). A soluble cytochrome P-450 functional in methylene hydroxylation. *The Journal of Biological Chemistry*, 243(12), 3543–3546.
16. Poulos, T. L., Finzel, B. C., Gunsalus, I. C., Wagner, G. C., & Kraut, J. (1985). The 2.6-Å crystal structure of *Pseudomonas putida* cytochrome P-450. *The Journal of Biological Chemistry*, 260(30), 16122–16130.
17. Narhi, L. O., & Fulco, A. J. (1986). Characterization of a catalytically self-sufficient 119,000-dalton cytochrome P-450 monooxygenase induced by barbiturates in *Bacillus megaterium*. *The Journal of Biological Chemistry*, 261(16), 7160–7169.

18. Schwalb, H., Narhi, L. O., & Fulco, A. J. (1985). Purification and characterization of pentobarbital-induced cytochrome P-450BM-1 from *Bacillus megaterium* ATCC 14581. *Biochimica Et Biophysica Acta*, *838*(3), 302–311.
19. Ravichandran, K. G., Boddupalli, S. S., Hasermann, C. A., Peterson, J. A., & Deisenhofer, J. (1993). Crystal structure of hemoprotein domain of P450BM-3, a prototype for microsomal P450's. *Science (New York, N.Y.)*, *261*(5122), 731–736.
20. Li, H., & Poulos, T. L. (1997). The structure of the cytochrome p450BM-3 haem domain complexed with the fatty acid substrate, palmitoleic acid. *Nature Structural & Molecular Biology*, *4*(2), 140–146. <https://doi.org/10.1038/nsb0297-140>
21. Sevrioukova, I. F., Li, H., Zhang, H., Peterson, J. A., & Poulos, T. L. (1999). Structure of a cytochrome P450-redox partner electron-transfer complex. *Proceedings of the National Academy of Sciences of the United States of America*, *96*(5), 1863–1868.
22. Joyce, M. G., Ekanem, I. S., Roitel, O., Dunford, A. J., Neeli, R., Girvan, H. M., ... Leys, D. (2012). The crystal structure of the FAD/NADPH-binding domain of flavocytochrome P450 BM3. *The FEBS journal*, *279*(9), 1694–1706. <https://doi.org/10.1111/j.1742-4658.2012.08544.x>
23. Cook, D. J., Finnigan, J. D., Cook, K., Black, G. W., & Charnock, S. J. (2016). Cytochromes P450: History, Classes, Catalytic Mechanism, and Industrial Application. *Advances in Protein Chemistry and Structural Biology*, *105*, 105–126. <https://doi.org/10.1016/bs.apcsb.2016.07.003>
24. Nelson, D. R. (2009). The Cytochrome P450 Homepage. *Human Genomics*, *4*(1), 59–65. <https://doi.org/10.1186/1479-7364-4-1-59>
25. Sanger, F., Nicklen, S., & Coulson, A. R. (1992). DNA sequencing with chain-terminating inhibitors. 1977. *Biotechnology (Reading, Mass.)*, *24*, 104–108.

26. Guengerich, F. P., & Cheng, Q. (2011). Orphans in the human cytochrome P450 superfamily: approaches to discovering functions and relevance in pharmacology. *Pharmacological Reviews*, 63(3), 684–699. <https://doi.org/10.1124/pr.110.003525>
27. Guengerich, F. P. (2015). Human Cytochrome P450 Enzymes. In *Cytochrome P450* (pp. 523–785). Springer, Cham. https://doi.org/10.1007/978-3-319-12108-6_9
28. Durairaj, P., Hur, J.-S., & Yun, H. (2016). Versatile biocatalysis of fungal cytochrome P450 monooxygenases. *Microbial Cell Factories*, 15. <https://doi.org/10.1186/s12934-016-0523-6>
29. Schuler, M. A. (2015). P450s in Plants, Insects, and Their Fungal Pathogens. In *Cytochrome P450* (pp. 409–449). Springer, Cham. https://doi.org/10.1007/978-3-319-12108-6_7
30. Kim, G.-T., & Tsukaya, H. (2002). Regulation of the biosynthesis of plant hormones by cytochrome P450s. *Journal of Plant Research*, 115(3), 0169–0177. <https://doi.org/10.1007/s102650200022>
31. Kelly, S. L., & Kelly, D. E. (2013). Microbial cytochromes P450: biodiversity and biotechnology. Where do cytochromes P450 come from, what do they do and what can they do for us? *Philosophical Transactions of the Royal Society of London. Series B, Biological Sciences*, 368(1612), 20120476. <https://doi.org/10.1098/rstb.2012.0476>
32. Kawano, S., Kamataki, T., Yasumori, T., Yamazoe, Y., & Kato, R. (1987). Purification of human liver cytochrome P-450 catalyzing testosterone 6 beta-hydroxylation. *Journal of Biochemistry*, 102(3), 493–501.
33. Kitagawa, W., Ozaki, T., Nishioka, T., Yasutake, Y., Hata, M., Nishiyama, M., ... Tamura, T. (2013). Cloning and heterologous expression of the aurachin RE biosynthesis gene cluster afford a new cytochrome P450 for quinoline N-hydroxylation. *Chembiochem: A European Journal of Chemical Biology*, 14(9), 1085–1093. <https://doi.org/10.1002/cbic.201300167>

34. Bauer, E., Guo, Z., Ueng, Y. F., Bell, L. C., Zeldin, D., & Guengerich, F. P. (1995). Oxidation of benzo[a]pyrene by recombinant human cytochrome P450 enzymes. *Chemical Research in Toxicology*, *8*(1), 136–142.
35. Kim, J. H., Stansbury, K. H., Walker, N. J., Trush, M. A., Strickland, P. T., & Sutter, T. R. (1998). Metabolism of benzo[a]pyrene and benzo[a]pyrene-7,8-diol by human cytochrome P450 1B1. *Carcinogenesis*, *19*(10), 1847–1853.
36. Nomura, T., Magome, H., Hanada, A., Takeda-Kamiya, N., Mander, L. N., Kamiya, Y., & Yamaguchi, S. (2013). Functional analysis of Arabidopsis CYP714A1 and CYP714A2 reveals that they are distinct gibberellin modification enzymes. *Plant & Cell Physiology*, *54*(11), 1837–1851. <https://doi.org/10.1093/pcp/pct125>
37. Brandle, J., & Richman, A. (2010, December 15). Composition and methods for producing steviol and steviol glycosides. Retrieved from <https://patents.google.com/patent/EP1897951B1/en>
38. Ceunen, S., & Geuns, J. M. C. (2013). Steviol Glycosides: Chemical Diversity, Metabolism, and Function. *Journal of Natural Products*, *76*(6), 1201–1228. <https://doi.org/10.1021/np400203b>
39. Palmer, C. N., Axen, E., Hughes, V., & Wolf, C. R. (1998). The repressor protein, Bm3R1, mediates an adaptive response to toxic fatty acids in *Bacillus megaterium*. *The Journal of Biological Chemistry*, *273*(29), 18109–18116.
40. English, N., Hughes, V., & Wolf, C. R. (1994). Common pathways of cytochrome P450 gene regulation by peroxisome proliferators and barbiturates in *Bacillus megaterium* ATCC14581. *The Journal of Biological Chemistry*, *269*(43), 26836–26841.
41. Bloemberg, G. V., & Lugtenberg, B. J. (2001). Molecular basis of plant growth promotion and biocontrol by rhizobacteria. *Current Opinion in Plant Biology*, *4*(4), 343–350.

42. Kaneda, T. (1977). Fatty acids of the genus *Bacillus*: an example of branched-chain preference. *Bacteriological Reviews*, *41*(2), 391–418.
43. Fulco, A. J. (1967). The effect of temperature on the formation of delta 5-unsaturated fatty acids by bacilli. *Biochimica Et Biophysica Acta*, *144*(3), 701–703.
44. Shimura, Y. (1988). A Quantitative Scale of the Spectrochemical Series for the Mixed Ligand Complexes of d⁶ Metals. *Bulletin of the Chemical Society of Japan*, *61*(3), 693–698.
<https://doi.org/10.1246/bcsj.61.693>
45. Hlavica, P., & Künzel-Mulas, U. (1993). Metabolic N-oxide formation by rabbit-liver microsomal cytochrome P-450B4: involvement of superoxide in the NADPH-dependent N-oxygenation of N,N-dimethylaniline. *Biochimica Et Biophysica Acta*, *1158*(1), 83–90.
46. Seto, Y., & Guengerich, F. P. (1993). Partitioning between N-dealkylation and N-oxygenation in the oxidation of N,N-dialkylarylamines catalyzed by cytochrome P450 2B1. *The Journal of Biological Chemistry*, *268*(14), 9986–9997.
47. Kashiwama, E., Yokoi, T., Odomi, M., Funae, Y., Inoue, K., & Kamataki, T. (1997). Cytochrome P450 responsible for the stereoselective S-oxidation of flosequinan in hepatic microsomes from rats and humans. *Drug Metabolism and Disposition: The Biological Fate of Chemicals*, *25*(6), 716–724.
48. Whitehouse, C. J. C., Bell, S. G., & Wong, L.-L. (2012). P450(BM3) (CYP102A1): connecting the dots. *Chemical Society Reviews*, *41*(3), 1218–1260. <https://doi.org/10.1039/c1cs15192d>
49. Girvan, H. M., Dunford, A. J., Neeli, R., Ekanem, I. S., Waltham, T. N., Joyce, M. G., ... Munro, A. W. (2011). Flavocytochrome P450 BM3 mutant W1046A is a NADH-dependent fatty acid hydroxylase: implications for the mechanism of electron transfer in the P450 BM3 dimer. *Archives of Biochemistry and Biophysics*, *507*(1), 75–85.
<https://doi.org/10.1016/j.abb.2010.09.014>

50. Makris, T. M., Denisov, I., Schlichting, I., & Sligar, S. G. (2005). Activation of Molecular Oxygen by Cytochrome P450. In *Cytochrome P450* (pp. 149–182). Springer, Boston, MA.
https://doi.org/10.1007/0-387-27447-2_5
51. Montellano, P. R. O. de, & Voss, J. J. D. (2005). Substrate Oxidation by Cytochrome P450 Enzymes. In *Cytochrome P450* (pp. 183–245). Springer, Boston, MA.
https://doi.org/10.1007/0-387-27447-2_6
52. Rittle, J., Younker, J. M., & Green, M. T. (2010). Cytochrome P450: The Active Oxidant and Its Spectrum. *Inorganic Chemistry*, *49*(8), 3610–3617. <https://doi.org/10.1021/ic902062d>
53. Groves, J. T., & McClusky, G. A. (1978). Aliphatic hydroxylation by highly purified liver microsomal cytochrome P-450. Evidence for a carbon radical intermediate. *Biochemical and Biophysical Research Communications*, *81*(1), 154–160.
54. Hjelmeland, L. M., Aronow, L., & Trudell, J. R. (1977). Intramolecular determination of primary kinetic isotope effects in hydroxylations catalyzed by cytochrome P-450. *Biochemical and Biophysical Research Communications*, *76*(2), 541–549.
[https://doi.org/10.1016/0006-291X\(77\)90758-6](https://doi.org/10.1016/0006-291X(77)90758-6)
55. Foster, A. B., Jarman, M., Stevens, J. D., Thomas, P., & Westwood, J. H. (1974). Isotope effects in O- and N-demethylations mediated by rat liver microsomes: an application of direct insertion electron impact mass spectrometry. *Chemico-Biological Interactions*, *9*(5), 327–340.
56. Gelb, M. H., Heimbrook, D. C., Mälkönen, P., & Sligar, S. G. (1982). Stereochemistry and deuterium isotope effects in camphor hydroxylation by the cytochrome P450cam monooxygenase system. *Biochemistry*, *21*(2), 370–377.

57. White, R. E., Miller, J. P., Favreau, L. V., & Bhattacharyya, A. (1986). Stereochemical dynamics of aliphatic hydroxylation by cytochrome P-450. *Journal of the American Chemical Society*, *108*(19), 6024–6031. <https://doi.org/10.1021/ja00279a059>
58. Groves, J. T., & Adhyam, D. V. (1984). Hydroxylation by cytochrome P-450 and metalloporphyrin models. Evidence for allylic rearrangement. *Journal of the American Chemical Society*, *106*(7), 2177–2181. <https://doi.org/10.1021/ja00319a044>
59. McClanahan, R. H., Huitric, A. C., Pearson, P. G., Desper, J. C., & Nelson, S. D. (1988). Evidence for a cytochrome P-450-catalyzed allylic rearrangement with double-bond topomerization. *Journal of the American Chemical Society*, *110*(6), 1979–1981. <https://doi.org/10.1021/ja00214a060>
60. Loida, P. J., & Sligar, S. G. (1993). Molecular recognition in cytochrome P-450: Mechanism for the control of uncoupling reactions. *Biochemistry*, *32*(43), 11530–11538. <https://doi.org/10.1021/bi00094a009>
61. Girhard, M., Bakkes, P. J., Mahmoud, O., & Urlacher, V. B. (2015). P450 Biotechnology. In *Cytochrome P450* (pp. 451–520). Springer, Cham. https://doi.org/10.1007/978-3-319-12108-6_8
62. Bernhardt, R., & Urlacher, V. B. (2014). Cytochromes P450 as promising catalysts for biotechnological application: chances and limitations. *Applied Microbiology and Biotechnology*, *98*(14), 6185–6203. <https://doi.org/10.1007/s00253-014-5767-7>
63. Lim, J. B., Barker, K. A., Eller, K. A., Jiang, L., Molina, V., Saifee, J. F., & Sikes, H. D. (2015). Insights into electron leakage in the reaction cycle of cytochrome P450 BM3 revealed by kinetic modeling and mutagenesis. *Protein Science: A Publication of the Protein Society*, *24*(11), 1874–1883. <https://doi.org/10.1002/pro.2793>

64. Cryle, M. J., Espinoza, R. D., Smith, S. J., Matovic, N. J., & De Voss, J. J. (2006). Are branched chain fatty acids the natural substrates for P450(BM3)? *Chemical Communications (Cambridge, England)*, (22), 2353–2355. <https://doi.org/10.1039/b601202g>
65. Dezvarei, S., Onoda, H., Shoji, O., Watanabe, Y., & Bell, S. G. (2018). Efficient hydroxylation of cycloalkanes by co-addition of decoy molecules to variants of the cytochrome P450 CYP102A1. *Journal of Inorganic Biochemistry*, 183, 137–145. <https://doi.org/10.1016/j.jinorgbio.2018.03.001>
66. Atkins, W. M., & Sligar, S. G. (1988). The roles of active site hydrogen bonding in cytochrome P-450cam as revealed by site-directed mutagenesis. *The Journal of Biological Chemistry*, 263(35), 18842–18849.
67. Paulsen, M. D., Filipovic, D., Sligar, S. G., & Ornstein, R. L. (1993). Controlling the regiospecificity and coupling of cytochrome P450cam: T185F mutant increases coupling and abolishes 3-hydroxynorcamphor product. *Protein Science: A Publication of the Protein Society*, 2(3), 357–365. <https://doi.org/10.1002/pro.5560020308>
68. Omura, T., & Sato, R. (1967). [90] Isolation of cytochromes P-450 and P-420. In *Methods in Enzymology* (Vol. 10, pp. 556–561). Academic Press. [https://doi.org/10.1016/0076-6879\(67\)10096-7](https://doi.org/10.1016/0076-6879(67)10096-7)
69. Mowat, C. G., Gazur, B., Campbell, L. P., & Chapman, S. K. (2010). Flavin-containing heme enzymes. *Archives of Biochemistry and Biophysics*, 493(1), 37–52. <https://doi.org/10.1016/j.abb.2009.10.005>
70. Schenkman, J. B., Remmer, H., & Estabrook, R. W. (1967). Spectral studies of drug interaction with hepatic microsomal cytochrome. *Molecular Pharmacology*, 3(2), 113–123.

71. Daff, S. N., Chapman, S. K., Turner, K. L., Holt, R. A., Govindaraj, S., Poulos, T. L., & Munro, A. W. (1997). Redox control of the catalytic cycle of flavocytochrome P-450 BM3. *Biochemistry*, *36*(45), 13816–13823. <https://doi.org/10.1021/bi971085s>
72. Leibman, K. C., Hildebrandt, A. G., & Estabrook, R. W. (1969). Spectrophotometric studies of interactions between various substrates in their binding to microsomal cytochrome P-450. *Biochemical and Biophysical Research Communications*, *36*(5), 789–794.
73. Mitani, F., & Horie, S. (1969). Studies on P-450. VI. The spin state of P-450 solubilized from bovine adrenocortical mitochondria. *Journal of Biochemistry*, *66*(2), 139–149.
74. Das, A., Zhao, J., Schatz, G. C., Sligar, S. G., & Van Duyne, R. P. (2009). Screening of Type I and II Drug Binding to Human Cytochrome P450-3A4 in Nanodiscs by Localized Surface Plasmon Resonance Spectroscopy. *Analytical chemistry*, *81*(10), 3754–3759.
<https://doi.org/10.1021/ac802612z>
75. Jefcoate, C. R. (1978). Measurement of substrate and inhibitor binding to microsomal cytochrome P-450 by optical-difference spectroscopy. *Methods in Enzymology*, *52*, 258–279.
76. Schwaneberg, U., Schmidt-Dannert, C., Schmitt, J., & Schmid, R. D. (1999). A Continuous Spectrophotometric Assay for P450 BM-3, a Fatty Acid Hydroxylating Enzyme, and Its Mutant F87A. *Analytical Biochemistry*, *269*(2), 359–366.
<https://doi.org/10.1006/abio.1999.4047>
77. Schwaneberg, U., Otey, C., Cirino, P. C., Farinas, E., & Arnold, F. H. (2001). Cost-effective whole-cell assay for laboratory evolution of hydroxylases in *Escherichia coli*. *Journal of Biomolecular Screening*, *6*(2), 111–117. <https://doi.org/10.1177/108705710100600207>
78. Wong, T. S., Wu, N., Roccatano, D., Zacharias, M., & Schwaneberg, U. (2005). Sensitive assay for laboratory evolution of hydroxylases toward aromatic and heterocyclic compounds.

- Journal of Biomolecular Screening*, 10(3), 246–252.
<https://doi.org/10.1177/1087057104273336>
79. Yoneda, F., Mori, K., Sakuma, Y., & Yamaguchi, H. (1980). A novel synthesis of pyrimido[4,5-b]quinoline-2(3H),4(10H)-diones (5-deazaflavins) and analogues by the oxidative cyclization of 5,5'-arylmethylenebis-(6-alkylamino-3-methyluracils). *Journal of the Chemical Society, Perkin Transactions 1*, 0(0), 978–981. <https://doi.org/10.1039/P19800000978>
80. Tee, K. L., & Schwaneberg, U. (2006). A screening system for the directed evolution of epoxygenases: importance of position 184 in P450 BM3 for stereoselective styrene epoxidation. *Angewandte Chemie (International Ed. in English)*, 45(32), 5380–5383.
<https://doi.org/10.1002/anie.200600255>
81. Cali, J. J., Ma, D., Sobol, M., Simpson, D. J., Frackman, S., Good, T. D., ... Liu, D. (2006). Luminogenic cytochrome P450 assays. *Expert Opinion on Drug Metabolism & Toxicology*, 2(4), 629–645. <https://doi.org/10.1517/17425255.2.4.629>
82. Lussenburg, B. M. A., Babel, L. C., Vermeulen, N. P. E., & Commandeur, J. N. M. (2005). Evaluation of alkoxyresorufins as fluorescent substrates for cytochrome P450 BM3 and site-directed mutants. *Analytical Biochemistry*, 341(1), 148–155.
<https://doi.org/10.1016/j.ab.2005.02.025>
83. Nakamura, K., Hanna, I. H., Cai, H., Nishimura, Y., Williams, K. M., & Guengerich, F. P. (2001). Coumarin substrates for cytochrome P450 2D6 fluorescence assays. *Analytical Biochemistry*, 292(2), 280–286. <https://doi.org/10.1006/abio.2001.5098>
84. Buters, J. T. M., Schiller, C. D., & Chou, R. C. (1993). A highly sensitive tool for the assay of cytochrome P450 enzyme activity in rat, dog and man: Direct fluorescence monitoring of the deethylation of 7-ethoxy-4-trifluoromethylcoumarin. *Biochemical Pharmacology*, 46(9), 1577–1584. [https://doi.org/10.1016/0006-2952\(93\)90326-R](https://doi.org/10.1016/0006-2952(93)90326-R)

85. Kenaan, C., Zhang, H., & Hollenberg, P. F. (2013). High-throughput fluorescence assay for cytochrome P450 mechanism-based inactivators. *Methods in Molecular Biology (Clifton, N.J.)*, 987, 61–69. https://doi.org/10.1007/978-1-62703-321-3_5
86. Venhorst, J., Onderwater, R. C. A., Meerman, J. H. N., Vermeulen, N. P. E., & Commandeur, J. N. M. (2000). Evaluation of a novel high-throughput assay for cytochrome P450 2D6 using 7-methoxy-4-(aminomethyl)-coumarin. *European Journal of Pharmaceutical Sciences*, 12(2), 151–158. [https://doi.org/10.1016/S0928-0987\(00\)00150-0](https://doi.org/10.1016/S0928-0987(00)00150-0)
87. Neufeld, K., Zu Berstenhorst, S. M., & Pietruszka, J. (2014). Evaluation of coumarin-based fluorogenic P450 BM3 substrates and prospects for competitive inhibition screenings. *Analytical Biochemistry*, 456, 70–81. <https://doi.org/10.1016/j.ab.2014.03.022>
88. Horecker, B. L., & Kornberg, A. (1948). The Extinction Coefficients of the Reduced Band of Pyridine Nucleotides. *Journal of Biological Chemistry*, 175(1), 385–390.
89. Beisenherz, G., Bücher, T., & Garbade, K.-H. (1955). [58] α -Glycerophosphate dehydrogenase from rabbit muscle: Dihydroxyacetone Phosphate + DPNH + H+ I- α -Glycerophosphate + DPN+. In *Methods in Enzymology* (Vol. 1, pp. 391–397). Academic Press. [https://doi.org/10.1016/0076-6879\(55\)01063-X](https://doi.org/10.1016/0076-6879(55)01063-X)
90. Ziegenhorn, J., Senn, M., & Bücher, T. (1976). Molar absorptivities of beta-NADH and beta-NADPH. *Clinical Chemistry*, 22(2), 151–160.
91. Guengerich, F. P. (2001). Uncommon P450-catalyzed reactions. *Current Drug Metabolism*, 2(2), 93–115.
92. Cryle, M. J., Stok, J. E., & Voss, J. J. D. (2003). Reactions Catalyzed by Bacterial Cytochromes P450. *Australian Journal of Chemistry*, 56(8), 749–762. <https://doi.org/10.1071/ch03040>
93. Bernhardt, R. (2006). Cytochromes P450 as versatile biocatalysts. *Journal of Biotechnology*, 124(1), 128–145. <https://doi.org/10.1016/j.jbiotec.2006.01.026>

94. Urlacher, V. B., & Eiben, S. (2006). Cytochrome P450 monooxygenases: perspectives for synthetic application. *Trends in Biotechnology*, *24*(7), 324–330.
<https://doi.org/10.1016/j.tibtech.2006.05.002>
95. Isin, E. M., & Guengerich, F. P. (2007). Complex reactions catalyzed by cytochrome P450 enzymes. *Biochimica Et Biophysica Acta*, *1770*(3), 314–329.
<https://doi.org/10.1016/j.bbagen.2006.07.003>
96. Ortiz de Montellano, P. R., & Nelson, S. D. (2011). Rearrangement reactions catalyzed by cytochrome P450s. *Archives of Biochemistry and Biophysics*, *507*(1), 95–110.
<https://doi.org/10.1016/j.abb.2010.10.016>
97. Urlacher, V. B., & Girhard, M. (2012). Cytochrome P450 monooxygenases: an update on perspectives for synthetic application. *Trends in Biotechnology*, *30*(1), 26–36.
<https://doi.org/10.1016/j.tibtech.2011.06.012>
98. Butler, C. F., Peet, C., McLean, K. J., Baynham, M. T., Blankley, R. T., Fisher, K., ... Munro, A. W. (2014). Human P450-like oxidation of diverse proton pump inhibitor drugs by “gatekeeper” mutants of flavocytochrome P450 BM3. *The Biochemical Journal*, *460*(2), 247–259. <https://doi.org/10.1042/BJ20140030>
99. Yun, C.-H., Kim, K.-H., Kim, D.-H., Jung, H.-C., & Pan, J.-G. (2007). The bacterial P450 BM3: a prototype for a biocatalyst with human P450 activities. *Trends in Biotechnology*, *25*(7), 289–298. <https://doi.org/10.1016/j.tibtech.2007.05.003>
100. Sono, M., Roach, M. P., Coulter, E. D., & Dawson, J. H. (1996). Heme-Containing Oxygenases. *Chemical Reviews*, *96*(7), 2841–2888. <https://doi.org/10.1021/cr9500500>
101. Edin, M. L., Cheng, J., Gruzdev, A., Hoopes, S. L., & Zeldin, D. C. (2015). P450 Enzymes in Lipid Oxidation. In *Cytochrome P450* (pp. 881–905). Springer, Cham.
https://doi.org/10.1007/978-3-319-12108-6_13

102. Jamieson, K. L., Endo, T., Darwesh, A. M., Samokhvalov, V., & Seubert, J. M. (2017). Cytochrome P450-derived eicosanoids and heart function. *Pharmacology & Therapeutics*. <https://doi.org/10.1016/j.pharmthera.2017.05.005>
103. Sugimoto Yukihiro, Narumiya Shuh, & Ichikawa Atsushi. (2004). Insight into Prostanoid Functions: Lessons from Receptor-Knockout Mice. *The Eicosanoids*. <https://doi.org/10.1002/0470020628.ch18>
104. Kadowitz P. J., Baber S. R., Mazim M. M., Keebler M., Champion H. C., Bivalacqua T. J., ... Hyman A. L. (2004). Generation of Vasoactive Prostanoids by the Cyclooxygenase-2 Pathway in the Cardiovascular System of the Rat. *The Eicosanoids*. <https://doi.org/10.1002/0470020628.ch34>
105. Henzl Milan R. (2004). Perspectives and Clinical Significance of Eicosanoids in Immunology, Endocrinology and Metabolic Regulation. *The Eicosanoids*. <https://doi.org/10.1002/0470020628.ch19>
106. Fleming Diana C., & Kelly Rodney W. (2004). Prostaglandins and the Immune Response. *The Eicosanoids*. <https://doi.org/10.1002/0470020628.ch20>
107. Sampson Anthony P., & Holgate Stephen T. (2004). Leukotrienes in Aspirin-Intolerant Asthma. *The Eicosanoids*. <https://doi.org/10.1002/0470020628.ch21>
108. Waxman, D. J., & Chang, T. K. H. (2015). Hormonal Regulation of Liver Cytochrome P450 Enzymes. In *Cytochrome P450* (pp. 813–850). Springer, Cham. https://doi.org/10.1007/978-3-319-12108-6_11
109. Auchus, R. J., & Miller, W. L. (2015). P450 Enzymes in Steroid Processing. In *Cytochrome P450* (pp. 851–879). Springer, Cham. https://doi.org/10.1007/978-3-319-12108-6_12
110. Sherif, K. (2013). *Hormone Therapy: A Clinical Handbook*. New York: Springer-Verlag. Retrieved from [//www.springer.com/gp/book/9781461462675](http://www.springer.com/gp/book/9781461462675)

111. Hiroi, T., Imaoka, S., & Funae, Y. (1998). Dopamine Formation from Tyramine by CYP2D6. *Biochemical and Biophysical Research Communications*, 249(3), 838–843.
<https://doi.org/10.1006/bbrc.1998.9232>
112. Niwa, T., Hiroi, T., Tsuzuki, D., Yamamoto, S., Narimatsu, S., Fukuda, T., ... Funae, Y. (2004). Effect of genetic polymorphism on the metabolism of endogenous neuroactive substances, progesterone and p-tyramine, catalyzed by CYP2D6. *Molecular Brain Research*, 129(1), 117–123. <https://doi.org/10.1016/j.molbrainres.2004.06.030>
113. Martínez, C., Agúndez, J. A., Gervasini, G., Martín, R., & Benítez, J. (1997). Tryptamine: a possible endogenous substrate for CYP2D6. *Pharmacogenetics*, 7(2), 85–93.
114. Yu, A.-M., Idle, J. R., Byrd, L. G., Krausz, K. W., Küpfer, A., & Gonzalez, F. J. (2003). Regeneration of serotonin from 5-methoxytryptamine by polymorphic human CYP2D6. *Pharmacogenetics*, 13(3), 173–181. <https://doi.org/10.1097/01.fpc.0000054066.98065.7b>
115. Di Nardo, G., & Gilardi, G. (2012). Optimization of the bacterial cytochrome P450 BM3 system for the production of human drug metabolites. *International Journal of Molecular Sciences*, 13(12), 15901–15924. <https://doi.org/10.3390/ijms131215901>
116. Cytochrome P450 Inhibition. (2010). *Human Drug Metabolism*.
<https://doi.org/10.1002/9780470689332.ch5>
117. Cacho, R. A., Chooi, Y.-H., Zhou, H., & Tang, Y. (2013). Complexity generation in fungal polyketide biosynthesis: a spirocycle-forming P450 in the concise pathway to the antifungal drug griseofulvin. *ACS chemical biology*, 8(10), 2322–2330.
<https://doi.org/10.1021/cb400541z>
118. Tian, Z., Cheng, Q., Yoshimoto, F. K., Lei, L., Lamb, D. C., & Guengerich, F. P. (2013). Cytochrome P450 107U1 is required for sporulation and antibiotic production in

- Streptomyces coelicolor*. *Archives of biochemistry and biophysics*, 530(2), 101–107.
<https://doi.org/10.1016/j.abb.2013.01.001>
119. Wu, S., & Chappell, J. (2008). Metabolic engineering of natural products in plants; tools of the trade and challenges for the future. *Current Opinion in Biotechnology*, 19(2), 145–152.
<https://doi.org/10.1016/j.copbio.2008.02.007>
120. Wink Michael. (2010). Introduction: Biochemistry, Physiology and Ecological Functions of Secondary Metabolites. *Annual Plant Reviews Volume 40: Biochemistry of Plant Secondary Metabolism*. <https://doi.org/10.1002/9781444320503.ch1>
121. Jordan, M. A., & Wilson, L. (2004). Microtubules as a target for anticancer drugs. *Nature Reviews. Cancer*, 4(4), 253–265. <https://doi.org/10.1038/nrc1317>
122. Schröder, G., Unterbusch, E., Kaltenbach, M., Schmidt, J., Strack, D., De Luca, V., & Schröder, J. (1999). Light-induced cytochrome P450-dependent enzyme in indole alkaloid biosynthesis: tabersonine 16-hydroxylase. *FEBS letters*, 458(2), 97–102.
123. Besseau, S., Kellner, F., Lanoue, A., Thamm, A. M. K., Salim, V., Schneider, B., ... Courdavault, V. (2013). A pair of tabersonine 16-hydroxylases initiates the synthesis of vindoline in an organ-dependent manner in *Catharanthus roseus*. *Plant Physiology*, 163(4), 1792–1803.
<https://doi.org/10.1104/pp.113.222828>
124. Morais, L. C., Barbosa-Filho, J. M., & Almeida, R. N. (1998). Central depressant effects of reticuline extracted from *Ocotea duckei* in rats and mice. *Journal of Ethnopharmacology*, 62(1), 57–61.
125. Wiart, C. (2014). Chapter 1 - Alkaloids. In *Lead Compounds from Medicinal Plants for the Treatment of Neurodegenerative Diseases* (pp. 1–188). San Diego: Academic Press.
<https://doi.org/10.1016/B978-0-12-398373-2.00001-7>

126. Frick, S., Kramell, R., & Kutchan, T. M. (2007). Metabolic engineering with a morphine biosynthetic P450 in opium poppy surpasses breeding. *Metabolic Engineering*, *9*(2), 169–176. <https://doi.org/10.1016/j.ymben.2006.10.004>
127. Teoh, K. H., Polichuk, D. R., Reed, D. W., Nowak, G., & Covello, P. S. (2006). *Artemisia annua* L. (Asteraceae) trichome-specific cDNAs reveal CYP71AV1, a cytochrome P450 with a key role in the biosynthesis of the antimalarial sesquiterpene lactone artemisinin. *FEBS Letters*, *580*(5), 1411–1416. <https://doi.org/10.1016/j.febslet.2006.01.065>
128. Kraus, P. F., & Kutchan, T. M. (1995). Molecular cloning and heterologous expression of a cDNA encoding berbamine synthase, a C–O phenol-coupling cytochrome P450 from the higher plant *Berberis stolonifera*. *Proceedings of the National Academy of Sciences of the United States of America*, *92*(6), 2071–2075.
129. Meng, Z., Li, T., Ma, X., Wang, X., Van Ness, C., Gan, Y., ... Huang, W. (2013). Berbamine inhibits the growth of liver cancer cells and cancer initiating cells by targeting Ca²⁺/Calmodulin-dependent protein kinase II. *Molecular cancer therapeutics*, *12*(10). <https://doi.org/10.1158/1535-7163.MCT-13-0314>
130. Zhao, Y., Lv, J. J., Chen, J., Jin, X. B., Wang, M. W., Su, Z. H., ... Zhang, H. Y. (2016). Berbamine inhibited the growth of prostate cancer cells *in vivo* and *in vitro* via triggering intrinsic pathway of apoptosis. *Prostate Cancer and Prostatic Diseases*, *19*(4), 358–366. <https://doi.org/10.1038/pcan.2016.29>
131. Parhi, P., Suklabaidya, S., & Sahoo, S. K. (2017). Enhanced anti-metastatic and anti-tumorigenic efficacy of Berbamine loaded lipid nanoparticles *in vivo*. *Scientific Reports*, *7*(1), 5806. <https://doi.org/10.1038/s41598-017-05296-y>
132. Liu, J. (1995). Pharmacology of oleanolic acid and ursolic acid. *Journal of Ethnopharmacology*, *49*(2), 57–68. [https://doi.org/10.1016/0378-8741\(95\)90032-2](https://doi.org/10.1016/0378-8741(95)90032-2)

133. Han, J.-Y., Kim, M.-J., Ban, Y.-W., Hwang, H.-S., & Choi, Y.-E. (2013). The involvement of β -amyrin 28-oxidase (CYP716A52v2) in oleanane-type ginsenoside biosynthesis in *Panax ginseng*. *Plant & Cell Physiology*, *54*(12), 2034–2046. <https://doi.org/10.1093/pcp/pct141>
134. Singh, H., Singh, P., Kumari, K., Chandra, A., Dass, S. K., & Chandra, R. (2013). A review on noscapine, and its impact on heme metabolism. *Current Drug Metabolism*, *14*(3), 351–360.
135. Dang, T.-T. T., & Facchini, P. J. (2014). CYP82Y1 is N-methylcanadine 1-hydroxylase, a key noscapine biosynthetic enzyme in opium poppy. *The Journal of Biological Chemistry*, *289*(4), 2013–2026. <https://doi.org/10.1074/jbc.M113.505099>
136. Dang, T.-T. T., & Facchini, P. J. (2014). Cloning and characterization of canadine synthase involved in noscapine biosynthesis in opium poppy. *FEBS letters*, *588*(1), 198–204. <https://doi.org/10.1016/j.febslet.2013.11.037>
137. Schoendorf, A., Rithner, C. D., Williams, R. M., & Croteau, R. B. (2001). Molecular cloning of a cytochrome P450 taxane 10 β -hydroxylase cDNA from *Taxus* and functional expression in yeast. *Proceedings of the National Academy of Sciences of the United States of America*, *98*(4), 1501–1506.
138. Jennewein, S., Rithner, C. D., Williams, R. M., & Croteau, R. B. (2001). Taxol biosynthesis: Taxane 13 α -hydroxylase is a cytochrome P450-dependent monooxygenase. *Proceedings of the National Academy of Sciences of the United States of America*, *98*(24), 13595–13600. <https://doi.org/10.1073/pnas.251539398>
139. Jennewein, S., Rithner, C. D., Williams, R. M., & Croteau, R. (2003). Taxoid metabolism: Taxoid 14 β -hydroxylase is a cytochrome P450-dependent monooxygenase. *Archives of Biochemistry and Biophysics*, *413*(2), 262–270. [https://doi.org/10.1016/S0003-9861\(03\)00090-0](https://doi.org/10.1016/S0003-9861(03)00090-0)

140. Papadopoulou, K., Melton, R. E., Leggett, M., Daniels, M. J., & Osbourn, A. E. (1999). Compromised disease resistance in saponin-deficient plants. *Proceedings of the National Academy of Sciences*, *96*(22), 12923–12928. <https://doi.org/10.1073/pnas.96.22.12923>
141. Qi, X., Bakht, S., Qin, B., Leggett, M., Hemmings, A., Mellon, F., ... Osbourn, A. (2006). A different function for a member of an ancient and highly conserved cytochrome P450 family: From essential sterols to plant defense. *Proceedings of the National Academy of Sciences*, *103*(49), 18848–18853. <https://doi.org/10.1073/pnas.0607849103>
142. Geisler, K., Hughes, R. K., Sainsbury, F., Lomonosoff, G. P., Rejzek, M., Fairhurst, S., ... Osbourn, A. (2013). Biochemical analysis of a multifunctional cytochrome P450 (CYP51) enzyme required for synthesis of antimicrobial triterpenes in plants. *Proceedings of the National Academy of Sciences*, *110*(35), E3360–E3367. <https://doi.org/10.1073/pnas.1309157110>
143. Jones, P. R., Moller, B. L., & Hoj, P. B. (1999). The UDP-glucose:p-hydroxymandelonitrile-O-glucosyltransferase that catalyzes the last step in synthesis of the cyanogenic glucoside dhurrin in *Sorghum bicolor*. Isolation, cloning, heterologous expression, and substrate specificity. *The Journal of Biological Chemistry*, *274*(50), 35483–35491.
144. Jørgensen, K., Morant, A. V., Morant, M., Jensen, N. B., Olsen, C. E., Kannangara, R., ... Bak, S. (2011). Biosynthesis of the Cyanogenic Glucosides Linamarin and Lotaustralin in Cassava: Isolation, Biochemical Characterization, and Expression Pattern of CYP71E7, the Oxime-Metabolizing Cytochrome P450 Enzyme. *Plant Physiology*, *155*(1), 282–292. <https://doi.org/10.1104/pp.110.164053>
145. J A D Zeevaart, & Creelman, and R. A. (1988). Metabolism and Physiology of Abscisic Acid. *Annual Review of Plant Physiology and Plant Molecular Biology*, *39*(1), 439–473. <https://doi.org/10.1146/annurev.pp.39.060188.002255>

146. Gray, W. M. (2004). Hormonal Regulation of Plant Growth and Development. *PLoS Biology*, 2(9). <https://doi.org/10.1371/journal.pbio.0020311>
147. Kumar, R., Khurana, A., & Sharma, A. K. (2014). Role of plant hormones and their interplay in development and ripening of fleshy fruits. *Journal of Experimental Botany*, 65(16), 4561–4575. <https://doi.org/10.1093/jxb/eru277>
148. Glawischnig, E. (2007). Camalexin. *Phytochemistry*, 68(4), 401–406. <https://doi.org/10.1016/j.phytochem.2006.12.005>
149. Daimon, T., & Shinoda, T. (2013). Function, diversity, and application of insect juvenile hormone epoxidases (CYP15). *Biotechnology and Applied Biochemistry*, 60(1), 82–91. <https://doi.org/10.1002/bab.1058>
150. Rewitz, K. F., O'Connor, M. B., & Gilbert, L. I. (2007). Molecular evolution of the insect Halloween family of cytochrome P450s: phylogeny, gene organization and functional conservation. *Insect Biochemistry and Molecular Biology*, 37(8), 741–753. <https://doi.org/10.1016/j.ibmb.2007.02.012>
151. Pondeville, E., David, J.-P., Guittard, E., Maria, A., Jacques, J.-C., Ranson, H., ... Dauphin-Villemant, C. (2013). Microarray and RNAi analysis of P450s in *Anopheles gambiae* male and female steroidogenic tissues: CYP307A1 is required for ecdysteroid synthesis. *PloS One*, 8(12), e79861. <https://doi.org/10.1371/journal.pone.0079861>
152. Bowers, W. S. (1971). Insect hormones and their derivatives as insecticides. *Bulletin of the World Health Organization*, 44(1-2-3), 379–389.
153. Fujita, T., & Nakagawa, Y. (2007). QSAR and mode of action studies of insecticidal ecdysone agonists. *SAR and QSAR in environmental research*, 18(1-2), 77–88. <https://doi.org/10.1080/10629360601053943>

154. Lonergan, P., Forde, N., & Spencer, T. (2016). Role of progesterone in embryo development in cattle. *Reproduction, Fertility, and Development*, 28(1–2), 66–74.
<https://doi.org/10.1071/RD15326>
155. Wiltbank, M. C., Souza, A. H., Carvalho, P. D., Cunha, A. P., Giordano, J. O., Fricke, P. M., ... Diskin, M. G. (2014). Physiological and practical effects of progesterone on reproduction in dairy cattle. *Animal: An International Journal of Animal Bioscience*, 8 Suppl 1, 70–81.
<https://doi.org/10.1017/S1751731114000585>
156. Meyer, H. H. (2001). Biochemistry and physiology of anabolic hormones used for improvement of meat production. *APMIS: acta pathologica, microbiologica, et immunologica Scandinavica*, 109(1), 1–8.
157. Schwendel, B. H., Wester, T. J., Morel, P. C. H., Tavendale, M. H., Deadman, C., Shadbolt, N. M., & Otter, D. E. (2015). Invited review: organic and conventionally produced milk—an evaluation of factors influencing milk composition. *Journal of Dairy Science*, 98(2), 721–746.
<https://doi.org/10.3168/jds.2014-8389>
158. Fontaine, M. (1976). Hormones and the Control of Reproduction in Aquaculture. *Journal of the Fisheries Research Board of Canada*, 33(4), 922–939. <https://doi.org/10.1139/f76-120>
159. Mylonas, C. C., Fostier, A., & Zanuy, S. (2010). Broodstock management and hormonal manipulations of fish reproduction. *General and Comparative Endocrinology*, 165(3), 516–534. <https://doi.org/10.1016/j.ygcen.2009.03.007>
160. Diaz-Chavez, M. L., Moniodis, J., Madilao, L. L., Jancsik, S., Keeling, C. I., Barbour, E. L., ... Bohlmann, J. (2013). Biosynthesis of Sandalwood Oil: Santalum album CYP76F Cytochromes P450 Produce Santalols and Bergamotol. *PLOS ONE*, 8(9), e75053.
<https://doi.org/10.1371/journal.pone.0075053>

161. Cankar, K., van Houwelingen, A., Bosch, D., Sonke, T., Bouwmeester, H., & Beekwilder, J. (2011). A chicory cytochrome P450 mono-oxygenase CYP71AV8 for the oxidation of (+)-valencene. *FEBS letters*, *585*(1), 178–182. <https://doi.org/10.1016/j.febslet.2010.11.040>
162. Furusawa, M., Hashimoto, T., Noma, Y., & Asakawa, Y. (2005). Highly efficient production of nootkatone, the grapefruit aroma from valencene, by biotransformation. *Chemical & Pharmaceutical Bulletin*, *53*(11), 1513–1514.
163. Substance that gives grapefruit its flavor and aroma could give insect pests the boot. (n.d.). *American Chemical Society*. Retrieved April 16, 2018, from <https://www.acs.org/content/acs/en/pressroom/newsreleases/2013/september/substance-that-gives-grapefruit-its-flavor-and-aroma-could-give-insect-pests-the-boot.html>
164. Shaw, P. E., & Wilson, C. W. (1981). Importance of nootkatone to the aroma of grapefruit oil and the flavor of grapefruit juice. *Journal of Agricultural and Food Chemistry*, *29*(3), 677–679. <https://doi.org/10.1021/jf00105a063>
165. Banerjee, A., & Giri, R. (2016). Chapter 9 - Nutraceuticals in Gastrointestinal Disorders. In R. C. Gupta (Ed.), *Nutraceuticals* (pp. 109–122). Boston: Academic Press. <https://doi.org/10.1016/B978-0-12-802147-7.00009-7>
166. Seki, H., Sawai, S., Ohyama, K., Mizutani, M., Ohnishi, T., Sudo, H., ... Muranaka, T. (2011). Triterpene Functional Genomics in Licorice for Identification of CYP72A154 Involved in the Biosynthesis of Glycyrrhizin. *The Plant Cell*, *23*(11), 4112–4123. <https://doi.org/10.1105/tpc.110.082685>
167. Godula, K., & Sames, D. (2006). C-H Bond Functionalization in Complex Organic Synthesis. *Science*, *312*(5770), 67–72. <https://doi.org/10.1126/science.1114731>

168. Chen, M. S., & White, M. C. (2007). A predictably selective aliphatic C-H oxidation reaction for complex molecule synthesis. *Science (New York, N.Y.)*, *318*(5851), 783–787.
<https://doi.org/10.1126/science.1148597>
169. Newhouse, T., & Baran, P. S. (2011). If C-H bonds could talk: selective C-H bond oxidation. *Angewandte Chemie (International Ed. in English)*, *50*(15), 3362–3374.
<https://doi.org/10.1002/anie.201006368>
170. Fasan, R. (2012). Tuning P450 Enzymes as Oxidation Catalysts. *ACS Catalysis*, *2*(4), 647–666.
<https://doi.org/10.1021/cs300001x>
171. Crabtree, R. H. (2001). Alkane C–H activation and functionalization with homogeneous transition metal catalysts: a century of progress—a new millennium in prospect. *Journal of the Chemical Society, Dalton Transactions*, *0*(17), 2437–2450.
<https://doi.org/10.1039/B103147N>
172. Welton, T. (2015). Solvents and sustainable chemistry. *Proceedings. Mathematical, Physical, and Engineering Sciences / The Royal Society*, *471*(2183).
<https://doi.org/10.1098/rspa.2015.0502>
173. Ilie, A., Harms, K., & Reetz, M. T. (2018). P450-Catalyzed Regio- and Stereoselective Oxidative Hydroxylation of 6-Iodotetralone: Preparative-Scale Synthesis of a Key Intermediate for Pd-Catalyzed Transformations. *The Journal of Organic Chemistry*.
<https://doi.org/10.1021/acs.joc.7b02878>
174. Roiban, G.-D., Agudo, R., Ilie, A., Lonsdale, R., & T. Reetz, M. (2014). CH-activating oxidative hydroxylation of 1-tetralones and related compounds with high regio- and stereoselectivity. *Chemical Communications*, *50*(92), 14310–14313. <https://doi.org/10.1039/C4CC04925J>

175. Liu, Q., Zhao, P., Li, X.-C., Jacob, M. R., Yang, C.-R., & Zhang, Y.-J. (2010). New α -Tetralone Galloylglucosides from the Fresh Pericarps of *Juglans sigillata*. *Helvetica Chimica Acta*, *93*(2). <https://doi.org/10.1002/hlca.200900177>
176. Liu, L., Li, W., Koike, K., Zhang, S., & Nikaido, T. (2004). New alpha-tetralonyl glucosides from the fruit of *Juglans mandshurica*. *Chemical & Pharmaceutical Bulletin*, *52*(5), 566–569.
177. Ito, H., Okuda, T., Fukuda, T., Hatano, T., & Yoshida, T. (2007). Two novel dicarboxylic Acid derivatives and a new dimeric hydrolyzable tannin from walnuts. *Journal of Agricultural and Food Chemistry*, *55*(3), 672–679. <https://doi.org/10.1021/jf062872b>
178. Turek, M., Szczęśna, D., Koprowski, M., & Bałczewski, P. (2017). Synthesis of 1-indanones with a broad range of biological activity. *Beilstein Journal of Organic Chemistry*, *13*, 451–494. <https://doi.org/10.3762/bjoc.13.48>
179. Yu, H., Kim, I. J., Folk, J. E., Tian, X., Rothman, R. B., Baumann, M. H., ... Rice, K. C. (2004). Synthesis and pharmacological evaluation of 3-(3,4-dichlorophenyl)-1-indanamine derivatives as nonselective ligands for biogenic amine transporters. *Journal of Medicinal Chemistry*, *47*(10), 2624–2634. <https://doi.org/10.1021/jm0305873>
180. Nagle, D. G., Zhou, Y. D., Park, P. U., Paul, V. J., Rajbhandari, I., Duncan, C. J., & Pasco, D. S. (2000). A new indanone from the marine cyanobacterium *Lyngbya majuscula* that inhibits hypoxia-induced activation of the VEGF promoter in Hep3B cells. *Journal of Natural Products*, *63*(10), 1431–1433.
181. Cossy, J., Belotti, D., & Maguer, A. (2003). Synthesis of Indatraline Using a Suzuki Cross-Coupling Reaction and a Chemoselective Hydrogenation: A Versatile Approach. *Synlett*, *2003*(10), 1515–1517. <https://doi.org/10.1055/s-2003-40868>

182. Ahmed, N. (2016). Chapter 8 - Synthetic Advances in the Indane Natural Product Scaffolds as Drug Candidates: A Review. In Atta-ur-Rahman (Ed.), *Studies in Natural Products Chemistry* (Vol. 51, pp. 383–434). Elsevier. <https://doi.org/10.1016/B978-0-444-63932-5.00008-5>
183. Chanda, T., & Singh, M. S. (2016). Developments toward the synthesis and application of 3-hydroxyindanones. *Organic & Biomolecular Chemistry*, *14*(38), 8895–8910. <https://doi.org/10.1039/c6ob01648k>
184. Dennig Alexander, Weingartner Alexandra Maria, Kardashliev Tsvetan, Müller Christina Andrea, Tassano Erika, Schürmann Martin, ... Schwaneberg Ulrich. (2017). An Enzymatic Route to α -Tocopherol Synthons: Aromatic Hydroxylation of Pseudocumene and Mesitylene with P450 BM3. *Chemistry – A European Journal*, *23*(71), 17981–17991. <https://doi.org/10.1002/chem.201703647>
185. Kato, M., Nguyen, D., Gonzalez, M., Cortez, A., Mullen, S. E., & Cheruzel, L. E. (2014). Regio- and stereoselective hydroxylation of 10-undecenoic acid with a light-driven P450 BM3 biocatalyst yielding a valuable synthon for natural product synthesis. *Bioorganic & Medicinal Chemistry*, *22*(20), 5687–5691. <https://doi.org/10.1016/j.bmc.2014.05.046>
186. Yamane, H., Konno, K., Sabelis, M., Takabayashi, J., Sassa, T., & Oikawa, H. (2010). 4.08 - Chemical Defence and Toxins of Plants. In H.-W. (Ben) Liu & L. Mander (Eds.), *Comprehensive Natural Products II* (pp. 339–385). Oxford: Elsevier. <https://doi.org/10.1016/B978-008045382-8.00099-X>
187. Kato, T., Yamaguchi, Y., Abe, N., Uyehara, T., Namai, T., Kodama, M., & Shiobara, Y. (1985). Structure and synthesis of unsaturated trihydroxy c18 fatty: Acids in rice plants suffering from rice blast disease. *Tetrahedron Letters*, *26*(19), 2357–2360. [https://doi.org/10.1016/S0040-4039\(00\)95098-6](https://doi.org/10.1016/S0040-4039(00)95098-6)

188. Kato, T., Yamaguchi, Y., Hirukawa, T., & Hoshino, N. (1991). Structural Elucidation of Naturally Occurring 9, 12, 13-Trihydroxy Fatty Acids by a Synthetic Study¹). *Agricultural and Biological Chemistry*, 55(5), 1349–1357. <https://doi.org/10.1271/bbb1961.55.1349>
189. Nagai, T., Kiyohara, H., Munakata, K., Shirahata, T., Sunazuka, T., Harigaya, Y., & Yamada, H. (2002). Pinellic acid from the tuber of *Pinellia ternata* Breitenbach as an effective oral adjuvant for nasal influenza vaccine. *International Immunopharmacology*, 2(8), 1183–1193.
190. Sunazuka, T., Shirahata, T., Yoshida, K., Yamamoto, D., Harigaya, Y., Nagai, T., ... Ōmura, S. (2002). Total synthesis of pinellic acid, a potent oral adjuvant for nasal influenza vaccine. Determination of the relative and absolute configuration. *Tetrahedron Letters*, 43(7), 1265–1268. [https://doi.org/10.1016/S0040-4039\(01\)02348-6](https://doi.org/10.1016/S0040-4039(01)02348-6)
191. Nagai, T., Shimizu, Y., Shirahata, T., Sunazuka, T., Kiyohara, H., Omura, S., & Yamada, H. (2010). Oral adjuvant activity for nasal influenza vaccines caused by combination of two trihydroxy fatty acid stereoisomers from the tuber of *Pinellia ternata*. *International Immunopharmacology*, 10(6), 655–661. <https://doi.org/10.1016/j.intimp.2010.03.004>
192. Papendorf, O., König, G. M., Wright, A. D., Chorus, I., & Oberemm, A. (1997). Mueggelone, a novel inhibitor of fish development from the fresh water cyanobacterium *Aphanizomenon flos-aquae*. *Journal of Natural Products*, 60(12), 1298–1300. <https://doi.org/10.1021/np970231s>
193. Mueller, M. J. (2004). Archetype signals in plants: the phytoprostanes. *Current Opinion in Plant Biology*, 7(4), 441–448. <https://doi.org/10.1016/j.pbi.2004.04.001>
194. Durand, T., Bultel-Poncé, V., Guy, A., Berger, S., Mueller, M. J., & Galano, J.-M. (2009). New bioactive oxylipins formed by non-enzymatic free-radical-catalyzed pathways: the phytoprostanes. *Lipids*, 44(10), 875–888. <https://doi.org/10.1007/s11745-009-3351-1>

195. Yokoyama, M., Yamaguchi, S., Inomata, S., Komatsu, K., Yoshida, S., Iida, T., ... Takimoto, A. (2000). Stress-induced factor involved in flower formation of *Lemna* is an alpha-ketol derivative of linolenic acid. *Plant & Cell Physiology*, *41*(1), 110–113.
196. Suzuki, M., Yamaguchi, S., Iida, T., Hashimoto, I., Teranishi, H., Mizoguchi, M., ... Yokoyama, M. (2003). Endogenous alpha-ketol linolenic acid levels in short day-induced cotyledons are closely related to flower induction in *Pharbitis nil*. *Plant & Cell Physiology*, *44*(1), 35–43.
197. Choi, J.-M., Han, S.-S., & Kim, H.-S. (2015). Industrial applications of enzyme biocatalysis: Current status and future aspects. *Biotechnology Advances*, *33*(7), 1443–1454.
<https://doi.org/10.1016/j.biotechadv.2015.02.014>
198. Wong, T. S., Arnold, F. H., & Schwaneberg, U. (2004). Laboratory evolution of cytochrome p450 BM-3 monooxygenase for organic cosolvents. *Biotechnology and Bioengineering*, *85*(3), 351–358. <https://doi.org/10.1002/bit.10896>
199. Munro, A. W., Lindsay, J. G., Coggins, J. R., Kelly, S. M., & Price, N. C. (1996). Analysis of the structural stability of the multidomain enzyme flavocytochrome P-450 BM3. *Biochimica Et Biophysica Acta*, *1296*(2), 127–137.
200. Salazar, O., Cirino, P. C., & Arnold, F. H. (2003). Thermostabilization of a cytochrome p450 peroxygenase. *Chembiochem: A European Journal of Chemical Biology*, *4*(9), 891–893.
<https://doi.org/10.1002/cbic.200300660>
201. Cirino, P. C., & Arnold, F. H. (2003). A self-sufficient peroxide-driven hydroxylation biocatalyst. *Angewandte Chemie (International Ed. in English)*, *42*(28), 3299–3301.
<https://doi.org/10.1002/anie.200351434>
202. Cirino, P. C., & Arnold, F. H. (2002). Regioselectivity and Activity of Cytochrome P450 BM-3 and Mutant F87A in Reactions Driven by Hydrogen Peroxide. *Advanced Synthesis &*

- Catalysis*, 344(9), 932–937. [https://doi.org/10.1002/1615-4169\(200210\)344:9<932::AID-ADSC932>3.0.CO;2-M](https://doi.org/10.1002/1615-4169(200210)344:9<932::AID-ADSC932>3.0.CO;2-M)
203. Ba, L., Li, P., Zhang, H., Duan, Y., & Lin, Z. (2013). Engineering of a hybrid biotransformation system for cytochrome P450sca-2 in *Escherichia coli*. *Biotechnology Journal*, 8(7), 785–793. <https://doi.org/10.1002/biot.201200097>
204. Ba, L., Li, P., Zhang, H., Duan, Y., & Lin, Z. (2013). Semi-rational engineering of cytochrome P450sca-2 in a hybrid system for enhanced catalytic activity: insights into the important role of electron transfer. *Biotechnology and Bioengineering*, 110(11), 2815–2825. <https://doi.org/10.1002/bit.24960>
205. Kumar, S., Liu, H., & Halpert, J. R. (2006). Engineering of cytochrome P450 3A4 for enhanced peroxide-mediated substrate oxidation using directed evolution and site-directed mutagenesis. *Drug Metabolism and Disposition: The Biological Fate of Chemicals*, 34(12), 1958–1965. <https://doi.org/10.1124/dmd.106.012054>
206. Kuper, J., Tee, K. L., Wilmanns, M., Roccatano, D., Schwaneberg, U., & Wong, T. S. (2012). The role of active-site Phe87 in modulating the organic co-solvent tolerance of cytochrome P450 BM3 monooxygenase. *Acta Crystallographica. Section F, Structural Biology and Crystallization Communications*, 68(Pt 9), 1013–1017. <https://doi.org/10.1107/S1744309112031570>
207. Vidal-Limón, A., Águila, S., Ayala, M., Batista, C. V., & Vazquez-Duhalt, R. (2013). Peroxidase activity stabilization of cytochrome P450(BM3) by rational analysis of intramolecular electron transfer. *Journal of Inorganic Biochemistry*, 122, 18–26. <https://doi.org/10.1016/j.jinorgbio.2013.01.009>

208. Valderrama, B., García-Arellano, H., Giansanti, S., Baratto, M. C., Pogni, R., & Vazquez-Duhalt, R. (2006). Oxidative stabilization of iso-1-cytochrome c by redox-inspired protein engineering. *The FASEB Journal*, *20*(8), 1233–1235. <https://doi.org/10.1096/fj.05-4173fje>
209. Guallar, V., & Olsen, B. (2006). The role of the heme propionates in heme biochemistry. *Journal of Inorganic Biochemistry*, *100*(4), 755–760. <https://doi.org/10.1016/j.jinorgbio.2006.01.019>
210. Guallar, V. (2008). Heme Electron Transfer in Peroxidases: The Propionate e-Pathway. *The Journal of Physical Chemistry B*, *112*(42), 13460–13464. <https://doi.org/10.1021/jp806435d>
211. Guallar, V., & Wallrapp, F. (2008). Mapping protein electron transfer pathways with QM/MM methods. *Journal of The Royal Society Interface*, *5*(Suppl 3), 233–239. <https://doi.org/10.1098/rsif.2008.0061.focus>
212. Kang, J.-Y., Kim, S.-Y., Kim, D., Kim, D.-H., Shin, S.-M., Park, S.-H., ... Yun, C.-H. (2011). Characterization of diverse natural variants of CYP102A1 found within a species of *Bacillus megaterium*. *AMB Express*, *1*, 1. <https://doi.org/10.1186/2191-0855-1-1>
213. Lim, J. B., & Sikes, H. D. (2015). Use of a genetically encoded hydrogen peroxide sensor for whole cell screening of enzyme activity. *Protein engineering, design & selection: PEDS*, *28*(3), 79–83. <https://doi.org/10.1093/protein/gzv003>
214. Talakad, J. C., Wilderman, P. R., Davydov, D. R., Kumar, S., & Halpert, J. R. (2010). Rational engineering of cytochromes P450 2B6 and 2B11 for enhanced stability: Insights into structural importance of residue 334. *Archives of Biochemistry and Biophysics*, *494*(2), 151–158. <https://doi.org/10.1016/j.abb.2009.11.026>
215. Saab-Rincón, G., Alwaseem, H., Guzmán-Luna, V., Olvera, L., & Fasan, R. (2018). Stabilization of the Reductase Domain in the Catalytically Self-Sufficient Cytochrome P450BM3 by

- Consensus-Guided Mutagenesis. *Chembiochem: A European Journal of Chemical Biology*, 19(6), 622–632. <https://doi.org/10.1002/cbic.201700546>
216. Chen, M. M. Y., Snow, C. D., Vizcarra, C. L., Mayo, S. L., & Arnold, F. H. (2012). Comparison of random mutagenesis and semi-rational designed libraries for improved cytochrome P450 BM3-catalyzed hydroxylation of small alkanes. *Protein Engineering, Design and Selection*, 25(4), 171–178. <https://doi.org/10.1093/protein/gzs004>
217. Peters, M. W., Meinhold, P., Glieder, A., & Arnold, F. H. (2003). Regio- and enantioselective alkane hydroxylation with engineered cytochromes P450 BM-3. *Journal of the American Chemical Society*, 125(44), 13442–13450. <https://doi.org/10.1021/ja0303790>
218. Glieder, A., Farinas, E. T., & Arnold, F. H. (2002). Laboratory evolution of a soluble, self-sufficient, highly active alkane hydroxylase. *Nature Biotechnology*, 20(11), 1135–1139. <https://doi.org/10.1038/nbt744>
219. Meinhold, P., Peters, M. W., Chen, M. M. Y., Takahashi, K., & Arnold, F. H. (2005). Direct conversion of ethane to ethanol by engineered cytochrome P450 BM3. *Chembiochem: A European Journal of Chemical Biology*, 6(10), 1765–1768. <https://doi.org/10.1002/cbic.200500261>
220. Fasan, R., Chen, M. M., Crook, N. C., & Arnold, F. H. (2007). Engineered alkane-hydroxylating cytochrome P450(BM3) exhibiting natively catalytic properties. *Angewandte Chemie (International Ed. in English)*, 46(44), 8414–8418. <https://doi.org/10.1002/anie.200702616>
221. Fasan, R., Meharena, Y. T., Snow, C. D., Poulos, T. L., & Arnold, F. H. (2008). Evolutionary history of a specialized p450 propane monooxygenase. *Journal of Molecular Biology*, 383(5), 1069–1080. <https://doi.org/10.1016/j.jmb.2008.06.060>

222. Lewis, J. C., & Arnold, F. H. (2009, June). Catalysts on Demand: Selective Oxidations by Laboratory-Evolved Cytochrome P450 BM3. Text.
<https://doi.org/info:doi/10.2533/chimia.2009.309>
223. Anzenbacher, P., & Hudecek, J. (2001). Differences in flexibility of active sites of cytochromes P450 probed by resonance Raman and UV-Vis absorption spectroscopy. *Journal of Inorganic Biochemistry*, 87(4), 209–213.
224. Karshikoff, A., Nilsson, L., & Ladenstein, R. (2015). Rigidity versus flexibility: the dilemma of understanding protein thermal stability. *The FEBS journal*, 282(20), 3899–3917.
<https://doi.org/10.1111/febs.13343>
225. Zou, C. L. (2001). [Conformational flexibility of enzyme active sites]. *Sheng Li Ke Xue Jin Zhan [Progress in Physiology]*, 32(1), 7–12.
226. Carmichael, A. B., & Wong, L. L. (2001). Protein engineering of *Bacillus megaterium* CYP102. The oxidation of polycyclic aromatic hydrocarbons. *European Journal of Biochemistry*, 268(10), 3117–3125.
227. Whitehouse, C. J. C., Rees, N. H., Bell, S. G., & Wong, L.-L. (2011). Dearomatisation of o-xylene by P450BM3 (CYP102A1). *Chemistry (Weinheim an Der Bergstrasse, Germany)*, 17(24), 6862–6868. <https://doi.org/10.1002/chem.201002465>
228. Lee, S. H., Kwon, Y.-C., Kim, D.-M., & Park, C. B. (2013). Cytochrome P450-catalyzed O-dealkylation coupled with photochemical NADPH regeneration. *Biotechnology and Bioengineering*, 110(2), 383–390. <https://doi.org/10.1002/bit.24729>
229. Kille, S., Zilly, F. E., Acevedo, J. P., & Reetz, M. T. (2011). Regio- and stereoselectivity of P450-catalysed hydroxylation of steroids controlled by laboratory evolution. *Nature Chemistry*, 3(9), 738–743. <https://doi.org/10.1038/nchem.1113>

230. Weber, E., Seifert, A., Antonovici, M., Geinitz, C., Pleiss, J., & Urlacher, V. B. (2011). Screening of a minimal enriched P450 BM3 mutant library for hydroxylation of cyclic and acyclic alkanes. *Chemical Communications (Cambridge, England)*, 47(3), 944–946. <https://doi.org/10.1039/c0cc02924f>
231. Dezvarei, S., Lee, J. H. Z., & Bell, S. G. (2018). Stereoselective hydroxylation of isophorone by variants of the cytochromes P450 CYP102A1 and CYP101A1. *Enzyme and Microbial Technology*, 111, 29–37. <https://doi.org/10.1016/j.enzmictec.2018.01.002>
232. Kawakami, N., Shoji, O., & Watanabe, Y. (2011). Use of perfluorocarboxylic acids to trick cytochrome P450BM3 into initiating the hydroxylation of gaseous alkanes. *Angewandte Chemie (International Ed. in English)*, 50(23), 5315–5318. <https://doi.org/10.1002/anie.201007975>
233. Kawakami, N., Shoji, O., & Watanabe, Y. (2013). Direct hydroxylation of primary carbons in small alkanes by wild-type cytochrome P450BM3 containing perfluorocarboxylic acids as decoy molecules. *Chemical Science*, 4(6), 2344–2348. <https://doi.org/10.1039/C3SC50378J>
234. Shoji, O., Kunimatsu, T., Kawakami, N., & Watanabe, Y. (2013). Highly selective hydroxylation of benzene to phenol by wild-type cytochrome P450BM3 assisted by decoy molecules. *Angewandte Chemie (International Ed. in English)*, 52(26), 6606–6610. <https://doi.org/10.1002/anie.201300282>
235. Shoji, O., & Watanabe, Y. (2015). Monooxygenation of small hydrocarbons catalyzed by bacterial cytochrome p450s. *Advances in Experimental Medicine and Biology*, 851, 189–208. https://doi.org/10.1007/978-3-319-16009-2_7
236. Cong, Z., Shoji, O., Kasai, C., Kawakami, N., Sugimoto, H., Shiro, Y., & Watanabe, Y. (2015). Activation of Wild-Type Cytochrome P450BM3 by the Next Generation of Decoy Molecules:

- Enhanced Hydroxylation of Gaseous Alkanes and Crystallographic Evidence. *ACS Catalysis*, 5(1), 150–156. <https://doi.org/10.1021/cs501592f>
237. Munday, S. D., Shoji, O., Watanabe, Y., Wong, L.-L., & Bell, S. G. (2016). Improved oxidation of aromatic and aliphatic hydrocarbons using rate enhancing variants of P450Bm3 in combination with decoy molecules. *Chemical Communications*, 52(5), 1036–1039. <https://doi.org/10.1039/C5CC09247G>
238. Shoji, O., Yanagisawa, S., Stanfield, J. K., Suzuki, K., Cong, Z., Sugimoto, H., ... Watanabe, Y. (2017). Direct Hydroxylation of Benzene to Phenol by Cytochrome P450BM3 Triggered by Amino Acid Derivatives. *Angewandte Chemie (International Ed. in English)*, 56(35), 10324–10329. <https://doi.org/10.1002/anie.201703461>
239. Karasawa, M., Stanfield, J. K., Yanagisawa, S., Shoji, O., & Watanabe, Y. (2018). Whole-Cell Biotransformation of Benzene to Phenol Catalysed by Intracellular Cytochrome P450BM3 Activated by External Additives. *Angewandte Chemie (International Ed. in English)*. <https://doi.org/10.1002/anie.201804924>
240. Shoji, O., Fujishiro, T., Nakajima, H., Kim, M., Nagano, S., Shiro, Y., & Watanabe, Y. (2007). Hydrogen Peroxide Dependent Monooxygenations by Tricking the Substrate Recognition of Cytochrome P450BS β . *Angewandte Chemie International Edition*, 46(20), 3656–3659. <https://doi.org/10.1002/anie.200700068>
241. Shoji, O., Fujishiro, T., Nagano, S., Tanaka, S., Hirose, T., Shiro, Y., & Watanabe, Y. (2010). Understanding substrate misrecognition of hydrogen peroxide dependent cytochrome P450 from *Bacillus subtilis*. *Journal of biological inorganic chemistry: JBIC: a publication of the Society of Biological Inorganic Chemistry*, 15(8), 1331–1339. <https://doi.org/10.1007/s00775-010-0692-4>

242. Shoji, O., Wiese, C., Fujishiro, T., Shirataki, C., Wünsch, B., & Watanabe, Y. (2010). Aromatic C–H bond hydroxylation by P450 peroxygenases: a facile colorimetric assay for monooxygenation activities of enzymes based on Russig's blue formation. *JBIC Journal of Biological Inorganic Chemistry*, *15*(7), 1109–1115. <https://doi.org/10.1007/s00775-010-0671-9>
243. Shoji, O., & Watanabe, Y. (2011). Design of H₂O₂-dependent oxidation catalyzed by hemoproteins. *Metallomics: Integrated Biometal Science*, *3*(4), 379–388. <https://doi.org/10.1039/c0mt00090f>
244. Fujishiro, T., Shoji, O., Kawakami, N., Watanabe, T., Sugimoto, H., Shiro, Y., & Watanabe, Y. (2012). Chiral-substrate-assisted stereoselective epoxidation catalyzed by H₂O₂-dependent cytochrome P450SP α . *Chemistry, an Asian Journal*, *7*(10), 2286–2293. <https://doi.org/10.1002/asia.201200250>
245. Onoda, H., Shoji, O., & Watanabe, Y. (2015). Acetate anion-triggered peroxygenation of non-native substrates by wild-type cytochrome P450s. *Dalton Transactions*, *44*(34), 15316–15323. <https://doi.org/10.1039/C5DT00797F>
246. Haines, D. C., Tomchick, D. R., Machius, M., & Peterson, J. A. (2001). Pivotal role of water in the mechanism of P450BM-3. *Biochemistry*, *40*(45), 13456–13465.
247. Eiben, S., Bartelmäs, H., & Urlacher, V. B. (2007). Construction of a thermostable cytochrome P450 chimera derived from self-sufficient mesophilic parents. *Applied Microbiology and Biotechnology*, *75*(5), 1055–1061. <https://doi.org/10.1007/s00253-007-0922-z>
248. Otey, C. R., Landwehr, M., Endelman, J. B., Hiraga, K., Bloom, J. D., & Arnold, F. H. (2006). Structure-guided recombination creates an artificial family of cytochromes P450. *PLoS biology*, *4*(5), e112. <https://doi.org/10.1371/journal.pbio.0040112>

249. Li, Y., Drummond, D. A., Sawayama, A. M., Snow, C. D., Bloom, J. D., & Arnold, F. H. (2007). A diverse family of thermostable cytochrome P450s created by recombination of stabilizing fragments. *Nature Biotechnology*, *25*(9), 1051–1056. <https://doi.org/10.1038/nbt1333>
250. Bloom, J. D., Labthavikul, S. T., Otey, C. R., & Arnold, F. H. (2006). Protein stability promotes evolvability. *Proceedings of the National Academy of Sciences of the United States of America*, *103*(15), 5869–5874. <https://doi.org/10.1073/pnas.0510098103>
251. Arnold, F. H. (2009). How proteins adapt: lessons from directed evolution. *Cold Spring Harbor Symposia on Quantitative Biology*, *74*, 41–46. <https://doi.org/10.1101/sqb.2009.74.046>
252. Buske, F. A., Their, R., Gillam, E. M. J., & Bodén, M. (2009). In silico characterization of protein chimeras: relating sequence and function within the same fold. *Proteins*, *77*(1), 111–120. <https://doi.org/10.1002/prot.22422>
253. Dietrich, M., Eiben, S., Asta, C., Do, T. A., Pleiss, J., & Urlacher, V. B. (2008). Cloning, expression and characterisation of CYP102A7, a self-sufficient P450 monooxygenase from *Bacillus licheniformis*. *Applied Microbiology and Biotechnology*, *79*(6), 931–940. <https://doi.org/10.1007/s00253-008-1500-8>
254. Fuziwara, S., Sagami, I., Rozhkova, E., Craig, D., Noble, M. A., Munro, A. W., ... Shimizu, T. (2002). Catalytically functional flavocytochrome chimeras of P450 BM3 and nitric oxide synthase. *Journal of Inorganic Biochemistry*, *91*(4), 515–526.
255. Jung, E., Park, B. G., Ahsan, M. M., Kim, J., Yun, H., Choi, K.-Y., & Kim, B.-G. (2016). Production of ω -hydroxy palmitic acid using CYP153A35 and comparison of cytochrome P450 electron transfer system in vivo. *Applied Microbiology and Biotechnology*, *100*(24), 10375–10384. <https://doi.org/10.1007/s00253-016-7675-5>

256. Scheps, D., Honda Malca, S., Richter, S. M., Marisch, K., Nestl, B. M., & Hauer, B. (2013). Synthesis of ω -hydroxy dodecanoic acid based on an engineered CYP153A fusion construct. *Microbial Biotechnology*, 6(6), 694–707. <https://doi.org/10.1111/1751-7915.12073>
257. Zhang, Y.-H. P. (2015). Production of biofuels and biochemicals by in vitro synthetic biosystems: Opportunities and challenges. *Biotechnology Advances*, 33(7), 1467–1483. <https://doi.org/10.1016/j.biotechadv.2014.10.009>
258. Rabe, K. S., Kiko, K., & Niemeyer, C. M. (2008). Characterization of the peroxidase activity of CYP119, a thermostable P450 from *Sulfolobus acidocaldarius*. *Chembiochem: A European Journal of Chemical Biology*, 9(3), 420–425. <https://doi.org/10.1002/cbic.200700450>
259. Lim, Y.-R., Eun, C.-Y., Park, H.-G., Han, S., Han, J.-S., Cho, K. S., ... Kim, D. (2010). Regioselective oxidation of lauric acid by CYP119, an orphan cytochrome P450 from *Sulfolobus acidocaldarius*. *Journal of Microbiology and Biotechnology*, 20(3), 574–578.
260. Koo, L. S., Tschirret-Guth, R. A., Straub, W. E., Moënne-Loccoz, P., Loehr, T. M., & Ortiz de Montellano, P. R. (2000). The active site of the thermophilic CYP119 from *Sulfolobus solfataricus*. *The Journal of Biological Chemistry*, 275(19), 14112–14123.
261. Suzuki, R., Hirakawa, H., & Nagamune, T. (2014). Electron donation to an archaeal cytochrome P450 is enhanced by PCNA-mediated selective complex formation with foreign redox proteins. *Biotechnology Journal*, 9(12), 1573–1581. <https://doi.org/10.1002/biot.201400007>
262. Sideso, O., Smith, K. E., Welch, S. G., & Williams, R. A. (1997). Thermostable cytochrome P450 steroid hydroxylase from a thermophilic bacillus strain. *Biochemical Society Transactions*, 25(1), 17S.

263. Eiben, S., Kaysser, L., Maurer, S., Kühnel, K., Urlacher, V. B., & Schmid, R. D. (2006). Preparative use of isolated CYP102 monooxygenases -- a critical appraisal. *Journal of Biotechnology*, 124(4), 662–669. <https://doi.org/10.1016/j.jbiotec.2006.02.013>
264. Mandai, T., Fujiwara, S., & Imaoka, S. (2009). Construction and engineering of a thermostable self-sufficient cytochrome P450. *Biochemical and Biophysical Research Communications*, 384(1), 61–65. <https://doi.org/10.1016/j.bbrc.2009.04.064>
265. Oku, Y., Ohtaki, A., Kamitori, S., Nakamura, N., Yohda, M., Ohno, H., & Kawarabayasi, Y. (2004). Structure and direct electrochemistry of cytochrome P450 from the thermoacidophilic crenarchaeon, *Sulfolobus tokodaii* strain 7. *Journal of Inorganic Biochemistry*, 98(7), 1194–1199. <https://doi.org/10.1016/j.jinorgbio.2004.05.002>
266. Ho, W. W., Li, H., Nishida, C. R., de Montellano, P. R. O., & Poulos, T. L. (2008). Crystal structure and properties of CYP231A2 from the thermoacidophilic archaeon *Picrophilus torridus*. *Biochemistry*, 47(7), 2071–2079. <https://doi.org/10.1021/bi702240k>
267. Schallmeyer, A., den Besten, G., Teune, I. G. P., Kembaren, R. F., & Janssen, D. B. (2011). Characterization of cytochrome P450 monooxygenase CYP154H1 from the thermophilic soil bacterium *Thermobifida fusca*. *Applied Microbiology and Biotechnology*, 89(5), 1475–1485. <https://doi.org/10.1007/s00253-010-2965-9>
268. Sideso, O., Williams, R. A., Welch, S. G., & Smith, K. E. (1998). Progesterone 6-hydroxylation is catalysed by cytochrome P-450 in the moderate thermophile *Bacillus thermoglucosidasius* strain 12060. *The Journal of Steroid Biochemistry and Molecular Biology*, 67(2), 163–169.
269. Govindaraj, S., & Poulos, T. L. (1996). Probing the structure of the linker connecting the reductase and heme domains of cytochrome P450BM-3 using site-directed mutagenesis. *Protein Science : A Publication of the Protein Society*, 5(7), 1389–1393.

270. Sharp, R. E., White, P., Chapman, S. K., & Reid, G. A. (1994). Role of the Interdomain Hinge of Flavocytochrome b2 in Intra- and Inter-Protein Electron Transfer. *Biochemistry*, *33*(17), 5115–5120. <https://doi.org/10.1021/bi00183a015>
271. Sibbesen, O., De Voss, J. J., & Montellano, P. R. (1996). Putidaredoxin reductase-putidaredoxin-cytochrome p450cam triple fusion protein. Construction of a self-sufficient *Escherichia coli* catalytic system. *The Journal of Biological Chemistry*, *271*(37), 22462–22469.
272. Kumar, S. (2010). Engineering cytochrome P450 biocatalysts for biotechnology, medicine and bioremediation. *Expert Opinion on Drug Metabolism & Toxicology*, *6*(2), 115–131. <https://doi.org/10.1517/17425250903431040>
273. Helvig, C., & Capdevila, J. H. (2000). Biochemical characterization of rat P450 2C11 fused to rat or bacterial NADPH-P450 reductase domains. *Biochemistry*, *39*(17), 5196–5205.
274. Gilardi, G., Meharena, Y. T., Tsotsou, G. E., Sadeghi, S. J., Fairhead, M., & Giannini, S. (2002). Molecular Lego: design of molecular assemblies of P450 enzymes for nanobiotechnology. *Biosensors and Bioelectronics*, *17*(1–2), 133–145. [https://doi.org/10.1016/S0956-5663\(01\)00286-X](https://doi.org/10.1016/S0956-5663(01)00286-X)
275. Porter, T. D. (1994). Mutagenesis at a highly conserved phenylalanine in cytochrome P450 2E1 affects heme incorporation and catalytic activity. *Biochemistry*, *33*(19), 5942–5946.
276. Larson, J. R., Coon, M. J., & Porter, T. D. (1991). Alcohol-inducible cytochrome P-450IIE1 lacking the hydrophobic NH2-terminal segment retains catalytic activity and is membrane-bound when expressed in *Escherichia coli*. *The Journal of Biological Chemistry*, *266*(12), 7321–7324.
277. Dong, J., & Porter, T. D. (1996). Coexpression of mammalian cytochrome P450 and reductase in *Escherichia coli*. *Archives of Biochemistry and Biophysics*, *327*(2), 254–259. <https://doi.org/10.1006/abbi.1996.0118>

278. Zerilli, A., Ratanasavanh, D., Lucas, D., Goasduff, T., Dréano, Y., Menard, C., ... Berthou, F. (1997). Both cytochromes P450 2E1 and 3A are involved in the O-hydroxylation of p-nitrophenol, a catalytic activity known to be specific for P450 2E1. *Chemical Research in Toxicology*, *10*(10), 1205–1212. <https://doi.org/10.1021/tx970048z>
279. Fairhead, M., Giannini, S., Gillam, E. M. J., & Gilardi, G. (2005). Functional characterisation of an engineered multidomain human P450 2E1 by molecular Lego. *Journal of biological inorganic chemistry: JBIC: a publication of the Society of Biological Inorganic Chemistry*, *10*(8), 842–853. <https://doi.org/10.1007/s00775-005-0033-1>
280. Albano, E., Tomasi, A., Persson, J.-O., Terelius, Y., Gorla-Gatti, L., Ingelman-Sundberg, M., & Dianzani, M. U. (1991). Role of ethanol-inducible cytochrome P450 (P450IIE1) in catalysing the free radical activation of aliphatic alcohols. *Biochemical Pharmacology*, *41*(12), 1895–1902. [https://doi.org/10.1016/0006-2952\(91\)90129-S](https://doi.org/10.1016/0006-2952(91)90129-S)
281. Chen, W., Peter, R. M., McArdle, S., Thummel, K. E., Sigle, R. O., & Nelson, S. D. (1996). Baculovirus expression and purification of human and rat cytochrome P450 2E1. *Archives of Biochemistry and Biophysics*, *335*(1), 123–130. <https://doi.org/10.1006/abbi.1996.0489>
282. Wang, M. H., Patten, C. J., Yang, G. Y., Paranawithana, S. R., Tan, Y., & Yang, C. S. (1996). Expression and coupling of human cytochrome P450 2E1 and NADPH-cytochrome P450 oxidoreductase in dual expression and co-infection systems with baculovirus in insect cells. *Archives of Biochemistry and Biophysics*, *334*(2), 380–388. <https://doi.org/10.1006/abbi.1996.0468>
283. Patten, C. J., & Koch, P. (1995). Baculovirus expression of human P450 2E1 and cytochrome b5: spectral and catalytic properties and effect of b5 on the stoichiometry of P450 2E1-catalyzed reactions. *Archives of Biochemistry and Biophysics*, *317*(2), 504–513. <https://doi.org/10.1006/abbi.1995.1194>

284. Rua, F., Sadeghi, S. J., Castrignanò, S., Di Nardo, G., & Gilardi, G. (2012). Engineering Macaca fascicularis cytochrome P450 2C20 to reduce animal testing for new drugs. *Journal of Inorganic Biochemistry*, *117*, 277–284. <https://doi.org/10.1016/j.jinorgbio.2012.05.017>
285. Dodhia, V. R., Fantuzzi, A., & Gilardi, G. (2006). Engineering human cytochrome P450 enzymes into catalytically self-sufficient chimeras using molecular Lego. *Journal Of Biological Inorganic Chemistry: JBIC: A Publication Of The Society Of Biological Inorganic Chemistry*, *11*(7), 903–916.
286. Hutzler, J. M., Wienkers, L. C., Wahlstrom, J. L., Carlson, T. J., & Tracy, T. S. (2003). Activation of cytochrome P450 2C9-mediated metabolism: mechanistic evidence in support of kinetic observations. *Archives of Biochemistry and Biophysics*, *410*(1), 16–24.
287. Perret, A., & Pompon, D. (1998). Electron shuttle between membrane-bound cytochrome P450 3A4 and b5 rules uncoupling mechanisms. *Biochemistry*, *37*(33), 11412–11424. <https://doi.org/10.1021/bi980908q>
288. Degregorio, D., D'Avino, S., Castrignanò, S., Di Nardo, G., Sadeghi, S. J., Catucci, G., & Gilardi, G. (2017). Human Cytochrome P450 3A4 as a Biocatalyst: Effects of the Engineered Linker in Modulation of Coupling Efficiency in 3A4-BMR Chimeras. *Frontiers in Pharmacology*, *8*, 121. <https://doi.org/10.3389/fphar.2017.00121>
289. Castrignanò, S., D'Avino, S., Di Nardo, G., Catucci, G., Sadeghi, S. J., & Gilardi, G. (2018). Modulation of the interaction between human P450 3A4 and B. megaterium reductase via engineered loops. *Biochimica Et Biophysica Acta*, *1866*(1), 116–125. <https://doi.org/10.1016/j.bbapap.2017.07.009>
290. Bostick, C. D., Hickey, K. M., Wollenberg, L. A., Flora, D. R., Tracy, T. S., & Gannett, P. M. (2016). Immobilized Cytochrome P450 for Monitoring of P450-P450 Interactions and

- Metabolism. *Drug Metabolism and Disposition: The Biological Fate of Chemicals*, 44(5), 741–749. <https://doi.org/10.1124/dmd.115.067637>
291. Paternolli, C., Antonini, M., Ghisellini, P., & Nicolini, C. (2004). Recombinant cytochrome p450 immobilization for biosensor applications. *Langmuir: the ACS journal of surfaces and colloids*, 20(26), 11706–11712. <https://doi.org/10.1021/la048081q>
292. Hirakawa, H., Kakitani, A., & Nagamune, T. (2013). Introduction of selective intersubunit disulfide bonds into self-assembly protein scaffold to enhance an artificial multienzyme complex's activity. *Biotechnology and Bioengineering*, 110(7), 1858–1864. <https://doi.org/10.1002/bit.24861>
293. Tan, C. Y., Hirakawa, H., & Nagamune, T. (2015). Supramolecular protein assembly supports immobilization of a cytochrome P450 monooxygenase system as water-insoluble gel. *Scientific Reports*, 5, 8648. <https://doi.org/10.1038/srep08648>
294. Tan, C. Y., Hirakawa, H., Suzuki, R., Haga, T., Iwata, F., & Nagamune, T. (2016). Immobilization of a Bacterial Cytochrome P450 Monooxygenase System on a Solid Support. *Angewandte Chemie (International Ed. in English)*, 55(48), 15002–15006. <https://doi.org/10.1002/anie.201608033>
295. Bahrami, A., Vincent, T., Garnier, A., Larachi, F., Boukouvalas, J., & Iliuta, M. C. (2017). Noncovalent Immobilization of Optimized Bacterial Cytochrome P450 BM3 on Functionalized Magnetic Nanoparticles. *Industrial & Engineering Chemistry Research*, 56(39), 10981–10989. <https://doi.org/10.1021/acs.iecr.7b02872>
296. Ryan, J. D., Fish, R. H., & Clark, D. S. (2008). Engineering cytochrome P450 enzymes for improved activity towards biomimetic 1,4-NADH cofactors. *Chembiochem: A European Journal of Chemical Biology*, 9(16), 2579–2582. <https://doi.org/10.1002/cbic.200800246>

297. Bahrami, A., Garnier, A., Larachi, F., & Iliuta, M. C. (n.d.). Covalent immobilization of cytochrome P450 BM3 (R966D/W1046S) on glutaraldehyde activated SPIONs. *The Canadian Journal of Chemical Engineering*, 0(0). <https://doi.org/10.1002/cjce.23208>
298. Maurer, S. C., Schulze, H., Schmid, R. D., & Urlacher, V. (n.d.). Immobilisation of P450 BM-3 and an NADP+ Cofactor Recycling System: Towards a Technical Application of Heme-Containing Monooxygenases in Fine Chemical Synthesis. *Advanced Synthesis & Catalysis*, 345(6–7), 802–810. <https://doi.org/10.1002/adsc.200303021>
299. Weber, E., Sirim, D., Schreiber, T., Thomas, B., Pleiss, J., Hunger, M., ... Urlacher, V. B. (2010). Immobilization of P450 BM-3 monooxygenase on mesoporous molecular sieves with different pore diameters. *Journal of Molecular Catalysis B: Enzymatic*, 64(1), 29–37. <https://doi.org/10.1016/j.molcatb.2010.01.020>
300. Do, M. Q., Henry, E., Kato, M., & Cheruzel, L. (2018). Cross-linked cytochrome P450 BM3 aggregates promoted by Ru(II)-diimine complexes bearing aldehyde groups. *Journal of Inorganic Biochemistry*, 186, 130–134. <https://doi.org/10.1016/j.jinorgbio.2018.06.001>
301. Zhao, L., Güven, G., Li, Y., & Schwaneberg, U. (2011). First steps towards a Zn/Co(III)sep-driven P450 BM3 reactor. *Applied Microbiology and Biotechnology*, 91(4), 989–999. <https://doi.org/10.1007/s00253-011-3290-7>
302. Panneerselvam, S., Shehzad, A., Mueller-Dieckmann, J., Wilmanns, M., Bocola, M., Davari, M. D., & Schwaneberg, U. (2018). Crystallographic insights into a cobalt (III) sepulchrate based alternative cofactor system of P450 BM3 monooxygenase. *Biochimica Et Biophysica Acta*, 1866(1), 134–140. <https://doi.org/10.1016/j.bbapap.2017.07.010>
303. Garny, S., Beeton-Kempen, N., Gerber, I., Verschoor, J., & Jordaan, J. (2016). The co-immobilization of P450-type nitric oxide reductase and glucose dehydrogenase for the

- continuous reduction of nitric oxide via cofactor recycling. *Enzyme and Microbial Technology*, 85, 71–81. <https://doi.org/10.1016/j.enzmictec.2015.10.006>
304. Lee, J. H., Nam, D. H., Lee, S. H., Park, J. H., Park, S. J., Lee, S. H., ... Jeong, K. J. (2014). New platform for cytochrome p450 reaction combining in situ immobilization on biopolymer. *Bioconjugate Chemistry*, 25(12), 2101–2104. <https://doi.org/10.1021/bc500404j>
305. Fulco, A. J. (1991). P450BM-3 and other Inducible Bacterial P450 Cytochromes: Biochemistry and Regulation. *Annual Review of Pharmacology and Toxicology*, 31(1), 177–203. <https://doi.org/10.1146/annurev.pa.31.040191.001141>
306. Maurer, S. C., Kühnel, K., Kaysser, L. A., Eiben, S., Schmid, R. D., & Urlacher, V. B. (2005). Catalytic Hydroxylation in Biphasic Systems using CYP102A1 Mutants. *Advanced Synthesis & Catalysis*, 347(7–8), 1090–1098. <https://doi.org/10.1002/adsc.200505044>
307. Torres Pazmiño, D. E., Winkler, M., Glieder, A., & Fraaije, M. W. (2010). Monooxygenases as biocatalysts: Classification, mechanistic aspects and biotechnological applications. *Journal of Biotechnology*, 146(1–2), 9–24. <https://doi.org/10.1016/j.jbiotec.2010.01.021>
308. Spaans, S. K., Weusthuis, R. A., van der Oost, J., & Kengen, S. W. M. (2015). NADPH-generating systems in bacteria and archaea. *Frontiers in Microbiology*, 6. <https://doi.org/10.3389/fmicb.2015.00742>
309. Beyer, N., Kulig, J. K., Bartsch, A., Hayes, M. A., Janssen, D. B., & Fraaije, M. W. (2017). P450_{BM3} fused to phosphite dehydrogenase allows phosphite-driven selective oxidations. *Applied Microbiology and Biotechnology*, 101(6), 2319–2331. <https://doi.org/10.1007/s00253-016-7993-7>
310. Johannes, T. W., Woodyer, R. D., & Zhao, H. (2005). Directed evolution of a thermostable phosphite dehydrogenase for NAD(P)H regeneration. *Applied and Environmental Microbiology*, 71(10), 5728–5734. <https://doi.org/10.1128/AEM.71.10.5728-5734.2005>

311. Woodyer, R., van der Donk, W. A., & Zhao, H. (2006). Optimizing a biocatalyst for improved NAD(P)H regeneration: directed evolution of phosphite dehydrogenase. *Combinatorial Chemistry & High Throughput Screening*, 9(4), 237–245.
312. Trivedi, A., Heinemann, M., Spiess, A. C., Dausmann, T., & Büchs, J. (2005). Optimization of adsorptive immobilization of alcohol dehydrogenases. *Journal of Bioscience and Bioengineering*, 99(4), 340–347. <https://doi.org/10.1263/jbb.99.340>
313. Iyer, R., Pavlov, V., Katakis, I., & Bachas, L. G. (2003). Amperometric Sensing at High Temperature with a “Wired” Thermostable Glucose-6-phosphate Dehydrogenase from *Aquifex aeolicus*. *Analytical Chemistry*, 75(15), 3898–3901. <https://doi.org/10.1021/ac026298o>
314. Winer, A. D., & Schwert, G. W. (1958). LACTIC DEHYDROGENASE IV. THE INFLUENCE OF pH ON THE KINETICS OF THE REACTION. *Journal of Biological Chemistry*, 231(2), 1065–1083.
315. Lowry, O. H., Passonneau, J. V., & Rock, M. K. (1961). The stability of pyridine nucleotides. *The Journal of Biological Chemistry*, 236, 2756–2759.
316. Lowry, O. H., Passonneau, J. V., Schulz, D. W., & Rock, M. K. (1961). The measurement of pyridine nucleotides by enzymatic cycling. *The Journal of Biological Chemistry*, 236, 2746–2755.
317. Wu, J. T., Wu, L. H., & Knight, J. A. (1986). Stability of NADPH: effect of various factors on the kinetics of degradation. *Clinical Chemistry*, 32(2), 314–319.
318. Kulishova, L., Dimoula, K., Jordan, M., Wirtz, A., Hofmann, D., Santiago-Schübel, B., ... Spiess, A. C. (2010). Factors influencing the operational stability of NADPH-dependent alcohol dehydrogenase and an NADH-dependent variant thereof in gas/solid reactors. *Journal of Molecular Catalysis B: Enzymatic*, 67(3–4), 271–283. <https://doi.org/10.1016/j.molcatb.2010.09.005>

319. Ian, P. R., & Elizabeth, S. A. (2005). *Cytochrome P450 Protocols* (Vol. 320). New Jersey: Humana Press. <https://doi.org/10.1385/1592599982>
320. Song, N., Zhang, M.-T., Binstead, R. A., Fang, Z., & Meyer, T. J. (2014). Multiple Pathways in the Oxidation of a NADH Analogue. *Inorganic Chemistry*, *53*(8), 4100–4105. <https://doi.org/10.1021/ic500072e>
321. Paul, C. E., Gargiulo, S., Opperman, D. J., Lavandera, I., Gotor-Fernández, V., Gotor, V., ... Hollmann, F. (2013). Mimicking nature: synthetic nicotinamide cofactors for C=C bioreduction using enoate reductases. *Organic Letters*, *15*(1), 180–183. <https://doi.org/10.1021/ol303240a>
322. Paul, C. E., & Hollmann, F. (2016). A survey of synthetic nicotinamide cofactors in enzymatic processes. *Applied Microbiology and Biotechnology*, *100*(11), 4773–4778. <https://doi.org/10.1007/s00253-016-7500-1>
323. Nowak, C., Beer, B., Pick, A., Roth, T., Lommès, P., & Sieber, V. (2015). A water-forming NADH oxidase from *Lactobacillus pentosus* suitable for the regeneration of synthetic biomimetic cofactors. *Frontiers in Microbiology*, *6*, 957. <https://doi.org/10.3389/fmicb.2015.00957>
324. Knaus, T., Paul, C. E., Levy, C. W., de Vries, S., Mutti, F. G., Hollmann, F., & Scrutton, N. S. (2016). Better than Nature: Nicotinamide Biomimetics That Outperform Natural Coenzymes. *Journal of the American Chemical Society*, *138*(3), 1033–1039. <https://doi.org/10.1021/jacs.5b12252>
325. Paul, C. E., Arends, I. W. C. E., & Hollmann, F. (2014). Is Simpler Better? Synthetic Nicotinamide Cofactor Analogues for Redox Chemistry. *ACS Catalysis*, *4*(3), 788–797. <https://doi.org/10.1021/cs4011056>

326. Gómez, E., Miguel, M., Jiménez, O., Rosa, G. de la, & Lavilla, R. (2005). 1,4-Dihydropicolinic acid derivatives: Novel NADH analogues with an altered connectivity pattern. *Tetrahedron Letters*, 46(20), 3513–3516. <https://doi.org/10.1016/j.tetlet.2005.03.069>
327. Goulioukina, N., Wehbe, J., Marchand, D., Busson, R., Lescrinier, E., Heindl, D., & Herdewijn, P. (2007). Synthesis of Nicotinamide Adenine Dinucleotide (NAD) Analogues with a Sugar Modified Nicotinamide Moiety. *Helvetica Chimica Acta*, 90(7), 1266–1278. <https://doi.org/10.1002/hlca.200790127>
328. Paul, C. E., Gargiulo, S., Opperman, D. J., Lavandera, I., Gotor-Fernández, V., Gotor, V., ... Hollmann, F. (2013). Mimicking Nature: Synthetic Nicotinamide Cofactors for C=C Bioreduction Using Enoate Reductases. *Organic Letters*, 15(1), 180–183. <https://doi.org/10.1021/ol303240a>
329. Hollmann, F., Witholt, B., & Schmid, A. (2002). [Cp*Rh(bpy)(H₂O)]²⁺: a versatile tool for efficient and non-enzymatic regeneration of nicotinamide and flavin coenzymes. *Journal of Molecular Catalysis B: Enzymatic*, 19–20, 167–176. [https://doi.org/10.1016/S1381-1177\(02\)00164-9](https://doi.org/10.1016/S1381-1177(02)00164-9)
330. Estabrook, R. W., Faulkner, K. M., Shet, M. S., & Fisher, C. W. (1996). Application of electrochemistry for P450-catalyzed reactions. *Methods in Enzymology*, 272, 44–51.
331. Bernhardt, P. V. (2006). Enzyme Electrochemistry — Biocatalysis on an Electrode. *Australian Journal of Chemistry*, 59(4), 233–256. <https://doi.org/10.1071/CH05340>
332. Krishnan, S., Schenkman, J. B., & Rusling, J. F. (2011). Bioelectronic delivery of electrons to cytochrome P450 enzymes. *The Journal of Physical Chemistry. B*, 115(26), 8371–8380. <https://doi.org/10.1021/jp201235m>

333. Sadeghi, S. J., Fantuzzi, A., & Gilardi, G. (2011). Breakthrough in P450 bioelectrochemistry and future perspectives. *Biochimica et Biophysica Acta (BBA) - Proteins and Proteomics*, 1814(1), 237–248. <https://doi.org/10.1016/j.bbapap.2010.07.010>
334. Shukla, A., Gillam, E. M., Mitchell, D. J., & Bernhardt, P. V. (2005). Direct electrochemistry of enzymes from the cytochrome P450 2C family. *Electrochemistry Communications*, 7(4), 437–442. <https://doi.org/10.1016/j.elecom.2005.02.021>
335. Holzinger, M., Le Goff, A., & Cosnier, S. (2014). Nanomaterials for biosensing applications: a review. *Frontiers in Chemistry*, 2, 63. <https://doi.org/10.3389/fchem.2014.00063>
336. Putzbach, W., & Ronkainen, N. J. (2013). Immobilization techniques in the fabrication of nanomaterial-based electrochemical biosensors: a review. *Sensors (Basel, Switzerland)*, 13(4), 4811–4840. <https://doi.org/10.3390/s130404811>
337. Alonso-Lomillo, M. A., Gonzalo-Ruiz, J., Domínguez-Renedo, O., Muñoz, F. J., & Arcos-Martínez, M. J. (2008). CYP450 biosensors based on gold chips for antiepileptic drugs determination. *Biosensors & Bioelectronics*, 23(11), 1733–1737. <https://doi.org/10.1016/j.bios.2008.01.030>
338. Udit, A. K., Hagen, K. D., Goldman, P. J., Star, A., Gillan, J. M., Gray, H. B., & Hill, M. G. (2006). Spectroscopy and electrochemistry of cytochrome P450 BM3-surfactant film assemblies. *Journal of the American Chemical Society*, 128(31), 10320–10325. <https://doi.org/10.1021/ja061896w>
339. Dodhia, V. R., Sassone, C., Fantuzzi, A., Nardo, G. D., Sadeghi, S. J., & Gilardi, G. (2008). Modulating the coupling efficiency of human cytochrome P450 CYP3A4 at electrode surfaces through protein engineering. *Electrochemistry Communications*, 10(11), 1744–1747. <https://doi.org/10.1016/j.elecom.2008.09.007>

340. Shumyantseva, V. V., Ivanov, Y. D., Bistolas, N., Scheller, F. W., Archakov, A. I., & Wollenberger, U. (2004). Direct electron transfer of cytochrome P450 2B4 at electrodes modified with nonionic detergent and colloidal clay nanoparticles. *Analytical Chemistry*, 76(20), 6046–6052. <https://doi.org/10.1021/ac049927y>
341. Alonso-Lomillo, M. A., Yardimci, C., Domínguez-Renedo, O., & Arcos-Martínez, M. J. (2009). CYP450 2B4 covalently attached to carbon and gold screen printed electrodes by diazonium salt and thiols monolayers. *Analytica Chimica Acta*, 633(1), 51–56. <https://doi.org/10.1016/j.aca.2008.11.033>
342. Yang, M., Kabulski, J. L., Wollenberg, L., Chen, X., Subramanian, M., Tracy, T. S., ... Wu, N. (2009). Electrocatalytic drug metabolism by CYP2C9 bonded to a self-assembled monolayer-modified electrode. *Drug Metabolism and Disposition: The Biological Fate of Chemicals*, 37(4), 892–899. <https://doi.org/10.1124/dmd.108.025452>
343. Müller, M., Agarwal, N., & Kim, J. (2016). A Cytochrome P450 3A4 Biosensor Based on Generation 4.0 PAMAM Dendrimers for the Detection of Caffeine. *Biosensors*, 6(3), 44. <https://doi.org/10.3390/bios6030044>
344. Xue, Q., Kato, D., Kamata, T., Guo, Q., You, T., & Niwa, O. (2013). Human cytochrome P450 3A4 and a carbon nanofiber modified film electrode as a platform for the simple evaluation of drug metabolism and inhibition reactions. *The Analyst*, 138(21), 6463–6468. <https://doi.org/10.1039/c3an01313h>
345. Walgama, C., Nerimetla, R., Materer, N. F., Schildkraut, D., Elman, J. F., & Krishnan, S. (2015). A Simple Construction of Electrochemical Liver Microsomal Bioreactor for Rapid Drug Metabolism and Inhibition Assays. *Analytical Chemistry*, 87(9), 4712–4718. <https://doi.org/10.1021/ac5044362>

346. Joseph, S., Rusling, J. F., Lvov, Y. M., Friedberg, T., & Fuhr, U. (2003). An amperometric biosensor with human CYP3A4 as a novel drug screening tool. *Biochemical Pharmacology*, *65*(11), 1817–1826.
347. Fleming, B. D., Tian, Y., Bell, S. G., Wong, L.-L., Urlacher, V., & Hill, H. A. O. (2003). Redox properties of cytochrome p450BM3 measured by direct methods. *European Journal of Biochemistry*, *270*(20), 4082–4088.
348. McLean, K. J., Warman, A. J., Seward, H. E., Marshall, K. R., Girvan, H. M., Cheesman, M. R., ... Munro, A. W. (2006). Biophysical characterization of the sterol demethylase P450 from *Mycobacterium tuberculosis*, its cognate ferredoxin, and their interactions. *Biochemistry*, *45*(27), 8427–8443. <https://doi.org/10.1021/bi0601609>
349. Shumyantseva, V. V., Bulko, T. V., Kumetsova, G. P., Lisitsa, A. V., Ponomarenko, E. A., Karuzina, I. I., & Archakov, A. I. (2007, April 20). Electrochemical Reduction of Sterol-14 alpha-demethylase from *Mycobacterium tuberculosis* (CYP51b1). *Biochemistry (Moscow)*. Retrieved May 20, 2018, from <https://eurekamag.com/research/015/686/015686234.php>
350. Udit, A. K., Hindoyan, N., Hill, M. G., Arnold, F. H., & Gray, H. B. (2005). Protein-surfactant film voltammetry of wild-type and mutant cytochrome P450 BM3. *Inorganic Chemistry*, *44*(12), 4109–4111. <https://doi.org/10.1021/ic0483747>
351. Xu, X., Wei, W., Huang, M., Yao, L., & Liu, S. (2012). Electrochemically driven drug metabolism via cytochrome P450 2C9 isozyme microsomes with cytochrome P450 reductase and indium tin oxide nanoparticle composites. *Chemical Communications (Cambridge, England)*, *48*(63), 7802–7804. <https://doi.org/10.1039/c2cc33575a>
352. Yoshioka, K., Kato, D., Kamata, T., & Niwa, O. (2013). Cytochrome P450 modified polycrystalline indium tin oxide film as a drug metabolizing electrochemical biosensor with a

- simple configuration. *Analytical Chemistry*, *85*(21), 9996–9999.
<https://doi.org/10.1021/ac402661w>
353. Mie, Y., Suzuki, M., & Komatsu, Y. (2009). Electrochemically driven drug metabolism by membranes containing human cytochrome P450. *Journal of the American Chemical Society*, *131*(19), 6646–6647. <https://doi.org/10.1021/ja809364r>
354. Panicco, P., Dodhia, V. R., Fantuzzi, A., & Gilardi, G. (2011). Enzyme-based amperometric platform to determine the polymorphic response in drug metabolism by cytochromes P450. *Analytical Chemistry*, *83*(6), 2179–2186. <https://doi.org/10.1021/ac200119b>
355. Faulkner, K. M., Shet, M. S., Fisher, C. W., & Estabrook, R. W. (1995). Electrocatalytically driven omega-hydroxylation of fatty acids using cytochrome P450 4A1. *Proceedings of the National Academy of Sciences of the United States of America*, *92*(17), 7705–7709.
356. Liu, S., Peng, L., Yang, X., Wu, Y., & He, L. (2008). Electrochemistry of cytochrome P450 enzyme on nanoparticle-containing membrane-coated electrode and its applications for drug sensing. *Analytical Biochemistry*, *375*(2), 209–216.
<https://doi.org/10.1016/j.ab.2007.12.001>
357. Rua, F., Sadeghi, S. J., Castrignanò, S., Valetti, F., & Gilardi, G. (2015). Electrochemistry of *Canis familiaris* cytochrome P450 2D15 with gold nanoparticles: An alternative to animal testing in drug discovery. *Bioelectrochemistry (Amsterdam, Netherlands)*, *105*, 110–116.
<https://doi.org/10.1016/j.bioelechem.2015.03.012>
358. Panicco, P., Astuti, Y., Fantuzzi, A., Durrant, J. R., & Gilardi, G. (2008). P450 versus P420: correlation between cyclic voltammetry and visible absorption spectroscopy of the immobilized heme domain of cytochrome P450 BM3. *The Journal of Physical Chemistry. B*, *112*(44), 14063–14068. <https://doi.org/10.1021/jp8050033>

359. Castrignanò, S., Sadeghi, S. J., & Gilardi, G. (2012). Entrapment of human flavin-containing monooxygenase 3 in the presence of gold nanoparticles: TEM, FTIR and electrocatalysis. *Biochimica Et Biophysica Acta*, 1820(12), 2072–2078.
<https://doi.org/10.1016/j.bbagen.2012.09.017>
360. Zilly, F. E., Taglieber, A., Schulz, F., Hollmann, F., & Reetz, M. T. (2009). Deazaflavins as mediators in light-driven cytochrome P450 catalyzed hydroxylations. *Chemical Communications (Cambridge, England)*, (46), 7152–7154. <https://doi.org/10.1039/b913863c>
361. Ener, M. E., Lee, Y.-T., Winkler, J. R., Gray, H. B., & Cheruzel, L. (2010). Photooxidation of cytochrome P450-BM3. *Proceedings of the National Academy of Sciences of the United States of America*, 107(44), 18783–18786. <https://doi.org/10.1073/pnas.1012381107>
362. Tran, N.-H., Huynh, N., Bui, T., Nguyen, Y., Huynh, P., Cooper, M. E., & Cheruzel, L. E. (2011). Light-initiated hydroxylation of lauric acid using hybrid P450 BM3 enzymes. *Chemical Communications (Cambridge, England)*, 47(43), 11936–11938.
<https://doi.org/10.1039/c1cc15124j>
363. Tran, N.-H., Huynh, N., Chavez, G., Nguyen, A., Dwaraknath, S., Nguyen, T.-A., ... Cheruzel, L. (2012). A series of hybrid P450 BM3 enzymes with different catalytic activity in the light-initiated hydroxylation of lauric acid. *Journal of Inorganic Biochemistry*, 115, 50–56.
<https://doi.org/10.1016/j.jinorgbio.2012.05.012>
364. Tran, N.-H., Nguyen, D., Dwaraknath, S., Mahadevan, S., Chavez, G., Nguyen, A., ... Cheruzel, L. E. (2013). An efficient light-driven P450 BM3 biocatalyst. *Journal of the American Chemical Society*, 135(39), 14484–14487. <https://doi.org/10.1021/ja409337v>
365. Lee, J. H., Nam, D. H., Lee, S. H., Park, J. H., Park, C. B., & Jeong, K. J. (2015). Solar-to-chemical conversion platform by Robust Cytochrome P450-P(3HB) complex. *Journal of Industrial and Engineering Chemistry*, 33. <https://doi.org/10.1016/j.jiec.2015.10.002>

366. Spradlin, J., Lee, D., Mahadevan, S., Mahomed, M., Tang, L., Lam, Q., ... Cheruzel, L. E. (2016). Insights into an efficient light-driven hybrid P450 BM3 enzyme from crystallographic, spectroscopic and biochemical studies. *Biochimica Et Biophysica Acta*, *1864*(12), 1732–1738. <https://doi.org/10.1016/j.bbapap.2016.09.005>
367. Shalan, H., Colbert, A., Nguyen, T. T., Kato, M., & Cheruzel, L. (2017). Correlating the para-Substituent Effects on Ru(II)-Polypyridine Photophysical Properties and on the Corresponding Hybrid P450 BM3 Enzymes Photocatalytic Activity. *Inorganic Chemistry*, *56*(11), 6558–6564. <https://doi.org/10.1021/acs.inorgchem.7b00685>
368. Das, A., Joshi, V., Kotkar, D., Pathak, V. S., Swayambunathan, V., Kamat, P. V., & Ghosh, P. K. (2001). Understanding the Facile Photooxidation of Ru(bpy)₃²⁺ in Strongly Acidic Aqueous Solution Containing Dissolved Oxygen. *The Journal of Physical Chemistry A*, *105*(28), 6945–6954. <https://doi.org/10.1021/jp0039924>
369. Paul, C. E., Churakova, E., Maurits, E., Girhard, M., Urlacher, V. B., & Hollmann, F. (2014). In situ formation of H₂O₂ for P450 peroxygenases. *Bioorganic & Medicinal Chemistry*, *22*(20), 5692–5696. <https://doi.org/10.1016/j.bmc.2014.05.074>
370. Churakova, E., Arends, I. W. C. E., & Hollmann, F. (2013). Increasing the Productivity of Peroxidase-Catalyzed Oxyfunctionalization: A Case Study on the Potential of Two-Liquid-Phase Systems. *ChemCatChem*, *5*(2), 565–568. <https://doi.org/10.1002/cctc.201200490>
371. Otey, C. R., Bandara, G., Lalonde, J., Takahashi, K., & Arnold, F. H. (2006). Preparation of human metabolites of propranolol using laboratory-evolved bacterial cytochromes P450. *Biotechnology and Bioengineering*, *93*(3), 494–499. <https://doi.org/10.1002/bit.20744>
372. Di Nardo, G., Fantuzzi, A., Sideri, A., Panicco, P., Sassone, C., Giunta, C., & Gilardi, G. (2007). Wild-type CYP102A1 as a biocatalyst: turnover of drugs usually metabolised by human liver

- enzymes. *Journal of biological inorganic chemistry: JBIC: a publication of the Society of Biological Inorganic Chemistry*, 12(3), 313–323. <https://doi.org/10.1007/s00775-006-0188-4>
373. Nazor, J., & Schwaneberg, U. (2006). Laboratory Evolution of P450 BM-3 for Mediated Electron Transfer. *ChemBioChem*, 7(4), 638–644. <https://doi.org/10.1002/cbic.200500436>
374. Nazor, J., Dannenmann, S., Adjei, R. O., Fordjour, Y. B., Ghampson, I. T., Blanusa, M., ... Schwaneberg, U. (2008). Laboratory evolution of P450 BM3 for mediated electron transfer yielding an activity-improved and reductase-independent variant. *Protein engineering, design & selection: PEDS*, 21(1), 29–35. <https://doi.org/10.1093/protein/gzm074>
375. Udit, A. K., Arnold, F. H., & Gray, H. B. (2004). Cobaltocene-mediated catalytic monooxygenation using holo and heme domain cytochrome P450 BM3. *Journal of Inorganic Biochemistry*, 98(9), 1547–1550. <https://doi.org/10.1016/j.jinorgbio.2004.06.007>
376. Zhao, J., Tan, E., Ferras, J., & Auclair, K. (2007). Activity of human P450 2D6 in biphasic solvent systems. *Biotechnology and Bioengineering*, 98(2), 508–513. <https://doi.org/10.1002/bit.21449>
377. Ryan, J. D., & Clark, D. S. (2008). P450cam biocatalysis in surfactant-stabilized two-phase emulsions. *Biotechnology and Bioengineering*, 99(6), 1311–1319. <https://doi.org/10.1002/bit.21772>
378. von Bühler, C. J., & Urlacher, V. B. (2014). A novel P450-based biocatalyst for the selective production of chiral 2-alkanols. *Chemical Communications (Cambridge, England)*, 50(31), 4089–4091. <https://doi.org/10.1039/c4cc00647j>
379. Schrewe, M., Julsing, M. K., Bühler, B., & Schmid, A. (2013). Whole-cell biocatalysis for selective and productive C-O functional group introduction and modification. *Chemical Society Reviews*, 42(15), 6346–6377. <https://doi.org/10.1039/c3cs60011d>

380. Huang, W.-C., Westlake, A. C. G., Maréchal, J.-D., Joyce, M. G., Moody, P. C. E., & Roberts, G. C. K. (2007). Filling a hole in cytochrome P450 BM3 improves substrate binding and catalytic efficiency. *Journal of Molecular Biology*, *373*(3), 633–651.
<https://doi.org/10.1016/j.jmb.2007.08.015>
381. Lundemo, M. T., Notonier, S., Striedner, G., Hauer, B., & Woodley, J. M. (2016). Process limitations of a whole-cell P450 catalyzed reaction using a CYP153A-CPR fusion construct expressed in *Escherichia coli*. *Applied Microbiology and Biotechnology*, *100*(3), 1197–1208.
<https://doi.org/10.1007/s00253-015-6999-x>
382. Ahn, T., & Yun, C.-H. (2004). High-level expression of human cytochrome P450 3A4 by co-expression with human molecular chaperone HDJ-1 (Hsp40). *Archives of Pharmacal Research*, *27*(3), 319–323.
383. Emmerstorfer, A., Wimmer-Teubenbacher, M., Wriessnegger, T., Leitner, E., Müller, M., Kaluzna, I., ... Pichler, H. (2015). Over-expression of ICE2 stabilizes cytochrome P450 reductase in *Saccharomyces cerevisiae* and *Pichia pastoris*. *Biotechnology Journal*, *10*(4), 623–635. <https://doi.org/10.1002/biot.201400780>
384. Wriessnegger, T., Moser, S., Emmerstorfer-Augustin, A., Leitner, E., Müller, M., Kaluzna, I., ... Pichler, H. (2016). Enhancing cytochrome P450-mediated conversions in *P. pastoris* through RAD52 over-expression and optimizing the cultivation conditions. *Fungal genetics and biology: FG & B*, *89*, 114–125. <https://doi.org/10.1016/j.fgb.2016.02.004>
385. de Carvalho, C. C. C. R. (2016). Whole cell biocatalysts: essential workers from Nature to the industry. *Microbial Biotechnology*, *10*(2), 250–263. <https://doi.org/10.1111/1751-7915.12363>

386. Chen, R. R. (2007). Permeability issues in whole-cell bioprocesses and cellular membrane engineering. *Applied Microbiology and Biotechnology*, 74(4), 730–738.
<https://doi.org/10.1007/s00253-006-0811-x>
387. Fujii, Y., Hirose, S., Fujii, T., Matsumoto, N., Agematu, H., & Arisawa, A. (2006). Hydroxylation of oleanolic acid to quercetin by cytochrome P450 from *Nonomuraea recticatena*. *Bioscience, Biotechnology, and Biochemistry*, 70(9), 2299–2302.
<https://doi.org/10.1271/bbb.60126>
388. Janocha, S., & Bernhardt, R. (2013). Design and characterization of an efficient CYP105A1-based whole-cell biocatalyst for the conversion of resin acid diterpenoids in permeabilized *Escherichia coli*. *Applied Microbiology and Biotechnology*, 97(17), 7639–7649.
<https://doi.org/10.1007/s00253-013-5008-5>
389. Ma, L., Du, L., Chen, H., Sun, Y., Huang, S., Zheng, X., ... Li, S. (2015). Reconstitution of the In Vitro Activity of the Cyclosporine-Specific P450 Hydroxylase from *Sebekia benihana* and Development of a Heterologous Whole-Cell Biotransformation System. *Applied and Environmental Microbiology*, 81(18), 6268–6275. <https://doi.org/10.1128/AEM.01353-15>
390. Ly, T. T. B., Schiffrin, A., Nguyen, B. D., & Bernhardt, R. (2017). Improvement of a P450-Based Recombinant *Escherichia coli* Whole-Cell System for the Production of Oxygenated Sesquiterpene Derivatives. *Journal of Agricultural and Food Chemistry*, 65(19), 3891–3899.
<https://doi.org/10.1021/acs.jafc.7b00792>
391. Zehentgruber, D., Drăgan, C.-A., Bureik, M., & Lütz, S. (2010). Challenges of steroid biotransformation with human cytochrome P450 monooxygenase CYP21 using resting cells of recombinant *Schizosaccharomyces pombe*. *Journal of Biotechnology*, 146(4), 179–185.
<https://doi.org/10.1016/j.jbiotec.2010.01.019>

392. Yan, Q., Machalz, D., Zöllner, A., Sorensen, E. J., Wolber, G., & Bureik, M. (2017). Efficient substrate screening and inhibitor testing of human CYP4Z1 using permeabilized recombinant fission yeast. *Biochemical Pharmacology*, *146*, 174–187.
<https://doi.org/10.1016/j.bcp.2017.09.011>
393. Cornelissen, S., Julsing, M. K., Volmer, J., Riechert, O., Schmid, A., & Bühler, B. (2013). Whole-cell-based CYP153A6-catalyzed (S)-limonene hydroxylation efficiency depends on host background and profits from monoterpene uptake via AlkL. *Biotechnology and Bioengineering*, *110*(5), 1282–1292. <https://doi.org/10.1002/bit.24801>
394. Schneider, S., Wubbolts, M. G., Sanglard, D., & Witholt, B. (1998). Biocatalyst engineering by assembly of fatty acid transport and oxidation activities for In vivo application of cytochrome P-450BM-3 monooxygenase. *Applied and Environmental Microbiology*, *64*(10), 3784–3790.
395. Kaderbhai, M. A., Ugochukwu, C. C., Lamb, D. C., & Kelly, S. L. (2000). Targeting of active human cytochrome P4501A1 (CYP1A1) to the periplasmic space of Escherichia coli. *Biochemical and Biophysical Research Communications*, *279*(3), 803–807.
<https://doi.org/10.1006/bbrc.2000.4001>
396. Kaderbhai, M. A., Ugochukwu, C. C., Kelly, S. L., & Lamb, D. C. (2001). Export of cytochrome P450 105D1 to the periplasmic space of Escherichia coli. *Applied and Environmental Microbiology*, *67*(5), 2136–2138. <https://doi.org/10.1128/AEM.67.5.2136-2138.2001>
397. Jose, J., Bernhardt, R., & Hannemann, F. (2002). Cellular surface display of dimeric Adx and whole cell P450-mediated steroid synthesis on E. coli. *Journal of Biotechnology*, *95*(3), 257–268.

398. Yim, S.-K., Kim, D.-H., Jung, H.-C., Pan, J.-G., Kang, H.-S., Ahn, T., & Yun, C.-H. (2010). Surface display of heme- and diflavin-containing cytochrome P450 BM3 in *Escherichia coli*: a whole cell biocatalyst for oxidation. *Journal of Microbiology and Biotechnology*, *20*(4), 712–717.
399. Schumacher, S. D., & Jose, J. (2012). Expression of active human P450 3A4 on the cell surface of *Escherichia coli* by Autodisplay. *Journal of Biotechnology*, *161*(2), 113–120. <https://doi.org/10.1016/j.jbiotec.2012.01.031>
400. Schumacher, S. D., Hannemann, F., Teese, M. G., Bernhardt, R., & Jose, J. (2012). Autodisplay of functional CYP106A2 in *Escherichia coli*. *Journal of Biotechnology*, *161*(2), 104–112. <https://doi.org/10.1016/j.jbiotec.2012.02.018>
401. Quehl, P., Hollender, J., Schüürmann, J., Brossette, T., Maas, R., & Jose, J. (2016). Co-expression of active human cytochrome P450 1A2 and cytochrome P450 reductase on the cell surface of *Escherichia coli*. *Microbial Cell Factories*, *15*, 26. <https://doi.org/10.1186/s12934-016-0427-5>
402. Blank, L. M., Ebert, B. E., Bühler, B., & Schmid, A. (2008). Metabolic capacity estimation of *Escherichia coli* as a platform for redox biocatalysis: constraint-based modeling and experimental verification. *Biotechnology and Bioengineering*, *100*(6), 1050–1065. <https://doi.org/10.1002/bit.21837>
403. Blank, L. M., Ebert, B. E., Buehler, K., & Bühler, B. (2010). Redox biocatalysis and metabolism: molecular mechanisms and metabolic network analysis. *Antioxidants & Redox Signaling*, *13*(3), 349–394. <https://doi.org/10.1089/ars.2009.2931>
404. Hollmann, F., Arends, I. W. C. E., Buehler, K., Schallmeyer, A., & Bühler, B. (2011). Enzyme-mediated oxidations for the chemist. *Green Chemistry*, *13*(2), 226–265. <https://doi.org/10.1039/C0GC00595A>

405. Kratzer, R., Woodley, J. M., & Nidetzky, B. (2015). Rules for biocatalyst and reaction engineering to implement effective, NAD(P)H-dependent, whole cell bioreductions. *Biotechnology Advances*, 33(8), 1641–1652.
<https://doi.org/10.1016/j.biotechadv.2015.08.006>
406. Siriphongphaew, A., Pisonpong, P., Wongkongkatep, J., Inprakon, P., Vangnai, A. S., Honda, K., ... Pongtharangkul, T. (2012). Development of a whole-cell biocatalyst co-expressing P450 monooxygenase and glucose dehydrogenase for synthesis of epoxyhexane. *Applied Microbiology and Biotechnology*, 95(2), 357–367. <https://doi.org/10.1007/s00253-012-4039-7>
407. Pongtharangkul, T., Chuekitkumchorn, P., Suwanampa, N., Payongsri, P., Honda, K., & Panbangred, W. (2015). Kinetic properties and stability of glucose dehydrogenase from *Bacillus amyloliquefaciens* SB5 and its potential for cofactor regeneration. *AMB Express*, 5(1), 68. <https://doi.org/10.1186/s13568-015-0157-9>
408. Mouri, T., Michizoe, J., Ichinose, H., Kamiya, N., & Goto, M. (2006). A recombinant *Escherichia coli* whole cell biocatalyst harboring a cytochrome P450cam monooxygenase system coupled with enzymatic cofactor regeneration. *Applied Microbiology and Biotechnology*, 72(3), 514–520. <https://doi.org/10.1007/s00253-005-0289-y>
409. Schewe, H., Kaup, B.-A., & Schrader, J. (2008). Improvement of P450(BM-3) whole-cell biocatalysis by integrating heterologous cofactor regeneration combining glucose facilitator and dehydrogenase in *E. coli*. *Applied Microbiology and Biotechnology*, 78(1), 55–65.
<https://doi.org/10.1007/s00253-007-1277-1>
410. Heller, K. B., Lin, E. C., & Wilson, T. H. (1980). Substrate specificity and transport properties of the glycerol facilitator of *Escherichia coli*. *Journal of Bacteriology*, 144(1), 274–278.

411. Stroud, R. M., Nollert, P., & Miercke, L. (2003). The glycerol facilitator GlpF its aquaporin family of channels, and their selectivity. *Advances in Protein Chemistry*, *63*, 291–316.
412. Stroud, R. M., Miercke, L. J. W., O'Connell, J., Khademi, S., Lee, J. K., Remis, J., ... Akhavan, D. (2003). Glycerol facilitator GlpF and the associated aquaporin family of channels. *Current Opinion in Structural Biology*, *13*(4), 424–431.
413. Lonsdale, T. H., Lauterbach, L., Honda Malca, S., Nestl, B. M., Hauer, B., & Lenz, O. (2015). H₂-driven biotransformation of n-octane to 1-octanol by a recombinant *Pseudomonas putida* strain co-synthesizing an O₂-tolerant hydrogenase and a P450 monooxygenase. *Chemical Communications (Cambridge, England)*, *51*(90), 16173–16175.
<https://doi.org/10.1039/c5cc06078h>
414. Park, J. H., Lee, S. H., Cha, G. S., Choi, D. S., Nam, D. H., Lee, J. H., ... Park, C. B. (2015). Cofactor-Free Light-Driven Whole-Cell Cytochrome P450 Catalysis. *Angewandte Chemie International Edition*, *54*(3), 969–973. <https://doi.org/10.1002/anie.201410059>
415. Müller, C. A., Weingartner, A. M., Dennig, A., Ruff, A. J., Gröger, H., & Schwaneberg, U. (2016). A whole cell biocatalyst for double oxidation of cyclooctane. *Journal of Industrial Microbiology & Biotechnology*, *43*(12), 1641–1646. <https://doi.org/10.1007/s10295-016-1844-5>
416. Müller, C. A., Dennig, A., Welters, T., Winkler, T., Ruff, A. J., Hummel, W., ... Schwaneberg, U. (2014). Whole-cell double oxidation of n-heptane. *Journal of Biotechnology*, *191*, 196–204.
<https://doi.org/10.1016/j.jbiotec.2014.06.001>
417. Tieves, F., Erenburg, I. N., Mahmoud, O., & Urlacher, V. B. (2016). Synthesis of chiral 2-alkanols from n-alkanes by a *P. putida* whole-cell biocatalyst. *Biotechnology and Bioengineering*, *113*(9), 1845–1852. <https://doi.org/10.1002/bit.25953>

418. Yan, J., Liu, Y., Wang, C., Han, B., & Li, S. (2015). Assembly of lipase and P450 fatty acid decarboxylase to constitute a novel biosynthetic pathway for production of 1-alkenes from renewable triacylglycerols and oils. *Biotechnology for Biofuels*, *8*, 34.
<https://doi.org/10.1186/s13068-015-0219-x>
419. Fasan, R., Crook, N. C., Peters, M. W., Meinhold, P., Buelter, T., Landwehr, M., ... Arnold, F. H. (2011). Improved product-per-glucose yields in P450-dependent propane biotransformations using engineered *Escherichia coli*. *Biotechnology and Bioengineering*, *108*(3), 500–510. <https://doi.org/10.1002/bit.22984>
420. Li, A., Ilie, A., Sun, Z., Lonsdale, R., Xu, J.-H., & Reetz, M. T. (n.d.). Whole-Cell-Catalyzed Multiple Regio- and Stereoselective Functionalizations in Cascade Reactions Enabled by Directed Evolution. *Angewandte Chemie International Edition*, *55*(39), 12026–12029.
<https://doi.org/10.1002/anie.201605990>
421. Favre-Bulle, O., Weenink, E., Vos, T., Preusting, H., & Witholt, B. (1993). Continuous bioconversion of n-octane to octanoic acid by recombinant *Escherichia coli* (alk(+)) growing in a two-liquid-phase Chemostat. *Biotechnology and Bioengineering*, *41*(2), 263–272.
<https://doi.org/10.1002/bit.260410213>
422. Royce, L. A., Liu, P., Stebbins, M. J., Hanson, B. C., & Jarboe, L. R. (2013). The damaging effects of short chain fatty acids on *Escherichia coli* membranes. *Applied Microbiology and Biotechnology*, *97*(18), 8317–8327. <https://doi.org/10.1007/s00253-013-5113-5>
423. Marounek, M., Skrivanová, E., & Rada, V. (2003). Susceptibility of *Escherichia coli* to C2-C18 fatty acids. *Folia Microbiologica*, *48*(6), 731–735.
424. Marques, M. P. C., Carvalho, F., Magalhães, S., Cabral, J. M. S., & Fernandes, P. (2009). Screening for suitable solvents as substrate carriers for the microbial side-chain cleavage of

- sitosterol using microtitre plates. *Process Biochemistry*, 44(5), 556–561.
<https://doi.org/10.1016/j.procbio.2009.01.014>
425. Gudimich, R. K., & Smit, M. S. (2011). Identification and characterization of 4-hexylbenzoic acid and 4-nonyloxybenzoic acid as substrates of CYP102A1. *Applied Microbiology and Biotechnology*, 90(1), 117–126. <https://doi.org/10.1007/s00253-010-3029-x>
426. Gao, P., Li, A., Lee, H. H., Wang, D. I. C., & Li, Z. (2014). Enhancing Enantioselectivity and Productivity of P450-Catalyzed Asymmetric Sulfoxidation with an Aqueous/Ionic Liquid Biphasic System. *ACS Catalysis*, 4(10), 3763–3771. <https://doi.org/10.1021/cs5010344>
427. Schrader, J. (2007). Microbial Flavour Production. In *Flavours and Fragrances* (pp. 507–574). Springer, Berlin, Heidelberg. https://doi.org/10.1007/978-3-540-49339-6_23
428. Schewe, H., Holtmann, D., & Schrader, J. (2009). P450(BM-3)-catalyzed whole-cell biotransformation of alpha-pinene with recombinant *Escherichia coli* in an aqueous-organic two-phase system. *Applied Microbiology and Biotechnology*, 83(5), 849–857.
<https://doi.org/10.1007/s00253-009-1917-8>
429. Braun, A., Geier, M., Bühler, B., Schmid, A., Mauersberger, S., & Glieder, A. (2012). Steroid biotransformations in biphasic systems with *Yarrowia lipolytica* expressing human liver cytochrome P450 genes. *Microbial Cell Factories*, 11, 106. <https://doi.org/10.1186/1475-2859-11-106>
430. Sahdev, S., Khattar, S. K., & Saini, K. S. (2008). Production of active eukaryotic proteins through bacterial expression systems: a review of the existing biotechnology strategies. *Molecular and Cellular Biochemistry*, 307(1–2), 249–264. <https://doi.org/10.1007/s11010-007-9603-6>

431. Aguiar, M., Masse, R., & Gibbs, B. F. (2005). Regulation of cytochrome P450 by posttranslational modification. *Drug Metabolism Reviews*, 37(2), 379–404.
<https://doi.org/10.1081/DMR-46136>
432. Rosano, G. L., & Ceccarelli, E. A. (2014). Recombinant protein expression in *Escherichia coli*: advances and challenges. *Frontiers in Microbiology*, 5, 172.
<https://doi.org/10.3389/fmicb.2014.00172>
433. Jenkins, C. M., & Waterman, M. R. (1994). Flavodoxin and NADPH-flavodoxin reductase from *Escherichia coli* support bovine cytochrome P450c17 hydroxylase activities. *The Journal of Biological Chemistry*, 269(44), 27401–27408.
434. Vary, P. S., Biedendieck, R., Fuerch, T., Meinhardt, F., Rohde, M., Deckwer, W.-D., & Jahn, D. (2007). *Bacillus megaterium*--from simple soil bacterium to industrial protein production host. *Applied Microbiology and Biotechnology*, 76(5), 957–967.
<https://doi.org/10.1007/s00253-007-1089-3>
435. Korneli, C., David, F., Biedendieck, R., Jahn, D., & Wittmann, C. (2013). Getting the big beast to work--systems biotechnology of *Bacillus megaterium* for novel high-value proteins. *Journal of Biotechnology*, 163(2), 87–96. <https://doi.org/10.1016/j.jbiotec.2012.06.018>
436. Biedendieck, R. (2016). A *Bacillus megaterium* System for the Production of Recombinant Proteins and Protein Complexes. *Advances in Experimental Medicine and Biology*, 896, 97–113. https://doi.org/10.1007/978-3-319-27216-0_7
437. Kleser, M., Hannemann, F., Hutter, M., Zapp, J., & Bernhardt, R. (2012). CYP105A1 mediated 3-hydroxylation of glimepiride and glibenclamide using a recombinant *Bacillus megaterium* whole-cell catalyst. *Journal of Biotechnology*, 157(3), 405–412.
<https://doi.org/10.1016/j.jbiotec.2011.12.006>

438. Bleif, S., Hannemann, F., Lisurek, M., von Kries, J. P., Zapp, J., Dietzen, M., ... Bernhardt, R. (2011). Identification of CYP106A2 as a regioselective allylic bacterial diterpene hydroxylase. *Chembiochem: A European Journal of Chemical Biology*, *12*(4), 576–582.
<https://doi.org/10.1002/cbic.201000404>
439. Bleif, S., Hannemann, F., Zapp, J., Hartmann, D., Jauch, J., & Bernhardt, R. (2012). A new *Bacillus megaterium* whole-cell catalyst for the hydroxylation of the pentacyclic triterpene 11-keto- β -boswellic acid (KBA) based on a recombinant cytochrome P450 system. *Applied Microbiology and Biotechnology*, *93*(3), 1135–1146. <https://doi.org/10.1007/s00253-011-3467-0>
440. Hussain, H., Al-Harrasi, A., Csuk, R., Shamraiz, U., Green, I. R., Ahmed, I., ... Ali, Z. (2017). Therapeutic potential of boswellic acids: a patent review (1990-2015). *Expert Opinion on Therapeutic Patents*, *27*(1), 81–90. <https://doi.org/10.1080/13543776.2017.1235156>
441. Schmitz, D., Zapp, J., & Bernhardt, R. (2014). Steroid conversion with CYP106A2 - production of pharmaceutically interesting DHEA metabolites. *Microbial Cell Factories*, *13*, 81.
<https://doi.org/10.1186/1475-2859-13-81>
442. Abdulmughni, A., Jóźwik, I. K., Putkaradze, N., Brill, E., Zapp, J., Thunnissen, A.-M. W. H., ... Bernhardt, R. (2017). Characterization of cytochrome P450 CYP109E1 from *Bacillus megaterium* as a novel vitamin D3 hydroxylase. *Journal of Biotechnology*, *243*, 38–47.
<https://doi.org/10.1016/j.jbiotec.2016.12.023>
443. Gerber, A., Kleser, M., Biedendieck, R., Bernhardt, R., & Hannemann, F. (2015). Functionalized PHB granules provide the basis for the efficient side-chain cleavage of cholesterol and analogs in recombinant *Bacillus megaterium*. *Microbial Cell Factories*, *14*, 107. <https://doi.org/10.1186/s12934-015-0300-y>

444. Ehrhardt, M., Gerber, A., Hannemann, F., & Bernhardt, R. (2016). Expression of human CYP27A1 in *B. megaterium* for the efficient hydroxylation of cholesterol, vitamin D3 and 7-dehydrocholesterol. *Journal of Biotechnology*, *218*, 34–40.
<https://doi.org/10.1016/j.jbiotec.2015.11.021>
445. Bentley, S. D., Chater, K. F., Cerdeño-Tárraga, A.-M., Challis, G. L., Thomson, N. R., James, K. D., ... Hopwood, D. A. (2002). Complete genome sequence of the model actinomycete *Streptomyces coelicolor* A3(2). *Nature*, *417*(6885), 141–147.
<https://doi.org/10.1038/417141a>
446. Ishikawa, J., Yamashita, A., Mikami, Y., Hoshino, Y., Kurita, H., Hotta, K., ... Hattori, M. (2004). The complete genomic sequence of *Nocardia farcinica* IFM 10152. *Proceedings of the National Academy of Sciences of the United States of America*, *101*(41), 14925–14930.
<https://doi.org/10.1073/pnas.0406410101>
447. Parajuli, N., Basnet, D. B., Chan Lee, H., Sohng, J. K., & Liou, K. (2004). Genome analyses of *Streptomyces peucetius* ATCC 27952 for the identification and comparison of cytochrome P450 complement with other *Streptomyces*. *Archives of Biochemistry and Biophysics*, *425*(2), 233–241. <https://doi.org/10.1016/j.abb.2004.03.011>
448. Ikeda, H., Ishikawa, J., Hanamoto, A., Shinose, M., Kikuchi, H., Shiba, T., ... Omura, S. (2003). Complete genome sequence and comparative analysis of the industrial microorganism *Streptomyces avermitilis*. *Nature Biotechnology*, *21*(5), 526–531.
<https://doi.org/10.1038/nbt820>
449. Anné, J., Maldonado, B., Van Impe, J., Van Mellaert, L., & Bernaerts, K. (2012). Recombinant protein production and streptomycetes. *Journal of Biotechnology*, *158*(4), 159–167.
<https://doi.org/10.1016/j.jbiotec.2011.06.028>

450. Gullón, S., & Mellado, R. P. (2018). The Cellular Mechanisms that Ensure an Efficient Secretion in *Streptomyces*. *Antibiotics (Basel, Switzerland)*, 7(2).
<https://doi.org/10.3390/antibiotics7020033>
451. Hussain, H. A., & Ward, J. M. (2003). Enhanced heterologous expression of two *Streptomyces griseolus* cytochrome P450s and *Streptomyces coelicolor* ferredoxin reductase as potentially efficient hydroxylation catalysts. *Applied and Environmental Microbiology*, 69(1), 373–382.
452. Ueno, M., Yamashita, M., Hashimoto, M., Hino, M., & Fujie, A. (2005). Oxidative activities of heterologously expressed CYP107B1 and CYP105D1 in whole-cell biotransformation using *Streptomyces lividans* TK24. *Journal of Bioscience and Bioengineering*, 100(5), 567–572.
<https://doi.org/10.1263/jbb.100.567>
453. Venkataraman, H., Te Poele, E. M., Rosłonec, K. Z., Vermeulen, N., Commandeur, J. N. M., van der Geize, R., & Dijkhuizen, L. (2015). Biosynthesis of a steroid metabolite by an engineered *Rhodococcus erythropolis* strain expressing a mutant cytochrome P450 BM3 enzyme. *Applied Microbiology and Biotechnology*, 99(11), 4713–4721.
<https://doi.org/10.1007/s00253-014-6281-7>
454. Larkin, M. J., Kulakov, L. A., & Allen, C. C. R. (2005). Biodegradation and *Rhodococcus*--masters of catabolic versatility. *Current Opinion in Biotechnology*, 16(3), 282–290.
<https://doi.org/10.1016/j.copbio.2005.04.007>
455. Hernández, M. A., Mohn, W. W., Martínez, E., Rost, E., Alvarez, A. F., & Alvarez, H. M. (2008). Biosynthesis of storage compounds by *Rhodococcus jostii* RHA1 and global identification of genes involved in their metabolism. *BMC genomics*, 9, 600.
<https://doi.org/10.1186/1471-2164-9-600>

456. van der Geize, R., & Dijkhuizen, L. (2004). Harnessing the catabolic diversity of rhodococci for environmental and biotechnological applications. *Current Opinion in Microbiology*, 7(3), 255–261. <https://doi.org/10.1016/j.mib.2004.04.001>
457. Mohn, W. W., van der Geize, R., Stewart, G. R., Okamoto, S., Liu, J., Dijkhuizen, L., & Eltis, L. D. (2008). The actinobacterial *mce4* locus encodes a steroid transporter. *The Journal of Biological Chemistry*, 283(51), 35368–35374. <https://doi.org/10.1074/jbc.M805496200>
458. van der Geize, R., Hessels, G. I., van Gerwen, R., van der Meijden, P., & Dijkhuizen, L. (2002). Molecular and functional characterization of *kshA* and *kshB*, encoding two components of 3-ketosteroid 9 α -hydroxylase, a class IA monooxygenase, in *Rhodococcus erythropolis* strain SQ1. *Molecular Microbiology*, 45(4), 1007–1018.
459. Hays, F. A., Roe-Zurz, Z., & Stroud, R. M. (2010). Overexpression and purification of integral membrane proteins in yeast. *Methods in Enzymology*, 470, 695–707. [https://doi.org/10.1016/S0076-6879\(10\)70029-X](https://doi.org/10.1016/S0076-6879(10)70029-X)
460. Hausjell, J., Halbwirth, H., & Spadiut, O. (2018). Recombinant production of eukaryotic cytochrome P450s in microbial cell factories. *Bioscience Reports*, 38(2). <https://doi.org/10.1042/BSR20171290>
461. Zahrl, R. J., Peña, D. A., Mattanovich, D., & Gasser, B. (2017). Systems biotechnology for protein production in *Pichia pastoris*. *FEMS yeast research*, 17(7). <https://doi.org/10.1093/femsyr/fox068>
462. Juturu, V., & Wu, J. C. (2018). Heterologous Protein Expression in *Pichia pastoris*: Latest Research Progress and Applications. *ChemBiochem: A European Journal of Chemical Biology*, 19(1), 7–21. <https://doi.org/10.1002/cbic.201700460>

463. Cereghino, G. P. L., Cereghino, J. L., Ilgen, C., & Cregg, J. M. (2002). Production of recombinant proteins in fermenter cultures of the yeast *Pichia pastoris*. *Current Opinion in Biotechnology*, *13*(4), 329–332.
464. Celik, E., & Calik, P. (2012). Production of recombinant proteins by yeast cells. *Biotechnology Advances*, *30*(5), 1108–1118. <https://doi.org/10.1016/j.biotechadv.2011.09.011>
465. Kolar, N. W., Swart, A. C., Mason, J. I., & Swart, P. (2007). Functional expression and characterisation of human cytochrome P45017alpha in *Pichia pastoris*. *Journal of biotechnology*, *129*(4), 635–644. <https://doi.org/10.1016/j.jbiotec.2007.02.003>
466. Siddiqui, M. S., Thodey, K., Trenchard, I., & Smolke, C. D. (2012). Advancing secondary metabolite biosynthesis in yeast with synthetic biology tools. *FEMS yeast research*, *12*(2), 144–170. <https://doi.org/10.1111/j.1567-1364.2011.00774.x>
467. Jiang, H., & Morgan, J. A. (2004). Optimization of an in vivo plant P450 monooxygenase system in *Saccharomyces cerevisiae*. *Biotechnology and Bioengineering*, *85*(2), 130–137. <https://doi.org/10.1002/bit.10867>
468. Takegawa, K., Tohda, H., Sasaki, M., Idiris, A., Ohashi, T., Mukaiyama, H., ... Kumagai, H. (2009). Production of heterologous proteins using the fission-yeast (*Schizosaccharomyces pombe*) expression system. *Biotechnology and Applied Biochemistry*, *53*(Pt 4), 227–235. <https://doi.org/10.1042/BA20090048>
469. Bureik, M., Schiffler, B., Hiraoka, Y., Vogel, F., & Bernhardt, R. (2002). Functional expression of human mitochondrial CYP11B2 in fission yeast and identification of a new internal electron transfer protein, etp1. *Biochemistry*, *41*(7), 2311–2321.
470. Drăgan, C.-A., Zearo, S., Hannemann, F., Bernhardt, R., & Bureik, M. (2005). Efficient conversion of 11-deoxycortisol to cortisol (hydrocortisone) by recombinant fission yeast

- Schizosaccharomyces pombe. *FEMS yeast research*, 5(6–7), 621–625.
<https://doi.org/10.1016/j.femsyr.2004.12.001>
471. Palabiyik, B., Karaer, S., Arda, N., Toker, S. E., Temizkan, G., Kelly, S., & Sarikaya, A. T. (2008). Expression of human cytochrome p450 3A4 gene in *Schizosaccharomyces pombe*. *Biologia*, 63(3), 450–454.
<https://doi.org/10.2478/s11756-008-0069-0>
472. Peters, F. T., Dragan, C.-A., Schwaninger, A. E., Sauer, C., Zapp, J., Bureik, M., & Maurer, H. H. (2009). Use of fission yeast heterologously expressing human cytochrome P450 2B6 in biotechnological synthesis of the designer drug metabolite N-(1-phenylcyclohexyl)-2-hydroxyethanamine. *Forensic Science International*, 184(1–3), 69–73.
<https://doi.org/10.1016/j.forsciint.2008.12.001>
473. Peters, F. T., Dragan, C.-A., Kauffels, A., Schwaninger, A. E., Zapp, J., Bureik, M., & Maurer, H. H. (2009). Biotechnological synthesis of the designer drug metabolite 4'-hydroxymethyl-alpha-pyrrolidinohexanophenone in fission yeast heterologously expressing human cytochrome P450 2D6--a versatile alternative to multistep chemical synthesis. *Journal of Analytical Toxicology*, 33(4), 190–197.
474. Zöllner, A., Dragan, C.-A., Pistorius, D., Müller, R., Bode, H. B., Peters, F. T., ... Bureik, M. (2009). Human CYP4Z1 catalyzes the in-chain hydroxylation of lauric acid and myristic acid. *Biological Chemistry*, 390(4), 313–317. <https://doi.org/10.1515/BC.2009.030>
475. Petrič, S., Hakki, T., Bernhardt, R., Zigon, D., & Crešnar, B. (2010). Discovery of a steroid 11 α -hydroxylase from *Rhizopus oryzae* and its biotechnological application. *Journal of Biotechnology*, 150(3), 428–437. <https://doi.org/10.1016/j.jbiotec.2010.09.928>
476. Neunzig, I., Widjaja, M., Peters, F. T., Maurer, H. H., Hehn, A., Bourgaud, F., & Bureik, M. (2013). Coexpression of CPR from various origins enhances biotransformation activity of

- human CYPs in *S. pombe*. *Applied Biochemistry and Biotechnology*, 170(7), 1751–1766.
<https://doi.org/10.1007/s12010-013-0303-2>
477. Fickers, P., Benetti, P.-H., Waché, Y., Marty, A., Mauersberger, S., Smit, M. S., & Nicaud, J.-M. (2005). Hydrophobic substrate utilisation by the yeast *Yarrowia lipolytica*, and its potential applications. *FEMS yeast research*, 5(6–7), 527–543.
<https://doi.org/10.1016/j.femsyr.2004.09.004>
478. Thevenieau, F., Beopoulos, A., Desfougeres, T., Sabirova, J., Albertin, K., Zinjarde, S., & Nicaud, J.-M. (2010). Uptake and Assimilation of Hydrophobic Substrates by the Oleaginous Yeast *Yarrowia lipolytica*. In K. N. Timmis (Ed.), *Handbook of Hydrocarbon and Lipid Microbiology* (pp. 1513–1527). Berlin, Heidelberg: Springer Berlin Heidelberg.
https://doi.org/10.1007/978-3-540-77587-4_104
479. Shiningavamwe, A., Obiero, G., Albertyn, J., Nicaud, J.-M., & Smit, M. (2006). Heterologous expression of the benzoate para-hydroxylase encoding gene (CYP53B1) from *Rhodotorula minuta* by *Yarrowia lipolytica*. *Applied Microbiology and Biotechnology*, 72(2), 323–329.
<https://doi.org/10.1007/s00253-005-0264-7>
480. Theron, C. W., Labuschagné, M., Gudiminchi, R., Albertyn, J., & Smit, M. S. (2014). A broad-range yeast expression system reveals *Arxula adenivorans* expressing a fungal self-sufficient cytochrome P450 monooxygenase as an excellent whole-cell biocatalyst. *FEMS yeast research*, 14(4), 556–566. <https://doi.org/10.1111/1567-1364.12142>
481. van Beilen, J. B., Duetz, W. A., Schmid, A., & Witholt, B. (2003). Practical issues in the application of oxygenases. *Trends in Biotechnology*, 21(4), 170–177.
[https://doi.org/10.1016/S0167-7799\(03\)00032-5](https://doi.org/10.1016/S0167-7799(03)00032-5)

482. O'Reilly, E., Köhler, V., Flitsch, S. L., & Turner, N. J. (2011). Cytochromes P450 as useful biocatalysts: addressing the limitations. *Chemical Communications (Cambridge, England)*, 47(9), 2490–2501. <https://doi.org/10.1039/c0cc03165h>
483. Jung, S. T., Lauchli, R., & Arnold, F. H. (2011). Cytochrome P450: taming a wild type enzyme. *Current Opinion in Biotechnology*, 22(6), 809–817. <https://doi.org/10.1016/j.copbio.2011.02.008>
484. Witholt, B., de Smet, M. J., Kingma, J., van Beilen, J. B., Kok, M., Lageveen, R. G., & Eggink, G. (1990). Bioconversions of aliphatic compounds by *Pseudomonas oleovorans* in multiphase bioreactors: background and economic potential. *Trends in Biotechnology*, 8(2), 46–52.
485. Julsing, M. K., Cornelissen, S., Bühler, B., & Schmid, A. (2008). Heme-iron oxygenases: powerful industrial biocatalysts? *Current Opinion in Chemical Biology*, 12(2), 177–186. <https://doi.org/10.1016/j.cbpa.2008.01.029>
486. Sligar, S. G., Lipscomb, J. D., Debrunner, P. G., & Gunsalus, I. C. (1974). Superoxide anion production by the autoxidation of cytochrome P450cam. *Biochemical and Biophysical Research Communications*, 61(1), 290–296. [https://doi.org/10.1016/0006-291X\(74\)90565-8](https://doi.org/10.1016/0006-291X(74)90565-8)
487. González-Pérez, V., Connolly, E. A., Bridges, A. S., Wienkers, L. C., & Paine, M. F. (2012). Impact of Organic Solvents on Cytochrome P450 Probe Reactions: Filling the Gap with (S)-Warfarin and Midazolam Hydroxylation. *Drug Metabolism and Disposition*, 40(11), 2136–2142. <https://doi.org/10.1124/dmd.112.047134>
488. Kühn-Velten, W. N. (1997). Effects of compatible solutes on mammalian cytochrome P450 stability. *Zeitschrift Fur Naturforschung. C, Journal of Biosciences*, 52(1–2), 132–135.
489. Reinen, J., van Hemert, D., Vermeulen, N. P. E., & Commandeur, J. N. M. (2015). Application of a Continuous-Flow Bioassay to Investigate the Organic Solvent Tolerability of Cytochrome

- P450 BM3 Mutants. *Journal of Biomolecular Screening*, 20(10), 1246–1255.
<https://doi.org/10.1177/10870571115607183>
490. Erkelenz, M., Kuo, C.-H., & Niemeyer, C. M. (2011). DNA-mediated assembly of cytochrome P450 BM3 subdomains. *Journal of the American Chemical Society*, 133(40), 16111–16118.
<https://doi.org/10.1021/ja204993s>
491. Lutz, J., Hollmann, F., Ho, T. V., Schnyder, A., Fish, R. H., & Schmid, A. (2004). Bioorganometallic chemistry: biocatalytic oxidation reactions with biomimetic NAD⁺/NADH co-factors and [Cp*Rh(bpy)H]⁺ for selective organic synthesis. *Journal of Organometallic Chemistry*, 689(25), 4783–4790. <https://doi.org/10.1016/j.jorganchem.2004.09.044>
492. Chi, E. Y., Krishnan, S., Randolph, T. W., & Carpenter, J. F. (2003). Physical stability of proteins in aqueous solution: mechanism and driving forces in nonnative protein aggregation. *Pharmaceutical Research*, 20(9), 1325–1336.
493. Nicoud, L., Owczarz, M., Arosio, P., & Morbidelli, M. (2015). A multiscale view of therapeutic protein aggregation: a colloid science perspective. *Biotechnology Journal*, 10(3), 367–378.
<https://doi.org/10.1002/biot.201400858>
494. Kopec, J., & Schneider, G. (2011). Comparison of fluorescence and light scattering based methods to assess formation and stability of protein-protein complexes. *Journal of Structural Biology*, 175(2), 216–223. <https://doi.org/10.1016/j.jsb.2011.04.006>
495. Neeli, R., Girvan, H. M., Lawrence, A., Warren, M. J., Leys, D., Scrutton, N. S., & Munro, A. W. (2005). The dimeric form of flavocytochrome P450 BM3 is catalytically functional as a fatty acid hydroxylase. *FEBS letters*, 579(25), 5582–5588.
<https://doi.org/10.1016/j.febslet.2005.09.023>
496. Cimperman, P., Baranauskiene, L., Jachimoviciūte, S., Jachno, J., Torresan, J., Michailoviene, V., ... Matulis, D. (2008). A quantitative model of thermal stabilization and

- destabilization of proteins by ligands. *Biophysical Journal*, 95(7), 3222–3231.
<https://doi.org/10.1529/biophysj.108.134973>
497. Ugwu, S. O., & Apte, S. P. (2004). The Effect of Buffers on Protein Conformational Stability. *Pharmaceutical Technology*, 28(3), 86–108.
498. Zbacnik, T. J., Holcomb, R. E., Katayama, D. S., Murphy, B. M., Payne, R. W., Coccaro, R. C., ... Manning, M. C. (2016). Role of Buffers in Protein Formulations. *Journal of Pharmaceutical Sciences*. <https://doi.org/10.1016/j.xphs.2016.11.014>
499. Ristic, M., Rosa, N., Seabrook, S. A., & Newman, J. (2015). Formulation screening by differential scanning fluorimetry: how often does it work? *Acta Crystallographica. Section F, Structural Biology Communications*, 71(Pt 10), 1359–1364.
<https://doi.org/10.1107/S2053230X15012662>
500. Anderson, B. M., & Anderson, C. D. (1963). The effect of buffers on nicotinamide adenine dinucleotide hydrolysis. *The Journal of Biological Chemistry*, 238, 1475–1478.
501. Colowick, S. P., Kaplan, N. O., & Ciotti, M. M. (1951). The reaction of pyridine nucleotide with cyanide and its analytical use. *The Journal of Biological Chemistry*, 191(2), 447–459.
502. Wong, C.-H., & Whitesides, G. M. (1981). Enzyme-catalyzed organic synthesis: NAD(P)H cofactor regeneration by using glucose-6-phosphate and the glucose-5-phosphate dehydrogenase from *Leuconostoc mesenteroides*. *Journal of the American Chemical Society*, 103(16), 4890–4899. <https://doi.org/10.1021/ja00406a037>
503. Schenkman, J. B., & Jansson, I. (2006). Spectral Analyses of Cytochromes P450. In I. R. Phillips & E. A. Shephard (Eds.), *Cytochrome P450 Protocols* (pp. 11–18). Totowa, NJ: Humana Press. <https://doi.org/10.1385/1-59259-998-2:11>
504. Pritchard, M. P., McLaughlin, L., & Friedberg, T. (2006). Establishment of Functional Human Cytochrome P450 Monooxygenase Systems in *Escherichia coli*. In I. R. Phillips & E. A.

- Shephard (Eds.), *Cytochrome P450 Protocols* (pp. 19–29). Totowa, NJ: Humana Press.
<https://doi.org/10.1385/1-59259-998-2:19>
505. Cheng, Q., & Guengerich, F. P. (2013). Identification of Endogenous Substrates of Orphan Cytochrome P450 Enzymes Through the Use of Untargeted Metabolomics Approaches. In I. R. Phillips, E. A. Shephard, & P. R. Ortiz de Montellano (Eds.), *Cytochrome P450 Protocols* (pp. 71–77). Totowa, NJ: Humana Press. https://doi.org/10.1007/978-1-62703-321-3_6
506. Rabe, K. S., & Niemeyer, C. M. (2013). Screening for Cytochrome P450 Reactivity with a Reporter Enzyme. In I. R. Phillips, E. A. Shephard, & P. R. Ortiz de Montellano (Eds.), *Cytochrome P450 Protocols* (pp. 149–156). Totowa, NJ: Humana Press.
https://doi.org/10.1007/978-1-62703-321-3_13
507. Oppenheimer, N. J., & Kaplan, N. O. (1974). Structure of the primary acid rearrangement product of reduced nicotinamide adenine dinucleotide (NADH). *Biochemistry*, *13*(23), 4675–4685.
508. Good, N. E., Winget, G. D., Winter, W., Connolly, T. N., Izawa, S., & Singh, R. M. (1966). Hydrogen ion buffers for biological research. *Biochemistry*, *5*(2), 467–477.
509. Chenault, H. K., Simon, E. S., & Whitesides, G. M. (1988). Cofactor regeneration for enzyme-catalysed synthesis. *Biotechnology & Genetic Engineering Reviews*, *6*, 221–270.
510. Ortiz de Montellano, P. R. (2010). Hydrocarbon hydroxylation by cytochrome P450 enzymes. *Chemical Reviews*, *110*(2), 932–948. <https://doi.org/10.1021/cr9002193>
511. Bernhardt, R., & Waterman, M. R. (2007). Cytochrome P450 and Steroid Hormone Biosynthesis. In A. Sigel, H. Sigel, & R. K. O. Sigel (Eds.), *The Ubiquitous Roles of Cytochrome P450 Proteins* (pp. 361–396). John Wiley & Sons, Ltd.
<https://doi.org/10.1002/9780470028155.ch12>

512. Andersen, J. F., & Hutchinson, C. R. (1992). Characterization of *Saccharopolyspora erythraea* cytochrome P-450 genes and enzymes, including 6-deoxyerythronolide B hydroxylase. *Journal of Bacteriology*, *174*(3), 725–735.
513. Shen, B., & Hutchinson, C. R. (1994). Triple hydroxylation of tetracenomycin A2 to tetracenomycin C in *Streptomyces glaucescens*. Overexpression of the *tcmG* gene in *Streptomyces lividans* and characterization of the tetracenomycin A2 oxygenase. *The Journal of Biological Chemistry*, *269*(48), 30726–30733.
514. Anzai, Y., Li, S., Chaulagain, M. R., Kinoshita, K., Kato, F., Montgomery, J., & Sherman, D. H. (2008). Functional Analysis of MycCl and MycG, Cytochrome P450 Enzymes Involved in Biosynthesis of Mycinamicin Macrolide Antibiotics. *Chemistry & Biology*, *15*(9), 950–959. <https://doi.org/10.1016/j.chembiol.2008.07.014>
515. Tian, L., Musetti, V., Kim, J., Magallanes-Lundback, M., & DellaPenna, D. (2004). The *Arabidopsis* LUT1 locus encodes a member of the cytochrome p450 family that is required for carotenoid epsilon-ring hydroxylation activity. *Proceedings of the National Academy of Sciences of the United States of America*, *101*(1), 402–407. <https://doi.org/10.1073/pnas.2237237100>
516. Thatcher, J. E., & Isoherranen, N. (2009). The role of CYP26 enzymes in retinoic acid clearance. *Expert opinion on drug metabolism & toxicology*, *5*(8), 875–886. <https://doi.org/10.1517/17425250903032681>
517. Jones, G., Prosser, D. E., & Kaufmann, M. (2014). Cytochrome P450-mediated metabolism of vitamin D. *Journal of Lipid Research*, *55*(1), 13–31. <https://doi.org/10.1194/jlr.R031534>
518. O’Keefe, D. P., Romesser, J. A., & Leto, K. J. (1988). Identification of constitutive and herbicide inducible cytochromes P-450 in *Streptomyces griseolus*. *Archives of Microbiology*, *149*(5), 406–412. <https://doi.org/10.1007/BF00425579>

519. Siminszky, B. (2006). Plant cytochrome P450-mediated herbicide metabolism. *Phytochemistry Reviews*, 5(2–3), 445–458. <https://doi.org/10.1007/s11101-006-9011-7>
520. Li, Q., Fang, Y., Li, X., Zhang, H., Liu, M., Yang, H., ... Wang, Y. (2013). Mechanism of the plant cytochrome P450 for herbicide resistance: a modelling study. *Journal of Enzyme Inhibition and Medicinal Chemistry*, 28(6), 1182–1191. <https://doi.org/10.3109/14756366.2012.719505>
521. Chiu, T.-L., Wen, Z., Rupasinghe, S. G., & Schuler, M. A. (2008). Comparative molecular modeling of *Anopheles gambiae* CYP6Z1, a mosquito P450 capable of metabolizing DDT. *Proceedings of the National Academy of Sciences of the United States of America*, 105(26), 8855–8860. <https://doi.org/10.1073/pnas.0709249105>
522. Kaplanoglu, E., Chapman, P., Scott, I. M., & Donly, C. (2017). Overexpression of a cytochrome P450 and a UDP-glycosyltransferase is associated with imidacloprid resistance in the Colorado potato beetle, *Leptinotarsa decemlineata*. *Scientific Reports*, 7(1), 1762. <https://doi.org/10.1038/s41598-017-01961-4>
523. Lewis, D. F., Dickins, M., Eddershaw, P. J., Tarbit, M. H., & Goldfarb, P. S. (1999). Cytochrome P450 substrate specificities, substrate structural templates and enzyme active site geometries. *Drug Metabolism and Drug Interactions*, 15(1), 1–49.
524. Lewis, D. F. (2000). Structural characteristics of human P450s involved in drug metabolism: QSARs and lipophilicity profiles. *Toxicology*, 144(1–3), 197–203.
525. Carver, P. L. (2007). Cytochrome P450 Enzymes: Observations from the Clinic. In A. Sigel, H. Sigel, & R. K. O. Sigel (Eds.), *The Ubiquitous Roles of Cytochrome P450 Proteins* (pp. 591–617). John Wiley & Sons, Ltd. <https://doi.org/10.1002/9780470028155.ch17>
526. Guengerich, F. P. (2008). Cytochrome p450 and chemical toxicology. *Chemical Research in Toxicology*, 21(1), 70–83. <https://doi.org/10.1021/tx700079z>

527. Li, Q. S., Schwaneberg, U., Fischer, P., & Schmid, R. D. (2000). Directed evolution of the fatty-acid hydroxylase P450 BM-3 into an indole-hydroxylating catalyst. *Chemistry (Weinheim an Der Bergstrasse, Germany)*, 6(9), 1531–1536.
528. van Vugt-Lussenburg, B. M. A., Damsten, M. C., Maasdijk, D. M., Vermeulen, N. P. E., & Commandeur, J. N. M. (2006). Heterotropic and homotropic cooperativity by a drug-metabolising mutant of cytochrome P450 BM3. *Biochemical and Biophysical Research Communications*, 346(3), 810–818. <https://doi.org/10.1016/j.bbrc.2006.05.179>
529. Munro, A. W., Leys, D. G., McLean, K. J., Marshall, K. R., Ost, T. W. B., Daff, S., ... Dutton, P. L. (2002). P450 BM3: the very model of a modern flavocytochrome. *Trends in Biochemical Sciences*, 27(5), 250–257.
530. Noble, M. A., Miles, C. S., Chapman, S. K., Lysek, D. A., MacKay, A. C., Reid, G. A., ... Munro, A. W. (1999). Roles of key active-site residues in flavocytochrome P450 BM3. *Biochemical Journal*, 339(Pt 2), 371–379.
531. Davies, M. J. (2012). Oxidative Damage to Proteins. In *Encyclopedia of Radicals in Chemistry, Biology and Materials*. John Wiley & Sons, Ltd.
<https://doi.org/10.1002/9781119953678.rad045>
532. Jung, C., Schünemann, V., Lenzian, F., Trautwein, A. X., Contzen, J., Galander, M., ... Barra, A.-L. (2005). Spectroscopic characterization of the iron-oxo intermediate in cytochrome P450. *Biological Chemistry*, 386(10), 1043–1053. <https://doi.org/10.1515/BC.2005.120>
533. Jung, C. (2007). Leakage in Cytochrome P450 Reactions in Relation to Protein Structural Properties. In A. Sigel, H. Sigel, & R. K. O. Sigel (Eds.), *The Ubiquitous Roles of Cytochrome P450 Proteins* (pp. 187–234). John Wiley & Sons, Ltd.
<https://doi.org/10.1002/9780470028155.ch7>

534. Otey, C. R., Silberg, J. J., Voigt, C. A., Endelman, J. B., Bandara, G., & Arnold, F. H. (2004). Functional evolution and structural conservation in chimeric cytochromes p450: calibrating a structure-guided approach. *Chemistry & Biology*, *11*(3), 309–318.
<https://doi.org/10.1016/j.chembiol.2004.02.018>
535. Munro, A. W., Lindsay, J. G., Coggins, J. R., Kelly, S. M., & Price, N. C. (1994). Structural and enzymological analysis of the interaction of isolated domains of cytochrome P-450 BM3. *FEBS Letters*, *343*(1), 70–74. [https://doi.org/10.1016/0014-5793\(94\)80609-8](https://doi.org/10.1016/0014-5793(94)80609-8)
536. Argos, P. (1990). An investigation of oligopeptides linking domains in protein tertiary structures and possible candidates for general gene fusion. *Journal of Molecular Biology*, *211*(4), 943–958. [https://doi.org/10.1016/0022-2836\(90\)90085-Z](https://doi.org/10.1016/0022-2836(90)90085-Z)
537. Govindaraj, S., & Poulos, T. L. (1995). Role of the linker region connecting the reductase and heme domains in cytochrome P450BM-3. *Biochemistry*, *34*(35), 11221–11226.
538. Lam, Q., Cortez, A., Nguyen, T. T., Kato, M., & Cheruzel, L. (2016). Chromogenic nitrophenolate-based substrates for light-driven hybrid P450 BM3 enzyme assay. *Journal of Inorganic Biochemistry*, *158*, 86–91. <https://doi.org/10.1016/j.jinorgbio.2015.12.005>
539. Tufvesson, P., Lima-Ramos, J., Nordblad, M., & Woodley, J. M. (2011). Guidelines and Cost Analysis for Catalyst Production in Biocatalytic Processes. *Organic Process Research & Development*, *15*(1), 266–274. <https://doi.org/10.1021/op1002165>
540. Girvan, H. M., & Munro, A. W. (2016). Applications of microbial cytochrome P450 enzymes in biotechnology and synthetic biology. *Current Opinion in Chemical Biology*, *31*, 136–145.
<https://doi.org/10.1016/j.cbpa.2016.02.018>
541. Grogan, G. (2011). Cytochromes P450: exploiting diversity and enabling application as biocatalysts. *Current Opinion in Chemical Biology*, *15*(2), 241–248.
<https://doi.org/10.1016/j.cbpa.2010.11.014>

542. Guengerich, F. P. (2002). Cytochrome P450 enzymes in the generation of commercial products. *Nature Reviews. Drug Discovery*, 1(5), 359–366. <https://doi.org/10.1038/nrd792>
543. Denisov, I. G., Makris, T. M., Sligar, S. G., & Schlichting, I. (2005). Structure and chemistry of cytochrome P450. *Chemical Reviews*, 105(6), 2253–2277. <https://doi.org/10.1021/cr0307143>
544. Guengerich, F. P., & Munro, A. W. (2013). Unusual cytochrome p450 enzymes and reactions. *The Journal of Biological Chemistry*, 288(24), 17065–17073. <https://doi.org/10.1074/jbc.R113.462275>
545. McLean, K. J., Leys, D., & Munro, A. W. (2015). Microbial Cytochromes P450. In P. R. Ortiz de Montellano (Ed.), *Cytochrome P450: Structure, Mechanism, and Biochemistry* (pp. 261–407). Cham: Springer International Publishing. https://doi.org/10.1007/978-3-319-12108-6_6
546. Narhi, L. O., & Fulco, A. J. (1987). Identification and characterization of two functional domains in cytochrome P-450BM-3, a catalytically self-sufficient monooxygenase induced by barbiturates in *Bacillus megaterium*. *The Journal of Biological Chemistry*, 262(14), 6683–6690.
547. Miura, Y., & Fulco, A. J. (1974). (Omega -2) hydroxylation of fatty acids by a soluble system from *Bacillus megaterium*. *The Journal of Biological Chemistry*, 249(6), 1880–1888.
548. Ahmed, F., Avery, K. L., Cullis, P. M., Primrose, W. U., Roberts, G. C. K., Ahmed, F., ... Willis, C. L. (1999). An unusual matrix of stereocomplementarity in the hydroxylation of monohydroxy fatty acids catalysed by cytochrome P450 from *Bacillus megaterium* with potential application in biotransformations. *Chemical Communications*, 0(20), 2049–2050. <https://doi.org/10.1039/A905974A>

549. Davis, S. C., Sui, Z., Peterson, J. A., & Ortiz de Montellano, P. R. (1996). Oxidation of omega-oxo fatty acids by cytochrome P450BM-3 (CYP102). *Archives of Biochemistry and Biophysics*, 328(1), 35–42.
550. Matson, R. S., Stein, R. A., & Fulco, A. J. (1980). Hydroxylation of 9-hydroxystearate by a soluble cytochrome P-450 dependent fatty acid hydroxylase from *Bacillus megaterium*. *Biochemical and Biophysical Research Communications*, 97(3), 955–961.
551. Miura, Y., & Fulco, A. J. (1975). Omega-1, Omega-2 and Omega-3 hydroxylation of long-chain fatty acids, amides and alcohols by a soluble enzyme system from *Bacillus megaterium*. *Biochimica Et Biophysica Acta*, 388(3), 305–317.
552. Adams, J., & Rosenzweig, F. (2014). Experimental microbial evolution: history and conceptual underpinnings. *Genomics*, 104(6 Pt A), 393–398.
<https://doi.org/10.1016/j.ygeno.2014.10.004>
553. Elena, S. F., & Lenski, R. E. (2003). Evolution experiments with microorganisms: the dynamics and genetic bases of adaptation. *Nature Reviews. Genetics*, 4(6), 457–469.
<https://doi.org/10.1038/nrg1088>
554. Shaw, G. C., & Fulco, A. J. (1992). Barbiturate-mediated regulation of expression of the cytochrome P450BM-3 gene of *Bacillus megaterium* by Bm3R1 protein. *Journal of Biological Chemistry*, 267(8), 5515–5526.
555. Fulco, A. J., Levy, R., & Bloch, K. (1964). THE BIOSYNTHESIS OF DELTA-9 AND DELTA-5-MONOSATURATED FATTY ACIDS BY BACTERIA. *The Journal of Biological Chemistry*, 239, 998–1003.
556. Nelson, D. R. (2006). Cytochrome P450 nomenclature, 2004. *Methods in Molecular Biology (Clifton, N.J.)*, 320, 1–10. <https://doi.org/10.1385/1-59259-998-2:1>

557. Jack, B. R., Meyer, A. G., Echave, J., & Wilke, C. O. (2016). Functional Sites Induce Long-Range Evolutionary Constraints in Enzymes. *PLOS Biology*, *14*(5), e1002452.
<https://doi.org/10.1371/journal.pbio.1002452>